Eesti Maaülikool
Estonian University of Life Sciences

ESTIMATING FOREST VARIABLES USING AIRBORNE LIDAR MEASUREMENTS IN HEMI-BOREAL FORESTS

PUISTUTE TAKSEERTUNNUSTE HINDAMINE AEROLIDARI MÕÕTMISANDMETE PÕHJAL HEMIBOREAALSETES METSADES

TAURI ARUMÄE

A Thesis
for applying for the degree of Doctor of Philosophy in Forestry

Väitekiri
filosoofiadoktori kraadi taotlemiseks metsanduse erialal

Tartu 2020

Eesti Maaülikooli doktoritööd

Doctoral Theses of the Estonian University of Life Sciences

Eesti Maaülikool
Estonian University of Life Sciences

ESTIMATING FOREST VARIABLES USING AIRBORNE LIDAR MEASUREMENTS IN HEMI-BOREAL FORESTS

PUISTUTE TAKSEERTUNNUSTE HINDAMINE AEROLIDARI MÕÕTMISANDMETE PÕHJAL HEMIBOREAALSETES METSADES

TAURI ARUMÄE

A Thesis
for applying for the degree of Doctor of Philosophy
in Forestry

Väitekiri
filosoofiadoktori kraadi taotlemiseks metsanduse erialal

Tartu 2020

Institute of Forestry and Rural Engineering
Estonian University of Life Sciences

According to verdict No 6-14/6-2, 7th of May, 2020, the Defence Board of PhD theses in Forestry of the Estonian University of Life Sciences has accepted the thesis for the defence of the degree of Doctor of Philosophy in Forestry.

Opponent: Professor **Petteri Packalén**, D.Sc (for)
School of Forest Sciences
University of Eastern Finland

Supervisor: Associate Professor **Mait Lang**, PhD
Institute of Forestry and Rural Engineering
Estonian University of Life Sciences

Defence of the thesis:
Estonian University of Life Sciences, room 2A1, Kreutzwaldi 5, Tartu on June 17th, 2020, at 10:00.

The English language was edited by Karit Jäärats and the Estonian by Urve Ansip.

Publication of this thesis is supported by the Estonian University of Life Sciences.

European Union
European Social Fund

Investing
in your future

ISSN 2382-7076
ISBN 978-9949-698-26-4 (printed)
ISBN 978-9949-698-27-1 (pdf)

CONTENTS

LIST OF ORIGINAL PUBLICATIONS

The thesis is based on the following papers; in the text references to them are given in Roman numerals. The papers are reproduced with the kind permission of the publishers.

I Lang, M., **Arumäe, T.**, Anniste, J. 2012. Estimation of main forest inventory variables from spectral and airborne lidar data in Aegviidu test site, Estonia. Forestry Studies, 56, 27−41.

II **Arumäe, T.**, Lang, M. 2013. A simple model to estimate forest canopy base height from airborne lidar data. Forestry Studies, 58, 46−56.

III **Arumäe, T.**, Lang, M. 2016. A validation of coarse scale global vegetation height map for biomass estimation in hemiboreal forests in Estonia. Baltic Forestry, 22(2), 275−282.

IV Olesk, A., Praks, J., Antropov, O., Zalite, K., **Arumäe, T.**, Voormansik, K. 2016. Interferometric SAR coherence models for characterization of hemiboreal forests using TanDEM-X data. Remote Sensing, 8(9), 700.

V **Arumäe, T.**, Lang, M. 2016. ALS-based wood volume models of forest stands and comparison with forest inventory data. Forestry Studies, 64, 5−16.

VI Lang, M., **Arumäe, T.**, Laarmann, D., Kiviste, A. 2017. Estimation of change in forest height growth. Forestry Studies, 67, 5−16.

VII **Arumäe, T.**, Lang, M. 2018. Estimation of canopy cover in dense mixed-species forests using airborne lidar data. European Journal of Remote Sensing, 51(1), 132−141.

VIII **Arumäe, T.**, Lang, M., Laarmann, D. 2020. Thinning- and tree-growth-caused changes in canopy cover and stand height and their estimation using low-density bitemporal airborne lidar measurements – a case study in hemi-boreal forests. European Journal of Remote Sensing, 53(1), 113−123.

The contributions from the authors to the papers are as follows:

	I	**II**	**III**	**IV**	**V**	**VI**	**VII**	**VIII**
Original idea	All	All	All	AO, JP, KV	All	All	All	All
Study design	All	All	All	AO, JP, KV	All	All	All	All
Data collection	All	All	All	AO, **TA**	All	All	All	All
Data analysis	All	All	All	All	All	All	All	All
Preparation of manuscript	All	All	All	All	All	All	All	All

AO – Aire Olesk, JP – Jaan Praks, KV – Kaupo Voormansik, **TA – Tauri Arumäe**

ABBREVIATIONS

ALS	Airborne laser scanning
AGC	Automatic Gain Control
CC	Canopy cover
CC_{ALS}	ALS-based canopy cover estimate
DTM	Digital terrain model
ENFRP	Estonian Network of Forest Research Plots
FI	Forest Inventory
GNSS	Global Navigation Satellite System
H_{ALS}	ALS-based plot/stand height prediction
H_{FI}	Forest inventory based forest height estimate
H_{LCB}	Live crown base height
H_{Px}	xth ALS point cloud height percentile
ICESat	Ice, Cloud, and Land Elevation Satellite
IMU	Inertial Measurement Unit
INS	Inertial Navigation System
InSAR	Interferometric synthetic-aperture radar
kNN	k-Nearest Neighbour algorithm
LAI	Leaf Area Index
Lidar	light detection and ranging
MEE	Mean estimate error
NFI	National Forest Inventory
NIR	Near-infrared
RSE	Residual standard error
RMSE	Root mean square error
r	Coefficient of correlation
R^2	Coefficient of determination
SAR	Synthetic Aperture Radar
VALERI	Validation of Land European Remote sensing Instruments

1. INTRODUCTION

Decision-making and planning for forest management requires up-to-date inventory data of forest stands – species composition, site fertility, forest stand height, standing wood volume, density, and age. The most common methods for retrieving such data are labour intensive in situ measurements. Nowadays, more and more of these measurements are being done via remote sensing techniques. One of the first and basic remote sensing method introduced to forestry was aerial and satellite photos (Spurr, 1948). At relatively small cost, large areas of forested land were inventoried and the information was used for stand delineation and basic visual interpretation. Using aerial images, estimation of tree species composition and main forest structure variables – tree height, tree count per unit area or even crown diameter – were computed (Spurr, 1948). With the introduction of stereo-photos, the estimation accuracy of forest height and stand density was improved. Although with a lot of manual work included, the visual interpretation of orthophotos is a common practice for forest managing and inventory even today.

Digital orthophotos can also be analysed using dedicated software and computers, as the photos consist of pixels (picture elements) assigned with a numeric value, which corresponds to the spectral radiance measured by the sensor cells. Using the numeric values of the photos has made it possible to automatize the processing of such data and with large amounts of big-data availability, global and country-wide wall-to-wall land cover monitoring has become available (Köhl et al., 2006). The biggest limitations for spectral data are clouds or illumination conditions.

In 1958, Charles Townes and Arthur Schawlow suggested that a narrow beam of very high intense monochromatic radiation could be precisely directed over large distances. The laser distance measurements in natural environments started shortly after, in 1960, when the first ruby laser was developed. Soon after, in 1966, the first laser distance-measuring instrument was developed (Large and Heritage, 2009).

Active remote sensing technologies like radar and lidar are independent from the sun illumination and radar also from most weather conditions, except heavy rain, whereas lidar technology is also limited by clouds. The advantage of radar and near-infrared (NIR) lidar technologies compared to spectral data is the ability to partially (Verhoeven, 2011) penetrate the green foliage and therefore better describe the vertical cross-section of the above-ground vegetation (Morsdorf et al., 2006; Saatchi et al., 2011).

With the possibility to receive detailed estimates of forest structure variables, the use of airborne laser scanning (ALS) over the two last decades has increased in forestry. ALS was introduced as a technique for terrain modelling and measuring (Krabill et al., 1980), using a near-infrared spectral region (0.75–1.4 µm) to receive information from beneath green foliage.

Estonian forestry has gone through several changes in the past century: the total forested land has increased from 1.3 million hectares in 1958 to 2.3 million hectares by the year 2016 and a fundamental transition in forest ownership, from 100% state-owned to 50% private-owned and managed forests. A little less than half of the forests are state-owned and the majority belongs to private owners or companies (Keskkonnaagentuur, 2017). With 51% of the land covered by forests, the forest management and wood industry is one of the largest economic incomes in the country. An overview of the forest resources is not only required for management and planning, but is also an obligation set by the European Union directives where the annual report of carbon flux is prescribed (Regulation 2018/481, 2018). Although forest monitoring methods rely mainly on field measurements (Adermann, 2010), the need for remote sensed data is becoming more and more essential for increasing estimation accuracy and reliability. Moreover, reliable estimates of forest resources increase the reputation of the forest sector for the public. Estonia has a national ALS program, which started in the 2008 and is intended for ground surface modelling. The airborne laser scanning is carried out by the Estonian Land Board and the measurements are conducted twice a year – in spring for ground monitoring and in summer for forestry purposes (Maa-amet, 2018). This national flight program is set to cover the country at a four-year cycle, both leaf-off and leaf-on data. By the end of 2016, Estonia had a double wall-to-wall ALS data coverage. Since 2017, the Estonian Land Board has used a new ALS scanner - Riegl VQ-1560i (Riegl, 2017), replacing the old Leica ALS50-II (Leica, 2007).

This PhD thesis focuses on developing models for the hemi-boreal forests in Estonia to utilise the routine country-wide ALS measurement data. The thesis is synthesised based on eight research papers focusing on ALS-based estimation of forest structure variables. The main studied variables are forest stand height (**I**, **III**, **IV**, **VI**, **VIII**) and standing wood volume (**I**, **V**). Additional variables were canopy base height (**II**), biomass (**III**) and canopy cover (**VII**, **VIII**). Phenology effects on ALS point clouds were studied (**VIII**). The ALS data was also used for validation of forest height, wood volume and biomass estimates obtained from radar and satellite laser scanners (**III**, **IV**). With the availability of multitemporal ALS data forest height increment and disturbance based structure changes were studied (**VI**, **VIII**).

2. REVIEW OF LITERATURE

2.1. Airborne lidar measurements

Lidar measurements most commonly use NIR wavelength for the purpose of penetrating the green foliage and to retrieve reflections from the ground. The common platforms used for ALS measurements are airplanes (Large and Heritage 2009), but with the rapid development of lightweight and compact laser scanners more and more small unmanned aerial vehicles (UAV) are used for ALS measurements (Sankey et al., 2017). Such lightweight scanners weigh up to 3 kg and with the continuing fast progress, their accuracy and flight time keep increasing (Pilarska et al., 2016)

ALS measurements are carried out similarly for all platforms – flying in the direction of X and emitting pulses in the direction of Z. The Leica ALS50-II system uses an oscillating mirror scanner, which sends out pulses in a zig-zag pattern towards the ground on the axis of Y (Figure 1). The emitted pulse diverges with the distance from the scanner and is in the shape of a cone (Figure 2). In the nadir the footprint of the laser beam on the ground is circular and with an increased scan-angle, the shape changes towards an ellipsoid. The size of the footprint (illumination on the ground) increases with the flight altitude and is also affected by the divergence of the pulse. Beam divergence is commonly referred to as the increase in beam diameter compared to the diameter at the start of the beam and is measured in radians (Gatziolis and Andersen, 2008).

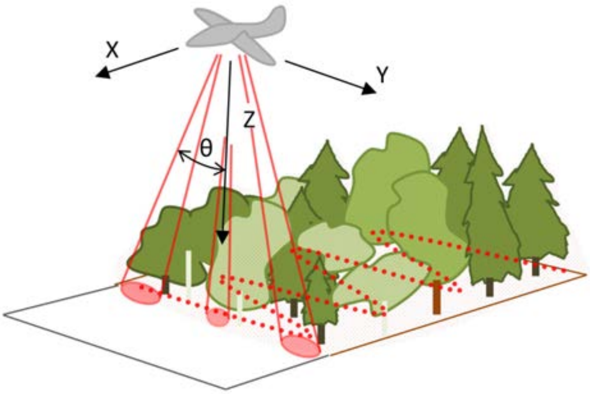

Figure 1. Airborne laser scanning zig-zag pattern used for Leica ALS50-II scanner. θ is the scanning angle.

The energy of emitted laser pulses is reflected specularly, scattered diffusely or absorbed by the vegetation or ground surface. The photons that are reflected back towards the scanner are timed. Using the flight time along the constant of the speed of light, the distance between the scanner and the reflection is calculated (Figure 2; Large and Heritage, 2009). Using the global navigation satellite system (GNSS), inertial navigation system (INS) of the carrier platform and the scanning angles from the scanner, location coordinates for each reflection are calculated and a three-dimensional point cloud is constructed, where each point represents a pulse reflection (Large and Heritage, 2009). Point clouds are later characterised by variables that correspond to point cloud height distribution percentiles, the density of points in horizontal layers and variability of point heights and densities. A general term "point cloud metrics" is used for these variables.

There are two ways of recording the returned signal of the emitted pulses. Most common and earlier scanners used an inner algorithm to define echoes based on the maximum of the signal strength. The amount of the returned photons (signal strength) required for a discrete scanner to register an echo is specific to the scanner and manufacturer and is also dependent on the amount of echoes per pulse the scanner is able to register (i.e. four echoes per pulse for Leica ALS50-II). The discrete return scanners also record the intensity which shows the amount of photons returned for each pulse. Simultaneously, based on the photons reflected back (Figure 2), the scanner Leica ALS50-II can automatically correct and change the power of the pulse emitted (how many photons are being emitted). This is coordinated by the automatic gain control (AGC; Vain et al., 2010) system.

Nowadays, more and more full-wave scanners are being used which, instead of defining the echoes using a scanner-specific algorithm, enable the data user to analyse the whole returned photon flux (Figure 2), thus giving more opportunities for manually filtering and selecting echo locations (Mallet and Bretar, 2009). The full waveform lidar has also shown to be more detailed and suited for describing the three-dimensional structure of vegetation, whereas the discrete returned lidar is more suitable for simple hard targets like buildings and roads (Anderson et al., 2015) and also for large-scale research or inventories due to its smaller demand for data storage capacities.

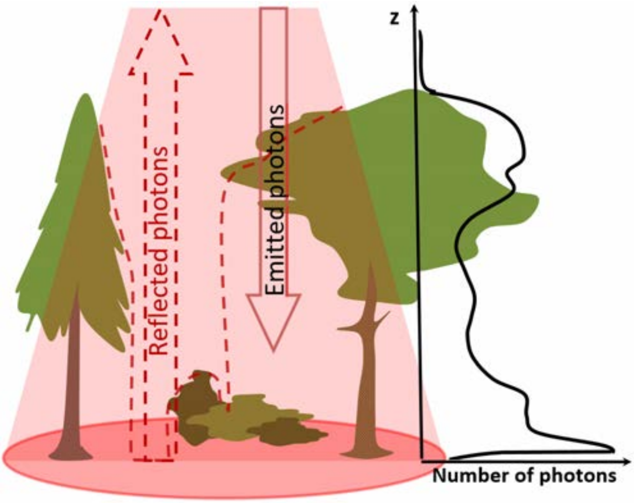

Figure 2. A single ALS pulse representation showing the potential "reflective" objects (dashed line). On the right is the distribution of the returning photons throughout the vertical cross-section of Z.

2.2. ALS in forest inventory

The first studies on tree height assessment using laser technology were already done in 1984 by Nelson et al., when they discovered that the canopy cover greatly affects the penetration and return of laser pulses. The laser was used for determining ground reflections, which were then compared with canopy reflections, defined as without strong ground reflection. This method could be used for forest height assessment with a one-metre difference compared to photogrammetrically measured heights. Further studies by Nelson et al. (1988a, 1988b) showed the possibilities to assess the total standing volume and biomass using ALS-based height and canopy density metrics.

Biomass and also standing wood volume are known to be well-correlated with forest height and basal area (Krigul, 1972; Lang et al., 2016). ALS-based forest height models are showing strong linear correlations with measured forest height. These height models are mostly based on the ALS point cloud height percentiles (Næsset, 1997a; 1997b; Yu et al., 2006; Lang, 2010; Bottalico et al., 2017). The reported precision of height estimations are within one to two metres. For the basal area substitution the ALS-based biomass or standing wood volume models, commonly vertical canopy cover – the proportional vertical projection of the tree crowns on the ground (Korhonen et al., 2006) – is used. Canopy cover is commonly estimated from ALS data using a threshold method (Korhonen et al., 2011), where the ratio of echoes above a certain threshold to the total number of echoes is calculated, and is commonly given as a percentage. This method, with restrictions to scan angle up to 15°, has showed strong correlation with the measured vertical canopy cover in the range of 30 to 95% (root mean square error, RMSE < 10%; Korhonen et al., 2011). With increasing scan angles (>30°) Korhonen et al. (2011) showed also an increase in ALS-based canopy cover estimate (CC_{ALS}) RMSE.

Biomass has shown strong correlations with using only ALS height metrics (RMSE 34%; Hawbaker et al., 2009). Combining the ALS height metrics with canopy cover indices has shown similar results ($R^2 = 0.81$, RMSE 11 t ha^{-1}; Nie et al., 2017) or could also be increased by including site indices (RMSE 31%; Shao et al., 2018). In direct correlation with biomass, the carbon flux can also be monitored as was shown by Simonson et al. (2016).

Biodiversity has been shown to correlate well with stand structure variation (Noss, 1990). Using this knowledge, methods using the ALS-based forest structure descriptive – canopy cover (CC) or density, height percentiles, height variation – have been developed for similar biodiversity estimations (Müller and Vierling, 2014). For example, light availability for understory vegetation is in strong correlation with canopy cover and upper layer vegetation density. In a recent study, Thers et al. (2017) studied ALS possibilities for mapping fungal species richness based on height and canopy cover and found a strong correlation ($R^2 > 0.5$). Guo et al. (2017) showed another possibility of using canopy cover calculated at different thresholds for monitoring biodiversity and different structure classes of forests.

Another input for biodiversity is species composition (Noss, 1990). ALS is rarely considered for species detection which is instead estimated using spectral data (Nagendra, 2001; Lang et al., 2018). Vauhkonen et al. (2009) showed the possibility of applying ALS data with high density of points per unit area of horizontal surface (40 p m^{-2}) with a computational geometry approach to distinguish common commercial tree species in Scandinavia. The down-side of such applications of geometry, 3D segmentation and single tree shape fitting methods, is the limitation by the high point density requirement. Most studies on single tree detection are based on at least 15 p m^{-2} (Holmgren et al., 2008; Eysn et al., 2015; Chen et al., 2018), but 10 p m^{-2} has also been shown to work with the 3D Adaptive Mean Shift algorithm to extract individual trees (Ferraz et al., 2016). With the high data density requirement, such methods are not feasible to implement in broad, wall-to-wall, country-based datasets, where the point density is in the range of 0.5 to 5 p m^{-2}. Another pre-requisite for single tree species extraction is the detectable difference between the tree crown shapes of different species. More promising results are shown by combining ALS-based point clouds with different data sources such as multi-spectral images (Holmgren et al., 2008), hyper-spectral data (Kandare et al., 2017) or by using the intensity values of laser impulses (Törmä, 2000), with the difference between coniferous and deciduous species being the most pronounced in the NIR wavelength (Kuusk et al., 2013).

With a rapid growth in applications and use, multitemporal data has become available, allowing monitoring of small-scale changes like tree mortality or wind-throw (Nyström et al., 2014), which for satellite-based change detection would be hidden by the measurement uncertainties and other factors that form the forest reflectance. Airborne lidar data has been shown to be applicable for detecting of small-scale disturbances like thinnings and even for monitor forest stand height or biomass increment (**VI**; **VIII**; Næsset and Gobakken, 2005; Kotivuori et al., 2016; Ene et al., 2017).

3. AIMS OF THE STUDY

With approximately 50% of the Estonian land area covered with forests (Keskkonnaagentuur, 2017) and ongoing routine ALS measurements, there is a need for ALS-based forest resource assessment models developed specifically for Estonia. This doctoral thesis synthesizes several studies on local ALS-based forest variable estimations.

The specific aims of the study were to:

1. Develop ALS-based models and methods for estimating forest structure variables and understanding the effects of scanning specifics on estimations when using the available country-wide low-density ALS data in Estonia. The studied structure variables were forest stand height (**I**, **III**, **IV**, **VI**, **VIII**), standing wood volume (**I**, **V**), live crown base height (**II**, **VII**), biomass (**III**), and canopy cover (**VII**, **VIII**).

2. Provide a better, up-to-date, overview of available forest resources for the State Forest Management Centre and to implement the developed models to improve forest management and planning (**I**, **II**, **V**, **VI**, **VII**, **VIII**). Find potential use for different phenological ALS measurements.

3. Use the ALS-based models for providing crucial validation data as an input for satellite-based remote sensing methods (**III**, **IV**). To improve ALS-based estimations with species-specific composition estimations (**I**, **V**).

The following hypotheses were tested:

1. Point cloud height distribution metrics can be used to predict live crown base height.

2. Monitoring of forest height growth and detecting small-scale disturbances like thinning is feasible with multitemporal lidar measurements.

3. Standing wood volume can be estimated using ALS data with similar precision to field-based forest mensuration.

4. MATERIALS AND METHODS

4.1. Test sites

The thesis is based on four test sites – Aegviidu, Laeva, Soomaa, and Järvselja (Figure 3). The test sites represent different forested landscapes in Estonia and most of the forests in the test sites are managed by the Estonian State Forest Management Centre.

Figure 3. Test site locations.

The first test site (15×15 km) is located near Aegviidu (59° 19’ 20” N, 25° 35’ 36” E) in North Estonia. The test site was established in 2008 by Anniste and Viilup (2011) for studying the use of ALS data for forest inventory and management planning in Estonia. The test site is mainly dominated by evergreen coniferous forests and, to a lesser extent, mixed forests where the dominating species are Scots pine (*Pinus sylvestris* L.), Norway spruce (*Picea abies* L.), and birch (*Betula pendula* Roth and *Betula pubescens* Ehrh.). The main site type according to the Estonian classification system by Lõhmus (2004) is *Rodococcum*. Aegviidu test site was used for forest structure variable research (**I**, **II**, **III**, **V**), the validation of coarse spatial resolution forest height map (**III**), assessment of forest management inventory wood volume estimates (**V**), and change detection based on bitemporal ALS data (**VIII**).

The second test site (15×15 km) was established in 2013 in south-eastern Estonia, near Laeva (58º 31’ 33” N, 26º 30’ 21” E). The forest land in Laeva is mostly covered by mixed multi-layered deciduous forests dominated by European aspen (*Populus tremula* L.), birch, Norway spruce, grey alder (*Alnus incana* (L.) Moench), and black alder (*Alnus glutinosa* (L.) Gaertn.). In most of the deciduous forests a second / lower layer is present, dominated by the shade-tolerant Norway spruce. Two main forest site types according to the classification of Lõhmus (2004) are dominant – *Aegopodium* and *Filipendula*. Laeva test site was used for developing a new method for processing digital hemispherical images (Lang et al., 2013), which was further used in the study **VII** for canopy cover estimation in contrasting phenological conditions using ALS data and hemispherical image based data as validation. Laeva test site was also used for satellite-based canopy height map validation (**III**) and analysis of wood volume data from forest management inventory database records and ALS-based models (**V**). The Estonian Network of Forest Research Plots (ENFRP) from Laeva test site was used for thinning simulation in the **VIII** study.

Järvselja test site (58º 15’ 42” N, 27º 19’ 39” E) is mostly dominated by mixed forests dominated by Scots pine, Norway spruce, birch or aspen. Järvselja test site was used for the live crown base height study (**II**) and for the interferometric synthetic-aperture radar (InSAR) coherence-based estimation of forest height (**IV**). The high-density bitemporal ALS measurements from Järvselja area were used for precise forest height increment measurements and comparisons with tree growth models (**VII**).

Soomaa test site (58° 24’ 06” N, 25° 07’ 52” E) was only used alongside Järvselja for the InSAR study **IV**. The 242 stands for Soomaa test site were mainly dominated by Scots pine, birch and black alder, with a total area of 591 ha.

4.1.1. The Estonian Network of Forest Research Plots

The Estonian Network of Forest Research Plots (EFNRP) has observations of 15, 20, 25 or 30 metres in radius. A detailed overview of the EFNRP project is given by Kiviste et al. (2015). The diameter at breast height for each tree in the sample plots is measured with a calliper and the trees are positioned. The plots are re-measured at a five-year-cycle and on each plot every fifth tree is selected for height and live crown base height measurements. The EFNRP data was acquired from Diana Laarmann (Estonian University of Life Sciences).

For in situ reference of CC change after thinning, a controlled simulation using the ENFRP sample plot in situ data was carried out. Data from 74 large (radius 15–30 m) ENFRP sample plots in Laeva test site were used for modelling CC change driven by thinning. The tree crowns were modelled and reshaped in accordance with neighbouring crown competition using models from Lang and Kurvits (2007). A thinning model developed by Korjus (1999; Table 1) was then applied that uses stand average diameter (D), main species and site index (H_{100}) as arguments to estimate the maximum allowable stand sparsity after thinning (L_{rj}). The thinning simulation was carried out by removing the tree neighbours that were located closer than estimated by the thinning model (Table 1). The simulation was run 15 times for each sample plot by starting at a random tree. Only the trees in the dominant/upper layer were used in the thinning simulation. All trees including those in the mid-storey and lower layers were included for CC calculations. The maximum allowable sparsity model is for forest stands; however, to keep the thinning simulation experiment simple, we applied the model at the single-tree level. To avoid excessively intensive thinning (i.e. the stands becoming too sparse) according to the thinning limit stated by law (Riigiteataja, 2018), the maximum sparsity that was predicted by the model had to be reduced to 70% of the estimated value. An example of a thinned ENFRP sample plot is shown in Figure (4).

Table 1. Models (Korjus, 1999) for estimating the minimum distance between remaining trees after a thinning (L_{rj}) has been carried out. The model is based on the stand average diameter (D) and site index (H_{100} or H_{50}).

Main species	Valid for range	Model
Scots pine	$D = 6\ldots26$ cm $H_{100} = 16\ldots28$ m	$L_{rj} = 166.8 + 15.2\cdot D - 3.7\cdot H_{100}$
Norway spruce	$D = 6\ldots26$ cm $H_{100} = 16\ldots32$ m	$L_{rj} = 121.6 + 13.3\cdot D - 1.9\cdot H_{100}$
Birch species	$D = 6\ldots26$ cm $H_{50} = 12\ldots22$ m	$L_{rj} = 105.0 + 16.8\cdot D$

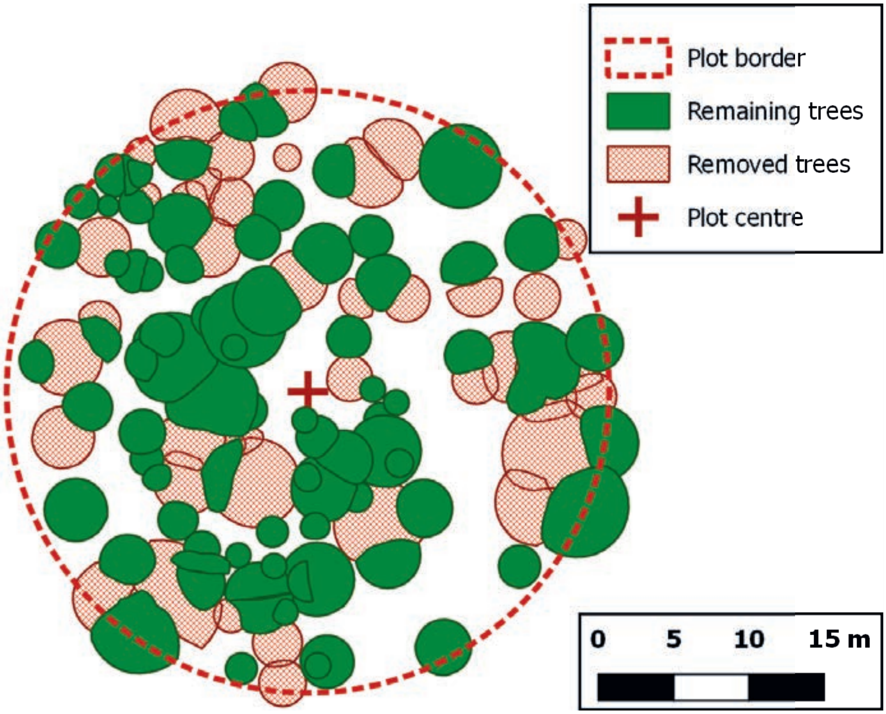

Figure 4. A thinning simulation example using data of Estonian Network of Forest Research Plots (ENFRP).

4.1.2. Field measurements in Aegviidu

Field measurements were carried out on 447 sample plots in 2008 (Anniste and Viilup, 2011). Sample plot radiuses varied from 8 to 15 metres. All the trees on the sample plots were callipered and model trees were selected for height measurements. A minimum of four model trees per plot were selected. The plot average height was then calculated for each sample plot using the model tree diameter to height models. Plot centre coordinates were measured with a precise GPS recorder Trimble R4. Sample plot placement was restricted to be representative of the stand and in a homogeneous part of the forest stand and with the centre of the plot at least 20 m from the stand border.

Additional measurements were carried out in the summer of 2011 in 46 stands. Within each stand, 8–12 circular plots were established and all the diameters at breast height on the plots were measured with callipers. Heights were measured for at least 3 model trees per plot and diameter to height models for each stand were developed using the diameter to height models then to calculate plot height for all trees on the sample plots. Based on the 8–12 sample plots in each stand, the stand-level estimates of forest inventory variables were calculated. Similar to the previous measurements, circular plots were limited to 20 m from the stand boarder.

The commercial thinning and management data for the study **VIII** were received from the State Forest Management Centre (RMK) database. The thinning years were updated using aerial images, as the thinning data are usually written in the database in bulks and after the actual thinning.

4.1.3. Field measurements in Laeva

Field measurements were mostly carried out by a special field crew on 401 sample plots with a 10-metre radius in 2013. All the trees within the sample plots were measured with callipers and model trees were selected for height measurements similar to Aegviidu test site measurements. A diameter to height model was developed and applied on all of the callipered trees to calculate the forest mean height for each plot.

Sample plot placement was inside a selected stand with at least 20 metres from the stand border and in a homogeneous representative spot. Centre coordinates of the plots were measured using regular hand-held GPS devices. This method gives the centre coordinate with an error of up to 10 metres, especially under dense forest canopies.

Hemispherical images were collected from 93 ENFRP sample plots (see chapter 4.3) for both leaf-off and leaf-on stages. For each plot, three photos in four cardinal directions were taken, a total of 12 photos per plot.

4.1.4. Field measurements in Järvselja

Measurements were carried out on 20 stands in the summer of 2010. Live crown base height (H_{LCB}) was measured on 10 randomly placed sample plots inside each stand. Average H_{LCB} of the sample plots was calculated for each stand.

4.2. Airborne laser scanning data

The ALS measurements for the test sites were carried out by the Estonian Land Board using the Leica ALS50-II scanner. The scanner operates in the NIR region of electromagnetic spectrum at 1064 nm and can register up to four echoes per pulse. The study **VI** used ALS measurements from two different scanners – the first measurements were carried out using the Leica ALS50-II scanner and the second ALS measurements were carried out using the Riegl VQ-1560i scanner. Riegl VQ-1560i is operating in a similar 1064 nm NIR wavelength, but has the ability to register up to 20 echoes per pulse and the distance limit between two registered echoes is also shorter compared to Leica ALS50-II, which has the minimum distance between two echoes of approximately 3 metres.

The point densities varied among test sites and are mainly dependent on the flying altitude – for Järvselja test site it was 0.5 p m^{-2} at a flight altitude of 2400 m (Table 2). The ALS measurements were carried out in the summer of 2010. Laeva test site was scanned twice to study leaf phenology effects. Point density for the leaf-on data was 2.0 p m^{-2} with a flight altitude of 1800 m. The leaf-on data was measured in July 2013. The leaf-off data was collected at 2400 m altitude, giving a point density of 0.45 p m^{-2}. The measurements were carried out in the beginning of May 2013. In Aegviidu test site the point density varied from 0.25 to 0.45 p m^{-2}. The flight height was 2400 m and 3800 m. Measurements were carried out in 2008, 2009, 2012 and 2013. The two high-density flights for Järvselja VALERI test sites were carried out in 2009 and 2017 during leaf-on conditions and the point density was correspondingly 23.7 p m^{-2} and 161.3 p m^{-2} (Table 2). This high point density was obtained by two low-altitude flights in perpendicular direction over the test stands.

Table 2. Flight specifications of the ALS measurements.

Test site	Year	Flight altitude (m)	Point density (p m^{-2})	Flight dates
Aegviidu	2008	2400	0.45	11.07, 27.07, 01.09
	2009	2400	0.45	15.05, 26.05
	2012	3800	0.25	20.06–04.07
	2013	2400	0.45	03.05–04.05
Laeva	2013	2400	0.45	06.05
	2013	1800	2.0	13.07, 14.07
Järvselja	2009	500	23.7	30.06
	2010	2400	0.45	29.06
	2017*	300	161.3	16.07
Soomaa	2010	2400	0.45	19.05

*Scanner Riegl VQ-1560i

4.2.1. ALS data processing

ALS data retrieved from the Estonian Land board (Maa-amet, 2018) was then processed using FUSION freeware (McGaughey, 2014). The main phases of ALS data processing were:

1. determining the ground points and creating a ground surface height model (5m pixel);

2. subtracting the ground surface height model from the point cloud and calculating point heights from the ground level;

3. using either stand border shapefiles or coordinates for cutting large point clouds into smaller polygons and calculating different metrics for each polygon.

The digital terrain model (DTM) for studies **I, II** and **III** was constructed using GroundFilter and GridSurfaceCreate modules in FUSION. The DTM for studies **IV-VIII** was downloaded from the Estonian Land Board public access server. Echoes above the DTM were extracted using ClipData and plot or stand-based clouds were cut using PolyClipData. The characteristics based on these point clouds were calculated using Cloudmetrics. For the forest height percentile increment calculations in the study **VI** the LAStools (Isenburg, 2017) modules were used.

For forest height estimation, the returns from near-ground and understory vegetation were excluded. This was done to avoid the bi-modal distribution (Figure 2) with the second peak near the ground, which would influence lower height percentiles and disturb the estimation of live canopy base height. The threshold for ground point exclusion was mostly set to 1.3 m above the DTM. A similar 1.3-metre minimum height filter was used for other height distribution characteristics studied in **VIII** – mode, skewness, kurtosis, and canopy relief ratio.

Canopy cover is defined as the vertical proportion of the crown projections to the total surface area (Korhonen et al., 2006). ALS-based canopy cover (CC_{ALS}) is calculated as the ratio of the first or first of many echoes above a certain threshold (z) over the DTM (CC_{ALS,z_1}). In the study **VII** both CC_{ALS,z_1} and all echoes above the set threshold CC estimation (CC_{ALS,z_A}) were compared. The threshold was also varied within the range of $1 \leq z \leq 10$ metres above the DTM up to the ALS-based live crown base height (H_{LCB_ALS}).

4.2.2 ALS-based models for forest structure variables and variable change estimation

Live crown base height (H_{LCB}) was measured in Aegviidu and Järvselja and then predicted from ALS point cloud height distribution using the point cloud height distribution mode (H_{Mode}) and standard deviation (H_{Stdev}) as follows (**II**):

$$H_{LCB\_ALS\_0} = H_{Mode} - \frac{H_{Stdev}}{2}. \tag{1}$$

The point clouds were tested for three different minimum height thresholds – 0.5 m, 1.0 m and 1.5 m. An additional linear model (2) was then fitted for site-specific measurements as follows (**III**):

$$H_{LCB\_ALS} = a \cdot H_{LCB\_ALS\_0} + b. \tag{2}$$

The ALS-based forest stand height (H_{ALS}) was predicted using the height percentiles of ALS point clouds (H_{Px}) in a linear model:

$$H_{ALS} = a \cdot H_{Px} + b. \tag{3}$$

The ALS-based standing wood volume (V_{ALS}) was predicted with four different models (4, 5, 6, and 7) using the ALS point cloud height parameters H_{P25}, H_{P80} and CC_{ALS} as follows:

$$V_{\mathrm{ALS}} = a \cdot {H_{P80}}^{b}, \tag{4}$$

$$V_{\mathrm{ALS}} = a \cdot {H_{P80}}^{b} + c \cdot H_{\mathrm{P25}}, \tag{5}$$

$$V_{\mathrm{ALS}} = a \cdot {H_{\mathrm{P80}}}^{b} \cdot {CC_{\mathrm{ALS}}}^{c}, \tag{6}$$

$$V_{\mathrm{ALS}} = \left(a \cdot {H_{\mathrm{P80}}}^{b} + c \cdot H_{\mathrm{P25}}\right) \cdot {CC_{\mathrm{ALS}}}^{d}, \tag{7}$$

where *a*, *b*, *c* and *d* are the fitted model parameters using ENRFP or measured test-site plots. The V_{ALS} model idea (**II**) is based on the classical Krigul (1972) standing wood volume (*V*) model (8):

$$V = G \cdot H \cdot F, \tag{8}$$

where *G* is the basal area of the stand, which has weak to no correlation with CC_{ALS}, but carries the similar information of stand density. The correlation is weaker in dense hemi-boreal forests where the crowns are overlapping and CC is near 100% and stronger in sparse boreal forests where the crowns are less overlapping. *H* is the forest height and *F* is the form factor describing the stem taper.

Forest height has many different definitions – Lorey's height, top height, mean height. For most case scenarios, Lorey's height is calculated, using tree basal area as the weight for height estimation. The top height is commonly referred to as the height of the 20% of the highest trees. Mean forest height is calculated as the average of all the trees on the plot. The different forest heights independent of their definitions are usually in strong linear relationship with most of the higher ALS point cloud height percentiles ($H_{Px} | x > 70$) (Hopkinson et al., 2006). The stem form factor *F* is not estimated from ALS and used in the V_{ALS} models; in forest inventory framework *F* is estimated from stand height. To account for the mid- and lower tree layers the 25th percentile H_{P25} was used as a descriptive variable in models 5 and 7.

The canopy relief ratio for the study **VIII** was calculated based on the mean ($\overline{H}_{\mathrm{ALS}}$), minimum ($H_{\mathrm{ALS,min}}$) and maximum ($H_{\mathrm{ALS,max}}$) height of echoes for each forest stand as follows (McGaughey, 2014):

$$CRR = (\overline{H}_{\mathrm{ALS}} - H_{\mathrm{ALS,min}}) \,/\, (H_{\mathrm{ALS,max}} - H_{\mathrm{ALS,min}}). \quad (8)$$

For the stand dominating species (SP) effect on CC_{ALS} or change of H_{P80}, we applied two linear models M_1 (9) and M_2 (10) as follows:

$$Y = b_0 + b_1 \cdot x + e, \quad (9)$$

$$Y = b_0 + b_1 \cdot x + SP + e, \quad (10)$$

where b_0 and b_1 were the model parameters, x was the ALS metric CC_{ALS} or H_{P80}, SP was the dummy variable (Fox and Weisberg, 2011), and e was the error term.

To estimate the significance of the additional variable SP in the linear model M_2, the analysis of variances (ANOVA) was used. The F statistic for model comparison was as follows (Faraway, 2005):

$$F = \frac{(RSS_{M1} - RSS_{M2})/(p_2 - p_1)}{RSS_{M2}/(n - p_2)}, \quad (11)$$

where RSS_{M1} and RSS_{M2} are the residual sums of squares for the models M_1 and M_2 respectively, p_1 and p_2 are the number of parameters for M_1 and M_2, and n is the number of observations.

The influence of the thinning year (T_{Year}), site fertility index (H_{100}), and stand age at the time of thinning (A_{Thinning}) on the change in H_{P80} (ΔH_{P80}) were studied using T_{Year} as a factor, using the generalized additive models (function gam, Mixed GAM Computation Vehicle package in R):

$$\Delta H_{\mathrm{P80}} = a_0 + a_1 \cdot T_{\mathrm{Year}} + a_2 \cdot A_{\mathrm{Thinning}} + a_3 \cdot H_{100} + e, \quad (12)$$

where a_x are the model parameters and e is the error term.

4.3. Hemispherical images

Hemispherical images for the canopy cover study (**VII**) were taken with two cameras. The first camera was a Nikon D5100 with Sigma's 4.5 mm

F2.8 EX DC HSM Circular Fisheye lens. The second camera was a Canon EOS 5D with Sigma 8 mm 1:3.5 EX DG Fisheye lens. Twelve photos for each EFNRP sample plot were taken in four cardinal directions, with a 3-metre difference between each take. The camera was levelled at 1.3 metres above the ground. The measuring protocol was according to the VALERI (Validation of Land European Remote Sensing Instruments, http://www.avignon.inra.fr/valeri/) method.

Hemispherical image processing was done with the HSP software. The HSP software uses raw data files to extract unprocessed sensor data from the camera-specific raw data files and uses these to correct for camera vignetting, correct the projection model and resample the images to a common dimension. Using the raw images the above canopy hemispherical sky image is restored and the ratio from the below canopy image to the above canopy is calculated and the gap fraction is estimated (Lang et al., 2013). Only the signal from authentic blue pixels was used, skipping interpolated values of the RGB and Complementary Metal-Oxide-Semiconductor (CMOS) sensors.

4.4. Satellite-based forest height estimations

The spaceborne lidar-based global vegetation height (GVH) map published by Simard et al., in 2011 is constructed using the Geoscience Laser Altimeter System (GLAS) data from the Ice, Cloud, and land Elevation Satellite (ICESat) mission. Simard et al. (2011) used a raster-based approach to construct the GVH map by dividing the global map into 1×1 km pixels. The ICESat mission satellite-lidar data has a 60 m footprint on ground. The pixels were classified as forest and non-forested pixels using the Global Land Cover Map (Glob-Cover, Hagolle et al., 2005), and for the pixels classified as forest, the forest height estimate was calculated. The GVH for pixels classified as forest, but with missing GLAS data, was estimated by using Moderate Resolution Imaging Spectroradiometer (MODIS) data, elevation data from the Shuttle Radar Topography mission and climatology map data. The GLAS data used for the GVH map over our test sites was collected in 2005 from May 20th to June 26th. The forest height estimates of 1×1 km pixels of the GVH map were validated using data from forest inventory and ALS-based height predictions. Biomass was predicted for the 1×1 km pixels using the biomass calculated for each stand with the diameter, age and, height from forest inventory data and Repola (2008, 2009) models. Biomass predictions were then compared with ALS-based height and satellite-lidar-based heights.

In the study **IV** ALS 3D point clouds over two forested test sites in Soomaa and Järvselja were used to validate forest height estimates obtained from the space-borne InSAR. InSAR is a radar technique, which uses a comparison of two or more synthetic aperture radar (SAR) images. The InSAR coherence was assumed to decrease due to forest density, and for the validation, ALS-based H_{P90} was used and showed promising results for estimating forest height and, through different allometric relations, above-ground biomass (AGB).

5. RESULTS

5.1. Forest stand height and live crown base height

In Laeva and Aegviidu test sites, forest height had strong linear correlation with all of the higher H_{Px} (x > 70%). In Laeva test site, the strongest correlation was found using the 80th height percentile (H_{P80}) $R^2 = 0.95$, the residual standard error of the linear model (RSE) was 1.84 m (p-value < 0.01; Table 3; Figure 5). The colours in the Figure (5) present different dominating tree species and are based on the forest inventory regulation (Metsa korraldamise juhend, 2009). The higher H_{Px} are based on a fewer amount of echoes and are therefore more sensitive to variability in canopy surface. For example, if we had 100 echoes in an ALS point cloud, the 95th percentile would be defined by just the top five echoes. In Aegviidu, the strongest correlation for the model (3) was shown using H_{P95} ($R^2 = 0.91$, RSE = 1.78), but when different percentiles were compared, no statistically significant differences were shown in predictive power using H_{P80} to H_{P99}. The linear relationship between H and H_{Px} (3) was not significantly influenced by stand dominating species when using H_{P50} or higher percentiles (p-value > 0.05) and leaf-on data. Lower H_{Px} linear models were significantly different (p-value < 0.05) for different dominating tree species, but the H_{ALS} estimation did not improve significantly for different species to be worthwhile to separate species-specific H_{ALS} models in leaf-on conditions. The reason for lower H_{Px} to be more influenced by the species could be related to differences in forest understory vegetation, as the deciduous species grow on more fertile soils with much more vegetation in the understory. A similar effect could be due to tree crown shapes, if for example we were to compare echoes received from the tops of canopies, spruces would have less chance compared to any deciduous species. Also canopy cover differs between different species, for example deciduous species with a large canopy cover (> 90%) have less echoes from beneath, due to strong signals from the top of the canopy.

Similarly to small circular sample plots, larger stand-sized point cloud polygon-based H_{P80} was strongly correlated with the average stand height ($R^2 = 0.95$, RSE = 0.99, p-value < 0.01) when the 46 stands in Aegviidu were studied (Table 3). Dominating species were statistically significant for pine and spruce-dominated stands (p-value < 0.05). However, the improvement by including dominating species in the H_{ALS} linear model was not significant enough to prove relevant.

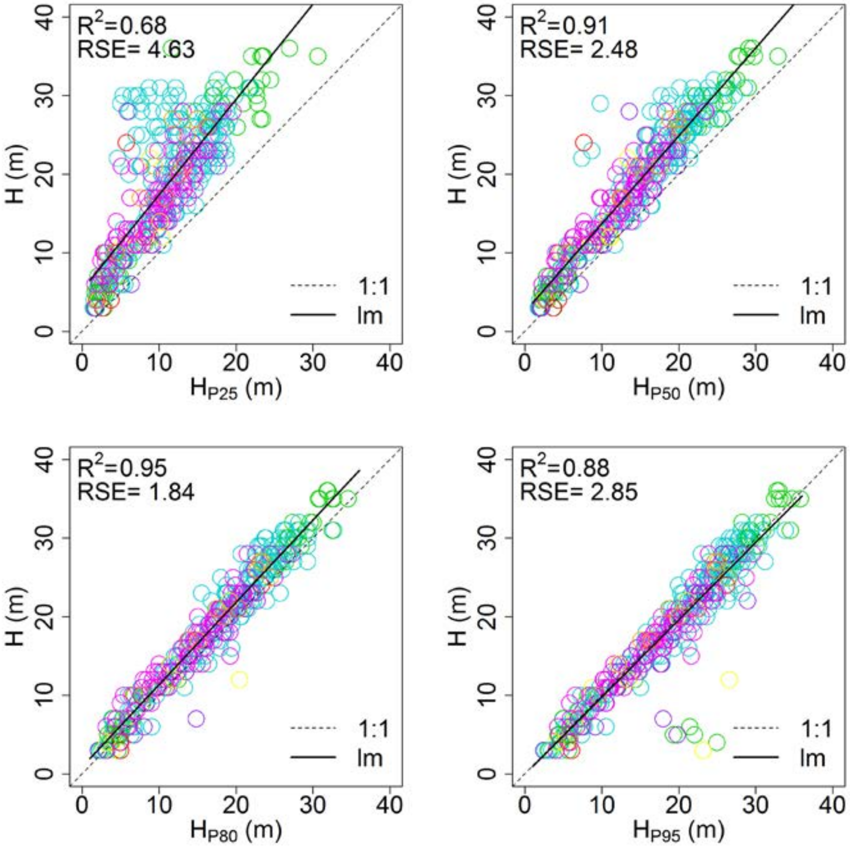

Figure 5. Relationships of different height percentiles (H_{P25}, H_{P50}, H_{P80}, H_{P95}) with the forest height estimate (H) in Laeva sample plots. Different colours represent different dominating tree species and the linear model (lm) parameters are given in Table 3.

Table 3. Regression model (3) parameters (*a*, *b*) and residual standard errors (RSE) using different height percentiles for forest height. The parameter values in italics are statistically insignificant.

Test site	Percentile	*a*	*b*	RSE	R^2
Laeva	H_{P25}	1.21	*5.26*	4.63	0.68
	H_{P50}	1.12	2.50	2.48	0.91
	H_{P80}	1.05	*0.89*	1.84	0.95
	H_{P95}	0.98	0.05	2.85	0.88
Aegviidu	H_{P25}	1.05	7.08	4.02	0.57
	H_{P50}	1.03	3.53	2.45	0.84
	H_{P80}	0.95	2.24	1.83	0.91
	H_{P95}	0.90	1.58	1.78	0.92
Aegviidu 46 stands	H_{P80}	1.03	*-0.12*	0.99	0.95

For large inhomogeneous pixels (1×1 km) of the forest landscape, the correlation of H_{ALS} with the forest inventory based height (H_{FI}) and satellite-lidar based height estimation was studied (**III**). The correlation of H_{ALS} with H_{FI} was strong in Aegviidu test site ($R^2 = 0.67$) and Laeva test site ($R^2 = 0.58$) using 1×1 km pixels. The satellite-lidar-based forest height (H_{GVH}) prediction, on the other hand, showed only a weak correlation with both H_{FI} and H_{ALS} in Aegviidu and Laeva test-site ($r < 0.3$; Figure 6, **III**). In contrast to the ICESat based forest height estimation, the InSAR study **IV** showed more promising results for predicting forest height using satellite-based data. The relationship between H_{ALS} and the InSAR coherence magnitude had a RMSE < 0.1 using stand-based plots. In the GVH study **III** it was also shown that biomass has a strong linear correlation with H_{ALS} and H_{FI} which is estimated based on plot or single-tree height.

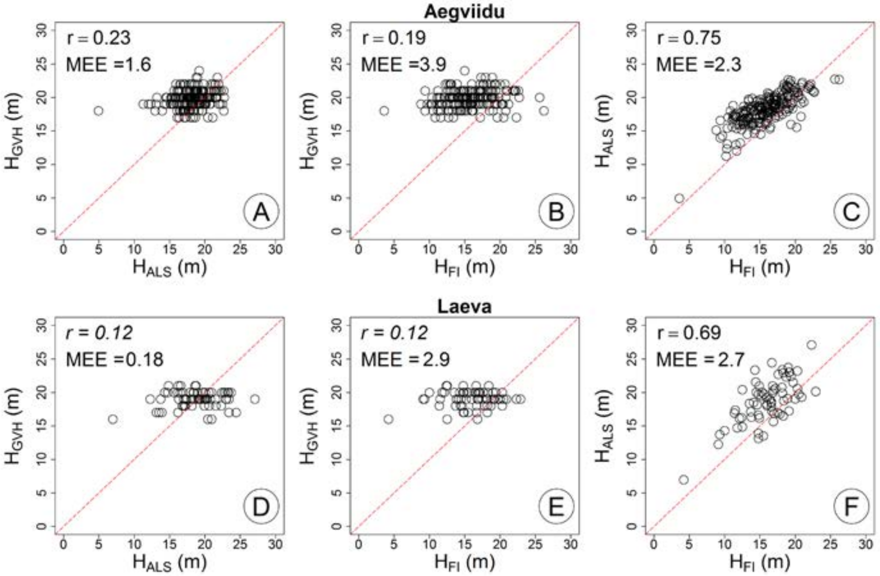

Figure 6. Space-borne lidar-based global vegetation height map values (H_{GVH}) compared to lidar-based prediction H_{ALS} and forest height estimate based on forest inventory data H_{FI} on 50 ha sampling units. MEE is the mean estimate error and r is the coefficient of correlation. Values in italics are statistically insignificant; reworked from Figure 2 in article **III.**

The forest canopy live crown base height $H_{\mathrm{LCB\_ALS}}$ predicted using the model (2) showed a strong linear correlation with the measured live crown base height (H_{LCB}). The coefficient of determination (R^2) was over 0.79 for all different point inclusion minimum height filters tested (**II**) and showed no significant difference for different thresholds. The RSE was 2.2 m in Järvselja test plots and 1.6 m in Aegviidu test plots. Site or area-specific parameters (*a*, *b*; model 2) should be estimated using the model (1).

5.2. Canopy cover

The CC_{ALS} based on the first or first of many echoes ($CC_{\mathrm{ALS,1.3\_1}}$) systematically overestimated the canopy cover estimated using hemispherical images (CC_{DHP}). The $CC_{\mathrm{ALS,1.3\_1}}$ saturated and lost relationship in dense forests with the measured canopy cover over 60% (Figure 7a, **VII**). Whereas including all echoes into the ratio calculation improved the correlation between $CC_{\mathrm{ALS,1.3\_A}}$ and CC_{DHP} with the RMSE, the best case scenario being 12% (Figure 7b, **VII**).

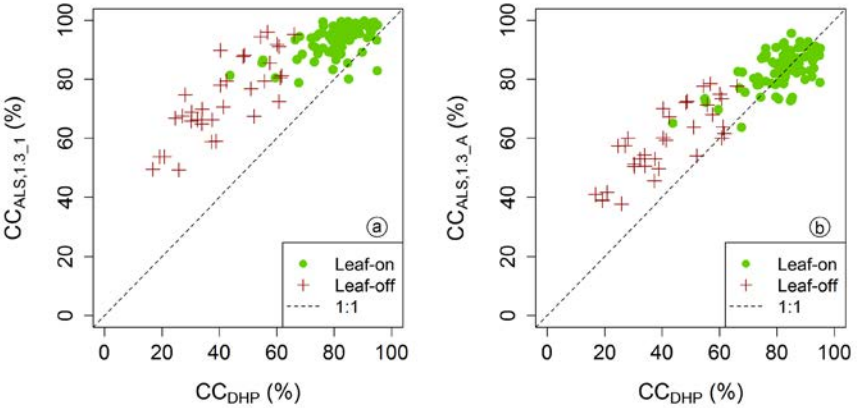

Figure 7. ALS-based canopy cover (CC_{ALS}) compared to the canopy cover estimate (CC_{DHP}) based on digital hemispherical photos using only ALS point cloud first echoes (a) or using all echoes (b), **VII.**

Increasing the threshold up to five metres showed no significant improvement on the correlation between CC_{ALS} and CC_{DHP}, but did systematically decrease the CC_{ALS} values. By raising the threshold up to H_{LCB_ALS} (model 2) no correlation was evident between CC_{ALS} and CC_{DHP} ($R^2 = 0$).

The phenology influence on the CC_{ALS} was substantial. The CC_{ALS} increased on average by 20% from the leaf-off to leaf-on stage in deciduous dominated plots with no known disturbances between the two ALS data acquisitions.

5.3. Standing wood volume and biomass

The model (7) using forest sample plot based lidar point clouds had an RSE of approximately 60 m^3 ha^{-1} in both Aegviidu and Laeva test sites and was even smaller when using the stand-level approach for the 46 Aegviidu stands (RSE = 38.4 m^3 ha^{-1}, Table 4, **V**). The model (7) parameters *a, b, c* and *d* are given in table (4), but should only be applied to similar forests of that region.

Table 4. Parameters for V_{ALS} models based on Aegviidu and Laeva circular sample plots and Aegviidu forest stands (**V**). RSE is the residual standard error; *a*, *b*, *c*, *d* are the model parameters.

Test site	RSE, m^3 ha^{-1}	Parameters							
		a	RSE	b	RSE	c	RSE	d	RSE
Aegviidu	59.8	3.48	0.96	1.55	0.08	9.22	1.76	1.08	0.07
Laeva	69.2	0.58	0.26	1.91	0.12	9.06	1.27	*0.17*	0.12
Aegviidu 46 stands	38.4	*2.1*	1.35	1.71	0.18	*3.99*	4.41	0.91	0.2

*Parameters in italics are statistically insignificant (p>0.05).

Standing wood volume showed systematic differences when compared with field-estimated FI volume (V_{FI}; **II**, **V**, **VII**). There was a systematic lack-of-fit between V_{ALS} and V_{FI} in both Aegviidu and Laeva test-sites using the stand-based approach. The difference is more pronounced in stands with V_{FI} > 250 m^3 ha^{-1} (Figure 8, **V**).

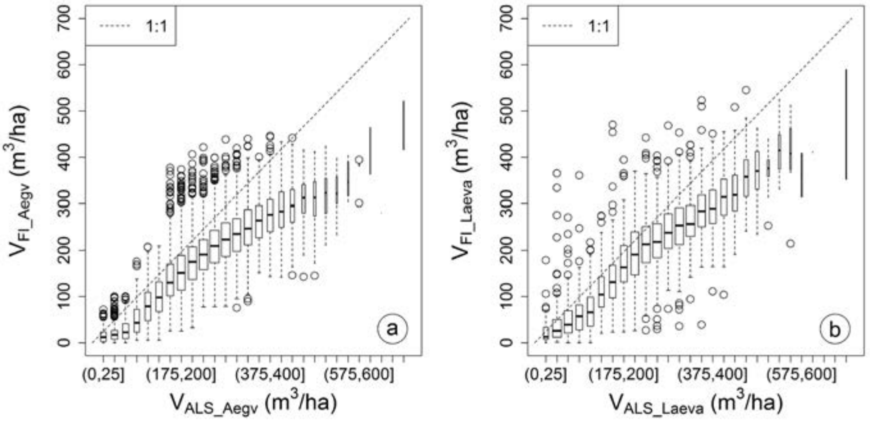

Figure 8. Comparison of ALS-based standing wood volume (V_{ALS}) predictions with FI dataset standing wood volume (V_{FI}) in Aegviidu and Laeva test sites; reworked from Figure 2 in article **V**.

Lidar-based predictions of wood volume can be used to assess the wood volume data available from forest inventory databases. Cross-validation of the V_{ALS} models (7) with models from Laeva applied to Aegviidu and vice versa showed a nonzero in mean estimate error (MEE) and increase in RMSE compared to the site-specific model RMSE. The Laeva model (Table 4) gave an MEE = 47 m^3 ha^{-1} and an RMSE = 92 m^3 ha^{-1} (Figure 9a, **V**) when used in Aegviidu. Similar results (Figure 9b, **V**) were found by applying the Aegviidu model (Table 4) to Laeva test plots and comparing it to the measured standing volume (MEE = -87 m^3 ha^{-1} and RMSE = 128 m^3 ha^{-1}; Figure 9b). The main reason for such a systematic difference is most likely due to the contrasting species compositions and forest types in Aegviidu and Laeva test sites.

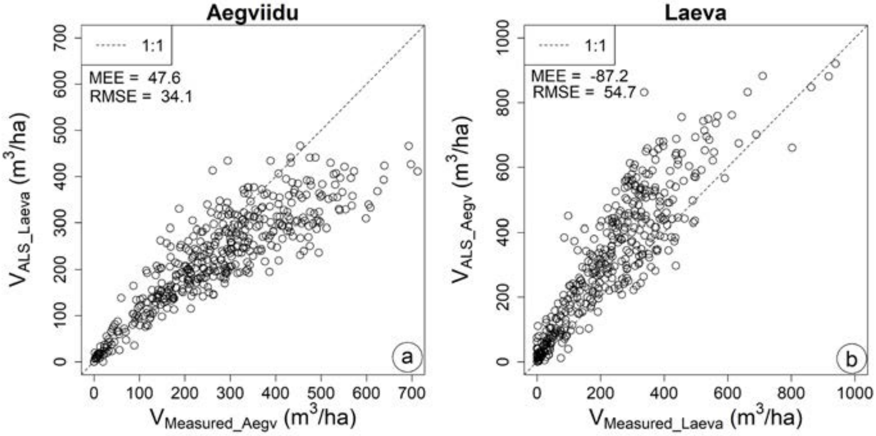

Figure 9. Cross-validation of Aegviidu (a) and Laeva (b) models (V_{ALS_Laeva}, V_{ALS_Aegv}) using the measured standing wood volume from sample plots ($V_{Measured\_Aegv}$, $V_{Measured\_Laeva}$); reworked from Figure 3 in article **V**.

In the satellite-based lidar study (**III**), 1×1 km pixels of biomass predictions were compared to H_{GVH} and H_{ALS}. The biomass was calculated for each of the GVH pixel using FI data and allometric regression models (Repola, 2008; 2009). The predicted biomass was strongly correlated with airborne lidar-based H_{ALS} (RSE of 12 t ha^{-1}, $R^2 = 0.64$; Figure 10, **III**) but when compared to the satellite-based height estimation H_{GVH}, the correlation was weak ($R^2 < 0.15$).

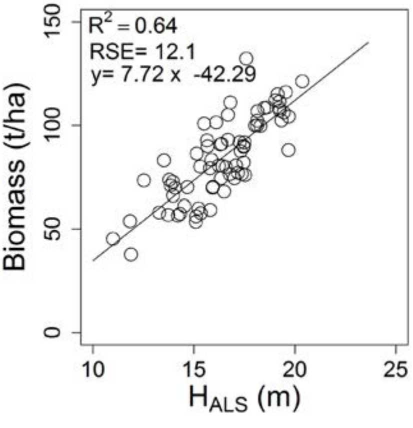

Figure 10. Relationship between the biomass estimate for 1×1 km pixels using Repola (2008; 2009) models with the ALS-based forest stand height estimate H_{ALS}; reworked from Figure 3 in article **III**.

5.4. Change detection and growth monitoring

Forest stand height increment was studied 1) using multitemporal high-density data from EFNRP plots with an eight-year difference in Järvselja and 2) applying regular flight low-density data on stand level using a four-year interval in Aegviidu with both leaf-off and leaf-on data acquisitions. The stand-based ALS point cloud height percentile increment (ΔH_{Px}) was similar for both leaf-off and leaf-on data (~25 cm year^{-1}), with small effects of phenology causing differences in the leaf-off data (**VIII**). The ΔH_{Px} showed no significant difference when compared for thinned and unthinned stands; instead the ΔH_{Px} was more dependent on phenological differences and on the time of flight in relation to the thinning year (T_{year}) (**VIII**). The ΔH_{Px} was systematically higher for stands thinned near the second data acquisition and this applied similarly to both leaf-off and leaf-on data (Figure 11 a, c). However, the results were influenced by the applied filters of minimum height. The ΔH_{Px} decreased significantly in a similar test using ALS data with no minimum height filters for the percentile calculations (Figure 11 b, d).

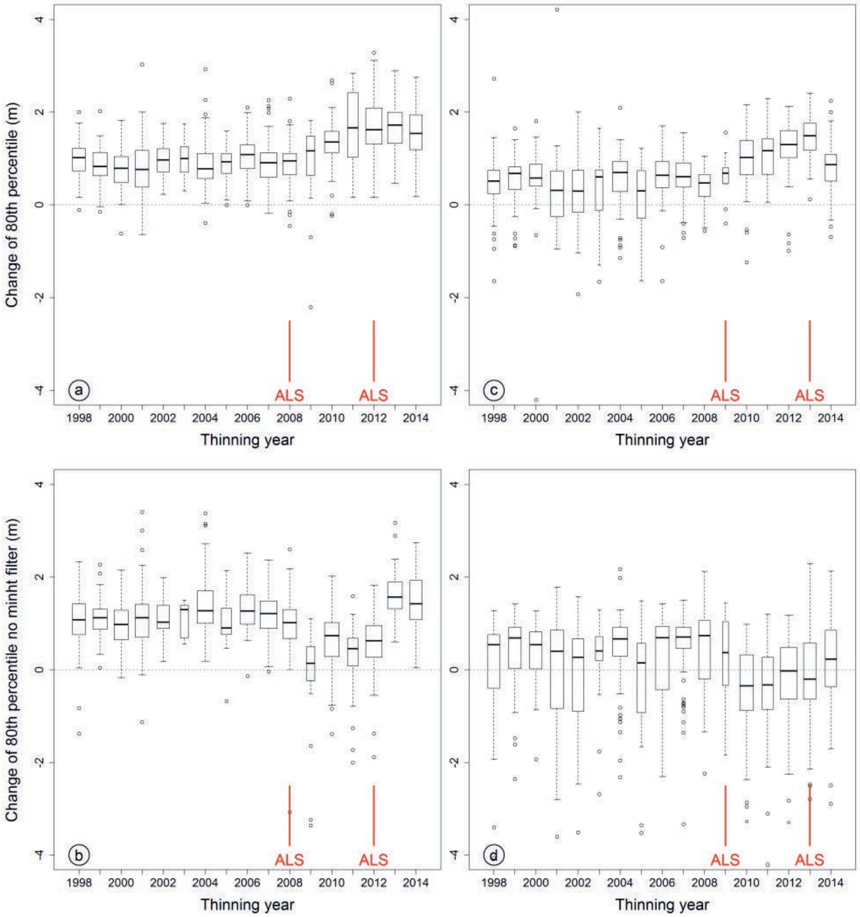

Figure 11. The change in the 80th percentile of point cloud height distribution using leaf-on data as a function of the thinning year: a) ground points excluded, b) all points included. Leaf-off data: c) ground points excluded, d) all points included; **VIII**.

The ΔH_{Px} was greater in younger forests and smaller in older forests (Figure 12; **VI**, **VIII**). The mean increment of H_{P80} using leaf-on data in the reference stands was 0.96 m for four years (RSE = 0.02 m, *p*-value < 0.01). The increment of H_{P80} in thinned stands was slightly greater (1.19 m; RSE = 0.06 m), which is most likely due to the better soil fertility (H_{100}) in thinned stands compared to the reference stands as appeared from forest inventory data. The ΔH_{Px} was also compared to the measured height increment on ENFRP sample plots and predicted height increment. The ΔH_{Px} showed systematically greater values compared to both (**VI**).

Disturbance detection was studied in Aegviidu test site using the data of commercial thinnings from the state forests and bi-temporal ALS data sets from the leaf-off and leaf-on season with a four-year difference. The commercial thinnings did not decrease the different point cloud height percentiles (Figure 13i to 13l) and other point cloud height metrics (mode, kurtosis, skewness and CRR). Instead, the thinnings significantly decreased CC_{ALS} in both leaf-on (Figure 13b, c) and leaf-off data (Figure 13f, g). CC_{ALS} decreased in stands thinned between the two ALS on average in the same range for both leaf-on (20.7%, interquartile range 15.4…25.1%) and leaf-off (21.5%, interquartile range 16.3…26.9%) data. For comparison, the thinning simulation showed a similar 22% average decrease in CC ($6\% \leq \mathrm{CC} \leq 37\%$; **VIII**).

The set of unthinned reference stands after filtering the clear-cuts and very young forests showed smaller CC changes compared to thinned stands. The difference over the four years using leaf-on data was insignificant (mean difference 0.4%) and the *t*-test showed no difference (*p*-value > 0.05). For leaf-off data the mean difference was larger (2%) and the systematic decrease was statistically significant. The decrease in CC_{ALS} compared for ALS_{2009} and ALS_{2013} is explained by the small differences in phenology for leaf-off data acquisition (**VIII**).

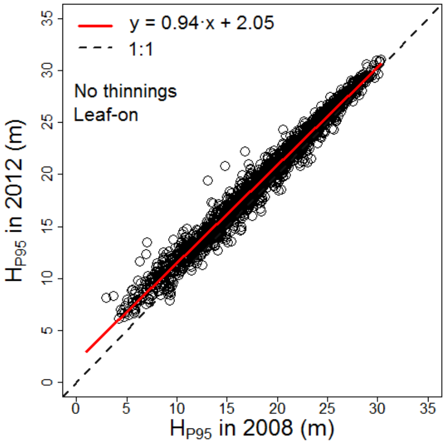

Figure 12. ALS point cloud height distribution percentile H_{p95} from 2008 and 2012 measurements in stands with no thinnings between the two ALS measurements; **VIII**.

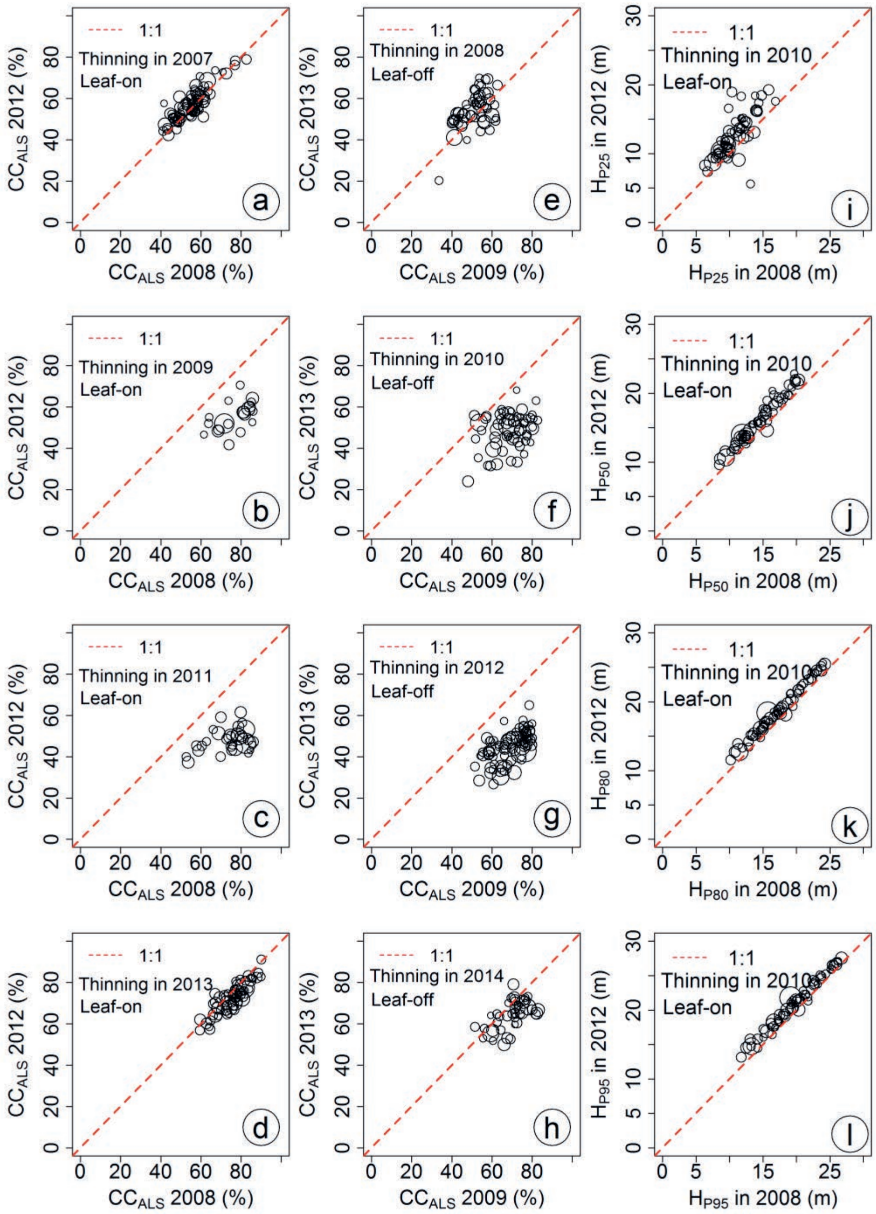

Figure 13. ALS-based canopy cover (*CC_{ALS}*) change over four years with thinnings carried out before, between and after the ALS measurements using leaf-on and leaf-off data. The symbols are scaled to indicate stand size; reworked from Figure 1 in manuscript **VIII**.

6. DISCUSSION

Estonia is currently one of the few countries to have freely available multitemporal airborne laser scanning (ALS) data covering the whole country. This allows developing methods for utilising ALS data for assessing forest mensuration data, monitoring changes in forest structure, tracking forest growth and increasing the precision of collected forest inventory data. The target group for different forest inventory variable maps are commonly large forest companies and national resource monitoring institutions; however, any forest manager with the skills of using GIS can benefit from the ALS-based predictions and estimates of forest inventory variables. On the other hand, field visits can be better utilised in forests where decision-making depends substantially on in situ observations. This information allows companies to make better forest management decisions and decrease the cost for manual labour needed to gather necessary data. For example the whole budget for a four-year wall-to-wall ALS data coverage cost at 1 p m^{-2} is around 450 000€ (Kirsimäe, 2020). For model development we would need around 100 permanent plots per year, with the cost of 200€ per plot, coming up to 80 000€ for a four-year period. With this in mind, the cost of basic forest inventory maps comes to around 15 cents per hectare.

These nation-wide maps of forest parameters could be of great value for forest management planning and inventories. Sample plot data could be obtained from already existing National Forest Inventories (NFI). Such remote sensing and NFI combination has already been widely applied in other countries (McRoberts & Tomppo, 2007) and with the persistent development in remote sensing applications has led to the question of "when, and not if" such data will be incorporated similarly in the Estonian NFI for constructing forest inventory variable maps.

The most basic and common forest structure variable predicted from ALS data is forest height. The method for forest height prediction using ALS data has been the percentile method, first calculating the distributions of the ALS point clouds from above-ground vegetation point clouds (Næsset, 1997a). These point clouds are commonly extracted representing either polygons of forest parcels or stands, or in other cases the extent of point clouds is determined by raster-based pixels, a common unit in remote sensing methods.

This study, similarly to the studies from other researchers (Goodwin et al., 2006; Noordermeer et al., 2019), showed that very strong correlation between forest height and any of the point cloud higher percentiles ($H_{\mathrm{Px}} | x > 75$) exist in the sparse Estonian ALS dataset. The higher percentiles showed strong relationships on a small-scale circular plot basis with radiuses up to 30 m, and also when using large (>1 ha) stand-level point clouds or even as large as 1 km pixels.

For applications using low-density ALS data (<1 p m^{-2}), the recommended and most stable predictor according to our results was the 80th height percentile (**I**, **III**, **VI**) and the results were in similar confidence levels as in other studies (Trier et al., 2018). Similar correlations were shown using any of the higher percentiles ($H_{\mathrm{Px}} | x > 90$), but with low-density ALS data the higher percentiles may cause problems in height prediction. For example, the prediction would be based on a smaller amount of ALS echoes, resulting in large randomness. This would be more pronounced as the footprint of a laser pulse at flying altitudes over 2000 m are quite large (>0.5 m in diameter). Emitted laser pulse return positions are calculated using airplane coordinates and position (X, Y, Z, tilt, roll, and yaw), scan angle and measured time of between emission and reception of signal. Airplane coordinates and position is measured but not fixed on repeated flights. Therefore the positions of echoes from forest canopy vary with each flight and point cloud statistics contain a random component. Also taking into consideration the diameter of the topmost shoot and the amount of reflecting material at the tree top, most likely we will never have a signal return from the topmost branches or treetops. The lack of echoes is most crucial for small parcels and plots or when using the pixel-based approaches with a common pixel size being < 20 m in the case of sparse ALS data. Such large randomness must be especially taken into account when developing applications based on bi-temporal data. For example – for a 10 m size pixel, the average echo count using the Estonian Land Board leaf-on ALS data would be around 30 points per pixel (data from missions in 2008–2016). Using the 90th percentile for forest height assessment would mean that the prediction would be defined by only the three topmost echoes. For stand-level approach, the amount of echoes is larger, but in the stands that are not homogeneous or, for example, consist of only a few higher retention trees we can expect a positive error in height prediction. This error is likely to happen in clear-cut stands where the exclusion of near-to-ground points from the point cloud would result in only having echoes from seed trees. The height percentiles will decrease after the young saplings have grown over the minimum height threshold used in the percentile calculations. The solution would be to use a pixel-based approach or lower height percentiles, but the lower percentiles ($H_{Px}|x<75$) also have weaker correlations with measured forest heights.

The ALS echo height distributions and point cloud distribution metrics also are able to predict the density of the understory (Campbell et al., 2018; Venier et al., 2019) and determine the live crown base height (**II**). These metrics are a valuable input for biodiversity assessment or for future development of management planning, for example thinnings. If we estimate the mean crown length through stand height and live crown base height, we have an indication of the stand density. This could then be possibly used for determining the thinning necessity, following the logic that the crowns remain longer when there is enough light and space between trees and vice versa, and shorter with less light and more competition between individual trees. Unpublished results (Kõks, 2018) have also shown the point cloud height mode (H_{Mode}) value to be a valuable predictor for determining the necessity of thinnings.

But all in all, with large confidence, one can say that forest height can be directly predicted or even measured from ALS data. This has led to the development of applications that are based on forest height being a predictor for other variables. Using the forest height alongside other variables, the most common estimated by-products are above-ground biomass (Lang et al., 2016; **III**), the standing wood volume (**I**; **V**), or even explaining forest albedo (Hovi et al., 2019). With the availability of bi-temporal data, forest height maps could be used for change detection (Nijland et al., 2015; **VI**; **VIII**). Height metric increment has also been shown to be a valuable input for forest site index prediction (Noordermeer et al., 2020). Although our study (**VIII)** showed that the stand-based ALS point cloud height percentiles were not suitable indicators for detecting weak disturbance (<20% canopy cover loss), in contrary to a study by Niljand et al. (2015), we did conclude that the height percentile increment ΔH_{Px} was somewhat influenced by the time passed from thinning. This applied to both leaf-off and leaf-on ALS data (**VIII**).

Therefore, for small-scale disturbances such as thinnings, instead, the ALS-based canopy cover estimate (CC_{ALS}) should be used. Our study using bi-temporal low-density ALS data confirmed a significant (>20 %) difference for stands thinned in between a four-year period of ALS data acquisition. For practical applications, such bi-temporal CC_{ALS} maps can be used for thinning detection alongside a forest database and the notice system of thinnings. The thinning detection could be potentially used in NFI for a better overview of management. The limit to such thinning detection would be the uncertainty of the CC_{ALS}. In the study (**VII)**, it was concluded that the error of CC_{ALS} for dense forests with a large canopy cover compared to field-measured DHP-based CC proxy was 10–15% in CC units. The error would be even larger, if the ALS data was acquired from different phenological periods (**VIII**). For such reasons, the leaf-on ALS data would be more suitable for change monitoring, as it excludes errors and differences caused by phenological differences. Additional problems might be caused by differences in scanner and flight settings, although as was shown by Keränen et al. (2016), the flight settings had a small impact on calculated metrics. At the same time, scan angle dependence on CC_{ALS} was shown by Korhonen et al. (2011). The study **VII** showed no significant differences between CC_{ALS} values obtained from point clouds with opposing scan angles, when using all-echoes included methods. Even after scan angle correction the dispersion between two opposition side CCALS proxies remained. This is most likely caused also by the dependence on the neighbouring pixels, which due to large scan angles have more influence on the actual point cloud of interest.

The combination of forest height and density is the basis for calculating the standing wood volume. Similarly to the in situ models of basal area, diameter and height (Krigul, 1972), ALS-based estimations are commonly the results of CC_{ALS} combination with H_{Px}. The study **V** showed a systematic difference for standing wood volume estimated from regular field work carried out by qualified field experts and estimated from ALS data on a stand-level basis. The plot-based estimations also showed a systematic difference between coniferous and deciduous tree species. The difference is most likely due to the weak correlation between basal area and canopy cover in dense forests with canopy covers over 80%. As airborne laser scanners are not able to directly see the tree stems, therefore we are also not able to measure tree diameter. In this case, the best indicator for a forest density variable, which carries similar information as basal area, is CC_{ALS}. Another option would be single-tree detection, but with today's country-wide sparse ALS data possibilities, this is not an applicable method. With methods developed for single-tree detection, combined with precise height estimations and allometric height-to-diameter models, standing wood volume precise estimations are possible. For now, this is commonly used in drone-based studies on small areas, but for state-level estimations and mapping such methods are not viable yet. The greatest limitation to drone-based and high-density ALS data is the flight time limitation for drones; additional limitations are related to instabilities due to flying conditions (Wallace et al., 2011), causing errors in positioning.

Standing wood volume is also the variable for direct measurement of carbon stock. With more and more forest management and policy-making being directed by the carbon monitoring and marketing, the demand for frequently updated, accurate and precise inventory data will grow even more in the near future. Therefore, the development of high-density ALS application is necessary, even though the practical perspectives from the economical point of view for large areas is limited.

7. CONCLUSIONS

Based on the results of this thesis, the following conclusions were drawn:

1. H_{P80} showed strong correlations with the measured plot-based and stand-based H. The fitted linear models for H_{ALS} were not significantly influenced by species distribution when using leaf-on ALS data. A weak influence was shown for lower height percentiles, most likely due to different species having different height distributions and crown shapes. Species-specific models for deciduous and coniferous trees would be required for leaf-off ALS data because of the phenological differences in deciduous forests during spring and summer.

2. Live crown base height (H_{LCB}) showed a strong correlation with the model (2) based on the ALS point cloud height distribution mode (H_{Mode}).

3. The ALS-based canopy cover (CC_{ALS}) estimate saturates at values >80% in hemi-boreal dense deciduous forests using the first or first of many echoes. The increase in the threshold for the CC_{ALS} estimate had no significant influence on improving the results. Such saturation was not observed when using all echoes above the threshold and at a 1.3 m threshold. This method showed an RMSE of 11% when CC_{ALS} was compared to the CC estimation (CC_{DHP}) based on digital hemispherical photos.

4. ALS-based standing wood volume (V_{ALS}) had a strong linear correlation with the measured wood volume V using the model (3) based on H_{P80}, H_{P25} and CC_{ALS}. V_{ALS} was at best estimated with an RSE < 40 $m^3 ha^{-1}$ when applied on large (>1 ha) stand-based polygons. The smaller, plot-based (diameter <30 m) approach had a slightly larger RSE of 60 $m^3 ha^{-1}$. V_{ALS} was also systematically greater compared to the forest inventory based wood volume (V_{FI}). The difference between V_{FI} and V_{ALS} increased exponentially at larger values (V_{ALS} >250 $m^3 ha^{-1}$).

5. V_{ALS} models showed systematic differences when cross-validated between broad-leaved deciduous forests and coniferous evergreen

forests, therefore species-specific models would be required to reduce systematic errors.

6. Forest inventory data based biomass estimations with a 1×1 km resolution showed strong linear correlation with ALS-based H_{P80} when using sparse ALS data (<0.5 p m^{-2}).

7. CC_{ALS} showed a strong response to small-scale forest disturbances (thinnings) using multitemporal ALS measurements over a four-year difference. The ALS point cloud height metrics showed no response to the disturbances.

8. The satellite-based lidar measurements showed weak correlations with ALS-based height measurements when compared over a 1×1 km pixel provided by the ICESat mission. Stronger correlations were found when ALS-based height estimations were compared with TanDEM-X based coherence measurements, showing promising results for future biomass and height estimations using radar missions.

REFERENCES

Adermann, V. 2010. Estonia – Country report. In: E. Tomppo et al., (Ed.), National Forest Inventories: Pathways for Common Reporting, 171−184.

Anderson, K., Hancock, S., Disney, M., Gaston, K.J. 2015. Is waveform worth it? A comparison of LiDAR approaches for vegetation and landscape characterization. Remote Sensing in Ecology and Conservation, 2(1): 5–15.

Anniste, J., Viilup, Ü. 2011. Determination of forest characteristics with the laser scanning. Artiklid ja uurimused, 10: 38–53. Luua Forestry School. (In Estonian with English summary).

Bottalico, F., Chirici, G., Giannini, R., Mele, S., Mura, M., Puxeddu, M., McRoberts, R., Valbuena, R. and Travaglini, D. 2017. Modeling Mediterranean forest structure using airborne laser scanning data. International Journal of Applied Earth Observations and Geoinformation, 57: 145–153.

Campbell, M.J., Dennison, P.E., Hudak, A.T., Parham, L.M., Butler, B.W. 2018. Quantifying understory vegetation density using small-footprint airborne lidar. Remote Sensing of Environment, 215: 330–342.

Chen, W., Hu, X., Chen, W., Hong, Y., Yang, M. 2018. Airborne LiDAR remote sensing for individual tree forest inventory using trunk detection-aided mean shift clustering techniques. Remote Sensing, 10: 1078.

Ene, L.T., Næsset, E., Gobakken, T., Bollandsås, O.M., Mauya, E.W., Zahabu, E. 2017. Large-scale estimation of change in aboveground biomass in miombo woodlands using airborne laser scanning and national forest inventory data. Remote Sensing of Environment, 188: 106–117.

Eysn, L., Hollaus, M., Lindberg, E., Berger, F., Monnet, J.-M., Dalponte, M., Kobal, M., Pellegrini, M., Lingua, E., Mongus, D., Pfeifer, N. 2015. A benchmark of lidar-based single tree detection methods using heterogeneous forest data from the Alpine space. Forests, 6(5): 1721–1747.

Faraway, J. J. 2005. Linear models with R (pp. 25–26). Florida: Chapman & Hall/CRC.

Ferraz, A., Saatchi, S., Mallet, C., Meyer, V. 2016. Lidar detection of individual tree size in tropical forests. Remote Sensing of Environment, 183: 318–333.

Fox, J., Weisberg, S. 2011. An R companion to applied regression (p. 163). California: SAGE Publications.

Gatziolis, D., Andersen, H.-E. 2008. A guide to LIDAR data acquisition and processing for the forests of the Pacific Northwest. United States Department of Agriculture Forest Service Pacific Northwest Research Station.

Goodwin, N.R., Coops, N.C., Culvenor, D.S. 2006. Assessment of forest structure with airborne LiDAR and the effects of platform altitude. Remote Sensing of Environment, 103: 140–152.

Guo, X., Coops, N.C., Tompalski, P., Nielsen, S.E., Bater, C.W., Stadt, J.J. 2017. Regional mapping of vegetation structure for biodiversity monitoring using airborne lidar data. Ecological Informatics, 38: 50–61.

Hagolle, O., Lobo, A., Maisongrande, P., Cabot, F., Duchemin, B. and De Pereyra, A. 2005. Quality assessment and improvement of temporally composited products of remotely sensed imagery by combination of VEGETATION 1 and 2 images. Remote Sensing of Environment, 94: 172–186.

Holmgren, J., Persson, Å., Söderman, U. 2008. Species identification of individual trees by combining high resolution LiDAR data with multi-spectral images. International Journal of Remote Sensing, 29(5): 1537–1552.

Hopkinson, C., Chasmer, L., Lim, K., Treitz, P., Creed, I. 2006. Towards a universal lidar canopy height indicator. Canadian Journal of Remote Sensing, 32: 139–152.

Hovi, A., Lindberg, E., Lang, M., Arumäe, T., Peuhkurinen, J., Sirparanta, S., Pyankov, S., Rautiainen, M. 2019. Seasonal dynamics of albedo across European boreal forests: analysis of MODIS albedo and structural metrics from airborne LiDAR. Remote Sensing of Environment, 224: 365–381.

Howard, J.A. 1991. Remote sensing of forest resources. Chapman & Hall. London. 420 pp.

Isenburg, M. 2017. LAStools – efficient LiDAR processing software. [WWW document]. – URL http://rapidlasso.com/LAStools [Downloaded on 17 October 2017, unlicensed].

Kandare, K., Dalponte, M., Ørka, H.O., Frizzera, L., Næsset, E. 2017. Prediction of species-specific volume using different inventory approaches by fusing airborne laser scanning and hyperspectral data. Remote Sensing, 9, 400, 19 pp.

Keränen, J., Maltamo, M., Packalen, P. 2016. Effect of flying altitude, scanning angle and scanning mode on the accuracy of ALS based forest inventory. International Journal of Applied Earth Observation and Geoninformation, 52: 349–360.

Keskkonnaagentuur. 2017. Yearbook forest 2016. Keskkonnaagentuur, Tallinn. 293 p.

Kirsimäe, P. 2020. Personal communication, 23.03.2020.

Kiviste, A., Hordo, M., Kangur, A., Kardakov, A., Laarmann, D., Lilleleht, A., Metslaid, S., Sims, A., Korjus, H. 2015. Monitoring and modeling of forest ecosystems: the Estonian Network of Forest Research Plots. Forestry Studies, 62: 26–38.

Korhonen, L., Korhonen, K.T., Rautiainen, M., Stenberg, P. 2006. Estimation of forest canopy cover: a comparison of field measurement technique. Silva Fennica, 40(4): 577–588.

Korhonen, L., Korpela, I., Heiskanen, J., Maltamo, M. 2011. Airborne discrete-return LIDAR data in the estimation of vertical canopy cover, angular canopy closure and leaf area index. Remote Sensing of Environment, 115: 1065–1080.

Korjus, H. 1999. Hooldusraiete mudelitest. [Models for forest thinning planning]. Transactions of the Faculty of Forestry, Estonian Agriculture University, 32: 44–49.

Kotivuori, E., Korhonen, L., Packalen, P. 2016. Nationwide airborne laser scanning based models for volume, biomass and dominant height in Finland. Silva Fennica 50, 1567, 28 p.

Krabill, W.B., Collins, J.G., Swift, R.N., Butler, M.L. 1980. Airborne laser topographic mapping results from Initial Joint NASA/U.S. Army Corps of Engineers Experiment, NASA Technical Memorandum 73287, Wallops Flight Center, Wallops Island, VA, p. 33.

Krigul, T. 1972. Metsatakseerimine. (Forest mensuration). Valgus, Tallinn. 358 pp. (In Estonian).

Kuusk, A., Lang, M., Kuusk, J. 2013. Database of optical and structural data for the validation of forest radiative transfer models. Light scattering reviews, 7: 109–148. Berlin, Heidelberg: Springer.

Köhl, M., Magnussen, S.S., Marchetti, M. 2006. Sampling methods, remote sensing and GIS multiresource forest inventory. Springer-Verlag, Berlin. 373 pp.

Kõks, M. 2018. Harvendusraie vajaduse hindamine aerolidari andmetelt Laeva katsealal. (Estimation of thinning necessity in Laeva test site using airborne laser scanning data). Eesti Maaülikool, Master's thesis. 43 pp. (in Estonian).

Lang, M. 2010. Estimation of crown and canopy cover from airborne lidar data. Forestry Studies, 52: 5–17.

Lang, M., Kaha, M., Laarmann, D., Sims, A. 2018. Construction of tree species composition map of Estonia using multispectral satellite images, soil map and a random forest algorithm. Forestry Studies, 68: 5–24.

Lang, M., Kodar, A., Arumäe, T. 2013. Restoration of above canopy reference hemispherical image from below canopy measurements for plant area index estimation in forests. Forestry Studies, 59: 13–27.

Lang, M., Kurvits, V. 2007. Restoration of tree crown shape for canopy cover estimation. Forestry Studies, 46: 23–34.

Lang, M., Lilleleht, A., Neumann, M., Bronisz, K., Rolim, S.G., Seedre, M., Uri, V., Kiviste, A. 2016. Estimation of above-ground biomass in forest stands from regression on their basal area and height. Forestry Studies, 64: 70–92.

Large, A.R.G., Heritage, G.L. 2009. Laser scanning – evolution of the discipline. In Laser scanning for the environmental sciences, editors Heritage,G.L., Large, A.R.G: 1–20. Chichester, West Sussex, John Wiley & Sons Ltd.

Leica. 2007. Leica ALS50-II. Airborne laser scanner product specification. Heerburg, Switzerland, Leica Geosystems AG. 12pp.

Lõhmus, E. 2004. Estonian habitation types. Eesti Loodusfoto, Tartu. 80 pp. (In Estonian).

Maa-amet. 2018. Aerolaserskaneerimise kõrguspunktid. [Aerial laserscanning heightpoints]. https://geoportaal.maaamet.ee/est/Andmed-ja-kaardid/Topograafilised-andmed/Korgusandmed/Aerolaserskaneerimise-korguspunktid-p499.html (Accessed on 25.07.2018)

Mallet, C., Bretar, F. 2009. Full-waveform topographic lidar: State-of-the-art. ISPRS Journal of Photogrammetry and Remote Sensing, 64: 1–16.

McGaughey, R.J. 2014. FUSION/LDV: Software for LIDAR data analysis and visualization. March 2014 – FUSION, Version 3.42. United States Department of Agriculture Forest Service Pacific Northwest Research Station.

McRoberts, R.E., Tomppo, E.O. 2007. Remote sensing support for national forest inventories. Remote Sensing of Environment, 110(4): 412–419.

Metsa korraldamise juhend. 2009. Forest management rules. https://www.riigiteataja.ee/akt/124112015006 (Accessed on 30.07.2018).

Müller, J., Vierling, K. 2014. Assessing biodiversity by airborne laser scanning. Dordrecht, Springer, pp. 357–374.

Morsdorf, F., Kötz, B., Meier, E., Itten, K.I., Allgöwer, B. 2006. Estimation of LAI and fractional cover from small footprint airborne laser scanning data based on gap fraction. Remote Sensing of Environment, 104: 50–61.

Nagendra, H. 2001. Using remote sensing to assess biodiversity. International Journal of Remote Sensing, 22(12): 2377–2400.

Næsset, E. 1997a. Determination of mean tree height of forest stands using airborne laser scanner data. ISPRS Journal of Photogrammetry & Remote Sensing, 52: 49–56.

Næsset, E. 1997b. Estimating timber volume of forest stands using airborne laser scanner data. Remote Sensing of Environment, 61: 246–253.

Næsset, E., Gobakken, T. 2005. Estimating forest growth using canopy metrics derived from airborne laser scanner data. Remote Sensing of Environment, 9: 453–465.

Nelson, R., Krabill, W., Maclean, G. 1984. Determining forest canopy characteristics using airborne laser data. Remote Sensing of Environment, 15: 201–212.

Nelson, R., Krabill, W., Tonelli, J. 1988a. Estimating forest biomass and volume using airborne laser data. Remote Sensing of Environment, 24: 247–267.

Nelson, R., Swift, R., Krabill, W. 1988b. Using airborne lasers to estimate forest canopy and stand characteristics. Journal of Forestry, 86(10), 31–38.

Nie, S., Wang, C., Zeng, H., Xi, X., Li, G. 2017. Above-ground biomass estimation using airborne discrete-return and full-waveform LiDAR data in a coniferous forest. Ecological Indicators, 78: 221–228.

Nijland, W., Coops, N.C., Macdonald, S.E., Nielsen, S.E., Bater, C.W., Stadt, J.J. 2015. Comparing patterns in forest stand structure following variable harvests using airborne laser scanning data. Forest Ecology and Management, 354: 272–280.

Noordermeer, L., Bollandsås, O.M., Ørka, H.O., Næsset, E., Gobakken, T. 2019. Comparing the accuracies of forest attributes predicted from airborne laser scanning and digital aerial photogrammetry in operational forest inventories. Remote Sensing of Environment, 226: 26–37.

Noordermeer, L., Gobakken, T., Næsset, E., Bollandsås, O.M. 2020. Predicting and mapping site index in operational forest inventories using bitemporal airborne laser scanner data. Forest Ecology and Management, 457: 117768.

Noss, R. 1990. Indicators for monitoring biodiversity: a hierarchical approach. Conservation Biology, 4(4): 355–364.

Nyström, M., Holmgren, J., Fransson, J.E.S., Ollson, H. 2014. Detection of windthrow trees using airborne laser scanning. International Journal of Applied Earth Observation and Geoinformation, 30: 21–29.

Pilarska, M., Ostrowski, W., Bakuła, K., Górski, K., Kurczyński, Z. 2016. The potential of light laser scanners developed for unmanned aerial vehicles – the review and accuracy. International Society for Photogrammetry and Remote Sensing, XLII-2/W2: 87–95.

Regulation 2018/481. 2018. Regulation (EU) 2018/841 of the European Parliament and of the council of 30 May 2018 on the inclusion of greenhouse gas emissions and removals from land use, land use change and forestry in the 2030 climate and energy framework, and amending Regulation (EU) No 525/2013 and Decision No 529/2013/EU. [WWW document]. – URL https://eur-lex.europa.eu/eli/reg/2018/841/oj

Repola, J. 2008. Biomass equations for birch in Finland. Silva Fennica, 42: 605–624.

Repola, J. 2009. Biomass Equations for Scots Pine and Norway Spruce in Finland. Silva Fennica, 43: 625–647.

Riegl. 2017. Dual channel waveform processing airborne LiDAR scanning system for high-point density and ultra-wide area mapping: Riegl VQ-1560i datasheet. [WWW document]. – URL http://www.riegl.com/nc/products/airborne-scanning/produktdetail/product/scanner/55/.

Riigiteataja. 2018. Forest Act. [WWW document]. – URL https://www.riigiteataja.ee/en/eli/ee/Riigikogu/act/528062018009/consolide.

Saatchi, S., Marlier, M., Chazdon, R.L., Clark, D.B., Russell, A.E. 2011. Impact of spatial variability of tropical forest structure on radar estimation of aboveground biomass. Remote Sensing of Environment, 115: 2836–2849.

Sankey, T., Donager, J., McVay, J., Sankey, J.B. 2017. UAV lidar and hyperspectral fusion for forest monitoring in the southwestern USA. Remote Sensing of Environment, 195: 30–43.

Shao, G., Shao, G., Gallion, J., Saunders, M.R., Frankenberger, J.R., Fei, S. 2018. Improving Lidar-based aboveground biomass estimation of temperatehardwood forests with varying site productivity. Remote Sensing of Environment 204: 872–882.

Simard, M., Pinto, N., Fisher, J.B., Baccini, A. 2011. Mapping forest canopy height globally with spaceborne lidar. Journal of Geophysical Research, 116.

Simonson, W., Ruiz-Benito, P., Valladares, F., Coomes, D. 2016. Modelling above-ground carbon dynamics using multi-temporal airborne lidar: insight from a Mediterranean woodland. Biogeosciences, 13: 961–973.

Spurr, S.H. 1948. Aerial photographs in forestry. New York, The Ronald Press Company. 340 pp.

Thers, H., Brunbjerg, A.K., Læssøe, T., Ejrnæs, R., Bøcher, P.K., Svenning, J.-C. 2017. Lidar-derived variables as a proxy for fungal species richness and composition in temperate Northern Europe. Remote Sensing of Environment, 200: 102–113.

Trier, Ø.D., Salberg, A.-B., Haarpaintner, J., Aarsten, D., Gobakken, T., Næsset, E. 2018. Multi-sensor forest vegetation height mapping methods for Tanzania. European Journal of Remote Sensing, 51: 587–606.

Törmä, M. 2000. Estimation of tree species proportions of forest stands using laser scanning. International Archives of Photogrammetry and Remote Sensing, 33:1524–1531

Vain, A., Yu, X., Kaasalainen, S., Hyyppä, J. 2010. Correcting airborne laser scanning intensity data for automatic gain control effect. IEEE Geoscience and Remote Sensing Letters, 7 (3): 511−514.

Vauhkonen, J., Tokola, T., Packalén, P., Maltamo, M. 2009. Identification of Scandinavian commercial species of individual trees from airborne laser scanning data using alpha shape metrics. Forest Science, 55(1): 37–47.

Venier, L.A., Swystun, T., Mazerolle, M.J., Kreutzweiser, D.P., Wainio-Keizer, K.L., McIlwrick, K.A., Woods, M.E., Wang, X. 2019. Modelling vegetation understory cover using LiDAR metrics. PLoS ONE, 14(11): e0220096.

Verhoeven, G.J. 2011. Near-infrared aerial crop mark archaeology: from its historical use to current digital implementations. Journal of Archaeological Method and Theory, 19:132–160.

Wallace, L., Lucieer, A., Turner, D., Watson, C. 2011. Error assessment and mitigation for hyper-temporal UAV-borne LiDAR surveys of forest inventory. In Proceedings of the 11th International Conference on LiDAR Applications for Assessing Forest Ecosystems, Tasmania, Australia, 16–20 October 2011; pp. 1–13.

Yu, X., Hyyppä, J., Kukko, A., Maltamo, M., Kaartinen, H. 2006. Change detection techniques for canopy height growth measurements using airborne laser scanner data. Photogrammetric Engineering and Remote Sensing, 72(12):1339–1348.

SUMMARY IN ESTONIAN

PUISTUTE TAKSEERTUNNUSTE HINDAMINE AEROLIDARI MÕÕTMISANDMETE PÕHJAL HEMIBOREAALSETES METSADES

Metsa majandamisotsuste langetamiseks on metsade kohta vaja andmeid, mida on harjumuspäraselt kogunud inimesed ja milleks on tehtud maapealseid mõõtmisi. Välitööde käigus hinnatakse puistu liigilist koosseisu, kõrgust, tagavara ja piiritletakse homogeensed üksused ehk eraldised, mida metsaseadusele tuginedes majandatakse. Üks esimesi kaugseire rakendusi metsanduses oli 1920-ndatel ortofotode kasutuselevõtt (Howard, 1991), mille abil oli metsaeraldiste piiritlemist võimalik teha eeltööna, ilma metsas käimata.

Ortofotode käsitsi töötlemisest järgmine samm on fotode numbriline töötlemine, kasutades digitaalfotodesse salvestatud numbrilisi väärtusi. Peale ortofotode hakati üha enam kasutama satelliidipilte, mille ruumiline lahutusvõime on küll väiksem kui ortofotodel, kuid suurema vaateväljaga on võimalik koguda laiemalt alalt andmeid odavama hinnaga. Satelliitsensorid salvestavad enamjaolt tagasihajunud päikesekiirgust, mis seejärel tõlgendatakse maapealsete mõõtmiste käigus kogutud andmete ja satelliitandmete seoste abil meile harjumuspärasteks tunnusteks – puuliik, metsa kõrgus, tagavara vms.

Kui erinevad spektraalsed mõõtmised pakuvad häid võimalusi metsade kahemõõtmeliseks mõõdistamiseks, siis metsa vertikaalse struktuuri kirjeldamiseks on sobivamad aktiivse kaugseire seadmed. Aktiivsed kaugseiresensorid ei kasuta andmete kogumiseks tagasipeegeldunud päikeseenergiat, vaid seadmed emiteerivad erinevatel lainepikkustel energiat, mille tagasihajumist hiljem registreeritakse. Kasutades vastavalt lähisinfrapunast lainepikkust või mikrolaineala on võimalik teavet koguda ka läbi lehestiku ja kogu metsa vertikaalses ulatuses.

Lähisinfrapunasel lainepikkusel töötavad aerolidarid on viimastel aastakümnetel muutunud peamiseks metsandusliku kaugseire vahendiks, mis võimaldab väga detailselt uurida metsa struktuuri. Eestis on aerolidari andmeid kogutud 2008. aastast ja mõõtmisega tegeleb Maaamet (Maaamet, 2016).

Selle doktoritöö eesmärk on Eesti metsadesse sobivate struktuuri- ja takseertunnuste prognoosimudelite koostamine ja rakenduste väljatöötamine Maa-ameti poolt rutiinselt kogutud aerolidari andmete jaoks. Peamised uuritud tunnused on metsa kõrgus (**I**, **III**, **IV**, **VI**, **VIII**) ja kasvava metsa tagavara (**I**, **V**). Klassikaliste ja enimkasutatavate metsanduslike tunnuste kõrval uuriti ka võimalust hinnata võrastiku alguskõrgust (**II**), biomassi (**III**) ja võrastiku katvust (**VII**, **VIII**) ning fenoloogia mõju katvusele (**VIII**). Lidarilt tuletatud metsa kõrgushinnanguid võrreldi ka satelliitidelt saadud kõrgushinnangutega nii satelliitlidarilt (**III**), kui ka radarkaugseirest (**IV**). Hilisemad uurimused keskendusid juba korduvmõõtmistest saadud andmekihtide võrdlemisele, mille abil uuriti metsade kõrguskasvu hindamist (**VI**, **VIII**) ja häiringute tuvastamise võimalusi harvendusraiete näitel (**VIII**).

Metoodika

Katsealad

Peamised katsealad asusid Aegviidus, Laevas, Soomaal ja Järvseljal. Katsealad kirjeldavad suurt osa Eesti metsade variatsioonist ning esindavad erinevaid metsatüüpe – viljakaid lehtpuu enamusega metsi Laeval kuni palu- ja rabamännikuteni Aegviidus.

Aegviidu 15×15 km katseala rajati aastal 2008 ja uuringute eesmärgiks oli uurida aerolidari andmetelt metsa takseertunnuste hindamise võimalikkust Eestis (Anniste ja Viilup, 2011). Peamised uuritavad takseertunnused olid metsa kõrgus ja kasvava metsa tagavara (**I**, **V**), lisaks otsiti meetodeid harvendusraiete ja kõrguskasvu tuvastamiseks (**VIII**).

Laeva katseala rajati 2013. aastal sarnase põhimõtte järgi nagu Aegviidu katseala (15×15 km ruut). Kahe katseala erinevus oli peamiselt puistute liigilises koosseisus – kui Aegviidu alal olid peamiselt, siis Laeva katsealal domineerisid lehtpuuenamusega puistud. Laeva katseala põhilised tulemused on seotud võrastiku katvuse hinnangu fenoloogiliste erinevuste uurimisega, milleks kasutati kahte erinevat aerolidari andmestikku kevadest ja suvest ning maapeal seniidi suunas tehtud poolsfääripilte (**VII**).

Soomaa ja Järvsela katsealasid kasutati vastavalt tehisavaradari andmete põhjal saadud puistute kõrguse hinnangu valideerimiseks (**IV**) ja võrastiku alguskõrguse mudeli väljatöötamiseks (**II**).

Aerolidari andmed

Aerolidari andmeid (ALS) on Eesti Maa-amet kogunud peamiselt Leica ALS50-II skanneriga (aastatel 2008–2016). Aastast 2016 on Maa-ametil kasutusel uus laserskanner Riegl VQ-1560i, mida Järvselja katsealal (**VI**) kasutati kõrguskasvu hindamiseks. Mõlemad Maa-ameti skannerid töötavad lähisinfrapunase spektri piirkonnas (1064 nm), kuid nende suurim erinevus on registreeritavate peegelduste minimaalne vahekaugus ja seeläbi ka kogutavate andmete punktitihedus - Riegl VQ-1560i skanneril on sama lennukõrguse juures pea neli korda tihedam andmestik, kui Leica ALS50-II skanneril. ALSi andmetöötluseks kasutati põhiliselt FUSIONi vabavara (McGaughey, 2014) ja LAStoolsi (Isenburg, 2017).

Tulemused

Elusvõra ja metsa kõrgus

Aegviidu ja Laeva katsealal andis tugevaima korrelatsiooni proovitükil mõõdetud metsa kõrguse ja aerolidarilt arvutatud punktipilve 80-protsentiili seos ($R^2 > 0{,}9$). Punktipilvedest eemaldati enne analüüsi maapinnalähedased peegeldused kuni 1,3 m kõrguseni. Kõrgemate protsentiilide ($H_{\mathrm{Px}}|\mathrm{x} > 90$) puhul oli seose tugevus küll ligilähedane, kuid üksikute kõrgemate puudega eraldistel tekkis kõrguse ülehindamine ja suurenes hinnangu juhuslik viga, kuna põhines vähemal arvul peegeldustel (**I**, **III**, **IV**, **VI**, **VIII**).

Elusvõra alguskõrguse hindamiseks aerolidari andmetelt osutus kõige paremaks punktipilve meetrikuks moodväärtus (H_{Mode}), kus sarnaselt kõrgusarvutusteks on eemaldatud maapinnalähedased peegeldused kuni 1,3 m kõrguseni. See väldib kõrgusjaotuse bimodaalsust ja moodväärtuse maapinnalähedast kõrgust. Elusvõra alguskõrguse ja moodväärtuse lineaarne seos oli tugev, mudeli $R^2 = 0{,}8$ (**II**), kuid igale uuele lennualale ja regioonile oleks soovitav lähendada uued mudeli parameetrid (**VIII**).

Aerolidari (H_{ALS}) ja satelliitlidari andmetel põhinevate metsakõrguse hinnangu (H_{GVH}) uurimuse tulemusel selgus, et H_{GVH} 50 ha pikslitele oli nõrgas seoses nii metsaregistris oleva metsa kõrgushinnangu (H_{FI}) kui ka aerolidarilt hinnatud metsa kõrgusega. Peamiseks põhjuseks võib pidada nii suure ala heterogeensust (**III**). Palju tugevamaid seoseid ALS andmete põhjal prognoositud metsa kõrguse ja satelliitidelt saadud kõrgushinnangute vahel saadi interferomeetrilise SARi andmeid kasutades (**IV**), kus vaatlusühik on 30 meetrine piksel.

Võrastiku katvus

Võrastiku katvuse hindamiseks katsetati erinevaid väljavõtteid punktipilvedest – kasutati kõiki või ainult esimesi aerolidari peegeldusi ning varieeriti katvuse arvutamiseks kasutatud nivood. Kõige tugevamad seosed poolsfääripiltidelt mõõdetud katvuse ja aerolidarilt hinnatud katvuse vahel andis kõiki peegeldusi kaasav katvushinnang 1,3 meetri kõrgusel nivool. Esimeste peegelduste kasutamine sarnaselt teiste Põhjamaade uurimustega küllastas katvushinnangu ning Eesti tihedamatesse metsadesse ei sobinud. Nivoo varieerimine ja tõstmine kuni 10 meetrini ei parandanud olulisel määral katvushinnangute seose tugevust (**VII**). Fenoloogia mõju lehtpuuenamusega puistutes aerolidari andmetelt arvutatud katvushinnangutele oli statistiliselt oluline – kevadised katvushinnangud olid keskmiselt 20% madalamad kui samadel proovitükkidel suvel (**VII**).

Kasvava metsa tagavara ja biomass

Aegviidu katseala proovitükkide alusel töötati välja Eestisse sobiv aerolidari andmetel põhinev mahumudel, mille sisendparameetrid on metsa kõrgusega tugevas seoses olev punktipilve 80-protsentiil, teise rinde infot sisaldav 25-protsentiil ja 1,3 meetrise nivoo pealt arvutatud punktipilve katvus (**I**). Mudeli ristvalideerimisel ja rakendamisel teise enamuspuuliigiga metsadele Laeva katsealal selgus, et lehtpuu ja okaspuu enamusega metsades käitub mudel süstemaatiliselt erinevalt, mistõttu mudelite rakendamisel tuleks igale piirkonnale ja puuliigile lähendada mudeli (7) järgi uued parameetrid (**V**). Väikeste ringproovitükkide korral andis mudel parimal juhul umbes 60 m^3 ha^{-1} suuruse standardvea, kuid mudeli lähendamisel ja rakendamisel eraldisepõhistele polügoonidele oli standardviga alla 40 m^3 ha^{-1} (Tabel 4). ALS andmetel ennustatud puistu tagavarad olid ka süstemaatiliselt suuremad, kui seda on metsaregistris olevad takseeritud tagavarad. Süstemaatiline erinevus suureneb suurema tagavaraga metsades (> 250 m^3 ha^{-1}).

Hemiboreaalsetes metsades on biomass hinnatav otseselt metsa kõrgust ja rinnaspindala teades, lisaks saab biomassi ja süsiniku arvutada otseselt kasvava metsa tagavara põhjal (Lang et al., 2016). Satelliitlidarilt saadud suurtele 1 × 1 km pikslitele arvutatud metsaregistri andmete põhine biomass näitas väga häid seoseid aerolidarilt hinnatud metsa kõrgusega ($R^2 = 0{,}64$; **III**), kuid seosed jäid nõrgaks kasutades satelliitlidari põhiseid kõrgushinnanguid.

Kõrguskasvu ja muutuste tuvastamine aerolidari andmetelt

Nelja-aastase vahega kogutud aerolidari andmete võrdlemisel selgus, et Maa-ameti rutiinlennul kogutud andmeid on võimalik edukalt kasutada kõrgusmuutuste ja metsa kõrguskasvu hindamiseks (**VII**, **VIII**). Kahe lennuandmestiku võrdlus Aegviidu katsealal näitas süstemaatilist kõrguskasvu nii kevadiste kui ka suviste andmete võrdlemisel. Võrdlemisel tuleks kasutada sarnasel fenoloogilisel perioodil kogutud ALS andmeid, et välistada fenoloogiast tulevadi erinevusi. Häiringute tuvastamise uuringus (**VIII**) selgus, et kahe lennu vahel harvendatud puistutes kõrgus ei vähenenud, vaid kasvas süstemaatiliselt. Kõrguskasvu põhjal harvendusraiete tuvastamine ei andnud sarnaselt teiste uurimustega (Nijland et al., 2015) tulemusi, kuid harvendusraied mõjutasid olulisel määral punktipilvest hinnatud katvust. Nii kevadise kui ka suvise andmepaari analüüsil selgus, et harvendusraie tagajärjel vähenes katvus olulisel määral (~20%; **VIII**), mis ületab ka katvushinnangu mõõtmisvea (12%; **VII**).

Kokkuvõte

Doktoritöö aluseks olevate uuringute põhjal saab teha järgmised järeldused.

Metsa kõrgus (H) ja aerolidari punktipilve 80-protsentiil (H_{P80}) on väga tugevas lineaarses korrelatsioonis ($R^2>0{,}9$). Aerolidari suviste andmete järgi ei sõltu kõrguse hinnang oluliselt lehtpuuliikide osakaalust puistus. Kevadiste aerolidari andmete kasutamisel tuleks kõrguse hindamiseks lähendada lehtpuudele ja okaspuudele eraldi mudeli parameetrid.

Puistu elusvõrastiku alguskõrgus (H_{LCB}) mõjutab peegelduste kõrgusjaotust ja on tugevas korrelatsioonis peegelduste kõrgusjaotuse moodväärtusega (H_{Mode}).

Aerolidaril punktipilve põhjal hinnatud võrastiku vertikaalne katvus (CC_{ALS}) on väga heas seoses poolsfääripiltidelt saadud metsa katvushinnangutega (CC_{DHP}), ruutkeskmine hinnanguviga (RMSE) on umbes 11%. Katvushinnang küllastus üle 80% katvuse juures, kui rakendati ainult esimeste peegelduste põhist arvutust, tugevaim korrelatsioon CC_{DHP}-ga saadi kõiki peegeldusi ja 1,3 meetrist nivood kasutades. Nivoo tõstmine ei andnud paremaid tulemusi. Katvushinnang erines raagus ja täislehes lehtpuupuistutes keskmiselt 20%.

Aerolidari andmetelt hinnatud kasvava metsa tagavara (V_{ALS}), kus sisendiks on H_{P80}, H_{P25} ja CC_{ALS} (mudel 7), on tugevas seoses metsas mõõdetud tagavaraga. Üle 1 hektari suurustele eraldisepõhistele punktipilvedele rakendatuna saadi parimaid tulemusi, RSE < 40 m^3 ha^{-1}. V_{ALS} hinnang oli süstemaatiliselt suurem võrreldes metsas tavalisel takseerimisel saadud tagavaraga, süstemaatiline erinevus suurenes tagavaradel $V_{FI} > 250$ m^3 ha^{-1}.

Mahumudelite ristvalideerimise lehtpuu ja okaspuu enamusega puistutel selgus, et mudeliprognoosid olid süstemaatiliselt erinevad, mistõttu tuleks igale regioonile lähendada oma mudeli parameetrid mudeli (7) kuju järgi.

Eraldise takseerandmete põhjal arvutatud biomassi hinnang 1×1 km pikslile ja aerolidari punktipilvedelt arvutatud kõrgusprotsentiili H_{P80} vahel oli tugev lineaarne seos. Kuna suurte pikslite puhul oli seos paljulubav, siis on lootust ka sarnasel põhimõttel rakendada puistupõhiseid biomassimudeleid.

Kahe lidarmõõdistuse vahel harvendusraietest tingitud muutused ei kajastunud eraldiste punktipilvedele arvutatud kõrgusprotsentiilis H_{P80} ja kõrguskasv (ΔH_{P80}) oli sarnane nii harvendatud kui ka harvendamata puistutes. Seevastu kahanes olulisel määral nii kevadiste kui ka suviste lidari andmete põhjal arvutatud katvushinnang (CC_{ALS}).

Satelliitlidarilt hinnatud metsa kõrgus oli nõrgas seoses nii takseeritud, kui ka aerolidarilt arvutatud metsa kõrgusega. Tehisavaradari (InSAR) andmete põhjal prognoositud metsa kõrguse seos lidariandmetel põhineva prognoosiga oli puistute tasemel tugeva korrelatsiooniga ja seega pakub InSAR mõõtmismeetod edaspidi võimalusi lidarmõõtmiste vahepeal kontrollida puistu kõrgust mõjutavaid häiringuid.

ACKNOWLEDGEMENTS

The road to this thesis has been awfully long and with lots of wrong turns, dead ends and long steep climbs. BUT, whenever I found myself struggling to find the purpose of this journey, I always had my co-pilot and supervisor Mait to guide me through, motivate and steer me onto the right path. To him, I owe the biggest gratitude of all.

The many years on this journey have led me to all sorts of new places and have given me the opportunity to meet new people that I from now on do not refer to as my colleagues, but as my friends – Diana, Eneli, Priit, Andres, Vivika, Teele, Sandra, Maris, Urmas, Paavo, Ando, Ahto, Henn – also known as the coffee break crew. I thank you from the bottom of my heart. My sincerest thanks go also out to Veiko Eltermann and Aigar Kallas from RMK, as this work would not have been possible without their support and belief in this topic.

For whenever I found myself thinking of quitting (and believe me, that happened more than once), my family was there to help me through and re-gain my focus. Every year, month, week and day, my wife Kaisa was there to support and love me, with absolutely no doubt in my success. Her belief and admiration have really helped me to go on even on the hardest days of this road. I also want to thank my mother and father who have raised me to be who I am today and who self-sacrificingly have provided me with everything and even more than I needed along all these years. To my brothers Tarvo, Rain and my sister Signe, I owe the stubbornness with a hint of competitiveness to take on this challenge and grin through for all these years. Thank you all!

Lastly, as the saying goes, "friends are the family we choose", I thank my chosen family – Maris, Maria, Brit, Marilin, Linda, Kaire, Liisi, Laura, Margit, Janek V., Janek S. They have given me the opportunity to shut off all the ferial struggles and have brought nothing but joy and laughter to my journey. These past years together have massively improved me as a person and have given me the strength mentally and physically to carry this burden.

I am also grateful to Jan Pisek for providing me with valuable input in the thesis and Karit Jäärats for the English language revision and Urve Ansip for the Estonian editing.

I

ORIGINAL PUBLICATIONS

Lang, M., **Arumäe, T.**, Anniste, J. 2012. Estimation of main forest inventory variables from spectral and airborne lidar data in Aegviidu test site, Estonia. Forestry Studies, 56, 27−41.

DOI: 10.2478/v10132-012-0003-7 Forestry Studies|Metsanduslikud Uurimused 56, 27–41, 2012

Lennukilidari ja spektraalse kaugseireandmestiku kasutamine metsa peamiste takseertunnuste hindamiseks Aegviidu katsealal

Mait Lang[1,2*], Tauri Arumäe[2] ja Johannes Anniste[3]

Lang, M., Arumäe, T., Anniste, J. 2012. Estimation of main forest inventory variables from spectral and airborne lidar data in Aegviidu test site, Estonia. – Forestry Studies | Metsanduslikud Uurimused 56, 27–41. ISSN 1406-9954.

Abstract. Field measurements from 450 sample plots, airborne lidar data and spectral images from Aegviidu, Estonia, 15 by 15 km test site were used to analyse options to estimate main forest inventory variables using remote sensing data. Up to 7 m random error in location of 15 m radius sample plots within homogeneous stands causes usually about 0.5 m standard deviation in lidar pulse return height distribution percentiles. Forest mean height can be predicted with linear relationship from 80th percentile of lidar pulse return height distribution. Upper percentiles of pulse return height distribution are not significantly affected by omitting returns from ground and forest understorey vegetation. Total stem volume in forest can be predicted by using 80th percentile, 25th percentile and canopy cover as model arguments with less than 70 m^3 ha^{-1} standard error. Best species specific stem volume models had 10 m^3 ha^{-1} smaller standard error.

Key words: airborne laser scanning, spectral information, forest inventory.

Authors' addresses: [1]Institute of Forestry and Rural Engineering, Estonian University of Life Sciences, Kreutzwaldi 5, Tartu 51014, Estonia; [2]Tartu Observatory, 61602, Tõravere, Tartumaa, Estonia; [3]OÜ Metsabüroo, Kadaka tee 86a, 12618, Tallinn, Estonia; [*]e-mail: mait.lang@emu.ee

Sissejuhatus

Metsandusliku kaugseire alguseks võib pidada 1920. aastat, mil Kanadas Quebecis inventeeriti aerofotode ja välitööde kombineeritud meetodiga pool miljonit aakrit metsi (Howard, 1991). Eestis on metsa takseerimisel kaugseiret kasutatud alates 1960ndatest aastatest, kui metsakorralduse aluseks võeti mustvalged nähtava ja lähiinfrapunase spektripiirkonna kujutist kandvad paberkujul aerofotod. Praegused digikaamerad salvestavad värvilise kujutise numbriliselt (Liang, 2004). Varasemalt oli peamiseks pilditöötlusmeetodiks aerofotode visuaalne tõlgendamine metsaeraldiste piiride määramiseks ja puistu koosseisu hindamiseks. Digitaalse ehk numbrilise kujutise korral saab aga kasutada andmestiku raaltöötlust nagu näiteks klassifitseerimist ja seoste analüüsi spektraalsete heleduste ning takseertunnuste vahel (Howard, 1991). Peamiseks takistuseks ainult spektraalsel andmestikul põhinevate automaatsete metsa takseerimise rakenduste loomisel on puistu spektraalse heleduse ja peamiste takseertunnuste nagu vanuse, tüvemahu ja rinnaspindala seose küllastumine. Üldiselt kahaneb puistu heledus esimese kolmekümne aasta jooksul ning jääb siis häiringute puudumisel vähemuutuvaks (Nilson, 1994; Nilson & Peterson, 1994). Põhjuseks on peamiste puistu heledust kujundava tegurite – alustaimestiku heleduse, võrastiku katvuse ja lehepinnaindeksi omavahelised tasalülitavad mõjud. Seetõttu on ainult spektraalse heleduse alusel saadud takseertunnuste hinnangud praktikas üksiku puistu jaoks tihti liiga suure veaga (Holmgren & Thuresson, 1998).

Lisaks spektraalsetele sensoritele kasutatakse maapeal ja lennukitel taimkatte kaugseires järjest rohkem laserskannereid ehk lidareid (Næsset *et al*., 2004, Heritage & Large, 2009). Maapinna topograafiliseks kaardistamiseks mõeldud diskreetsed lidarid (topolidarid) on aktiivsed kaugseireseadmed, mis saadavad välja kindla lainepikkusega elektromagnetkiirguse impulsse ja registreerivad sensori suunas tagasi hajunud signaali maksimumide kohalt niinimetatud peegeldusi. Peegeldusele kolmemõõtmeliste koordinaatide (x,y,z) arvutamiseks kasutatakse lennuki asendiandurist (IMU, *Inertial measurement unit*) saadud kaldenurki, diferentsiaalparandusega asukohamääramissüsteemi (GPS) andmeid, impulsi suunda ja signaali teeloleku aega (Heritage & Large, 2009). Enamik kaasaegseid topolidareid registreerib emiteeritud impulsi kohta kuni neli peegeldust. Tulemuseks saadavas lidarandmestikus (punktiparves ehk pilves) sõltub horisontaalpinna ühiku kohta tekkiv peegelduste arv veel lennukõrgusest ja skaneerimisnurgast. Iga peegelduse kohta salvestatakse ka signaali tugevus (*intensity*), kuid selle info kasutamine on kaliibrimisprobleemide tõttu keeruline (Vain *et al*., 2009; Korpela *et al*., 2010).

Mingi metsaosa või puistu takseertunnuste ja lidarandmete seostamiseks kasutatakse puistu piires või sobiva ruumilise lahutusega rastri pikslite kaupa arvutatud statistikuid (Næsset, 1997). Punktipilvest on võimalik saada peegelduste kõrgusjaotused, mis on üsna tihedas seoses puistu võrastiku struktuuriga ja seega ka metsa peamiste takseertunnustega (Nilson, 2005; Frey, 2009). Kolmemõõtmelisest punktiparvest saab arvutada katvuse hinnangu (Lang, 2010), mis puu võra ja puu üldise suuruse seoseid arvestades (Krigul, 1972a; Nilson, 2005) kannab informatsiooni rinnasdiameetri, puude arvu, rinnaspindala ja täiuse kohta.

Käesoleva uuringu eesmärgiks oli testida 2008. aastal Aegviidu katsealal lennukilt tehtud lidarmõõtmiste, multispektraalsete kosmose- ja aeropiltide ja maapealsete proovitükkide kasutamist metsa takseertunnuste hindamiseks. Andmestiku varasema töötluse käigus oli selgunud, et Soomes kasutatavad algoritmid ja mudelid Aegviidu andmestiku jaoks hästi ei sobi (Anniste & Viilup, 2011). Seekord otsiti võimalusi koostada mudelid, mis oleksid väheste sisendtunnustega ja järgiksid metsa peamiste takseertunnuste omavahelisi seoseid. Lisaks uuriti proovitüki asukohavea mõju lidarandmetest saadavale puistu kõrguse hinnangule.

Metoodika

Testala ja proovitükkide takseerandmed

Katseala jääb Aegviidust ja Jänedast läände ja kujutab endast enamasti metsaga kaetud 15 × 15 km ruutu. Metsaregistri andmebaas sisaldas katsetööde objektil riigi- ja erametsade 1999–2008. aasta metsainventeerimise andmeid, mis võeti aluseks proovialade paigutamisel. Katsetööde objektil kasvasid valdavalt männikud, moodustades 55% puistute pindalast, järgnesid kaasikud (22%) ja kuusikud (20%), muude puistute osatähtsus oli väike (Anniste & Viilup, 2011).

Katsealale rajati 2008. aastal 453 proovitükki selliselt (tabel 1), et oleks tagatud sellel esinevate metsade proportsionaalne esindatus (Anniste & Viilup, 2011). Kõikidele välitöödel klupitud puudele (v.a. männid) oli arvutatud 2008. aasta andmestikku kõrgus puu diameetril, vanusel, rinde määrangul, puistu boniteedil, kasvukohatüübil ja täiusel põhineva statistilise metsainventuuri (SMI) metoodikas kasutatava avaldamata mudeliga (Veiko Adermann, Keskkonnteabe Keskus, Riikliku metsainventeerimise osakond). Mändide kõrguse mudel oli lähendatud Aegviidu mudelpuude järgi. Käesoleva katse jaoks arvutati

Tabel 1. Testala puistute jagunemine enamuspuuliigi järgi ja välitöödeks valitud puistute arv.
Table 1. Forest area distribution according to dominant species in Aegviidu test site and preliminary number of selected stands for fieldwork.

Peapuuliik *Dominant species*	Lühend *Code*	Pindala *Area*		Eralduste arv *Number of stands*		Valitud eraldisi *Selected stands*	
		ha	%	arv / *count*	%	arv / *count*	%
Mänd / *Scots pine*	MA	8911	54,9	4745	47,7	207	41,5
Kuusk / *Norway spruce*	KU	3243	20,0	2359	23,7	95	19,0
Kask / *Silver birch*	KS	3581	22.1	2395	24,1	109	21,8
Haab / *Trembling aspen*	HB	115	0,7	118	1,2	30	6,0
Sanglepp / *Black alder*	LM	207	1,3	158	1,6	32	6,4
Hall lepp / *Gray alder*	LV	176	1,1	178	1,8	26	5,2
Kokku / *Total*		16233	100,0	9953	100,0	499	100,0

igal proovitükil puistu keskmine kõrgus Lorey valemiga (Vaus, 2005) kõikide proovitükil klupitud puude põhjal. Välitöödel noorendikes puid ei klupitud, vaid loendati puude arv, hinnati kohe puistu keskmine kõrgus ja rinnasdiameeter (Anniste & Viilup, 2011). Tüvemahud arvutati metsakorralduse juhendi mudelite järgi (Metsa korraldamise juhend, 2009). Hilisemast andmetöötlusest jäi välja kolm ilmsete asukoha vigadega proovitükki.

Multispektraalne kosmosepilt ja aeropildid

Katsetes kasutati SPOT-4 HRVIR pilti, mis oli tehtud selge ilmaga 04. juunil 2008. Kosmosepilt koosnes kujutistest spektri rohelisest, punasest ja NIR (lähiinfrapunane) alast sarnaselt lähiinfrapuna ortofotodega ning lisaks lühilainelises infrapunasest spektripiirkonnast (1580–1750 nm). Pilt sobitati Eesti põhikaardi koordinaatsüsteemi ja piksli suuruseks maapinnal võeti 20 m. Tööks kasutati pildi pikslite algseid väärtusi ja atmosfäärikorrektsiooni ei tehtud. Aeropildid tegi Maa-amet kaameraga Leica ADS40 samaaegselt lidarmõõdistamisega. Käesolevas töös kasutati aeropildina Maa-ameti standardset visuaalseks tõlgendamiseks mõeldud ortokorrigeeritud toodet. Heleduste ja takseerandmete seoste analüüsiks arvutati kosmose- ja aeropildilt proovitükkidele spektraalsed signatuurid ehk tunnusvektorid (Nilson, 1994) programmiga helex32 (Lang *et al*., 2005).

Lidarandmed

Lidarmõõtmised tegi Maa-amet skanneriga Leica ALS50-II (11.07.2008, 27.07.2008 ja 01.09.2008) lennates maapinnast keskmiselt 2400 m kõrgusel. Skanner ALS50-II registreerib impulsi kohta kuni neli peegeldust ja töötab lainepikkusel 1064 nm (Leica, 2007). Andmed olid salvestatud standardsesse LAS failivormingusse lennuribade kaupa. Enamik lennuribadest olid ida-läänesuunalised, aga kaks olid põhja-lõunasuunalised. Skaneerimise nadiirnurk oli andmestikus kuni 20 kraadi. Impulsitihedus maapinnal esimeste peegelduste järgi oli keskmiselt 0,7–0,9 imp m^{-2} (impulssi ruutmeetrile). Lennuribade keskel oli impulsitihedus 0,45–0,50 imp m^{-2}. Lennuribade servades oli impulsside ja peegelduste tihedus horisontaalpinna ühiku kohta kõrgem skanneri peegli suuna muutusega seotud liikumise aeglustumise tõttu. Keskmine peegelduste (P) tihedus lennuribal oli 1–1,2 P m^{-2}. Lennuribade ülekattega aladel oli peegeldusi pinnaühiku kohta rohkem. Punktipilvede töötluseks kasutati vabavara FUSION (McGaughey, 2010).

Igale peegeldusele arvutati kõrgus maapinnast. Selleks eraldati mooduliga Groundfilter ribade kaupa eeldatavalt maapinnalt tekkinud peegeldused. Groundfilter kasutab iteratiivset algoritmi rasterkujul modelleeritava maapinna sobitamiseks punktiparve (McGaughey, 2010). Maapinda esindavate peegelduste eraldamiseks valiti katseliselt rastri piksli suuruseks neli meetrit. Liiga madal ruumiline lahutusvõime siluks tuntavalt lokaalset maapinna reljeefi. Liiga kõrge ruumilise lahutusvõime korral on madalas tihedas taimestikus (näiteks pajuvõsas) piksli alal maapinnalt peegelduste tekkimise tõenäosus väike. Kuna Groundfilter algoritm otsib piksli ulatuses pilvest kõige alumisi punkte, siis võib väikestel pikslitel maapinna lähend osutuda hoopis tiheda taimestiku pinnaks. Peale maapinnapeegelduste eraldamist koostati nende järgi GridSurfaceCreate abil iga riba jaoks rasterkujul digitaalne maapinna mudel (DEM) ruumilise lahutusega 4,0 m.

Maapealsete takseertunnustega saab punktipilve statistikuid siduda kahel viisil 1) lõigates puistu või proovitüki piires välja punktipilve või 2) kasutades rasterkihi piksleid virtuaalsete süstemaatiliste paigutusega proovitükkidena ja arvutades puistu või tegeliku prooviala kohta keskmised hinnangud juba rastrilt. Rasterkihi kasutamine punktiparve analüüsi vaheetapina on üsna levinud meetod ja lihtsustab tehniliselt andmetöötlust (Næsset, 1997). Rasterkihtidena olevate andmete kasutamine on võrreldes punktipilvega lihtne metsanduslikus kaugseires k- lähima naabri meetodiga takseertunnuste ülepinnaliste kaartide koostamisel (McRoberts & Tomppo, 2007).

Enne punktipilve statistikute ja takseertunnuste seoste uurimist testiti proovitüki asukohavea mõju lidarandmetest arvutatus statistikutele. Iga prooviala algse GPS abil mõõdetud asukoha (Anniste & Viilup, 2011) ümbert eraldati kuni seitsme meetri raadiuses 100 juhuslikult paiknevat 15 meetri raadiust pilve. Seitsme meetri suurune viga vastab keskmiselt tavaliste käsi-GPS seadmete reaalsele täpsusele metsas (Anniste & Viilup, 2011). Juhusliku paigutusega pilvedest arvutati iga prooviala jaoks peegelduste keskmine kõrgusjaotus ja jaotuse kvantiilide standardhälbed.

Proovitükkide takseerandmete ja lidarandmete seostamiseks arvutati punktipilve kirjeldavad statistikud 20 m ruumilise lahutusega rastri pikslitele. Takseertunnuste ja lidarandmete regressioonmudelite koostamises arvutati igale proovitükile lidarandmete statistikute keskmised väärtused proovitüki alale jäävatelt pikslitelt programmiga helex32. Kuna proovitükid olid meelega paigutatud puistute keskossa aga mitte rasterkihi pikslite järgi, siis võrreldes pilvemeetodiga kasvab rastri vaheetapina kasutamisel veidi regressioonimudelite jääkstandardviga S_e.

Mudelite süsteem

Reaalse puistu naturaalseid takseertunnuseid kirjeldava mudelite süsteemi keskmeks on puistu tüvemahu M, rinnaspindala G, keskmise kõrguse H ja vormiarvu F seosed, millest üldkasutatav on $M = GHF$ (Krigul, 1972a; Tappo, 1981; Vaus, 2005). Normaalpuistu on (kokkuleppeliselt) kasvutingimusi täielikult kasutav puistu, mille takseertunnused saab leida niinimetatud standardtabelitest (Krigul, 1972a). Tegeliku puistuga seob normaalpuistut täius T, mis arvutatakse puistu tagavara ja normaaltagavara M_{norm} või rinnaspindala ja normaalrinnaspindala G_{norm} suhtena. Frey (2009) näitab, et metsa takseertunnuseid saab üldiselt hinnata võrastiku struktuuri kaudu. Praktilisest metsatakseerimisest on hästi teada puistu võrastiku katvuse K ja täiuse eeldatav lineaarne seos (Krigul, 1972a; Lang *et al*., 2001). Võrastiku katvus on puude võraprojektsioonide pindala S_V ja puistu pindala suhe, kusjuures projektsioonide ülekatted arvestatakse ühekordselt (Jennings *et al*., 1999). Katvuse mõõtmiseks sobivad niinimetatud poolsfääri, punktide ja visiiride meetodid (Krigul, 1972a; Kull, 1999; Rautiainen *et al*., 2005; Korhonen *et al*., 2006). Puistu tihedus, katvus ja vormiarv on samuti omavahel seotud (Krigul, 1972a; Nilson, 2005; Frey, 2009), mis võimaldab kasutada lidariandmetest saadud katvust näiteks täiuse ja puistu rinnaspindala hindamiseks. Aerofotodel põhineval metsatakseerimise metoodikas hinnatakse võra läbimõõdu järgi nii puude kõrgust kui ka rinnasdiameetrit ja katvuse järgi hinnatakse puistu täiust (Krigul, 1972b).

Katvuse saab määratleda lidarandmete

puhul maapinnast kõrgemal tekkinud peegelduste arvu ja kõigi peegelduste arvu suhtena (Morsdorf, 2006; Lang, 2010; Korhonen *et al.*, 2011). Tegelikust maapinnast erineva kõrguse kasutamine näiteks alustaimestiku mõju vältimiseks annab katvuse taustkõrgusel z

$$K(z) = \sum (P_n \mid h_p > z) \,/\, \sum P_n\,, \qquad (1)$$

kus h_p on on peegelduse kõrgus ja P_n sobivalt valitud peegeldusjärkude komplekt. Eeskirja (1) kohaselt on katvuse muutumisvahemik 0–1. Lidarilt saadud katvuse hinnang kahaneb taustpinna kõrguse kasvades ja sõltub peegeldusjärkude valikust (Lang, 2010).

Kolmemõõtmelise punktiparve statistikute nagu näiteks kõrgusjaotuse (joonis 1) või spektraalse heleduse eeldatavaid üldisi seaduspärasusi saame kasutada metsa takseertunnuste hindamiseks, võt-

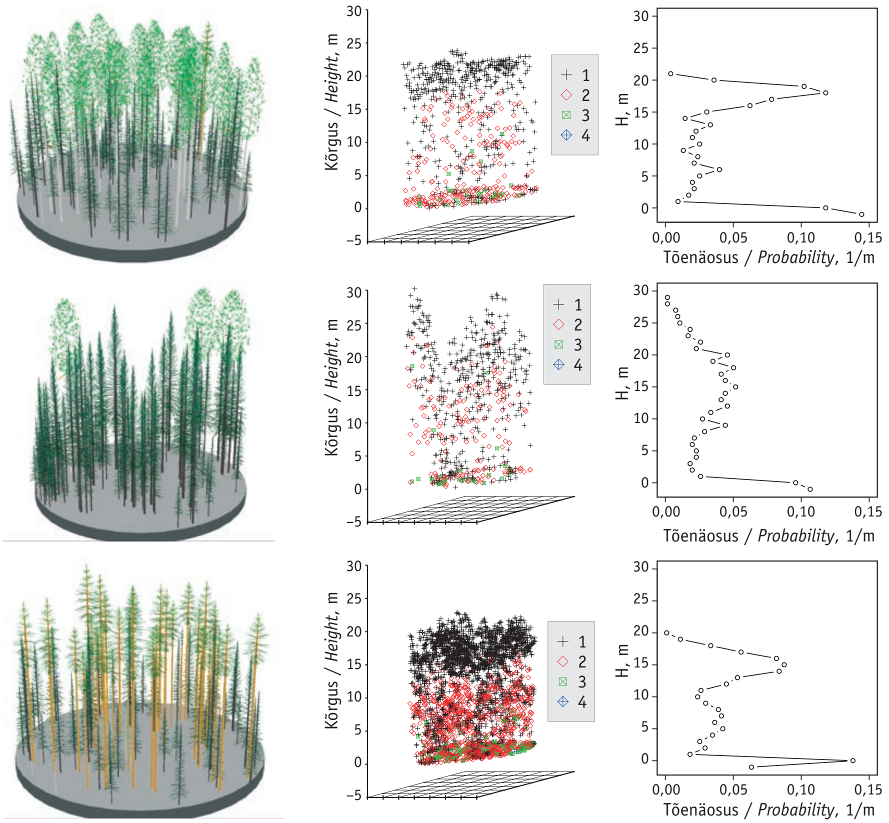

Joonis 1. Näiteid proovitükkide (andmete visualiseering programmiga SVS) punktipilvedes olevate peegelduste kõrgusjaotust kohta. Tavaliselt on kõrgusjaotused kahemodaalsed – moodid on võrastiku keskel ning maapinnal. Numbrid punktipilvede legendil näitavad peegeldusjärku.

Figure 1. Some examples of point clouds and corresponding height distribution of lidar pulse returns from sample plots. Height distribution has two modes: one within canopy and second near to ground. Labels on point cloud subfigure indicate pulse return number.

tes mudelisse hinnatava tunnusega loogiliselt seotud argumendid. Puistu keskmise kõrguse hindamiseks võiks sobida punktiparve kõrgusjaotuse mingil protsentiilil H_q põhinev lineaarne mudel. Aegviidu andmete analüüsile ja varasematele kogemustele tuginedes (Arumäe, 2011) valiti puistu keskmise kõrguse ennustamiseks peegelduste kõrgusjaotuse 80-protsentiilil H_{80} põhinev mudel

$$H = a + bH_{80} \,. \tag{2}$$

Puistu tüvemahu ennustamiseks lidarandmetest testiti mudelid, mille argumentideks olid maapinnalähedaste peegeldusteta ($h_p > 0{,}8$ m) punktiparve kõrgusjaotuse 80-protsentiil, alumine kvartiil H_{25} ja 0,8 m kõrgusel nivool kõikide peegelduste järgi arvutatud katvus $K_{0,8}$:

$$M = aH_{80}^{b} \,, \tag{3}$$

$$M = aH_{80}^{b} + cH_{25} \,, \tag{4}$$

$$M = aH_{80}^{b} * K_{0,8}^{c} \,, \tag{5}$$

$$M = (aH_{80}^{b} + cH_{25}) * K_{0,8}^{d} \,, \tag{6}$$

kus a, b ja c on hinnatavad parameetrid.

Spektraalse heleduse või impulsi peegelduse tugevuse (I) järgi tüvemahu ennustamiseks testiti mudelit

$$M = a(c \,/\, I) \,. \tag{7}$$

Takseertunnuste hindamise mudelid (2–7) koostati nii puuliigist sõltumatult kui puuliigiti. Puuliigist sõltumatu mudel võimaldab lihtsalt ja lausaliselt teisendada kaugseireandmeid takseertunnuste hinnanguteks. Mudelite (2–7) argumentide kordajad lähendati paketi R (www.r-project.org) meetodi nls abil.

Tulemused ja arutelu

Asukohavea mõju katsest selgus, et proovitükkide puistusisese paigutusskeemi puhul ulatub kuni seitsme meetrise eksimuse korral kõrgusjaotuse kvantiilide standardhälve poole meetrini (joonis 2). Mõnedel proovitükkidel oli kvantiilide standardhälve üle meetri ning ühel (KS-120) ulatus kümne meetrini. Asukohavea mõju sõltub antud proovialal oleva puistu ühtlusest, vaadeldava punktiparve suurusest ja kaugusest tegelikust asukohast.

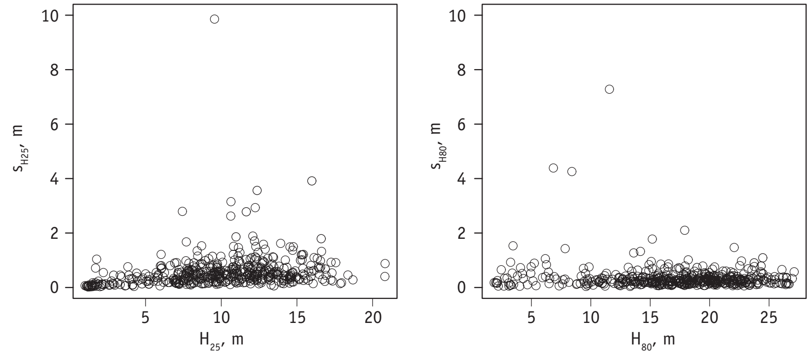

Joonis 2. Kuni seitsme meetri suuruse asukohavea mõju puistu sees asuva proovitüki punktipilve kõrgusjaotuse alumise kvartiili (H_{25}) ja 80-protsentiili (H_{80}) hinnangu standardhälbena (s_{H25}, s_{H80}) 100 katse alusel. Iga punkt tähistab proovitükki.

Figure 2. The influence of up to 7 meters random error in plot position to the lidar return height distribution lower quartile (H_{25}) and 80th percentile (H_{80}). Standard deviation (s_{H25}, s_{H80}) is calculated from 100 clouds. Each point represents one sample plot.

Väiksemate punktipilvede, ebaühtlase tiheduse või struktuuriga puistute puhul on hajuvus suurem. Proovitüki asukohaviga mõjub ka rasterkujul andmetelt statistikute arvutamisel. Sõltuvalt sellest, kas proovitükile võetakse rastrilt lähima piksli väärtus või rastri pikslite ja proovitüki ala lõigetega kaalutud väärtused, võivad muutused olla hüppelised või sujuvad. Lang *et al.* (2005) näitavad, et metsa kasvukäigu proovitükkidele Landsat ETM+ 30 m ruumilise lahutusega rastrilt arvutatud heleduste jaotused võivad proovitüki asukoha veast tingituna olla üsna erinevad.

Peegelduste kõrgusjaotuste kvantiilide väärtused sõltuvad maapinna lähedalt tekkinud peegelduste kaasamisest. Puurinde kõrguse hindamisel mõjutavad kõrgusjaotuse kvantiile ka rohu-, puhma- ja põõsarindelt tekkivad peegeldused. Mõju on oluline just alumistele kvantiilidele ja isegi mediaanile H_{50} (joonis 3c, 3f). Kõrgusjaotuste ülemistele kvantiilidele ei ole maapinnalähedaste peegelduste kaasamise mõju üldiselt enam märgatav (joonis 3), välja arvatud harvikutes või üksikute kõrgete puudega (säilikpuud) aladel, kus kvantiilide väärtused on veidi suuremad maapinnalähedaste peegeldusteta kõrgusjaotuse korral. Kõrgemate kvantiilide puhul koondub puistu keskmise kõrguse ja lidarimpulsi peegelduste seos üsna hästi tunnetatava lineaarseose ümber olenemata sellest, kas maapinnalähedasi peegeldusi kaasata või mitte.

Impulsside peegelduste 0,95-kvantiili seos puistu keskmise kõrgusega on praktiliselt üks-ühene (joonis 3c, 3f). Noorte puis-

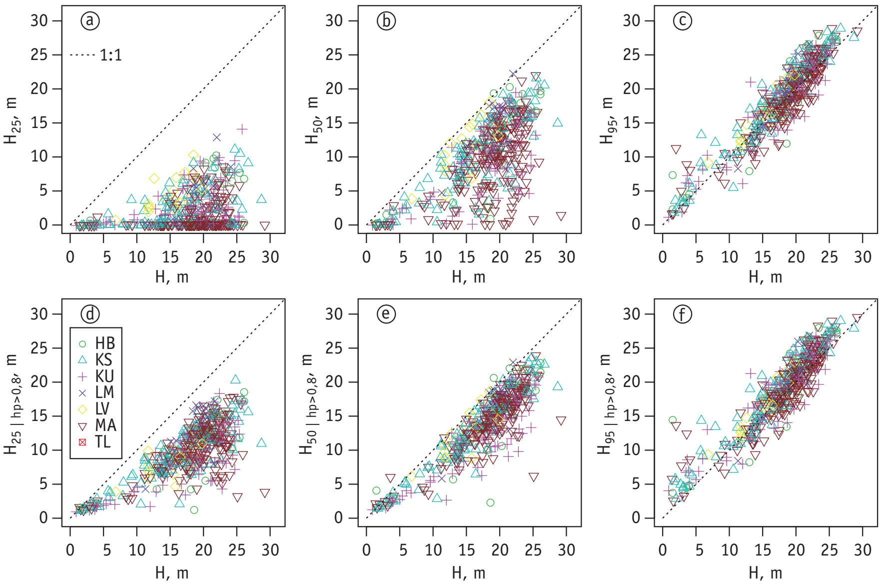

Joonis 3. Lidarimpulsi peegelduste kõrgusjaotuse mõnede protsentiilide ja puistu keskmise kõrguse H seosed. Võrdlusena on toodud kõikide peegeldustega (a,b,c) ja maapinnapeegeldusteta jaotused (d,e,f). h_p on peegelduse kõrgus maapinnast meetrites. Puuliikide lühendid on tabelis 1.

Figure 3. Relationship between lidar point cloud height distribution percentiles and stand mean height H using all returns (a,b,c) or when excluding ground returns (d,e,f). h_p *is pulse return height relative to ground. Species codes are given in Table 1, „TL“ is for other species.*

tute kõrgusjaotuse 0,95-kvantiil on süstemaatiliselt kõrgem, kui võiks eeldada üksühesest seosest puistu keskmise kõrgusega. Arvatavasti on üheks põhjuseks noortes ja vanemates puistutes kasutatud erinev takseerimismetoodika. Vanemates puistutes arvutati puude kaupa kõrgusmudelil põhinev puistu keskmise kõrguse hinnang, aga noortes puistutes hinnati välitöödel puistu keskmist kõrgust. Teisalt kasutati peegelduste kõrgusjaotuse koostamiseks kõiki nelja võimalikku impulsist tekkinud peegeldust. Teist ja kõrgemat järku peegelduste registreerimine sõltub lidaril ajamõõtmise täpsusest väljendatuna impulsi kohta registreeritavate peegelduste vähimas kauguses (Baltsavias, 1999), mis ALS50-II puhul on 3,5 m (Leica, 2007). Seega tekib kõrgemates puistutes madalamal asuvaid teisi, kolmandaid ja neljandaid peegeldusi suurema tõenäosusega. Niisiis kahandab impulsi jagunemine kõikidel peegeldustel põhineva kõrgusjaotuse kvantiilide väärtust just kõrgemates puistutes. Keskmiselt tekkis lennuribades iga impulsi kohta 0,25–0,30 teist peegeldust, 0,030–0,045 kolmandat peegeldust ja neljandate peegelduste arv oli tühine. Kolmandaks põhjuseks eelkirjeldatud kõrguste seose nihkele võib olla rastri kasutamine andmesalvestuse vaheetapina kõrgusjaotuse kvantiilide arvutamisel. Kuna proovitükid ei olnud planeeritud rastri pikslite keskpunktidesse vaid puistu keskele, siis arvatavasti avaldas noorendikes arvutatud peegelduste kõrgusjaotusele olulist mõju ka proovitüki väliste kõrgete puude võimalik olemasolu metsas.

Puistu kõrguse hindamiseks lidarandmetest lähendati lineaarmudeliga puistu kõrguse ja $H_{80|hp>0,8}$ seos üle kogu andmestiku ning eraldi männikute, kaasikute, kuusikute ja ülejäänud puuliikide jaoks (tabel 2). Determinatsioonikordaja R^2 tuli kõikidel juhtudel üle 0,81 ja mudeli jääkstandardviga kahe meetri lähedale. Mudeli parameetrite hinnanguid ja standardvigu arvestades võib Aegviidu andmestiku põhjal väita, et kõrgusjaotuse protsentiili $H_{80|hp>0,8}$ seos puistu keskmise kõrgusega ei ole oluliselt puuliigiomane.

Puistu rinnaspindala kasvades suureneb kõikide peegelduste põhjal arvutatud katvus $K_{P_k|hp>0,8}$ logaritmiliselt (joonis 4a). Maapinnalähedaste punktideta kõikide peegelduste kõrgusjaotuse 90-protsentiil $H_{90|hp>0,8}$ kasvab praktiliselt lineaarselt (joonis 4b). Puistu heledus SPOT-4 HRVIR keskmises infrapunases kanalis kahaneb mittelineaarselt rinnaspindala kasvades (joonis 4c), mis on ka varasematest kaugseirealastest töödest hästi teada (Nilson, 1994; Nilson & Peterson, 1994). Rinnaspindala seos impulsi peegelduste tugevusega oli sarnane spektraalsele heledusele NIR kanalis, mis on ka eeldatav ALS50-II nimilainepikkuse järgi.

Erinevalt puistu kõrgusest on rinnaspindala ja täiuse seosed punktiparvest arvutatud katvust kirjeldavate tunnustega tavaliselt mittelineaarsed ja oluliselt suurema hajuvusega. Rinnaspindala seoste hajuvusdiagrammidelt on aimatav ka puuliigi mõju (joonis 4). Puistu täiuse ja lidarilt arvutatud katvuse seostes on hajuvus suu-

Tabel 2. Peegelduste kõrgusjaotuse 80-protsentiilil $H_{80|hp>0,8}$ põhineva puistu keskmise kõrguse ennustamise lineaarseose (2) statistikud, parameetrid ja nende standardvead.
Table 2. Parameters and descriptive statistics for $H_{80|hp>0,8}$ *based forest mean height regressioon model (2).*

Puistu / *Stand*	Parameetrid / *Parameters*				Mudel / *Model*	
	a	$S_{e,\,a}$	b	$S_{e,\,b}$	R^2	S_e
Kõik / *All*	2,221	0,315	0,927	0,018	0,857	2,13
Männikud /*Pine stands*	3,139	0,567	0,897	0,032	0,812	2,07
Kuusikud / *Spruce stands*	2,543	0,723	0,934	0,042	0,842	2,38
Kaasikud / *Birch stands*	1,189	0,449	0,945	0,026	0,928	1,71
Teised / *Other*	2,002	0,804	0,905	0,045	0,857	2,10

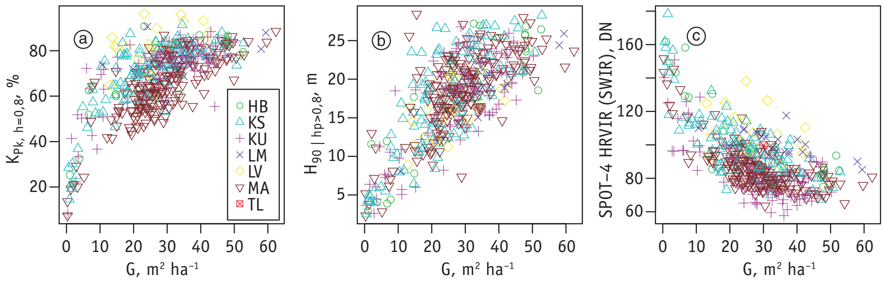

Joonis 4. Takseeritud rinnaspindala *G* seosed kõikidel peegeldustel põhineva katvuse K_{Pk} peegelduste kõrgusjaotuse 90-protsentiili H_{90} ja SPOT HRVIR pildilt arvutatud heledusega. Sama rinnaspindala korral on lehtpuupuitutes suuremad nii punktipilvel põhinev katvuse hinnang kui ka spektraalne heledus.

Figure 4. Relationships of stand basal area G with all return based canopy cover K_{Pk}, *pulse return height distribution 90th-percentile* H_{90} *and spectral reflectance in SWIR band of SPOT-4 HRVIR scanner.*

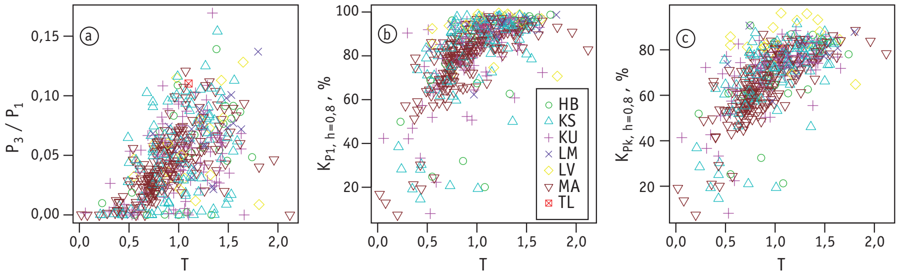

Joonis 5. Takseeritud täiuse T seosed peegelduse jagunemise statistikuga (P_3/P_1) ning katvusega esimeste peegelduste K_{P1} ja kõikidel peegelduste K_{Pk} järgi.

Figure 5. Relationships of stand relative density T with pulse split indicator P_3/P_1, *first return based canopy cover* K_{P1} *and all return based canopy cover* K_{Pk}.

rem kui seostes rinnaspindalaga (joonis 5). Esimestel peegeldustel P_1 põhineva katvuse hinnang saab taustkõrgusel $z = 0,8$ m tihti väärtuse 100% (joonis 5b), kuna nivool $z < 0,8$ m peegeldusi pole. Küllastunud hinnangud edasise analüüsi jaoks infot ei sisalda. Taustkõrguse *z* suurendamisel küllastumise võimalus kahaneks (Lang, 2010). Kõikide peegelduste arvu järgi arvutatud katvuse hinnangud jäävad üldiselt alla 90% (joonis 5c) ja seos täiusega ei küllastu. Nii P_1 kui ka kõikidel peegeldustel P_k põhineva katvuse seos täiusega oli kasvav ja mittelineaarne (joonis 5b, 5c). Impulsi jagunemist kirjeldav suhe P_3/P_1 kasvab koos täiusega – tihedamates puistutes on impulsi jagunemise tõenäosus suurem. Siiski ei anna seose $T = f(P_3/P_1)$ hajuvus lootust selle praktiliseks kasutamiseks (joonis 5a).

Puistute spektraalsed heledused arvutati SPOT-4 HRVIR pildi neljast kanalist, lidarandmetega samaaegselt tehtud aeropiltide kolmest kanalist ja lidari peegelduste tugevusest. Aegviidu katsealal olevate puistute tüvemahu seos spektraalse infoga on sarnane varasematest uuringutest teadaolevaga (Nilson & Peterson, 1994): puistu kasvades üldiselt spektraalne heledus kahaneb esimese kahekümne aasta jooksul ning jääb siis häiringute puudumisel stabiilseks või edaspidi kahaneb oluliselt aeglasemalt (joonis 6). Aeropiltide ja SPOT-4 HRVIR pildi rohelise ning punase kanali heleduse ning tüvemahu seoses kvalitatiivseid erinevusi ei olnud, puuliikide mõju oluliselt ei ilmnenud (joonis 6a, 6d). Aeropiltidel oli siiski seose hajuvus suurem, mille põhjuseks on arvatavasti vaatenurgast ja valgustatusest tekkivad moonutused. Kuna ei kasutatud aeropiltide toorandmeid vaid Maa-ameti rutiinse automaatse pilditöötlusprotseduuri tulemust, siis esines arvatavalt ka värvisignaali moonutusi. NIR kanalis ilmnes selge erinevus okas- ja lehtpuude heleduse ning tüvemahu seoses: sama tüvemahu juures on lehtpuupuistud selgelt heledamad nii SPOT-4 HRVIR pildil kui ka aerofotodel (joonis 6b, 6e). Kvalitatiivselt sarnane kuid lehtpuu- ja okaspuupuistuid pigem mitte eristav oli seos lidari impulsi (samuti NIR spektripiirkond) peegelduste tugevuse ja puistu tüvemahu vahel. Võimalik, et liigilise erinevuse summutab lidari automaatne tundlikkuse kontroll (AGC), mille eesmärgiks on kindlustada, et igast välja saadetud impulsist registreeritakse vähemalt üks peegeldus ja samas jääks registreeritav signaal sensori lineaarse tundlikkuse piirkonda (Vain *et al*., 2009). Parimad lähendid spektraalsel heledusel põhineva puistu tüvemahu ennustamiseks olid jääkstandardveaga üle 110 m^3 ha^{-1} ehk praktiliseks kasutamiseks sobimatud ja siinkohal neid täpsemalt toodud ei ole.

Puistu tüvemahu ennustamiseks sobivad punktipilve statistikud märgatavalt paremini kui spektraalne heledus, sest pee-

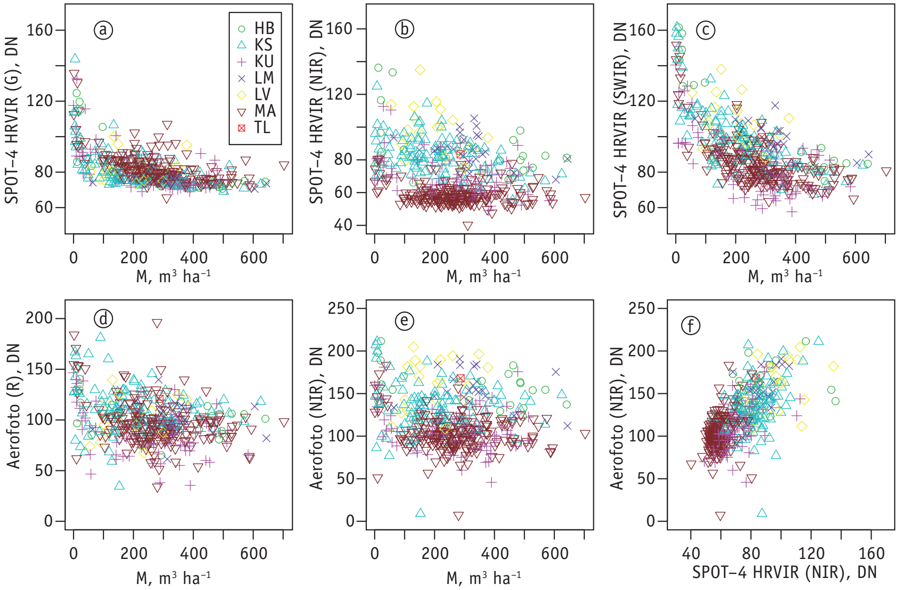

Joonis 6. Puistu tüvemahu *M* seosed kosmosepildilt ning aerofotolt saadud spektraalsete tunnustega. Lähiinfrapunases kanalis (NIR) on lehtpuud okaspuudest tuntavalt heledamad.

Figure 6. Relationships between total stem volume M and spectral variables from satellite image and aerial image. Deciduous and coniferous are well distinguished in near infrared (NIR) band.

gelduste kõrgusjaotus kirjeldab hästi puistu kõrgust, mis on otseselt seotud tüvemahuga (joonis 7a, 7b). Seosed ei ole lineaarsed, kuid neis ei esine sarnast küllastumist nagu spektraalse heleduse puhul. Kvalitatiivselt ei ilmne seostes olulisi erinevusi, kui jätta välja maapinnalähedased peegeldused.

Tüvemahu ennustamiseks maapinnalähedaste peegeldusteta kõrgusjaotuse järgi lähendati esmalt puuliigist sõltumatud üldised mudeleid (3–6), mis põhinesid tunnustel $H_{25|hp>0,8}$, $H_{80|hp>0,8}$ ja $K_{P_k|hp>0,8}$ (tabel 3). Ainult kõrgusjaotusel põhinevad mudelid lähendasid algandmestikku jääkveaga veidi üle 80 $m^3\ ha^{-1}$. Katvuse hinnangu lisamisel mudelisse kahanes jääkviga u. 10 $m^3\ ha^{-1}$ (tabel 3). Parima mahumudeli ennustuse ja takseeritud tüvemahu hajuvusdiagrammilt ilmnes, et üldine mudel võib tekitada süstemaatilisi vigu puuliigiti. Jääkide uurimisel selgus, et keskmiselt alahinnatakse üldise mudeliga tüvemahtu männikutes 21,6 $m^3\ ha^{-1}$ ja kuusikutes 15,7 $m^3\ ha^{-1}$ ning ülehinnatakse kaasikutes 45,9 $m^3\ ha^{-1}$ ja teistes puistutes 15,7 $m^3\ ha^{-1}$. Kuna peegelduste kõrgusjaotuse ja puistu kõrguse seoses puuliigiomasust ei esinenud (tabel 2), siis on arvatavasti põhjuseks nii katvuse hinnangute sõltuvus puuliigist kui ka kõrguse ja tüvemahu seoste erinevused puuliigiti.

Enamuspuuliigiti lähendatud mudelitel saadi ennustuse jääkviga kuni 60 $m^3\ ha^{-1}$ parima mahumudeli korral (joonis 7c, tabel 4). Puuliigiomaste mudelite rakendamisel praktikas on aga probleemiks vajadus teada eelnevalt puuliiki, mis punktipilve statistikute põhjal ei ole hästi eristatav.

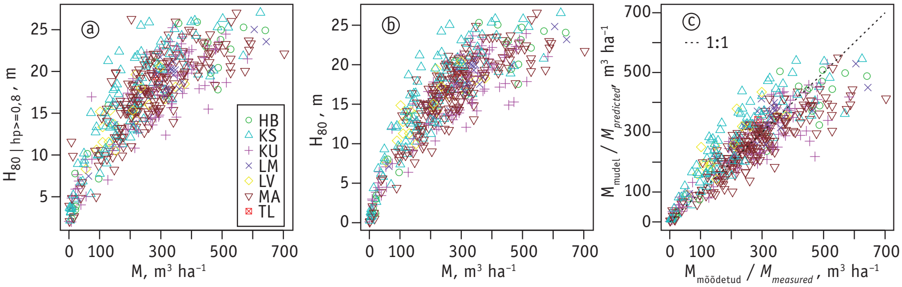

Joonis 7. Peegelduste kõrgusjaotuse 80-protsentiili H_{80} ja puistu tüvemahu M seos maapinnalähedasi peegeldusi arvestades (a) ja ilma (b). Parima üldise mahumudeli (6) ennustuse ja mõõdetud tüvemahu võrdlus (c).

Figure 7. Relationships between total stem volume M and lidar return height distribution 80th percentile (a) ground returns included, (b) ground returns excluded. Comparison of best volume model (6) predictions to measured values (c).

Tabel 3. Peegelduste kõrgusjaotusel ja katvusel põhinevate puuliigist sõltumatute tüvemahu mudelite parameetrite väärtuste hinnangud ja standardvead.

Table 3. Parameters for species-independent stem volume estimation models.

Mudel / *Model*		Parameetrid / *Parameters*							
Nr. / *Eq. Nr*	S_e, $m^3\ ha^{-1}$	a	$S_{e,\ a}$	b	$S_{e,\ b}$	c	$S_{e,\ c}$	d	$S_{e,\ d}$
3	80,4	4,603	0,903	1,422	0,065	-	-	-	-
4	80,0	3,147	0,947	1,501	0,087	3,724	1,604	-	-
5	70,5	9,721	1,784	1,269	0,058	0,907	0,085	-	-
6	69,1	5,784	1,622	1,361	0,081	8,649	2,069	0,957	0,085

Tabel 4. Lidari impulsi peegelduste kõrgusjaotusel ja katvuse hinnangul põhineva parima tüvemahu mudeli (6) parameetrite väärtuste hinnangud ja standardvead enamuspuuliigiti.

Table 4. Parameters for the best stem volume estimation model (6) by dominant species.

Enamuspuuliik	S_e,	Parameetrid / *Parameters*							
Dominant species	$m^3\ ha^{-1}$	a	$S_{e,\ a}$	b	$S_{e,\ b}$	c	$S_{e,\ c}$	d	$S_{e,\ d}$
Mänd / *Scots pine*	58,27	7,559	3,187	1,297	0,127	13,425	3,121	1,204	0,105
Kuusk / *Norway spruce*	62,85	17,627	7,752	1,006	0,140	11,181	5,164	1,174	0,229
Kask / *Silver birch*	61,81	4,335	2,845	1,452	0,179	7,561	5,185	1,495	0,247
Teised / *Other*	67,21	0,364	0,514	2,180	0,403	13,269	5,575	0,806	0,305

Käesolevas katses olid peegelduste statistikud proovitükile arvutatud 20 m ruumilise lahutusega rastrit vaheetapina kasutades, mis lisab hinnangutesse hajuvust. Teisalt on praktiliste rakenduste puhul mudeli jääkhälbest isegi olulisem see, kui tundlikud on mudelid sisendtunnuste vigadele. Varasemas uuringus (Anniste & Viilup, 2011) sai Blom Kartta OY Aegviidu andmestikul hinnangu keskmiseks ruutveaks puistu kõrgusele 1,67 m ja üldisele tüvemahule 62,94 $m^3\ ha^{-1}$. Käesoleva uuringuga võrreldes väiksemate lähendivigade taga oli oluline vaatluste arvu vähendamine – nimelt kasutas Blom Kartta OY andmestikust ainult 318 proovitüki andmeid võrreldes siinse 450 vaatlusega.

Koostatud mudelite kasutamine on võimalik arvatavasti ka mujal Eestis, kui lidarmõõtmised on tehtud fenoloogiliselt samal ajal ja samasuguselt seadistatud skanneriga. Lehepinnaindeksi muutused mõjutavad oluliselt peegelduste kõrgusjaotust kasvuperioodi jooksul (Næsset, 2005) ja seega tuleks näiteks kevadiste topograafilise kaardistamise tarbeks tehtud lendude käigus kogutud lidarmõõtmiste kasutamisel lähendada mudelitele uued parameetrite väärtused. Puuliigiomaste tüvemahumudelite rakendamine nõuab spektraalse info või olemasoleva andmebaasi kasutamist, sest ainult madala punktitihedusega lidarmõõtmistest ei ole võimalik puistu liigilist koosseisu usaldusväärselt hinnata. Edasist uurimist vajab katvuse hindamisel sobivaima taustkõrguse valik ja praktilistes rakendustes metsade takseerimisel kaugseireandmetele lisaks vajalik maapealsete proovitükkide hulk.

Kokkuvõte

Lidarimpulsi peegelduste kõrgusjaotuse kvantiilide standardhälve ei ületa 15 m raadiuste proovitükkide puistusisese paigutuse korral oluliselt poolt meetrit, kui asukohaviga ulatub seitsme meetrini. Puistu kõrguse ja lidarimpulsi peegelduste kõrgusjaotuse ülemiste kvantiilide lineaarseos võimaldab hinnata metsa keskmist kõrgust kuni kahe meetrise jääkveaga Aegviidu katsealal. Täpsust on võimalik edaspidi suurendada, kui kasutada paremat maapinna kõrgusmudelit ja proovitüki puude kõrguste arvutamisel üldisse katseala mudelisse lisada juurde konkreetse proovitüki mudelpuude kõrguste arvestamine. Selgus, et Aegviidu katsealal ei ole lidarandmetest metsa kõrguse ennustamise mudel oluliselt puuliigiomane. Metsa tüvemahtu on võimalik hinnata puuliigist sõltumatu kõikide peegelduste kõrgusjaotustel ja katvuse hinnangul põhineva mudeliga alla 70 $m^3\ ha^{-1}$ jääkveaga ning puuliiki arvestades kuni 10 $m^3\ ha^{-1}$ täpsemalt. Testitud mudelite kujud on kasutatavad ka mujal Eestis, aga muul fenoloogilisel ajal või teistsuguse skanneriseadistusega kogutud andmete puhul tuleb lähendada uued parameetrite väärtused.

Tänuavaldused. Aegviidu katseala andmete analüüsimist toetas Riigimetsa Majandamise Keskus. Artikli valmimist toetasid Keskkonnakaitse ja -tehnoloogia programmi projekt ERMAS, Eesti Teadusfondi grant ETF8290 ja riikliku sihtfinantseerimise grandid SF0060115s08 ja SF0170014s08. Autorid tänavad retsensente kasulike soovituste ja märkuste eest.

Kasutatud kirjandus

Anniste, J., Viilup Ü. 2011. Metsa takseertunnuste määramisest laserskanneerimise abil. (Determination of forest characteristics with the laser scanning). – Artiklid ja uurimused, 10, 38–53. Luua Metsanduskool. (In Estonian).

Arumäe, T. 2011. Laserskanneri andmete kasutamine takseertunnuste hindamiseks. (Using lidar to assess forest characteristics). MSc thesis. Metsandus- ja maaehitusinstituut, Eesti Maaülikool. Tartu. 45pp. (In Estonian with English summary).

Baltsavias, E.P. 1999. Airborne laser scanning: basic relations and formulas. – ISPRS Journal of Photogrammetry & Remote Sensing, 54, 199–214.

Frey, T. 2009. Stand structure links up canopy processes and forest management. – Forestry Studies / Metsanduslikud Uurimused, 51, 40–48.

Heritage, G.L., Large, A.R.G. 2009. Principles of 3D Laser Scanning. Laser Scanning for the Environmental Sciences. Eds Heritage, G.L., Large. John Wiley & Sons, Ltd., Publication, West Sussex, UK, 21–34.

Holmgren, P., Thuresson, T. 1998. Satellite remote sensing for forestry planning – a review. – Scandinavian Journal of Forest Research, 13, 90–100.

Hopkinson, C., Chasmer, L. 2009. Testing LiDAR models of fractional cover across multiple forest ecozones. – Remote Sensing of Environment, 113, 275–288.

Howard, J.A. 1991. Remote sensing of forest resources. Chapman & Hall. London. 420 pp.

Jennings, S.B., Brown, N.D., Sheil, D. 1999. Assessing forest canopies and understorey illumination: canopy closure, canopy cover and other measures. – Forestry, 72, 59–73.

Korhonen, L., Korhonen, K.T., Rautiainen, M., Stenberg, P. 2006. Estimation of forest canopy cover: a comparison of field measurement techniques. – Silva Fennica, 40(4), 577–588.

Korhonen, L., Korpela, I., Heiskanen, J., Maltamo, M. 2011. Airborne discrete-return LIDAR data in the estimation of vertical canopy cover, angular canopy closure and leaf area index. – Remote Sensing of Environment, 115, 1065–1080.

Korpela, I., Ørka, H.O., Hyyppä, J., Heikkinen, V., Tokola, T. 2010. Range AGC normalization in airborne discrete-return LiDAR data for forest canopies. – ISPRS Journal of Photogrammetry and Remote Sensing, 65, 369–379.

Krigul, T. 1972a. Metsatakseerimine. (Forest mensuration). Valgus, Tallinn. 358 pp. (In Estonian).

Krigul, T. 1972b. Aerofotomõõdistamise metoodiline juhend metsamajanduse osakonna üliõpilastele. (Interpretation of aerial images). Eesti Põllumajanduse Akadeemia, Tartu. 84 pp. (In Estonian).

Kull, E. 1999. Lehepinnaindeksi ja võrastiku liituse määramine palumetsades poolsfäärifotode ja vertikaalse toru meetodil. (Relationship of leaf area index and canopy closure in mesotrophic pine forest: an assessment by hemispherical photographs and by the vertical tube methods). – Forestry Studies / Metsanduslikud Uurimused, 31, 98–103. (In Estonian with English summary).

Lang, M., Nilson, T., Lükk, T. 2001. Puistu kasvufunktsioonide kasutamisest kaugseires. (Using forest growth functions in satellite remote sensing). – Forestry Studies / Metsanduslikud Uurimused, 37, 80–88. (In Estonian with English summary).

Lang, M. Lükk, T., Rähn, A., Sims, A. 2005. Kasvukäiguproovitükkide kaugseire võimalusi. (Change detection on permanent forest growth sample plots using satellite images). – Metsanduslikud Uurimused / Forestry Studies, 43, 24–37. (In Estonian with English summary).

Lang, M. 2010. Metsa katvuse ja liituse hindamine lennukilt laserskanneriga. (Estimation of crown and canopy cover from airborne lidar data). – Forestry Studies / Metsanduslikud Uurimused, 52, 5–17. (In Estonian with English summary).

Leica. 2007. Leica ALS50-II. Airborne laser scanner product specifications (760344en-V.07-INT). Leica Geosystems AG, Heerbrugg, Switzerland. 12 p.

Liang, S. 2004. Quantitative remote sensing of land surfaces. John Wiley & Sons, Inc. Hoboken, New Jersy. 543 pp.

McGaughey, R.J. 2010. FUSION/LDV: Software for LIDAR Data Analysis and Visualization. July2010 – FUSION Version 2.90. United States Department of Agriculture Forest Service Pacific Northwest Research Station.

McRoberts, R. E., Tomppo, E. O. 2007. Remote sensing support for national forest inventories. – Remote Sensing of Environment 110, 412–419.

Metsa korraldamise juhend. (Forest inventory guidlines in Estonia). RTL 2009, 9, 104. (In Estonian). – URL https://www.riigiteataja.ee/akt/13124148. [Accessed January 30, 2013].

Morsdorf F., Kötz, B., Meier, E., Itten, K.I., Allgöwer, B. 2006. Estimation of LAI and fractional cover from small footprint laser scanning data based on gap fraction. – Remote Sensing of Environment, 104, 50–61.

Næsset, E. 1997. Determination of mean tree height of forest stands using airborne laser scanner data. – ISPRS Journal of Photogrammetry & Remote Sensing, 52, 49–56.

Næsset, E. 2005. Assessing sensor effects and effects of leaf-off and leaf-on canopy conditions on biophysical stand properties derived from small footprint airborne laser data. – Remote Sensing of Environment, 95, 356–370.

Næsset, E., Gobakken, T., Holmgren, J., Hyyppä, H., Hyyppä, J., Maltamo, M., Nilsson, M., Olsson, H., Persson, Å., Söderman, U. 2004. Laser scanning of forest resources: the Nordic experience. – Scandinavian Journal of Forest Research, 19(6), 482–499.

Nilson, A. 2005. Fitness of allometric equation N = aD^b and equation N = $(a + bD)^{-2}$ for modelling the dependence of the number of trees N on their mean diameter D in yield tables. – Forestry Studies / Metsanduslikud Uurimused, 43, 159–172.

Nilson, T. 1994. Metsade kaugseire alused. (Remote sensing of forests). Eesti Põllumajandusülikooli Metsakorralduse Instituut. 160 pp. (In Estonian).

Nilson, T., Peterson, U. 1994. Age Dependence of Forest Reflectance – Analysis of Main Driving Factors. Remote Sensing of Environment, 48(3), 319–331.

Rautiainen, M., Stenberg, P., Nilson, T. 2005. Estimating canopy cover in Scots pine stands. – Silva Fennica, 39(1), 137–142.

Tappo, E. 1981. Eesti NSV puistute keskmised takseertunnused puistu enamuspuuliigi, boniteedi ja vanuse järgi. (Forest stand average characteristics in Estonia by dominant species, site fertility and age). Eesti NSV Põllumajandusministeeriumi Informatiooni ja Juurutamise Valitsus, Tallinn. 72 pp. (In Estonian).

Vain, A., Kaasalainen, S., Pyysalo, U., Krooks, A., Litkey, P. 2009. Use of naturally available reference targets to calibrate airborne laser scanning intensity data. – Sensors, 9, 2780–2796; DOI:10.3390/s90402780.

Vaus, M. 2005. Metsatakseerimine. (Forest mensuration). OÜ Halo kirjastus, Tartu. 178 pp. (In Estonian).

Estimation of main forest inventory variables from spectral and airborne lidar data in Aegviidu test site, Estonia

Mait Lang, Tauri Arumäe and Johannes Anniste

Summary

Point clouds from airborne laser scanners and spectral information from spaceborne or airborne sensors contain information about forest structure. In Aegviidu, Estonia, 450 sample plots were used from 15 × 15 km test site to assess options to estimate main forest inventory variables from remote sensing data and to build models for forest height and stem volume estimation. SPOT-4 HRVIR image from 04.07.2008, Leica ALS50-II scanning data (11.07.2008, 27.07.2008, 01.09.2008; about one return per m^2) and aerial images (Leica ADS40 camera) were used. General description of test site is in Table 1.

Basic relationships $M = GHF$ and $M = TM_{norm}$ relate total stem volume *M*, stand basal area *G*, mean forest height *H*, stem form factor *F*, stand relative density *T* and stem volume of normal stand M_{norm} (Krigul, 1972a; Vaus, 2005). Tappo (1981) shows that M_{norm} and stand form height *HF* can be well estimated from measured forest height. Close relationships between forest cover *K* and stand relative density *T* are well known (Krigul, 1972a; Nilson, 2005; Frey, 2009). Since height and cover are the basic variables obtained from lidar data (Figure 1; Næsset, 2005; Korhonen *et al*., 2011) we followed the logic of forest inventory models and designed equations (Eq. 2–6) for stem volume estimation where H_{80} and H_{25} are respective percentiles of lidar return height distribution and $K_{0.8}$ is cover estimate at reference height $z = 0.8$ m. We also assessed the influence of ground returns to percentiles of lidar pulse return height distribution. Influence of errors in sample plot location to the lidar pulse return height distribution was studied by adding up to 7 m random error to original position in 100 tests for 15 m sample plots.

Plot shift test revealed that in case of 15 m sample plots that are located within homogeneous stands up to 7 m random error in plot location causes usually less

than 0.5 m standard deviation in pulse return height percentiles (Figure 2). Upper percentiles of lidar pulse return height distribution are not significantly affected if ground returns are excluded (Figure 3). Mean forest height can be estimated with linear model (2) having residual standard error around 2 m (Table 2). Stand basal area and relative density are related to lidar variables and spectral information but the relationships are rather scattered (Figures 4, 5). Stem volume and spectral radiance *I* were related as known before (Nilson & Peterson, 1994), the relationships are different for deciduous and coniferous stands (Figure 6). Smallest residual standard error 110 m^3 ha^{-1} for single spectral channel based model (7) does not encourage to build forest inventory system based on spectral data only. On the other hand, lidar variables based models fitted stem volume data rather well (Figure 7, Tables 3 and 4). However, in case of species specific model (Table 4), the dominating species has to be determined beforehand using spectral data or existing database over the area of interest. The elaborated models can be used elsewhere if phenological time, scanner settings and forests are similar to this study. Model equations (Eq. 2–7) are universal, only new local parameters (*a*, *b*, *c*) have to be estimated for models if applying them in different conditions or when reference height for cover estimate is changed.

Received January 31, 2013, revised February 18, 2013, accepted March 25, 2013

II

Arumäe, T., Lang, M. 2013. A simple model to estimate forest canopy base height from airborne lidar data. Forestry Studies, 58, 46−56.

Forestry Studies | Metsanduslikud Uurimused 58, 46–56, 2013 DOI: 10.2478/fsmu-2013-0005

Puistu esimese rinde võrastiku alguse kõrguse hindamine lennukilidari mõõdistusandmete järgi

Tauri Arumäe[1,2*] **ja Mait Lang**[1,3]

Arumäe, T., Lang, M. 2013. A simple model to estimate forest canopy base height from airborne lidar data. – Forestry Studies | Metsanduslikud Uurimused 58, 46–56. ISSN 1406-9954.

Abstract. Airborne laser scanner (ALS) measurements from two test sites in Estonia were used to estimate forest canopy-base height (H_{VL}). The ALS data was collected by Estonian Land Board using Leica ALS50-II scanner. The H_{VL} was estimated by using mode value and standard deviation of the ALS pulse reflection position height distribution. The pulse reflections which had height less than 0.5 m over the estimated digital terrain model were excluded from the analysis. In situ measurements of canopy base height (H_{VA}) were carried out in 20 mesotrophic Norway spruce and silver birch forest stands in Järvselja and in 45, mostly Scots pine dominant, mesotrophic forest stands in Aegviidu. Determination coefficients of linear regression between H_{VL} and H_{VA} for both test sites were over 0.8 and the residual standard errors of the models were less than two meters. The influence of forest understory vegetation to the estimation of H_{VL} was tested by excluding the near-to-ground vegetation reflections which had height less than 1.5 m. The test results revealed no significant impact of forest understory to the H_{VL} models. The cross validation showed that the H_{VL} models were independent of test sites and tree species composition. The Järvselja data based H_{VL} model had 1.3 m negative bias if applied to Aegviidu forests and the Aegviidu data based H_{VL} model had 1.4 m positive bias if applied to Järvselja forests. In the Aegviidu test site, difference of H_{VL} models of coniferous and deciduous stands was tested and the difference was found not to be significant.

Key words: airborne laser scanning, forest, canopy-base height.

Authors' addresses: [1]Institute of Forestry and Rural Engineering, Estonian University of Life Sciences, Kreutzwaldi 5, Tartu 51014, Estonia; [2]State Forest Management Centre, 10149, Toompuiestee 24, Tallinn; [3]Tartu Observatory, 61602, Tõravere, Tartumaa, Estonia, *e-mail: tauri.arumae@rmk.ee

Sissejuhatus

Lidar (*Light Detection And Ranging*) on kaugseires kasutatav seade, mis koosneb kolmest põhimõtteliselt osast: impulsi edastaja/saatja, salvesti/vastuvõtja ja opto-mehhaaniline seade. Lidar saadab kindlaks määratud suunas välja valgusimpulsse, mis sõltuvalt uuritava pinna või keskkonna omadustest kas peegelduvad tagasi, neelduvad või hajuvad edasisuunas. Tagasipeegeldunud signaali töötlemisel saadakse kolmemõõtmeline punktiparv, mille iga punkt kirjeldab objekti pinda, millelt impulss tagasi peegeldus. Aerolidari impulsside peegelduste asukoha-koordinaadid (X, Y, Z) arvutatakse impulsi edasi-tagasi liikumiseks kulunud aja ning lennuki GPS süsteemist ja asendianduritest saadud andmete järgi. Maapealse punktitiheduse horisontaalpinnal määrab impulsisagedus, skanneri peegli võnkesagedus, lennukõrgus, lennuki kiirus, suurim vaatenurk nadiiri suhtes ja impulsi kohta registreeritavate peegelduste arv (Heritage & Large, 2009; Large & Heritage, 2009; Leica, 2007).

Lennukilt lidarite abil kogutav kolmemõõtmelist andmestikku kasutatakse peamiselt maapinna topoloogilisel kaardistamisel (Wehr & Lohr, 1999; Hodgson *et al.*, 2003), kuid ka arheoloogilistel uuringutel (Large & Heritage, 2009; Crutchley, 2009). Skandinaaviamaades ja ka Põhja-Ameerikas on viimase paarikümne aasta jooksul arendatud aerolidaril põhinevaid poolautomaatseid metsade inventeerimise süsteeme (Næsset, 1997a; Næsset, 1997b; Drake *et al.*, 2002; Patenaude *et al.*, 2004; Korhonen *et al.*, 2011).

Enamik topograafiliseks kaardistamiseks mõeldud aerolidareid kasutab lähiinfrapunase spektripiirkonna (NIR, *near infrared*) kiirgust. NIR lainepikkusel (0,78–1,3 μm) on roheline lehestik poolläbipaistev struktuur ja seega saadakse infot ka maapinna kõrguste kohta taimkatte all (Hodgson *et al.*, 2003). Samas tekivad laserimpulsi peegeldused ka võrastikult (Liang, 2004; Heritage & Large, 2009) ja toimub lidarimpulsi jagunemine ehk ühest impulsist mitme peegelduse teke. Jagunemist mõjutab metsas puude kõrgus ja võrastiku läbipaistvus (Næsset, 1997a; Jennings *et al.*, 1999; Drake *et al.*, 2002; Patenaude *et al.*, 2004; Disney *et al.*, 2010), aga ühe impulsi kohta registreeritav peegelduste arv sõltub konkreetsest lidarist.

Metsa kõrgus on üks olulisemaid puistu struktuuri kirjeldavaid tunnuseid metsakorralduses, mille kohta on ka enim uurimusi (Krigul, 1972; Næsset, 1997a; Næsset, 2002; Vaus, 2005; Heurich, 2008). Metsa läbipaistvus omakorda on seotud võrastiku tihedusega ja seeläbi puistu rinnaspindalaga ja katvusega, mis omakorda on seoses täiusega (Howard, 1991; Nilson & Kuusk, 2004; Frey, 2009; Lang, 2010; Lang, 2012). Varasemates uurimustes on selgunud (Hall *et al.*, 2005; Dean *et al.*, 2009; Lang *et al.*, 2010), et tüüpiline lidarimpulsside peegeldumise kõrgusjaotus metsas on kahemodaalne. Jaotuse esimene mood asub võrastiku tihedaimas osas ning teine mood maapinna lähedal. Niisugune jaotuse kuju on hästi kooskõlas kiirgust peegeldavate ja hajutavate elementide ja pindade ruumilise jaotusega metsas. Peegelduste kõrgusjaotuse mood, mis asub võrastikus, võiks seega olla lähtepunktiks puistu võrastiku alguse kõrguse hindamiseks.

Erinevalt puistu kõrgusest ja läbipaistvusest on puistu võrastiku alguse kõrgus meil üsna vähe uuritud tunnus, mis aga võiks anda ülevaate metsa elujõulisuse (võrade pikkuse ja puistu kõrguse suhe), puistu sortimentidest (oksavaba palgi osa) ja rinnasdiameetrist, mis on otseses seoses võra diameetriga ja puu kõrgusega (Krigul, 1968; Zarnoch *et al.*, 2004; Nilson, 2005; Kato *et al.*, 2009; Zhao *et al.*, 2011). Lisaks on näiteid, kus puistu võrastiku alguse kõrgust kasutatakse metsade tuleohutuse kaardistamiseks (Riaño *et al.*, 2004), biomassi hindamiseks (Marklund, 1987) ja info allikana harvendusraiete planeerimisel (Popescu & Zhao, 2008; Dean *et al.*, 2009). Põhimõtteliselt saab aerolidari andmetest tuvastada ka puu liiki eeldusel, et erinevat liiki puude võrade struktuur ja profiilid on tuvastatavad kolmemõõtmelisest punktiparvest (Holmgren & Persson, 2004; Yao *et al.*, 2012).

Käesoleva töö eesmärgiks oli testida puistu võrastiku alguse kõrguse hindamist aerolidari impulsi peegelduste kõrgusjaotuse moodi ja standardhälbe järgi. Uuriti ka kuni 1,5 m paksuse maapinnalähedase kihi peegelduste eemaldamise (filtreerimise) mõju peegelduste kõrgusjaotusele, mis on aluseks võrastiku alguse kõrguse hindamisel. Analüüsiti saadud mudelite sõltuvust testala asukohast ja puistu peapuuliigist.

Materjal ja metoodika

Testalad

Uuringus kasutati kahe katseala andmeid. Lõuna-Eestisse Järvseljale rajati 2010. aastal katseala (Arumäe, 2011) tsentrikoordinaatidega 6463392,6 N, 694362,9 E (EPSG:3301), kus oli 12 kuusikut ja 8 kaasikut. Puistute keskmine vanus oli kuusikutel 52 aastat ja kaasikutel 61 aastat (tabel 1). Puistud asusid peamiselt jänesekapsa-mustika, mustika ja jänesekapsa-kõdusoo (Lõhmus, 2004) kasvukohatüüpides, kus alusmets oli hõre ning põõsa ja rohurinne madalakasvuline. Puistute üldkirjeldus on tabelis (1).

Igas puistus mõõdeti vähemalt kümne puu elusa võra alguskõrgus (h_{vm}) ja rinnasdiameeter (d_m), mille keskmised võeti puistu hinnanguteks (puistu võraalguse kõrgus (H_{VA}), puistu ruutkeskmine rinnasdiameeter (D_m)). Puude elusvõra alguse kõrguse mõõtmiseks kasutati Vertex III kõrgusemõõtjat ja T3 transponderit. Kõrguse lugem võeti suurema lehemassiivi algusest, mis on ka antud artikli kontekstis elusvõrastiku alguskõrguse piiriks (joonis 1).

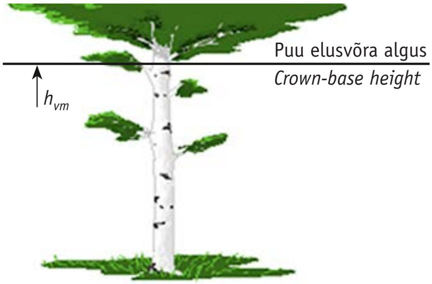

Joonis 1. Puu elusvõra alguse (*crown-base height*) kõrguse (h_{vm}) määratlemine (Arumäe, 2011).

Figure 1. The definition of the tree live crown base height (h_{vm}) according to Arumäe (2011).

Põhja-Eestis Aegviidu katsealal (Anniste & Viilup, 2010), mille tsentrikoordinaadid on 6573468,3 N, 587991,8 E (EPSG:3301) tehti 2012. aastal lisamõõtmisi ja puistu elusvõrastiku alguse kõrguse analüüsiks saadi andmed 45 metsaeraldiselt. Puistud asusid peamiselt angervaksa, mustika ja jänesekapsa-kõdusoo kasvukohatüüpides. Alusmets neil proovitükkidel oli hõre ja alustaimestik madalakasvuline, kui välja arvata angervaksa kasvukohatüübi puistud. Puude elusvõra alguse kõrguse mõõtmiseks ning puistu võrastiku alguse kõrguse hinnangu saamiseks rajati igasse eraldisse vähemalt 10 juhuslikult asetsevat ringproovitükki raadiusega 8–12 m. Proovitükil klupiti kõik puud ning mõõdeti kuni kolme mudelpuu kõrgus ja elusvõra alguse kõrgus Vertex III kõrgusemõõtja ja T3 transponderi abil. Hiljem arvutati Eesti Metsakorralduskeskuses väljatöötatud mudelite (Pärt, 2013) abil proovitükkide ja metsaeraldiste takseerkirjeldused. Katseala puistute liigiline jaotus ja põhilised takseertunnused on esitatud tabelis 1.

Lidarimõõdistuste andmed

Lasermõõdistuse tegi mõlemal testalal Eesti Maa-amet aerolidariga Leica ALS50-II,

Tabel 1. Aegviidu ja Järvselja katsealade proovitükkide jagunemine puuliikide järgi. Järvselja puistute kõrgusandmed pärinevad 2010. aasta takseerkirjeldusest.

Table 1. The distribution of sample plots in the Aegviidu and Järvselja test sites according to the main species. Järvselja data is from the forest inventory database from the year 2010.

Katseala *Test site*	Peapuuliik *Main species*	Puistute arv *Stands*	Keskmine vanus (a) *Average age (y)*	Puistute keskmine kõrgus (m) *Stand average height (m)*	Teise rinde kõrgus (m) *Second layer height (m)*
Aegviidu	Haab (*Common aspen* L.)	3	57	24,3	13,80
	Kask (*Silver birch* Roth)	11	45	18,7	9,76
	Kuusk (*Norway spruce* L.)	9	59	19,8	10,00
	Sanglepp (*Common alder* L.)	2	64	19,8	9,60
	Mänd (*Scots pine* L.)	20	79	21,6	11,10
Järvselja	Kask (*Silver birch* Roth)	8	52	29,3	-
	Kuusk (*Norway spruce* L.)	12	61	28,6	-

mis registreerib kuni neli peegeldust ühe impulsi kohta (Leica, 2007). Aegviidu andmestik koguti aastal 2008 (Anniste & Viilup, 2010) ning Järvseljal lennati aastal 2010. Lennu kõrgus mõlemal katsealal oli keskmiselt 2400 meetrit, mis koos skanneri muude seadistustega tagas umbes 0,5 peegeldust ruutmeetri kohta. Lidarandmete töötluseks kasutati programmi FUSION/LDV (v 3.20) erinevaid mooduleid (McGaughey, 2010).

Esimene etapp lidarandmete töötluses oli maapinna kõrgusmudeli loomine, milleks eraldati üldisest punktiparvest *Groundfilter* mooduli abil eeldatavalt maapinnalt tekkinud peegeldused. Seejärel tükeldati lidariandmestik puistute kaupa *PolyClipData* mooduliga, kasutades selleks eraldise piiride vektorpolügoone. Järgnevalt eemaldati *Clipdata* mooduliga andmestikust maapinna lähedased punktid (h_r < 0,5 m, kus h_r on peegelduse kõrgus maapinnast). Järele jäänud peegelduste alusel arvutati protseduuri *Cloudmetrics* abil iga eraldiste punktiparvede statistikud.

Võimalike alustaimestikult tekkinud peegelduste mõju uurimiseks võrastiku alguse kõrguse hinnangule H_{VL} rakendati punktiparvele enne kõrgusjaotuse arvutamist lisaks esialgsele filtrile ($h_r \leq 0{,}5$ m) veel filtertingimusi $h_r \leq 1$ m ja $h_r \leq 1{,}5$ m.

Kõikides testides arvutati lidarandmetest puistu võrastiku alguse kõrguse H_{VL} hinnang valemiga

$$H_{VL} = H_{Mood} - \frac{H_{Stdev}}{2}\,, \qquad (1)$$

kus H_{Mood} ja H_{Stdev} on vastavalt peegelduste kõrgusjaotuse mood ja standardhälve. Peegelduste kõrgusjaotuse mood ja standardhälve on mõlemad FUSIONi mooduli *CloudMetrics* poolt arvutatud parameetrid. Moodväärtuse leidmiseks jagab *Cloudmetrics* peegeldused 64 kõrgusklassi (McGaughey, 2010).

Maapealsete mõõtmiste järgi hinnatud H_{VA} ning lidarandmetest mudeliga (1) arvutatud puistu võrastiku alguse kõrguse seost lähendati vähimruutude meetodil lineaarse mudeliga $H_{VL} = aH_{VA}+b$, kus a ja b on võrrandi hinnatavad parameetrid. Seoseid uuriti testala kaupa, testalal puuliigiti ning erinevate h_r filtertingimuste korral.

Tulemused

Maapinnalähedaste peegelduste eemaldamise järel edasiseks analüüsiks kasutatud peegelduste ühemodaalsete kõrgusjaotuste näited on joonisel (2), kus on esitatud Aegviidu katsealalt näited kaasiku, männiku ja kuusiku kohta.

Maapinna lähedaste peegelduste väljajätmise katsest selgus (tabel 2), et peegel-

Tabel 2. Maapinnalähedaste peegelduste filtreerimine ei avaldanud olulist mõju mõõdetud ja lidarandmetest arvutatud puistu võrastiku alguse kõrguse seose parameetritele ega jääkhälbele.

Table 2. The exclusion of near to ground reflections did not significantly influence the estimated parameters for the relationship $H_{VL} = aH_{VA} + b$, where H_{VL} is estimated using Eq.(1) and H_{VA} is the measured canopy base height.

Katseala *Test site*	Filter *Filter*	Katse number *Test number*	R^2 R^2	H_{VL} mudeli parameetrid *Parameters of H_{VL} model*		Standardviga (m) *Standard error (m)*	Olulisus *Significance*
				a	b		
Järvselja	$F_{h>0,5\ m}$	H_{VL_1}	0,874	0,8511	−1,5553	2,20	***
	$F_{h>1,0\ m}$	H_{VL_2}	0,867	0,8309	−1,4177	2,27	***
	$F_{h>1,5\ m}$	H_{VL_3}	0,869	0,8431	−1,4104	2,25	***
Aegviidu	$F_{h>0,5\ m}$	H_{VL_4}	0,795	0,7707	0,9955	1,62	***
	$F_{h>0,8\ m}$	H_{VL_5}	0,791	0,7698	0,9906	1,63	***
	$F_{h>1,5\ m}$	H_{VL_6}	0,801	0,7710	0,8951	1,59	***

*** *p < 0,05*

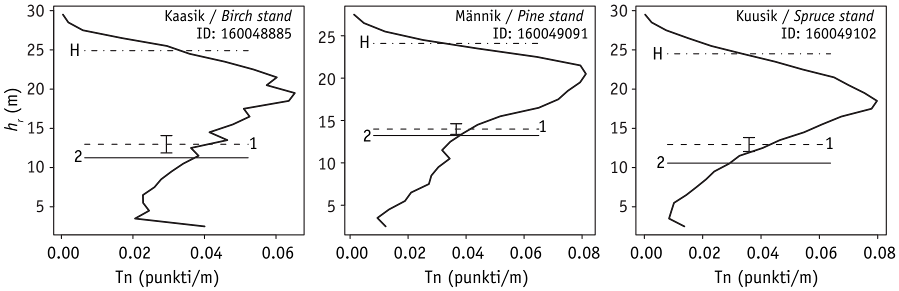

Joonis 2. Punktiparve kõrgusjaotused kolmest Aegviidu puistust. Katkendlik joon „1" – lidarandmetest arvutatud puistu elusvõrastiku alguskõrgus mudeli H_{VL_6} (tabel 2) abil, pidevjoon „2" – puistus mõõdetud elusvõrastiku alguskõrgus, h_r – peegelduste kõrgus (m), H – puistu esimese rinde mõõdetud kõrgus, Tn – tõenäosus.

Figure 2. Examples of the lidar pulse return height distribution in three Aegviidu test stands. The returns with height $h_r \leq 1.5$ m from the ground were excluded. X-axis – probability (returns per meter), dashed line "1" is the crown-base height according to model H_{VL_6} (Table 2), continuous line "2" is the measured stand crown-base height, H is the average height of the stand, and h_r is the pulse reflection height.

dused, mis jäävad madalamale kui 1,5 m, ei avalda lidariandmetest arvutatud ja maapeal mõõdetud puistu elusvõrastiku alguse kõrguse seosele olulist mõju. Lineaarse regressioonimudeli parameetrid ja lähendi R^2 oluliselt ei muutunud. Parimaid tulemusi andis Aegviidu katsealal filter $h_r \leq 1,5$ m ja Järvseljal esialgne filter $h_r \leq 0,5$ m, kuid statistiliselt olulist erinevust kõrgusfiltrid ei põhjustanud.

Järvselja mudeliga H_{VL_3} Aegviidu puistutele ennustatud võrastiku alguse kõrgus osutus keskmiselt 1,33 meetri võrra mõõdetust madalamaks. Vastupidises katses saadi Aegviidu mudeliga H_{VL_6} Järvseljal keskmiselt 1,42 meetrit suurem võrastiku alguskõrguse hinnang. Erinevuste põhjuste selgitamiseks võrreldi katsealade puistute ruutkeskmise rinnasdiameetri (D_m) ja puistute elusvõrastiku alguskõrguse (H_{VA}) seost (joonis 3), arvestades, et puistu võrastiku alguse kõrgus on seoses puistu kõrgusega, mis omakorda on seoses diameetriga (Valentine & Mäkelä, 2005). Ilmnes, et Järvselja ja Aegviidu metsade vahel olulist erinevust selle võrdluse põhjal ei olnud ja võrastiku alguse kõrguse H_{VL} mudeleid saab kasutada asukohast sõltumatuna. Üheks süstemaatilise vea põhjuseks on arvatavasti see, et Aegviidu katseala lidarandmed on neli aastat maapealsetest mõõtmistest vanemad.

Et selgitada okas- ja lehtpuupuistute eristamise vajadust lidarmõõdistuse andmete alusel puistute võrastiku alguse kõrguse hindamiseks, lähendati mudelid H_{VL_3} ja H_{VL_6} puuliigist lähtuvalt. Selgus, et mõlemal katsealal suudeti täpsemalt hinnata võraalguse kõrgust okaspuupuistutes – parimate mudelite $R^2 > 0,88$ (tabel 3). Joonisel 4 on esitatud eraldi Aegviidu ja Järvselja oksas- ning lehtpuupuistute regressioonimudelid ning tabelis 3 vastavad korrelatsioonikordajad ning tõusude hinnangud ning usalduspiirid. Kuna leht- ja okaspuude mudelite tõusu alumine ja ülemine 95% usalduspiir peaaegu kattusid ja vabaliikmed ei olnud mudelis statistilisest olulised, siis võime järeldada, et eelnevalt ei ole vaja eristada eraldisi peapuuliigiti.

Tabel 3. Lehtpuupuistute (LP) ja okaspuupuistute (OP) elusvõrastiku alguse kõrguse mudelite H_{VL_3} ja H_{VL_6} tõusude võrdlus Aegviidu ja Järvselja katsealal.

Table 3. The comparison of the crown-base height models H_{VL_3} and H_{VL_6} for coniferous stands (OP) and deciduous stands (LP) in the Aegviidu test site and Järvselja test site.

Testala *Test site*	Liik *Main species*	Mudeli tõusu hinnang *Model gain*	R^2 R^2	Hinnangu standardviga (m) *Standard Error (m)*	t-statistik *t-stat*	Olulisuse tõenäosus *p-value*	Usaldusspiirid *Confidence intervalls*	
							5%	95%
Aegviidu	LP	1,39	0,799	0,13	10,49	***	1,1	1,67
	OP	0,96	0,884	0,09	11,01	***	0,78	1,14
Järvselja	LP	0,89	0,908	0,12	7,26	***	0,58	1,21
	OP	0,82	0,913	0,09	9,4	***	0,62	1,01

*** *$p < 0,05$*

Joonis 3. Puistu ruutkeskmise rinnasdiameetri (D_m) ja puistu elusvõrastiku alguse (H_{VA}) suhe Järvselja ja Aegviidu katsealal, mis näitab, et katsealade metsad omavahel oluliselt ei erine.

Figure 3. The relationship of stand mean breast height diameter (D_m) to crown-base height (H_{VA}) in the Järvselja and Aegviidu test sites are similar.

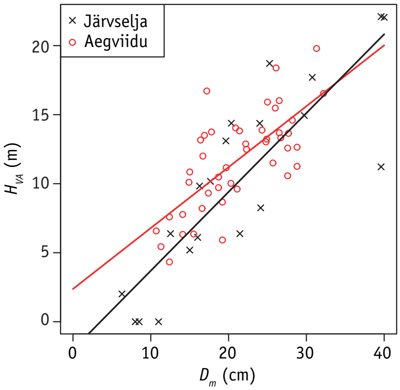

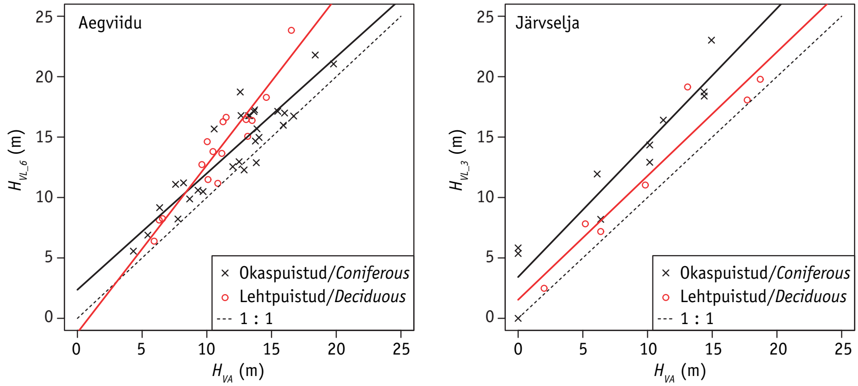

Joonis 4. Mõõdetud elusvõrastiku alguskõrguse ja mudelite H_{VL_3} ning H_{VL_6} puuliigiti lähendite võrdluskatse Aegviidu ja Järvselja katsealal.

Figure 4. The comparison of the measured and estimated with model H_{VL_3} and H_{VL_6} (Table 2) crown-base height by main species in Aegviidu and Järvselja test site.

Arutelu

Puistu võrastiku alguse kõrguse hindamiseks on näiteks Zhao *et al*. (2011) pakkunud mudeli, millel on neli argumenti: kõikide peegelduste kõrgusjaotuse 1-protsentiil, esimeste peegelduste kõrgusjaotuse 98-protsentiil ning maapinnast mõõtes kõrguste vahemikkesse 15–20 m ja 20–25 m jääv suhteline osa kõikide peegelduste arvust. Zhao *et al.* (2011) mudeli kasutamisel eeldatakse, et andmestikus on iga teise peegelduse jaoks leitav vastava impulsi esimene peegeldus. Zhao *et al.* (2011) mudeli kasutamine Eestis on problemaatiline, kuna Maa-amet väljastab lidarandmeid tavaliselt kaardilehtede kaupa mitte algsete lennuribade järgi ja peegeldusi ei ole üldiselt enam võimalik konkreetse impulsiga seostada. Peegelduste kõrgusjaotuse 1-protsentiili mõjutab üsna oluliselt alusmetsa tihedus ja kõrgus ning fikseeritud kõrgusvahemiku kasutamise tõttu võivad ennustustesse tekkida järsud muutused ja müra. Käesolevas töös välja pakutud mudelis (1) kasutatakse maapinnalähedaste peegeldusteta punktiparve kõrgusjaotuse moodi ja standardhälbe hinnangut. See mudel ei pruugi sobida metsades, kus peegelduste kõrgusjaotuse mood pole hästi eristuv.

Mudeli (1) järgi leitud laserimpulsi peegelduste kõrgusjaotuse kvantiili sobivust võrastiku alguse kõrguse hindamiseks kinnitas mõlemal katsealal mõõdetud ja lidarandmetest ennustatud võrastiku alguse kõrguse lineaarseose determinatsioonikordaja väärtus $R^2 > 0,8$. Maapinna lähedaste peegelduste eemaldamise filtri ($h_r \leq 1,5$ m) mõjul muutus katseala piires võrastiku alguse kõrguse mudeli jääkstandardviga maksimaalselt 12 cm, aga mudelid omavahel oluliselt ei erinenud. Ligilähedased olid nii seose $H_{VL} = aH_{VA} + b$ parameetrid kui ka R^2 (tabel 2) kolme testitud maapinnalähedaste peegelduste eemaldamise filtri ($h_r \leq 0,5$ m, $h_r \leq 1,0$ m, $h_r \leq 1,5$ m) puhul. Arvestades, et alustaimestik ja alusmets näiteks angervaksa kasvukohas võib olla kuni 2 meetri kõrgune, siis võib metsa esimese ja teise rinde võrastiku alguse kõrguse hindamisel jätta lidarimpulsside peegelduste kõrgusjaotusest välja alla 1,5 kuni 2 meetri kõrgusel olevad peegeldused. Esialgu pole selge, kuivõrd sobib selline reegel näiteks noorendike võraalguse kõrguse hindamisel.

Mõningane erinevus ilmnes Aegviidu ja Järvselja mudelite võrdlemisel, nii oli mudeli jääkstandardviga Järvseljal kuni 0,6 m suurem kui Aegviidu katsealal. Samuti saime mudelite risttesti tulemusel Aegviidu katsealal võrastiku alguse kõrguse 1,33 meetrise alahinnangu ning Järvseljal 1,42 meetrise ülehinnangu. Järvselja ja Aegviidu katsealade puistute keskmise rinnasdiameetri ja elusvõrastiku alguse kõrguse suhte võrdluse põhjal võib väita, et need metsad olid sarnased, seega võraalguse kõrguse mudelite võrdluses tekkinud erinevuse põhjuseid tuleks otsida mujalt. Näiteks Aegviidu laserandmete ja mõõtmiste vahel oli nelja aastane paus, mille jooksul puistud kasvasid keskmiselt 0,5–1 m võrra kõrgemaks vastavalt Kiviste (1997) mudelile. Samas vahemikus oli arvatavasti ka muutus võrastiku alguse kõrguses (Valentine & Mäkelä, 2005), mis võis tingida Aegviidus võrastiku alguskõrguse alahindamise. Lisaks võisid tulemustele mõju avaldada teise rinde kasv ning maapealse mõõtmismetoodika erinevus kahel katsealal või mõõtmisvead – elusvõra alguspiir võib kohati olla hägune ja õige kõrguse defineerimine on üsna subjektiivne. Samuti tuleks arvestada laserskanneri enda seadistuste erisuste mõju ja võimalikku tundlikkuse muutust aja jooksul.

Tulevikku silmas pidades on laserandmete kõrvale vaja kindlasti juurde teha maapealseid tugimõõtmisi, sest pole teada, kuidas mõjutab võrastikust tekkivate peegelduste kõrgusjaotust näiteks skanneri automaatne tundlikkuse kontroll (AGC – *Automatic Gain Control*) (Vain *et al*., 2010). Kolmemõõtmelisest punktiparvedest arvutatud statistikutel põhinevate mudelite kaliibrimiseks võiks edaspidi hästi sobida ka statistilise metsainventuuri andmekogu

(Adermann, 2010). See võiks märgatavalt suurendada laserandmete kasutusvõimalusi. Samas annab käesolevas uuringus ilmnenud Aegviidu ja Järvselja puistute mudelite sarnasus lootust, et põhimõtteliselt on võimalik isegi Eesti mandriosa metsade jaoks universaalse lidarandmetele tugineva võraalguse kõrguse mudeli koostamine.

Kokkuvõte

Aegviidu ja Järvselja andmete põhjal selgus, et lidarimpulsside peegelduste kõrgusjaotuse moodväärtusel ja standardhälbel põhinev mudel (1) on sobilik puistu elusvõrastiku alguse kõrguse hindamiseks. Maapealsete mõõtmiste ja laserimpulsi peegelduste järgi hinnatud puistu elusvõrastiku alguse kõrguse regressioonimudeli standardviga oli 1,85 m, determinatsioonikordaja $R^2 > 0{,}8$ ja seosed olid kõik olulised. Okas- ja lehtpuupuistute mudelid olid sarnased.

Alusmetsa ja alustaimestiku peegelduste eemaldamisel ei olnud märkimisväärset mõju filtreerimiskõrguste vahemikus $h_r \geq 0{,}5$–1,5 m. Parimaid, aga mitte oluliselt erinevaid, tulemusi andis Aegviidu katsealal $h_r \leq 1{,}5$ m ja Järvseljal $h_r \leq 0{,}5$ m. Kokkvõttes filterkõrguse valik mudelite parameetrite hinnanguid oluliselt ei mõjuta, eeldusel, et alusmets ja rohurinne on rakendatud filtrikõrgusest madalamad.

Uurimuse tulemusena selgus ka, et Aegviidu ja Järvselja katsealadel saadud mudelid ei ole kohaomased, kuigi mudelite risttestimisel kaasnes Aegviidul 1,33 meetrine võrastiku alguse alahindamine ja Järvseljal samas suurusjärgus võraalguse ülehindamine. Vahe võis olla tingitud lasermõõtmiste ja maapealsete mõõtmiste ajalisest vahest või erinevatest võrastiku peegeldusomadustest ning skaneerimistingimustest, kuna puistute keskmise diameetri ja elusvõrastiku alguse kõrguse seosed mõlemal katsealal olid tegelikult sarnased.

Tänuavaldused. Aegviidu katseala andmete analüüsimist toetas Riigimetsa Majandamise Keskus. Teema on seotud Eesti Teadusfondi grandiga ETF8290 ja riikliku sihtfinantseerimise grantidega SF0180009Bs11 ja SF0170014s08 ning institutsionaalse uurimistoetusega IUT21-04 (B21004MIMK). Andmete kogumisel oli suureks abiks Keskkonnateabekeskus eesotsas Enn Pärdiga. Autorid tänavad Andres Kuuske ja anonüümset retsensenti kasulike märkuste ja soovituste eest.

Kasutatud kirjandus

Adermann, V. 2010. Development of Estonian National Forest Inventory. – Tomppo, E., Gschwantner, T., Lawrencem, M., McRoberts, R.E. (eds.). National Forest Inventories. Springer, 171–184.

Anniste, J., Viilup Ü. 2010. Metsa takseertunnuste määramisest laserskanneerimise abil. (Determination of forest characteristics with the laser scanning). – Artiklid ja uurimused, 10, 38–53. Luua Metsanduskool. (In Estonian with English summary).

Arumäe, T. 2011. Laserskanneri andmete kasutamine takseertunnuste hindamiseks. (Using lidar data to assess forest characteristics). MSc thesis. Metsandus- ja maaehitusinstituut, Eesti Maaülikool. Tartu. 45 pp. (In Estonian with English summary).

Crutchley, S. 2009. Using LIDAR in Archaeological Contexts: The English Heritage Experience and Lessons Learned. – Heritage, G.L., Large, A.R.G. (eds.). Laser Scanning for the Environmental Sciences. John Wiley & Sons, Ltd., Publication, West Sussex, 180–200.

Dean, T.J., Cao, Q.V., Roberts, S.D., Evans, D.L. 2009. Measuring heights to crown base and crown median with LiDAR in a mature even-aged loblolly pine stand. – Forest Ecology and Management, 257, 126–133.

Disney, M.I., Kalogirou, V., Lewis, P., Prieto-Blanco, A., Hancock, S., Pfeifer, M. 2010. Simulating the impact of discrete-return lidar system and survey characteristics over young conifer and broadleaf forests. – Remote Sensing of Environment, 114, 1546–1560.

Drake, J.B., Dubayah, R.O., Clark, D.B., Knox, R.G., Blair, J.B., Hofton, M.A., Chazdon, R.L., Weishampel, J.F., Prince, S.D. 2002. Estimation of tropical forest structural characteristics using large-footprint lidar. – Remote Sensing of Environment, 79, 30–319.

Frey, T. 2009. Stand structure links up canopy processes and forest management. – Forestry Studies / Metsanduslikud Uurimused, 51, 40–48.

Hall, S.A., Burke, I.C., Box, D.O., Kaufmann, M.R., Stoker, J.M. 2005. Estimating stand structure using discrete-return lidar: an example from low density, fire prone ponderosa pine forests. – Forest Ecology and Management, 208, 189–209.

Heritage, G.L., Large, A.R.G. 2009. Principles of 3D Laser Scanning. – Heritage, G.L., Large, A.R.G. (eds.). Laser Scanning for the Environmental Sciences. John Wiley & Sons, Ltd., Publication, West Sussex, 21–34.

Heurich, M. 2008. Automatic recognition and measurement of single trees based on data from airborne laser scanning over the richly structured natural forests of the Bavarian Forest National Park. – Forest Ecology and Management, 255, 2416–2433.

Hodgson, M.E., Jensen, J.R., Schmidt, L., Schill, S., Davis, B. 2003. An evaluation of LIDAR- and IFSAR-derived digital elevation models in leaf-on conditions with USGS level 1 and level 2 DEMs. – Remote Sensing of Environment, 84, 295–308.

Holmgren, J., Persson, Å. 2004. Identifying species of individual trees using airborne laser scanner. – Remote Sensing of Environment, 90, 415–423.

Howard, J.A. 1991. Remote Sensing of Forest Resources. Theory and application, London, Chapman & Hall. 420 pp.

Jennings, S.B., Brown, N.D., Sheil, D. 1999. Assessing forest canopies and understory illumination: canopy closure, canopy cover and other measures. – Forestry, 72, 59−74.

Kato, A., Moskal, L.M., Schiess, P., Swanson, M.E., Calhoun, D., Stuetzle, W. 2009. Capturing tree crown formation through implicit surface reconstruction using airborne lidar data. – Remote Sensing of Environment, 113, 1148–1162.

Kiviste, A. 1997. Eesti riigimetsa puistute kõrguse, diameetri ja tagavara vanuseridade diferentsmudel 1984–1993. a. metsakorralduse takseerkirjelduste andmeil. (Difference equations of stand height, diameter and volume depending on stand age and site factors for Estonian state forests on the basis of 1984–1993 forest inventory data). – Teadustööde kogumik, Eesti Põllumajandusülikool, 189, 63–75. (In Estonian with English summary).

Korhonen, L., Korpela, I., Heiskanen, J., Maltamo, M. 2011. Airborne discrete-return LIDAR data in the estimation of vertical canopy cover, angular canopy closure and leaf area index. – Remote Sensing of Environment, 115, 1065–1080.

Krigul, T. 1968. Laasimise rakendamisest metsamajanduses. (Practicing pruning in Forest Management). – Eesti Põllumajanduse Akadeemia teaduslike tööde kogumik, 50, 121–137. (In Estonian).

Krigul, T. 1972. Metsatakseerimine. (Forest mensuration). Tallinn, Valgus. 358 pp. (In Estonian).

Lang, M. 2010. Metsa katvuse ja liituse hindamine lennukilt laserskanneriga. (Estimation of crown and canopy cover from airborne lidar data). – Forestry Studies / Metsanduslikud Uurimused, 52, 5–17. (In Estonian with English summary).

Lang, M., Arumäe, T., Anniste, J. 2012. Estimation of main forest inventory variables from spectral and airborne lidar data in Aegviidu test site, Estonia. (Lennukilidari ja spektraalse kaugseireandmestiku kasutamine metsa peamiste takseertunnuste hindamiseks Aegviidu katsealal). – Forestry Studies / Metsanduslikud Uurimused, 56, 27–41.

Large, A.R.G., Heritage, G.L. 2009. Laser Scanning – Evolution of the Discipline. – Heritage, G.L., Large, A.R.G. (eds.). Laser Scanning for the Environmental Sciences. John Wiley & Sons, Ltd., Publication, West Sussex, 1–20.

Leica. 2007. Leica ALS50-II. Airborne laser scanner product specifications (760344en-V.07-INT). Leica-Geosystems AG, Heerbrugg, Switzerland. 12 p.

Liang, S. 2004. Quantitative remote sensing of land surfaces. John Wiley & Sons, Inc. Hoboken, New Jersy. 543 pp.

Lõhmus, E. 2004. Eesti metsakasvukohatüübid. (Estonian habitation types). Eesti Loodusfoto, Tartu. 80 pp. (In Estonian).

Marklund, L.G. 1987. Biomass functions for Norway spruce (*Picea abies* (L.) Karst.) in Sweden. Swedish University of Agricultural Sciences, Department of Forest Survey, Report 43.

McGaughey, R.J. 2010. FUSION/LDV: Software for LIDAR Data Analysis and Visualization. March 2010 – FUSION, Version 2.80. United States Department of Agriculture Forest Service Pacific Northwest Research Station.

Næsset, E. 1997a. Determination of mean tree height of forest stands using airborne laser scanner data. – ISPRS Journal of Photogrammetry & Remote Sensing, 52, 49–56.

Næsset, E. 1997b. Estimating Timber Volume of Forest Stands Using Airborne Laser Scanner Data. – Remote Sensing of Environment, 61, 246–253.

Næsset, E., Økland, T. 2002. Estimating tree height and tree crown properties using airborne scanning laser in a boreal nature reserve. – Remote Sensing of Environment, 79, 105–115.

Nilson, A. 2005. Fitness of allometric equation $N = aD^b$ and equation $N = (a + bD)^{-2}$ for modelling the dependence of the number of trees N on their mean diameter D in yield tables. (Allomeetria võrrandi $N = aD^b$ ja võrrandi $N = (a + bD)^{-2}$ sobivusest puude arvu N ja nende keskmise diameetri D seose kirjeldamiseks metsa kasvukäigu tabelites). – Forestry Studies / Metsanduslikud Uurimused, 43, 159–172.

Nilson, T., Kuusk, A. 2004. Improved algorithm for estimating canopy indices from gap fraction data in forest canopies. – Agricultural and Forest Meteorology, 124, 157–169.

Pärt, E. 2013. Personaalne vestlus Keskkonnaagentuuri metsaosakonna juhatajaga. (Interview with The Estonian Environment Agency forest department chairman).

Patenaude, G., Hill, R.A., Milne, R., Gaveau, D.L.A., Briggs, B.B.J., Dawson, T.P. 2004. Quantifying forest above ground carbon content using LiDAR remote sensing. – Remote Sensing of Environment, 93, 368–380.

Popescu, S.C., Zhao, K. 2008. A voxel based lidar method for estimating crown base height for deciduous and pine trees. – Remote Sensing of Environment, 112, 767–781.

Riaño, D., Chuvieco, E., Condés, S., González-Matesanz, J., Ustin, S.L. 2004. Generation of crown bulk density for *Pinus sylvestris* L. from lidar. – Remote Sensing of Environment, 92, 345–352.

Vain, A., Yu, X., Kaasalainen, S., Hyypä, J. 2010. Correcting airborne laser scanning intensity data for automatic gain control effect. – IEEE Geoscience and Remote Sensing Letters, 7, 511–514.

Valentine, H.T., Mäkelä, A. 2005. Bridging process-based and empirical approaches to modeling tree growth. – Tree Physiology, 25, 769–779.

Vaus, M. 2005. Metsatakseerimine. (Forest mensuration). OÜ Halo kirjastus, Tartu. 178 pp. (In Estonian).

Wehr, A., Lohr, U. 1999. Airborne laser scanning – an introduction and overview. – ISPRS Journal of Photogrammetry & Remote Sensing, 54, 68–82.

Yao, W., Krzystek, P., Heurich, M. 2012. Tree species classification and estimation of stem volume and DBH based on single tree extraction by exploiting airborne full-waveform LiDAR data. – Remote Sensing of Environment, 123, 368–380.

Zarnoch, S.J., Bechtold, W.A., Stolte, K.W. 2004. Using crown condition variables as indicators of forest health. Canadian Journal of Forest Research, 34, 1057−1070

Zhao, K., Popescu, S., Meng, X., Pang, Y., Agca, M. 2011. Characterizing forest canopy structure with lidar composite metrics and machine learning. – Remote Sensing of Environment, 115, 1978–1996.

A simple model to estimate forest canopy base height from airborne lidar data

Tauri Arumäe and Mait Lang

Summary

Airborne laser scanning (ALS) is widely used for topological mapping, urban planning (Large & Heritage, 2009) and even archeological studies (Crutchley, 2009). During the last two decades ALS has been used to estimate forest structural characteristics (Næsset, 1997a; Næsset, 1997b; Lang, 2010).

ALS data (Leica ALS50-II) from Järvselja (flight in 2010), South-East Estonia, and Aegviidu (flight in 2008), North-Estonia, test sites (Table 1) was used. Field measurements of tree crown base height were carried out in 2010 in Järvselja and in 2012 in Aegviidu. The lidar data based estimate of canopy base height (H_{VL}) for each forest stand was calculated with the model (1) using the mode value (H_{Mood}) and half of the standard deviation (H_{Stdev}) of the lidar pulse reflection height distribution. The near to ground reflections with the height $h_r \leq 0.5$ m were excluded, to ensure a unimodal height distributions (Figure 2). In Järvselja, the stand canopy base height (H_{VA}) was calculated as the average of the crown-base height (h_{vm}, Figure 1) of ten sample trees. The H_{VA} in Aegviidu was calculated using two or three h_{vm} per sample plot, with the total of eight to twelve sample plots per stand. Simple linear regression was then used to analyze relationships between the measured stand H_{VA} and lidar data based H_{VL}. The influence of forest understory vegetation to the H_{VL} estimations was tested by using reflections with height $h_r \geq 0.5$ m, $h_r \geq 1.0$ m and $h_r \geq 1.5$ m. The dependence of the H_{VL} to H_{VA} relationship on the stand main species (coniferous or deciduous) was analyzed. The regression models were cross-validated on test sites.

The stand canopy base height (H_{VL}) had strong linear relationship to H_{VA}, since coefficient of determination was over 0.8. There was no significant impact on H_{VL} if the lower reflections of point cloud were excluded with the additional filters (Table 2). The H_{VL} was not dependent on main species of forest (Table 3, Figure 4).

The cross-validation of models H_{VL_3} and H_{VL_6} (Table 2) revealed the 1.33 m overestimation of H_{VL} in Aegviidu and the 1.42 m underestimation of H_{VL} in Järvselja. It was, however, concluded that the models are not site specific (Figure 4). This hypothesis is confirmed by the relationship similarities of forest stand canopy base height and stand mean diameter in both test-sites. The differences may have been caused by the four years time gap between the lidar measurements and in-situ data gathering.

Received November 11, 2013, revised January 20, 2014, accepted March 5, 2014

III

Arumäe, T., Lang, M. 2016. A validation of coarse scale global vegetation height map for biomass estimation in hemiboreal forests in Estonia. Baltic Forestry, 22(2), 275−282.

A Validation of Coarse Scale Global Vegetation Height Map for Biomass Estimation in Hemiboreal Forests in Estonia

TAURI ARUMÄE [1,2*] AND MAIT LANG [1,3]

[1]*Institute of Forestry and Rural Engineering, Estonian University of Life Sciences, Kreutzwaldi 5, 51014, Tartu, Estonia; *e-mail: tauri.arumae@rmk.ee*

[2]*State Forest Management Centre, 10149, Tallinn, Estonia*

[3]*Tartu Observatory, 61602, Tõravere, Tartumaa, Estonia*

Arumäe, T.* and Lang, M. 2016. A Validation of Coarse Scale Global Vegetation Height Map for Biomass Estimation in Hemiboreal Forests in Estonia. *Baltic Forestry* 22(2): 275-282.

Abstract

A public release of global vegetation height map, based on data from spaceborne lidar GLAS, was validated using forest management inventory (FI) data and airborne laser (ALS) data from two 15 × 15 km test sites in Estonia: the first one in Aegviidu and the second one in Laeva. For each global vegetation height (GVH) map pixel located in the test sites we calculated forest height based on the FI data and on ALS data. Linear regression analysis was then used to evaluate the relationships between GVH map values (H_{GVH}), FI forest height (H_{FI}) and ALS-based Lorey's forest height (H_{ALS}). In the second test H_{GVH} and H_{ALS} were evaluated for estimating forest biomass using regression analysis. The biomass was calculated for each GVH pixel using FI data and allometric regression models.

The correlation between H_{GVH} and H_{FI} or H_{ALS} in both test sites was weak – in Aegviidu $r < 0.25$ and in Laeva $r < 0.15$; and, the relationship was not statistically significant in Laeva. The airborne lidar based H_{ALS} had a strong positive correlation with forest biomass and the determination coefficient of linear regression was $R^2 > 0.6$ ($p < 0.01$) in both test sites. The relationship between H_{GVH} and biomass was scattered and determination coefficient for linear model was small ($R^2 < 0.15$, $p < 0.01$).

Although in this study only weak correlation between measured forest heights (H_{FI} and H_{ALS}) and spaceborne lidar based HGVH was found, the GVH type estimates are essential for the areas, where forest inventory data or airborne lidar data is not available. The obtained results show that forest height estimates from ALS or spaceborne lidar could be used directly for estimating biomass in managed hemiboreal forests at coarse spatial resolution.

Keywords: hemiboreal forests, airborne laser data, forest inventory data, global vegetation height map, forest biomass.

Introduction

Airborne laser scanning (ALS) has been a success story in operational forest inventories in many countries. The ALS data based forest structure variables (Næsset 1997, Korhonen et al. 2011, Lang et al. 2012) can further be used for monitoring carbon balance and biomass stocks (Patenaude et al. 2004, Popescu and Zhao 2008, Popescu et al. 2011, Zhang et al. 2014). In addition to the regional laser scanning from airplanes or drones, spaceborne laser scanning has also gained importance for global scale applications (Lefsky 2010). The Geoscience Laser Altimeter System (GLAS) aboard Ice, Cloud, and Land Elevation Satellite (ICESat, Schutz et al. 2005) has been used to construct global wall-to-wall maps of biomass and carbon (Hese et al. 2005, Boudreau et al. 2008, Yu et al. 2015, Lefsky et al. 2005, Zhang et al. 2014), to estimate vegetation height (Gwenzi and Lefsky 2014, Miller et al. 2011, Lefsky 2010, Simard et al. 2011), for monitoring and mapping forest disturbances (Dolan et al. 2011, Hayashi et al. 2015) and for digital elevation maps (Duncanson et al. 2010, Chen 2010). The spaceborne products cover wider areas with smaller time-lapse providing a fast overview at coarser spatial resolution compared to airborne laser data. However, before these global products can be used for local estimation of biomass or other variables, a careful validation should be conducted.

The height of a forest or a tree is the basic variable in forest description and modelling. Forest height is also the most important parameter for estimating volumes, biomass, carbon stocks etc. The most commonly used tree height definition is the vertical distance from the root collar of the tree to the highest branch or top (Van Laar and Akça 2010). While the height definition seems to be clear, the determination of root collar position is already a source of error - for example in drained forests in former swamps, where the soil surface sinks due to the organic matter decay after draining (Jürimäe 1966).

Average height of several trees growing on an area can be calculated in different ways. For a rather homogeneous part of a forest (forest stand), the height may be calculated as an average of single measured tree heights. More commonly Lorey's height is used, which is stem basal area weighted average height. The average height of multiple forest stands, as found within a larger area corresponding for example to a global scale map pixel, is not a usual variable in forest inventories. The area of the global vegetation height (GVH) map (Simard et al. 2011) pixel used in this study is about 50 hectares in Estonia coordinate system. The average forest stand size in our test sites is about 2 hectares, and the 50 hectare pixels are internally heterogeneous with forests up to 30 metres in height mixed with crop fields and other land use types at the edges of forest patches. Depending on where the GLAS pulse hits the pixel, the estimated height might not reflect the average forest height at all.

Forest height and biomass are known to be well correlated (Marklund 1987, Repola 2009, Zianis et al. 2005) and biomass monitoring is another common by-product of global vegetation height maps especially for areas with no ALS data cover or forest inventory (FI) data. Forest biomass is also the key variable for estimating carbon stocks (Latifi et al. 2015, Main-Knorn et al. 2013); therefore, the validation of global vegetation height map products is important before making any further analyses.

The goal of this study was to validate the freely available global vegetation height map (GVH) published by Simard et al. (2011), in our two Estonian test sites with diverse multi-layer and mixed hemiboreal forests. Biomass estimates were calculated using the forest management inventory (FI) database and Repola (2008, 2009) biomass models. Biomass was then calculated for each GVH map pixel found in our test sites. Then the forest height from the GVH map (H_{GVH}) and ALS based forest height (H_{ALS}) were tested as biomass predictor variables using regression analysis.

Material and Methods

Test sites and forest inventory data

The first validation site (15×15 km) is located near Aegviidu (centre coordinates in EPSG:3301 projection: 6572701 N; 587333 E), in North Estonia (Figure 1) and was established by Anniste and Viilup (2011) for ALS data based forest inventory study. The second 15×15 km test site is located near Laeva (centre coordinates in EPSG:3301 projection: 6490854 N; 642472 E), in the south-eastern part of Estonia (Figure 1) and was established in 2013. The test site is described in more detail by Lang et al. (2014).

Aegviidu test site is dominated by coniferous forests with the main species being Scots pine (*Pinus sylvestris* L.). Laeva test site is dominated by deciduous forests where the most widespread species are silver birch (*Betula pendula* Roth) and trembling aspen (*Populus tremula* L.). These two contrasting test sites represent typical hemiboreal managed forests.

The FI database contained data for 14,263 stands in Aegviidu test site and data for 8950 stands in Laeva. The forest stands in Aegviidu test site were inventoried during 2007-2010, the data for Laeva test site was collected mostly in 2013 during regular forest management inventory. The forest height in FI is defined as the average height of trees with the square mean diameter. To match the GLAS data collection time period used by Simard et al. (2011) the FI data was predicted to the year 2005 using algebraic difference model published by Kangur et al. (2007).

The biomass for each GVH pixel was calculated using Repola (2008, 2009) models based on data from the FI database. Next, the FI stand map was split and sampled according to the GVH pixel shape files (Figure 1). For each GVH pixel forest inventory data based height (H_{FI}) and biomass were then calculated as the stand polygon area weighted mean values.

Global vegetation height map

The spaceborne lidar based GVH map published by Simard et al. (2011) is constructed using GLAS data from ICESat mission. They used a raster based approach to construct the GVH map: the global map was first divided into 1×1 km pixels, which then were classified as forest and non-forest using the Global Land Cover Map (GlobCover, Hagolle et al. 2005). The GLAS transmits laser pulses (1064 nm), which have a footprint of about 60 m in diameter on ground and records the reflected signal waveform (Schutz et al. 2005), so each pulse covers less than one percent of the GVH map pixel area in Estonia. The data used for the map was collected in 2005 from May 20th to June 26th. This is the period just after the active bud burst and time of rapid increase of foliage mass and the time of leaf properties change in Estonia. Therefore for the validation we used two ALS datasets, one from leaf-off and second from leaf-on conditions as the leaf properties and canopy transmittance vary substantially between spring and summer time, especially in deciduous forests (Brandtberg 2007). For calculating the forest canopy height (H_{GVH}) Simard et al. (2011) used the GLAS level-2 altimetry GLA14 product version 31, which is designed for land surface elevation assessment. The GLA14 product defines the pulse return signal start as the location, at which the signal is 3.5 times the noise standard deviation. Ground is defined as the last Gaussian peak of the signal. The relative height RH100 is then defined as

Figure 1. Aegviidu and Laeva test sites (left). An example of the Global Vegetation Height (GVH) pixel borders over the forest inventory (FI) stand map in Aegviidu test site (right)

the distance between these two signal peaks and is then used for modelling the top canopy for GVH map (H_{GVH}).

Simard et al. (2011) used validation data from 66 globally distributed FLUXNET sites, which have measured canopy height data available and showed the linear relationship with $R^2 = 0.49$ (with outliers excluded $R^2 = 0.69$). Due to sparse or missing GLAS data in some regions, Moderate Resolution Imaging Spectroradiometer (MODIS) data, elevation data from the Shuttle Radar Topography mission and climatology map data etc., were used to estimate vegetation height in for the pixels.

We extracted the pixel boundaries of the GVH raster map as a new map of vector polygons, which was then resampled into Estonian basic map coordinate system (EPSG:3301). This approach decreases substantially the errors related to georeferencing of the large pixels for spatial queries from detailed maps. The size of each GVH polygon was after the coordinate system transformation about 500 by 1000 metres (Figure 1). The polygons were used as the elementary observation units and are further in the text referred as GVH pixels.

The list of the GVH pixels was filtered to select those which had forest land over 75 percent and clear cut area during 1996…2013 less than 50 percent. The stand replacing disturbance map was obtained from Urmas Peterson (Tartu Observatory, personal contacts) and the map construction methods are described by Peterson et al. (2004). The total count of GVH pixels left after the filtering in Aegviidu test site was 226 and in Laeva test site we had 69 GVH pixels.

Airborne lidar data

The leaf-on ALS data for Aegviidu was collected in 2008 summer from July to beginning of September and leaf-off ALS data set was collected in May 2009. In Laeva test site, both leaf-off and leaf-on datasets were collected in 2013: leaf-off dataset in May and leaf-on dataset in July. All ALS data was collected by Estonian Land Board using the Leica ALS50-II scanner on board a Cessna Grand Caravan 208B airplane. This Leica scanner operates on the same 1,064 nm wavelength as does the GLAS. In Aegviidu test site the average point density in the ALS data was 0.45 points m^{-2}. In Laeva test site the point density was approximately 2 points m^{-2}. The ALS data was processed using FUSION/LDV freeware (McGaughey 2014) modules GroundFilter, GridSurfaceCreate, PolyClipData and CloudMetrics. ALS data based digital terrain model with a 5 metres pixel was created with GroundFilter and GridSurfaceCreate and was then used to calculate pulse return height relative to the ground. The ALS point clouds were extracted using the GVH pixel polygon shapefiles and the FI stand polygons with PolyClipData module. Based on previous research in Aegviidu test site (Lang et al. 2012), different height statistics were calculated with CloudMetrics and 80-percentile was chosen to estimate H_{ALS} with linear model 1. Reflections below two metres were excluded from the percentile calculations to reduce the influence of near ground vegetation.

$$H_{ALS} = a_i \times P_{80} + b_i, \qquad (1)$$

where

H_{ALS} is the ALS-based forest height (m) for the GVH pixel,

P_{80} is 80-percentile of the ALS point cloud,

a_i, b_i are estimated parameters depending on test site and leaf-on/leaf-off flights. Values for a_i and b_i are given in Table 1.

Table 1. Model (1) parameter values and model statistics for test sites and different phenology stages

Test site	ALS flight time	Model (1) parameters and statistics				
		a_i	b_i	R^2	RSE (m)	*p*-value
Laeva	Leaf-off	1.27	- 3.65	0.93	1.83	< 0.01
	Leaf-on	1.21	- 4.01	0.96	1.32	< 0.01
Aegviidu	Leaf-off	0.94	3.63	0.96	0.83	< 0.01
	Leaf-on	0.94	3.48	0.94	1.04	< 0.01

The site and phenology specific models (Eq.(1), Table 1) for H_{ALS} were created using measurements from 46 forest stands in Aegviidu (Arumäe and Lang 2013) and using data from 94 permanent forest growth study sample plots (Kiviste et al. 2015) in Laeva test site. The plots in Laeva were measured in 2010 and 2011 and in Aegviidu measurements were done in 2011. The parameters for the regression model (1) were estimated using R (R Core Team 2014) lm procedure.

Using the same lm procedure we compared all the derived forest heights (H_{FI}, H_{ALS} and H_{GVH}). Bias estimates for these regression analyses were calculated as $\sum(Y - X) / N$, where N is the number of observations, X is the independent variable and Y is the dependent variable.

Results

Forest height

We found only a weak correlation ($r < 0.25$, $p < 0.01$) between H_{GVH} calculated by Simard et al. (2011) and H_{ALS} in both test sites (Figure 2A and 2D). In Laeva the correlation between H_{GVH} and H_{ALS} was not statistically significant ($p > 0.05$). Similar weak correlations ($r < 0.2$) were found for H_{GVH} and H_{FI} in Aegviidu and Laeva as seen in Figure 2B and 2E. The relationship was significant in Aegviidu ($p < 0.01$), but in Laeva the relationship was not statistically significant ($p > 0.05$). Figure 2 shows the lack of variation in H_{GVH} compared to H_{ALS} and H_{FI} and a large error in estimating heights below 15 metres. On the other hand, as found in many previous studies, there was a strong correlation between H_{ALS} and H_{FI} using linear model in both test sites (Figure 2C and 2F) with coefficient of correlation over 0.6 ($p < 0.01$).

The bias on Figure 2F is caused partially by the time difference between FI height data (predicted to year 2005) and ALS data acquisition (2013). *T*-test confirmed that bias in all cases was statistically significant ($p < 0.01$). The large bias may also be caused by using the same 80-percentile (P_{80}) height method for estimating canopy height for a large 50 hectare pixel and a small 10-15 metre radius plot. To estimate the model (1) small sample plots were used as is the usual approach in forest inventory. The model was then applied to the GVH pixel-based point clouds. The explanation for the extracted point cloud size influence to the H_{ALS} follows from the definition of P_{80}: this is the height in ALS point cloud from which 80 % of points are located lower. While P_{80} is usually well correlated with canopy top height we do not know, how high the rest 20 % of points are located. In point clouds extracted for 50 hectare GVH pixels containing different forest stands, the P_{80} is determined by the highest stands (or groups of trees) covering roughly 20 % of the area. For comparison, in Laeva test site we calculated P_{80} of ALS point height distribution for GVH pixels from a 20 m resolution raster map of P_{80} instead of 50 ha large original point clouds. The average forest height in Laeva test site was then 2.8 metres lower when calculated with the model (1) and using P_{80} averaged from the 20 m raster map for each GVH pixel.

There was no substantial difference in relationship between H_{GVH} and H_{ALS} in leaf-off and leaf-on ALS data in Aegviidu test site, where evergreen coniferous forests are dominating (Table 2). In Laeva test site, where deciduous broadleaf forests are in majority, the linear correlation between H_{GVH} and H_{ALS} was not significant (Table 2).

The H_{GVH} relationship to H_{ALS} or H_{FI} at GVH pixel level was absent or weak (Figure 2A, 2D). To verify if H_{GVH} estimates are reasonable, when the GVH pixel values are averaged over a larger area we compared the mean H_{GVH}, H_{FI} and H_{ALS} on test site basis. The results (Table 3) showed no significant differences for leaf-on and leaf-off ALS datasets in Aegviidu and mean H_{ALS} for both spring and summer datasets were about 1.8 metres lower than H_{GVH}. To compare the significance of differences of test site mean forest height estimations *t*-test was used. In Laeva the difference between leaf-off and leaf-on ALS height estimates was significant (Table 3). Based on leaf-off ALS dataset, the mean H_{ALS} was 3.0 metres lower than using leaf-on ALS dataset. This decrease in test site mean height is probably related to the ALS pulse being split more per pulse in leaf-off conditions compared to leaf-on conditions in deciduous forests. In Laeva, the share of first returns from total number of returns was 85.5 % in leaf-on conditions and 76.5 % in leaf-off condition. In Aegviidu, where evergreen coniferous forests dominate, the corresponding shares were 75 % and 71.8 %. The overall mean of H_{GVH} and H_{ALS} in leaf-on ALS datasets was not significantly different in Laeva. H_{ALS} was calculated using the large 50-hectare point clouds and possible influence of the ALS point cloud sample was discussed earlier in the text.

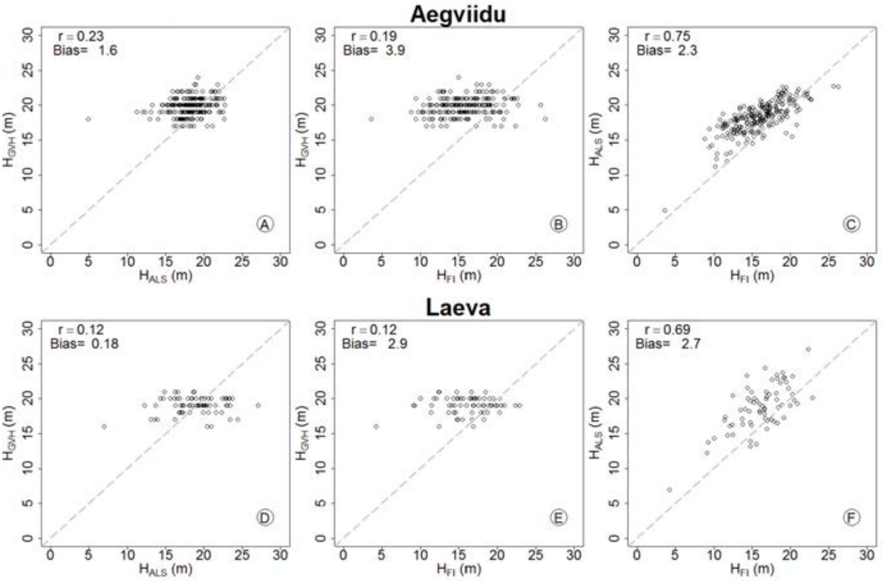

Figure 2. Correlation between forest height estimates using GVH map pixels as observations. Leaf-on ALS data is used for the Figures

Table 2. The relationship between H_{GVH} and H_{ALS} described by linear regression model ($H_{GVH} = aH_{ALS} + b$)

Test site	ALS flight time	H_{GVH} and H_{ALS} linear regression model parameters				
		b	a	RSE	R^2	*p*-value
Laeva	Leaf-off	19.58	*- 0.04*	1.22	0.00	> 0.45
	Leaf-on	18.19	*0.04*	1.22	0.00	> 0.32
Aegviidu	Leaf-off	16.98	0.16	1.27	0.08	< 0.01
	Leaf-on	17.42	0.13	1.29	0.05	< 0.01

Table 3. Overall average of H_{GVH} compared to H_{ALS} and H_{FI} averages in Aegviidu and Laeva test sites. Standard error is given in brackets

Test site	ALS flight time	Forest height estimate		
		H_{ALS} (m)	H_{GVH} (m)	H_{FI} (m)
Aegviidu	Leaf-off	18.0 (0.15)	19.8 (0.10)	15.9 (0.21)
	Leaf-on	18.2 (0.15)		
Laeva	Leaf-off	15.8 (0.38)	19.0 (0.15)	16.1 (0.40)
	Leaf-on	18.8 (0.41)		

Biomass

H_{GVH} and biomass (Figure 3A) had only weak correlation but the relationship was still significant ($R^2 = 0.11$, $p < 0.01$). Residual standard error (RSE) was 19.1 t/ha (22 %). Figure 3B shows that H_{ALS} is well correlated to biomass, which was calculated for each GVH pixel in Aegviidu test site and there is a strong linear relationship ($R^2 > 0.6$, $p < 0.01$). RSE for H_{ALS} and biomass relationship was 12.1 t/ha (14 %). Similar results were found in Laeva test site, but as the H_{GVH} relations to H_{ALS} and H_{FI} were weaker compared to Aegviidu (Figure 2), the biomass to H_{GVH} relationship was also weaker ($R^2 < 0.1$, $p < 0.01$).

Discussion

The goal of this study was to validate the spaceborne lidar based vegetation height map product in two contrasting hemiboreal forest test sites and validate how forest height estimated from spaceborne lidar is applicable for biomass estimation. Such products are viable for large forested areas in Eastern Europe, where access to ALS or FI data is limited.

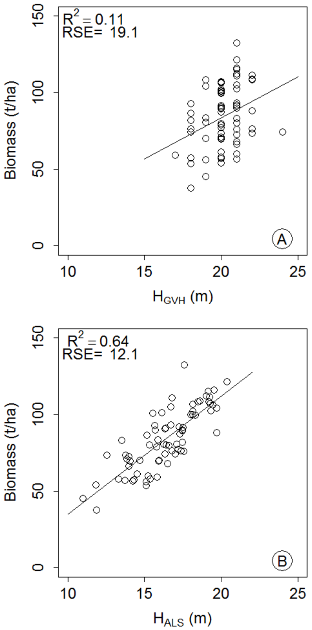

Figure 3. The biomass of forest trees calculated using Repola (2008, 2009) models in Aegviidu test site in relation to H_{GVH} (A) and H_{ALS} (B)

Forest height from global vegetation height map H_{GVH} showed weak correlations on pixel based comparison with FI data and ALS data based forest heights and this can be due to several reasons.

Firstly, there is difference in forest height definition: Simard et al. (2011) modelled the top canopy height whereas in our dataset the average forest height was available.

Secondly, part of the scatter in the relationships could be due to geometric inaccuracy and resampling. The forest stand border errors in forest inventory map are known to be in average about 10 metres. The coordinate errors of the used *in situ* sample plots for estimating the forest height model for ALS point cloud samples were also with up to 10 m location errors. However, much larger position errors with the size of about half a pixel (250...500 m) may be present in the coarse spatial resolution global GVH map. There is also an influence to H_{GVH} calculated from additional gap filling procedure via MODIS data, as MODIS single observation location is known to have substantial differences with the final gridded image as described by Tan et al. (2006).

Thirdly, some mismatch of H_{GVH} and H_{ALS} could be the result of the chosen percentile method for extracting data from the large ALS point clouds for each GVH pixel. To calculate ALS point cloud statistics for the large GVH pixels and small sample plots we selected the same 80-percentile method. The P_{80} based forest height model (1) was estimated from point clouds extracted for small circular plots and applied to large point clouds with the size of 50 hectares. We compared the average H_{ALS} for Laeva test site calculated from large GVH pixel size point clouds and alternatively from 20 by 20 m small point clouds. The mean forest height estimate was 2.8 metres lower when using small point cloud samples compared to large ALS point cloud subsets. So, in heterogeneous forests the point cloud sampling procedure has an influence to the forest height estimates.

Simard et al. (2011) also stated that the GVH product accuracy was lower in tall broadleaved forests (> 40 metres) with high canopy cover. Although the forest height in our test sites were usually lower than 30 m, this could also be the reason for weaker correlations in Laeva test site, which is dominated by broadleaved forest with high canopy cover. The explanation for the 2.8 metres smaller average height in leaf-off compared to leaf-on datasets in Laeva (Table 3) can also be caused by the dominance of deciduous forests in Laeva, as such difference in test site average height for Aegviidu was not found. Another possible reason for differences could be due to the time difference in data acquisition – the GLAS data was from 2005 and ALS scanning for Laeva was done in 2013.

Our analysis showed that the forest height range of H_{GVH} was narrower than the range of H_{ALS} or H_{FI}. We excluded at the beginning the GVH pixels with large disturbances to exclude outdated H_{FI}, but this resulted in removing also a substantial part of the young forests with smaller height and the forest height range was due to that narrower. Further tests proved that the removal of the filters didn't increase H_{GVH} height variation meaning that the height estimates for forest lower than 15 m are problematic for this GVH map in managed hemiboreal forests. However, Simard et al. (2011) modelled canopy top height and if we take in consideration that the 50 hectare GVH pixels are heterogeneous (average stand size in our test site is 2 hectares) then the GVH map values could be to some extent correct, since within 50 ha of forest land in Laeva or Aegviidu the occurrence of a high forest patch is common. To reduce the error caused by the heterogeneous landscapes we also applied the filter of forest land cover over 75 percent which improved the height correlations of H_{FI} and H_{ALS} but still gave no significant improvement on H_{GVH} to H_{FI} or H_{ALS} correlations. The large pixel based sampling error could be solved by using smaller pixel size.

If carefully validated, such wall-to-wall vegetation height maps could be well used for biomass and carbon monitoring, especially in areas where FI and ALS data are not available. As shown in Figure 3 GVH pixel based H_{ALS} had a strong linear correlation to biomass with a RSE of 12 t/ha. When we compare pixel level H_{GVH} and biomass relationship the results showed only a weak correlation with a 19 t/ha error. The spaceborne lidar based biomass estimation could also be improved by using forest cover (Sexton et al. 2013, Langanke 2013) maps additionally to the vegetation height maps.

To make a better error analysis of H_{GVH} estimates, we propose that next versions of global vegetation height maps must incorporate data quality description layer similarly to MODIS products with information of the number of GLAS measurements within the pixel and applied gap filling producers. In addition to ALS synthetic aperture radar (SAR) could be used for H_{GVH} validation or development, since SAR coherence has been found to have a strong relationship to ALS based forest height estimates (Olesk et al. 2015). There is a regular ALS scanning done by Estonian Land Board covering 1/4 of Estonia each year in spring and 1/5 of Estonia in summer, which could be a valuable data for testing the next versions of GVH or other similar products. Simard et al. (2011) show that GLAS data cover decreases with increasing latitude of geographic location. Our two test sites, Laeva and Aegviidu, are located almost at the limit of the GLAS data cover. Some additional test sites from Finland, Latvia and Lithuania could provide a latitudinal gradient for validating the next versions of GVH maps.

Conclusion

Based on this research we can conclude that the global vegetation height map (Simard et al. 2011) is not well applicable for forest height estimation in managed mixed species hemiboreal forests. Comparison on a pixel basis showed only weak correlation between H_{GVH} and H_{ALS} ($r < 0.25$, $p < 0.01$) and H_{GVH} to H_{FI} ($r < 0.2$, $p < 0.01$). Average forest height from GVH map was similar to H_{ALS} except in deciduous forests in spring. Mean height of GVH pixel is underestimated by 3 m from ALS data when sampling by small e.g. 10 m radius subsets instead of 50 ha subset.

Biomass estimates had a strong linear correlation to H_{ALS}, so in the future global vegetation height products, if carefully validated, could be used directly for biomass estimates, as similar correlations were shown for H_{GVH} and biomass relationship. The global vegetation height maps could also be improved by having a smaller pixel size, which would reduce the heterogeneity inside a pixel and additional forest cover maps would improve biomass estimates.

To improve the validation of such products, these maps should also include an additional layer showing pixel data quality and information on the number of used GLAS pulses per pixel.

Acknowledgements

The authors would like to thank the Estonian Land Board for the airborne lidar data. Data acquisition was financed by Estonian State Forest Management Centre. Data analysis was supported by the Ministry of Education and Research through grant IUT21-4. Estonian Network of Forest Research Plots is supported by the Estonian State Forest Management Centre and the Estonian Environmental Investment Centre. Authors are also thankful for the helpful and constructive comments from the anonymous reviewers.

References

Anniste, T. and Viilup, Ü. 2011. Metsa takseertunnuste määramisest laserskanneerimise abil [Estimation of forest characteristics with the laser scanning.]. *Artiklid ja uurimused* 10: 38–53 (in Estonian).

Arumäe, T. and Lang, M. 2013. A simple model to estimate forest canopy base height from airborne lidar data. *Forestry Studies* 58: 46–56 (in Estonian).

Boudreau, J., Nelson, R.F., Margolis, H.A., Beaudoin, A., Guindon, L. and Kimes, D.S. 2008. Regional aboveground forest biomass using airborne and spaceborne LiDAR in Québec. *Remote Sensing of Environment* 112: 3876-3890.

Brandtberg, T. 2007. Classifying individual tree species under leaf-off and leaf-on conditions using airborne lidar. *ISPRS Journal of Photogrammetry & Remote Sensing* 61: 325-340.

Chen, Q. 2010. Assessment of terrain elevation derived from satellite laser altimetry over mountainous forest area using airborne lidar data. *ISPRS Journal of Photogrammetry and Remote Sensing* 65: 111-122.

Dolan, K.A., Hurtt, G.C., Chambers, J.Q., Dubayah, R.O., Frolking, S. and Masek, J.G. 2011. Using ICESat's Geoscience Laser Altimeter System (GLAS) to assess large-scale forest disturbance caused by hurricane Katrina. *Remote Sensing of Environment* 115: 86-96.

Duncanson, L.I., Niemann, K.O. and Wulder, M.A. 2010. Estimating forest canopy height and terrain relief from GLAS waveform metrics. *Remote Sensing of Environment* 114: 138-154.

Gwenzi, D. and Lefsky, M.A. 2014. Modelling canopy height in a savanna ecosystem using spaceborne lidar waveforms. *Remote Sensing of Environment* 154: 338-344.

Hagolle, O., Lobo, A., Maisongrande, P., Cabot, F., Duchemin, B. and De Pereyra, A. 2005. Quality assessment and improvement of temporally composited products of remotely sensed imagery by combination of VEGETATION 1 and 2 images. *Remote Sensing of Environment* 94: 172–186.

Hayashi, M., Saigusa, N., Oguma, H., Yamagata, Y. and Takao, G. 2015. Quantitative assessment of the impact of typhoon disturbance on a Japanese forest using satellite laser altimetry. *Remote Sensing of Environment* 156: 216-225.

Hese, S., Lucht, W., Schmullius, C., Barnsley, M., Dubayah, R., Knorr, D., Neumann, K., Riedel, T. and Schröter, K. 2005. Global biomass mapping for an improved understanding of the CO_2 balance – the Earth observation mission Carbon-3D. *Remote Sensing of Environment* 94: 94-104.

Jürimäe, A. 1966. Metsamaade kuivendamine [Drainage of forest-lands]. Tartu, Eesti, Põllumajanduse Akadeemia, 199 pp. (in Estonian).

Kangur, A., Sims, A., Jõgiste, K., Kiviste, A., Korjus, H. and von Gadow, K. 2007. Comparative modeling of stand development in Scots pine dominated forests in Estonia. *Forest Ecology and Management* 250: 109-118.

Kiviste, A., Hordo, M., Kangur, A., Kardakov, A., Laarmann, D., Lilleleht, A., Metslaid, S., Sims, A. and Korjus, H. 2015. Monitoring and modelling of forest ecosystems: the Estonian Network of Forest Research Plots. *Forestry Studies* 62: 26-38.

Korhonen, L., Korpela, I., Heiskanen, J. and Maltamo, M. 2011. Airborne discrete-return LIDAR data in the estimation of vertical canopy cover, angular canopy closure and leaf area index. *Remote Sensing of Environment* 115: 1065-1080.

Lang, M., Arumäe, T. and Anniste, J. 2012. Estimation of main forest inventory variables from spectral and airborne lidar data in Aegviidu test site, Estonia. *Forestry Studies* 56: 27-41.

Lang, M., Arumäe, T., Lükk, T. and Sims, A. 2014. Estimation of standing wood volume and species composition in managed nemoral multi-layer mixed forests by using nearest neighbor classifier, multispectral satellite images and airborne lidar data. *Forestry Studies* 61: 47-68 (in Estonian).

Langanke, T. 2013. GIO land (GMES/Copernicus initial operations land) High Resolution Layers (HRLs) – summary of product specifications. GIO land team at the EEA, Manual, electronic document, 15 pp.

Latifi, H., Fassnacht, F.E., Hartig, F., Berger, C., Hernández, J., Corvalán, P. and Koch, B. 2015. Stratified aboveground forest biomass by remote sensing data. *International Journal of Applied Earth Observation and Geoinformation* 38: 229-241.

Lefsky, M.A., Turner, D.P., Guzy, M. and Cohen, W.B. 2005. Combining lidar estimates of aboveground biomass and Landsat estimates of stand age for spatially extensive validation of modeled forest productivity. *Remote Sensing of Environment* 95: 549-558.

Lefsky, M.A. 2010. A global forest canopy height map from the Moderate Resolution Imaging Spectroradiometer and the Geoscience Laser Altimeter System. *Geophysical Research Letters* 37, L15401.

Main-Knorn, M., Cohen, W.B., Kennedy, R.E., Grodzki, W., Pflugmacher, D., Griffiths, P. and Hostert, P. 2013. Monitoring coniferous forest biomass change using Landsat trajectory-based approach. *Remote Sensing of Environment* 139: 277-290.

Marklund, L.G. 1987. Biomass functions for Norway spruce (*Picea abies* (L.) Karst.) in Sweden. Swedish University of Agricultural Sciences, Department of Forest Survey, Report 43.

McGaughey, R.J. 2014. FUSION/LDV: Software for LIDAR Data Analysis and Visualization. March 2010 – FUSION, Version 3.42. United States Department of Agriculture Forest Service Pacific Northwest Research Station, 179 pp.

Miller, M.E., Lefsky, M. and Pang, Y. 2011. Optimization of Geoscience Laser Altimeter System waveform metrics to support vegetation measurements. *Remote Sensing of Environment* 115: 298-305.

Næsset, E. 1997. Estimating timber volume of forest stands using airborne laser scanner data. *Remote Sensing of Environment* 61: 246-253.

Olesk, A., Voormansik, K., Tamm, T., Noorma, M. and Praks, J. 2015. Seasonal effects of estimation of height of boreal and deciduous forests from intererometric TanDEM-X coherence data. *IEEE Journal of Selected Topics in Applied Earth Observations and Remote Sensing* 99: 1-8.

Patenaude, G., Hill, R.A., Milne, R., Gaveau, D.L.A, Briggs, B.B.J. and Dawson, T.P. 2004. Quantifying forest above ground carbon content using LiDAR remote sensing. *Remote Sensing of Environment* 93: 368-380.

Peterson, U., Püssa, K. and Liira, J. 2004. Issues related to delineation of forest boundaries on Landsat Thematic Mapper winter images. *International Journal of Remote Sensing* 25 (24): 5617-5628.

Popescu, S.C. and Zhao, K. 2008. A voxel based lidar method for estimating crown base height for deciduous and pine trees. *Remote Sensing of Environment* 112: 767-781.

Popescu, S.C., Zhao, K., Neuenschwander, A. and Lin, C. 2011. Satellite lidar vs. small footprint airborne lidar: Comparing the accuracy of aboveground biomass estimates and forest structure metrics at footprint level. *Remote Sensing of Environment* 115: 2786-2797.

R Core Team. 2014. R: A language and environment for statistical computing. R Foundation for Statistical Computing, Vienna, Austria. URL http://www.R-project.org/.

Repola, J. 2008. Biomass Equations for Birch in Finland. *Silva Fennica* 42: 605–624.

Repola, J. 2009. Biomass Equations for Scots Pine and Norway Spruce in Finland. *Silva Fennica* 43: 625-647.

Schutz, B.E., Zwally, H.J., Shuman, C.A., Hancock, D. and DiMarzio, J.P. 2005. Overview of the ICESat Mission. *Geophysical Research Letters*, 32.

Sexton, J.O., Bax, T., Siqueira, P., Swenson, J.J. and Hensley, S. 2009. A comparison of lidar, radar, and field measurements of canopy height in pine and hardwood forests of southeastern North America. *Forest Ecology and Management* 257: 1136-1147.

Simard, M., Pinto, N., Fisher, J.B. and Baccini, A. 2011. Mapping forest canopy height globally with spaceborne lidar. *Journal of Geophysical Research* 116.

Tan, B., Woodcock, C., Hu, J., Zhang, P., Ozdogan, M., Huang, D., Yang, W., Knyazikhin, Y. and Myneni, R. B. 2006. The impact of gridding artifacts on the local spatial properties of MODIS data: Implications for validation, compositing, and band-to-band registration across resolutions. *Remote Sensing of Environment* 105: 98 – 114.

Van Laar, A. and Akça, A. 2010. Forest Mensuration. United Kingdom, Springer, 384 pp.

Yu, Y., Xiguang, Y. and Fan, W. 2015. Estimates of forest structure parameters from GLAS data and multi-angle imaging spectrometer data. *International Journal of Applied Earth Observation and Geoinformation* 38: 65-71.

Zhang, G., Ganguly, S., Nemani, R.R., White, M.A., Milesi, C., Hashimoto, H., Wang, W., Saatchi, S., Yu, Y. and Myneni, R.B. 2014. Estimation of forest aboveground biomass in California using canopy height and leaf area index estimated from satellite data. *Remote Sensing of Environment* 151: 44-56.

Zianis, D., Muukkonen, P., Mäkipää, R. and Mencuccini, M. 2005. Biomass and stem volume equations for tree species in Europe. *Silva Fennica Monographs* 4, 63 pp.

Received 26 October 2015
Accepted 25 January 2016

IV

Olesk, A., Praks, J., Antropov, O., Zalite, K., **Arumäe, T.**, Voormansik, K. 2016. Interferometric SAR coherence models for characterization of hemiboreal forests using TanDEM-X data. Remote Sensing, 8(9), 700.

remote sensing

MDPI

Article

Interferometric SAR Coherence Models for Characterization of Hemiboreal Forests Using TanDEM-X Data

Aire Olesk [1,2,*], **Jaan Praks** [3], **Oleg Antropov** [3,4], **Karlis Zalite** [2,5], **Tauri Arumäe** [6] **and Kaupo Voormansik** [2]

[1] University of Tartu, Institute of Physics, W. Ostwaldi 1, 50411 Tartu, Estonia
[2] Department of Space Technology, Tartu Observatory, 61602 Tõravere, Tartumaa, Estonia; karlis.zalite@to.ee (K.Z.); kaupo.voormansik@to.ee (K.V.)
[3] Department of Radio Science and Engineering, Aalto University, P.O. Box 13000, 00076 AALTO, Finland; jaan.praks@aalto.fi (J.P.); oleg.antropov@vtt.fi (O.A.)
[4] VTT Technical Research Centre of Finland, P.O. Box 1000, 02044 VTT, Finland
[5] Department of Physical Geography and Ecosystem Science, Lund University, Sölvegatan 12, 223 62 Lund, Sweden
[6] Institute of Forestry and Rural Engineering, Estonian University of Life Sciences, Kreutzwaldi 5, 51014 Tartu, Estonia; tauri.arumae@rmk.ee
* Correspondence: aire@ut.ee; Tel.: +372-696-2571

Academic Editors: Sangram Ganguly, Zhong Lu and Prasad S. Thenkabail
Received: 31 May 2016; Accepted: 15 August 2016; Published: 25 August 2016

Abstract: In this study, four models describing the interferometric coherence of the forest vegetation layer are proposed and compared with the TanDEM-X data. Our focus is on developing tools for hemiboreal forest height estimation from single-pol interferometric SAR measurements, suitable for wide area forest mapping with limited a priori information. The multi-temporal set of 19 TanDEM-X interferometric pairs and the 90th percentile forest height maps are derived from Airborne LiDAR Scanning (ALS), covering an area of 2211 ha of forests over Estonia. Three semi-empirical models along with the Random Volume over Ground (RVoG) model are examined for applicable parameter ranges and model performance under various conditions for over 3000 forest stands. This study shows that all four models performed well in describing the relationship between forest height and interferometric coherence. Use of an advanced model with multiple parameters is not always justified when modeling the volume decorrelation in the boreal and hemiboreal forests. The proposed set of semi-empirical models, show higher robustness compared to a more advanced RVoG model under a range of seasonal and environmental conditions during data acquisition. We also examine the dynamic range of parameters that different models can take and propose optimal conditions for forest stand height inversion for operationally-feasible scenarios.

Keywords: forest height; radar interferometry; Synthetic Aperture Radar (SAR); TanDEM-X; vegetation mapping; X-band; InSAR; semi-empirical models, coherence; LiDAR

---

1. Introduction

Forest Above Ground Biomass (AGB) is a key variable in the assessment of the state of global forest resources and monitoring its change [1]. Forests are subject to a variety of disturbances, including deforestation, forest degradation, logging operations, forest regrowth and regeneration. Due to the essential role of forests in the global carbon cycle, uncertainties in the AGB estimation affect the accuracy of the carbon stock accounting and can lead to significant uncertainties in the model output. This requires development and implementation of reliable and robust AGB estimation and monitoring methods.

Remote Sens. **2016**, *8*, 700; doi:10.3390/rs8090700 www.mdpi.com/journal/remotesensing

Ground-based inventories are often insufficient for providing frequent up-to-date information on the extent, spatial distribution and dynamics of forests covering vast areas. A more economical approach lies in systematic integration of Earth Observation data with high quality ground measurements. There exists a variety of methods for mapping forest biomass [2], most notably airborne [3] and spaceborne LiDAR (Light Detection And Ranging) scanning [4], satellite optical remote sensing [5] and space-borne imaging radar [6]. Airborne surveys, however, are relatively costly, while approaches using satellite optical data are often obscured by clouds and suffer from a lack of solar illumination, particularly in high latitudes. Furthermore, optical satellite data have limited value for forest biomass estimation, since the reflectance primarily originates from the upper layer of the forest canopy, and the vertical structure is not assessed. In this situation, using Synthetic Aperture Radar (SAR) satellite data might be the most practical option for large-scale forest mapping [7] by being a cost-effective and time-efficient way to obtain regular estimates of forest resources and to provide accurate input for carbon cycle models.

Two widely-known techniques for radar-based AGB estimation are: (1) direct interpretation of the backscattered SAR signal; and (2) radar-based forest height estimation combined with allometric relations. The first approach typically suffers from signal saturation [8], which renders the method unusable for high biomass forests. The saturation level is affected by wavelength, radar polarization, forest characteristics and environmental conditions during the image acquisition. Relationships between AGB and SAR backscatter can be both model-based and empirical. However, training data are typically necessary for this approach to be effective [9–11]. The second widely-adopted family of approaches uses interferometric SAR (InSAR) images to estimate forest height, which is an important forest variable. Furthermore, radargrammetry, a technique that relies on a reference ALS-based DTM, is giving promising results for potential applications in large-area boreal forest AGB mapping [12–14]. The radar estimated forest height can be applied for deriving aboveground forest biomass [15–19], canopy density [20], estimating carbon flux [21], detecting changes in forests [22] or improving the inventory data for remote areas [23].

Most InSAR techniques use coherence, which is a measure of the complex correlation between two SAR images, and it can be related to forest height using appropriate physics-based [24] or empirical relationships. Unfortunately, the estimation of forest height exclusively from interferometric coherence requires a fully-polarimetric measurement that is not routinely and widely available in the case of spaceborne SAR. Another important factor affecting the usability of InSAR coherence is the level of temporal decorrelation when image acquisitions are separated by a time interval. In the case of bistatic TanDEM-X single pass acquisitions, the latter factor can be neglected.

Supervised semi-empirical and empirical methods particularly using linear [19,25–27] and non-linear regression [26–28] and non-parametric models [23] are popular tools for relating InSAR coherence and forest parameters. Approaches relying on InSAR coherence magnitude (e.g., [19,26]) and phase (e.g., [23,27,28] in the presence of external DTM), as well as their combination (as suggested in [24]) were found useful in estimating forest variables. Promising results for model-based forest height estimation were demonstrated over a variety of frequency bands and sites from boreal [17,29–31] to tropical forests [32–34]. However, practically all of these studies were performed only over relatively small test sites and typically required auxiliary data.

Despite successful demonstrations of the potential sophisticated algorithms in several empirical studies, a framework for operational forest height retrieval has not yet been established. In the current work, we try to fill this gap and provide a set of simple, theoretically-justified models and associated methods for relating forest height to available single-polarization coherence data, particularly suitable for wide area (e.g., country-level) mapping. We consider the operational forest height inversion scenarios in the hemiboreal forest environment for enabling downstream services, using only coherence magnitude in absence of any other auxiliary information. Focus is on the coherence magnitude-based forest stand height retrieval, as phase inversion requires additional ground DEM, which is not available globally or is of poor quality. We investigate several simple models suitable for this inversion scenario subject to their suitability, robustness and adequacy of data description and determine the range of validity of these models and the dynamic range of their parameters. The influence of forest tree species is studied, as well, in order to determine if this aspect should be considered during forest height retrieval. Experimental data are represented by bistatic TanDEM-X acquisitions.

Firstly, we establish a simple theoretical framework based on the RVoG model and derive models with different complexity levels. We then investigate the performance of the proposed models by comparing the models with extensive multi-temporal coherence magnitude data acquired over Estonia. This is followed by defining the range of validity of these models for reliable inversion and assessing the inversion parameters for the feasible operational production scenario for three main forest types in the hemiboreal zone.

The paper is organized as follows. In Section 2, we discuss model-based approaches for forest height extraction from InSAR data and present the models examined in the study. Section 3 describes the study areas, TanDEM-X data and reference data used. Section 4 provides an overview of the data processing. Experimental results are presented and discussed in Section 5, and the article is concluded in Section 6.

2. Forest Parameter Relation with Interferometric SAR Measurement

2.1. Interferometric SAR Measurements of Forests

In the case of interferometric SAR (InSAR) measurement, the measured variable is coherence, which is the normalized complex cross-correlation between two complex signals (two SAR images, separated by a baseline) s_1 and s_2 and is defined as:

$$\gamma = \frac{\langle s_1 s_2^* \rangle}{\sqrt{\langle s_1 s_1^* \rangle \langle s_2 s_2^* \rangle}}, 0 \leq |\gamma| \leq 1 \tag{1}$$

where $\langle .. \rangle$ denotes an average over the ensemble of pixels, usually selected by a sliding window of size (azimuth × range) in a single look complex image. Interferometric coherence is essentially a complex variable, combining both the coherence magnitude and interferometric phase. In general, the measured coherence γ can be described as a product of the following factors:

$$\gamma = \gamma_{System} \gamma_{SNR} \gamma_{Temp} \gamma_{Vol} \tag{2}$$

where γ_{System} combines decorrelation caused by measurement system quantization, ambiguities, relative shift of the Doppler spectra and the baseline, γ_{SNR} describes the coherence decrease caused by the finite sensitivity of the system (the signal to noise ratio), γ_{temp} accounts for changes in the target over time and γ_{Vol} describes decorrelation caused by volume scattering over vegetated areas where several scatterers at different heights contribute to scattering [35]. The two last terms depend on target properties and have the largest dynamics when measuring natural targets.

Forest parameter estimation from InSAR measurements assumes that forest causes a decrease of coherence due to volume scattering (referred to as volume decorrelation) and can therefore be characterized by interpreting the coherence (1). The amount of decorrelation depends on the imaging configuration and also on the properties of the volume.

One of the most important descriptors of the volume is the thickness of the volume layer and the attenuation properties of the medium. As can be seen from (2), distinguishing between temporal and volume scattering-induced effects is difficult, and therefore, the measurement is arranged in a way that the temporal decorrelation can be neglected, for example by making measurements for both signals simultaneously.

2.2. RVoG Coherence Model

One of the simplest physics-based models describing volume scattering effects to InSAR coherence γ_{Vol} is the Random Volume over Ground (RVoG) model. It relates the volume induced decorrelation γ_{Vol} in observed interferometric coherence (1) to the physical properties (structure) of the forest layers [36–38]. RVoG is closely associated with the interferometric water cloud model [39], [24] and can be considered a simplified version of the latter when gaps in vegetation are excluded from the analysis [16].

The RVoG is a two-layer model that assumes that a homogeneous layer of volume scatterers, representing the forest canopy, is located over a reflective ground layer, while ignoring the even-bounce scattering mechanism and higher order interactions. The model has been used for retrieving forest parameters from polarimetric interferometric SAR data, which are able to provide a sufficient number of independent measurements. The RVoG model presents the interferometric coherence as a normalized sum of volume coherence γ_V and the polarization ω-dependent ground reflection term $\mu(\omega)$ as:

$$\gamma_{RVoG} = e^{i\phi}\left(\frac{\gamma_V + \mu(\omega)}{1 + \mu(\omega)}\right) \tag{3}$$

where the common ground phase is taken into account with the coefficient, reliant on the ground phase ϕ. The term γ_V is dependent on both the volume layer properties and also on the imaging configuration. The equation (3) can also be presented in the form of:

$$\gamma_{RVoG} = e^{i\phi}\left(1 - \frac{1 - \gamma_V}{1 + \mu(\omega)}\right) \tag{4}$$

where the variable μ occurs only once, as proposed in [31].

The volume decorrelation term γ_V is the Fourier transform of the normalized scattering profile in the vertical direction. When assuming a random isotropic volume, the profile can be modeled with an exponential distribution and γ_V can be written as:

$$\gamma_V = \frac{\int_0^h e^{\sigma z} e^{i\kappa_z z} dz}{\int_0^h e^{\sigma z} dz} \tag{5}$$

where the parameter σ describes the attenuation in the volume layer and is called extinction, and imaging geometry is described by the vertical wavenumber κ_z. It is important to note that in this simplified notation, the extinction parameter σ depends also on the incidence angle θ because $\sigma = \frac{2\sigma_m}{cos(\theta)}$, where σ_m is the extinction coefficient of the medium. After integration, one can write:

$$\gamma_V = \frac{\sigma(e^{h\sigma} e^{i\kappa_z h} - 1)}{(\sigma + i\kappa_z)(e^{h\sigma} - 1)} \tag{6}$$

The RVoG model is obtained by combining Equations (6) and (3). The model depends on imaging geometry κ_z and on three variables characterizing the volume: volume extinction σ, volume layer height h and the polarization-dependent term $\mu(\omega)$ that defines the contribution of the scattering from the ground. The model also depends on the SAR instrument wavelength via κ_z and extinction, which is a function of wavelength.

As seen, the model connects forest height to measured interferometric coherence and provides the opportunity to derive the height directly from InSAR coherence. However, despite being a relatively simple approach, this model still has four unknown parameters and, therefore, needs at least four independent measurements for rigorous inversion. Therefore, at least two independent complex measurements are required for model inversion at the pixel level. Typically, fully-polarimetric SAR data are used to provide a sufficient amount of measurements to derive the coherence region and allow meaningful model inversion. However, such data are not routinely available from space. To overcome this difficulty and obtain height estimates using dual-polarization (dual-pol) or even single-polarization (single-pol) InSAR data [31,34], additional assumptions, auxiliary data or further regularization are needed. Including the auxiliary Digital Terrain Model (DTM) representing ground surface, fixing the phase center height location, discarding the ground scattering contribution and fixing the forest extinction to a predefined value are among the commonly-used solutions [31,33,34,40].

3. Simplified Coherence Models for Forests

The performance of a coherence model is influenced by several factors, such as the selection of the perpendicular baseline (affecting the vertical wavenumber) [34], the seasonal variability of the volume extinction and ground reflectance [41,42]. For example, the dependence of the model-based inversion on weather conditions has been studied to a very limited extent [43,44], and no studies focused on the peculiarities of forest height retrieval for different forest species. When working with space-borne coherence data, the quantity of independent measurements is usually limited, and various error sources cannot be entirely controlled. Therefore, in practice, often, simpler models than the RVoG are applied in order to retrieve forest height from coherence magnitude measurement. Despite its relative simplicity, the RVoG model is still too complicated for operational forest height estimation, and a variety of simplifications, such as regression models or the sinc model, are typically used. Moreover, practically all pf the above-mentioned studies using RVoG were carried out over relatively small test sites (at the extent of one scene), typically with a specific dominating type of forest. Wide area mapping, however, requires a somewhat different, more robust approach, which would allow model inversion based on available single-polarization data. Reliable inversion is needed over all service areas, and a set of applicable models and the dynamic range of their parameters should be well defined for different inversion scenarios. A regression model cannot answer to those demands, and in the following, we propose an RVoG model simplification to provide a set of semi-empirical models to form a physics-based framework for coherence modeling for forest height retrieval.

3.1. RVoG Model Simplifications

As was noted above, simpler models have several benefits during practical forest height retrieval, mainly in terms of invertibility. One straightforward way to simplify the RVoG model is to eliminate some of its variables. This can be, for example, done by considering the volume decorrelation integral (5) in the case where extinction parameter σ approaches zero. The $\sigma = 0$ condition should be applied prior to the integration in order to derive a defined function. Effectively, this means that the profile function in (5) is assumed to be constant instead of exponential. The simplification can be derived in the form of:

$$\gamma_{V0} = \frac{(e^{ih\kappa_z} - 1)}{ih\kappa_z} \tag{7}$$

This can be presented using trigonometric functions as:

$$\gamma_{V0} = e^{i\frac{h\kappa_z}{2}} \frac{sin\left(\frac{h\kappa_z}{2}\right)}{\frac{h\kappa_z}{2}} = e^{i\frac{h\kappa_z}{2}} sinc\left(\frac{h\kappa_z}{2}\right) \tag{8}$$

which provides the equation as a product of the imaginary and real functions [45]. As can be noted from (7) and (8), a convenient argument for this problem is not h, but $h\kappa_z$. Moreover, when taking into account the definition of InSAR height of ambiguity, defined as:

$$HoA = \frac{\lambda R_D \sin(\theta)}{2\pi LN} = \frac{2\pi}{\kappa_z} \tag{9}$$

where λ is the wavelength, θ is incidence angle, L is baseline, R_D is the range distance, $N = 2$ denotes monostatic and $N = 1$ for bistatic measurement and κ_z is the vertical wavenumber, the zero extinction volume decorrelation can be presented as:

$$\gamma_{V0} = \frac{i}{2\pi}\left(1 - e^{i2\pi\frac{h}{HoA}}\right)\frac{HoA}{h} = e^{i\pi\frac{h}{HoA}} sinc\left(\pi\frac{h}{HoA}\right) \tag{10}$$

Here, the $\frac{h}{HoA}$ can be interpreted as a relative (fringe-height-normalized) height of the forest stand. The $\frac{h}{HoA}$ is a dimensionless parameter, which provides comparable reference for volume-induced coherence, measured with different baselines.

When substituting the simplified volume decorrelation function (10) into RVoG model (3) and assuming zero ground contribution $\mu = 0$, the so-called sinc-model can be derived as:

$$|\gamma_{sinc}| = sinc\left(\pi\frac{h}{HoA}\right) \tag{11}$$

A particular benefit of the sinc model is that it can be used for coherence magnitude-based inversion [31,43,44] or, alternatively, in hybrid inversion scenarios where both the magnitude and the phase of the InSAR coherence are used [24]. The drawback is that it is harder to explain model performance in the typical terms in which the RVoG operates, i.e., ground-to-volume ratio and extinction. Furthermore, the simple sinc model does not take into account the interferometric phase.

3.2. Linear Model for Coherence

An even simpler model can be constructed using the RVoG model to establish a linear relation between coherence and forest height. The motivation for that is given by the fact that often, a linear relation between forest height and interferometric coherence is established empirically. This can be done using linear approximation for the sinc function. It is known that for height estimation with the RVoG model, the forest height should generally be in the range, or smaller, than the height of ambiguity. This means that the argument range of (11) is restricted to an area between zero and π. In this region, the sinc function can be approximated rather well with a simple linear function $(1 - \frac{x}{\pi})$. By replacing the sinc in (10) with this linear function, one can derive a simple linear approximation for the coherence and height relation as:

$$\gamma_l = e^{i\phi} e^{i\pi\frac{h}{HoA}}\left(1 - \frac{h}{HoA}\right) \tag{12}$$

where h denotes the thickness of forest volume (forest height), HoA is the Height of Ambiguity of the SAR system and ϕ is the interferometric phase on the ground. When only the coherence magnitude is considered, the above model (12) represents a simple linear relationship between the volume height and InSAR coherence and shows that the RVoG model can be used to explain theobserved linear relationship between the forest height and interferometric coherence amplitude.

It will be demonstrated later that when plotting $\frac{h}{HoA}$ against coherence values, the result depends on the imaging configuration much less than on the actual forest stand height. Therefore, in the following, we will use $\frac{h}{HoA}$ as an argument for empirical models.

3.3. RVoG-Based Semi-Empirical Models

In the following, we assume that the derived simplifications of the RVoG model capture the essential dependencies between the forest height, imaging parameters and the interferometric coherence. We assume that with additional empirical parametrization, the models can provide viable robust tools for forest height derivation from coherence images. However, in this work, we only investigate the plausibility of such models by comparing various possible models with ALS forest height and TanDEM-X coherence magnitude measurements. Here, we propose three semi-empirical models (13), (14) and (15):

$$|\gamma_{linear}| = 1 - \frac{h}{HoA}C_{lin} \tag{13}$$

$$|\gamma_{sinc}| = 0.95 \cdot sinc\left(C_{sinc}\pi\frac{h}{HoA}\right) \tag{14}$$

$$\gamma_{0ext} = \left[\left(1 - e^{i2.4\pi\frac{h}{HoA}}\right)\frac{HoA}{h}\frac{i}{2.4\pi} - 1\right]\frac{1}{C_{0ext}} + 0.95 \tag{15}$$

where C_{lin}, C_{sinc} and C_{0ext} are empirical parameters for the derived models. The linear model (13) is based on (12); the sinc-model (14) is based on (11); and the $0ext$ model (15) is derived by combining (7) with (4). The last model can be presented and constructed also in terms of a sinc function, but it is important to include both the imaginary and real components of the model for additional empirical parametrization. The magnitude of the model depends also on the imaginary component, and a simple real sinc model fails to agree with the data. There are also many more ways to parametrize (10) and get good empirical models. The parametrization here is performed in a way that keeps the shape of the original functions, but allows one to adjust slightly the model range to fit with the data. The models also contain a few constants, which are selected to adjust the model shape to meet the majority of the data. For example, the coherence maximum is adjusted to a lower value than one (0.95 was selected according to the $0ext$ model fit to the entire dataset). The models are depicted graphically in Figure 1, where the general shape of the functions can be seen. As can be noted, all proposed models behave in a similar way for a coherence magnitude range of 0.4–0.8. Furthermore, linear and sinc models do not describe the phase, as they use only real functions. It has to be noted that the linear, sinc and $0ext$ model shapes do not contain additional dependencies on the baseline when the h/HoA argument is used, but, the RVoG model has a more complex dependence on HoA; and the model shape is actually slightly different for different baselines also in the h/HoA axis reference.

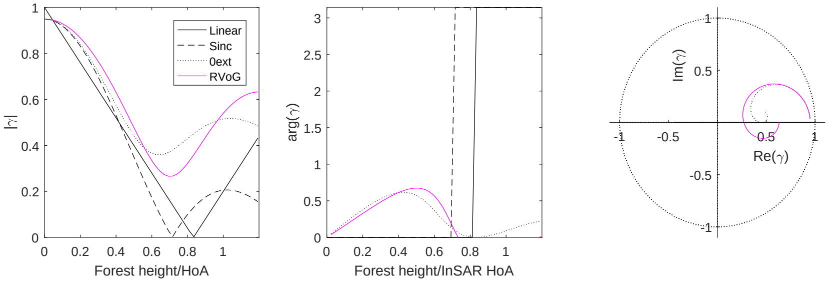

Figure 1. Proposed semi-empirical models for modeling InSAR coherence as a function of stand height (black lines) along with the RVoG model (magenta line). The amplitude of the coherence is on the left; the phase is presented in the middle; and the complex plane on the right. On the x-axis is forest stand height over the Height of Ambiguity (HoA).

In the following, we proceed to assess the potential of the proposed models for forest height retrieval and define the applicable region of model parameters by using an extensive dataset of X-band multitemporal coherence magnitude images and ALS-based forest height maps.

4. Test Sites and Description of the Data

4.1. Study Area

The study areas are located in southern Estonia (Figure 2). The first test site (12 km × 15 km) is situated in Soomaa National Park in southwestern Estonia (58°24′N, 25°6′E), and the second Peipsiveere test site covered a larger region (46 km × 61 km) in southeastern Estonia (58°8′N, 27°19′E). It is located in Tartu and Põlva County and includes the Peipsiveere Nature Reserve and the old-growth forests of the Järvselja Primeval Forest Reserve.

The Soomaa site is situated on a flat terrain (elevations ranging from 20–30 m above sea level) between large mires and rivers of the Pärnu River basin (Halliste, Raudna and Lemmjõgi). The Peipsiveere site contains the primeval forests of Järvselja Nature Reserve and Peipsiveere Nature Reserve that are located around the estuary of the Emajõgi River on the southwestern coast of Lake Peipus. The region is relatively flat (30–40 m above sea level) and surrounded by wetlands and forest.

As demonstrated in Figure 2, the forest data from the Estonian Forest Registry [46] are divided into three main classes according to the dominant tree species. A total of 242 forest stands covering 591 hectares of forests were selected over the Soomaa site, with the average stand size of 2.44 ha. The dominating tree species for more than half of the forests (116 stands) is Scots pine (*Pinus sylvestris* L.). The deciduous stands are represented by 101 stands, dominated by silver birch (*Betula pendula* Roth) with 57 stands and followed by black alder (*Alnus glutinosa* L.) with 36 stands, grey alder (*Alnus incana* L.) with five stands and trembling aspen (*Populus tremula* L.) with three stands. Norway spruce (*Picea abies* L.) has the smallest presence with a total of 25 stands.

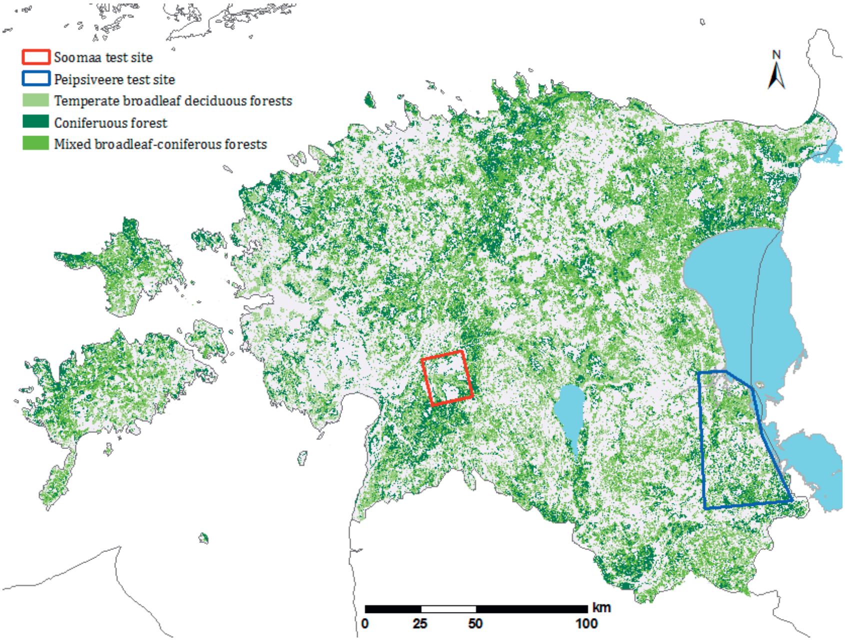

Figure 2. Locations of the Soomaa and Peipsiveere test sites in southern Estonia. Forest data are divided into three classes according to the forest type.

The Peipsiveere site includes 563 forest stands covering over 1620 ha. The average stand size is 2.88 ha. The site conditions are influenced by the large wetlands and are also reflected in the distribution of the tree species common for wet locations and moist soils. The majority of the forests are deciduous (333 stands), composed of 303 silver birch and 26 black alder stands. The remaining four stands are represented by grey alder, larch (*Larix decidua)* Mill.) and aspen stands. The Scots pine forests include altogether 173 stands, while the smallest class is Norway spruce with 57 stands.

4.2. Forest Inventory Data

The forest inventory data were provided by the Estonian Environment Information Centre [46]. The data were used to select forest sub-compartments from the State Forest Registry for accounting of forest resources, which are integrated, sufficiently homogeneous in their origin, composition, age, basal area, height, standing volume and site type and subject to common methods of management [47].

The average stand height over the Soomaa test site is 16.7 m, with the stand height ranging from 1.4 m–29.7 m. The mean standing volume density over the test site is 140 m^3/ha, ranging between 1 and 327 m^3/ha. For the Peipisveere test site, the mean stand height is 14.8 m, with the stand height ranging from 1.5 m–30.2 m. The mean standing volume density over the test site is 121 m^3/ha, ranging between 0 and 449 m^3/ha.

The mean size of the 242 Soomaa stands is 2.44 ha (median 1.70 ha), ranging from 1.0 ha–15.2 ha. The mean size of the 563 Peipsiveere stands is 2.88 ha (median 1.96 ha), where the smallest stand is 1.0 ha and the largest 47.0 ha.

4.3. TanDEM-X Dataset

The interferometric SAR dataset consists of 19 TanDEM-X bistatic Stripmap (SM) dual polarization (HH/VV) and single polarization (HH) images acquired from 2010–2012 over the Soomaa (Table 1) and Peipsiveere test sites (Table 2). In order to have a consistent dataset, only the HH-polarization component of dual-pol TanDEM-X Coregistered Single look Slant range Complex (CoSSC) scenes is used. As was demonstrated in our earlier study [44], there is typically a small difference between HH and VV polarizations due to a weak double-bounce mechanism as a result of the forest floor conditions and flat terrain. The VV polarization should mainly be considered when dealing with flooded environments, as inundated forest floor is better seen in the HH channel and has less impact on the VV channel coherence [44,48,49].

The images for Soomaa and Peipsiveere sites were acquired with effective baselines ranging from 64–259 m and incidence angles ranging from 18°–45°. The satellite look direction is to the right for all images. The minimum ground temperature in Tables 1 and 2 shows the lowest ground temperature over a 24-h period, while the precipitation information is the sum of total rainfall over 24 h prior to the satellite data acquisition. Data in the temperature column were recorded in the nearest weather station [50] and reflect weather conditions during the data acquisition. The given water level in Table 1 is measured from the Halliste River and is relative to a long-term minimum [50].

4.4. ALS Data

Airborne LiDAR scanning (ALS) measurements over both test sites were carried out by the Estonian Land Board in June 2010 using a Leica ALS50-II scanner. The ALS data point density is 0.45 per m^2 with a pulse repetition frequency of 94 kHz MPiA (multiple pulses in air).

The 90th percentile (P_{90}) of the point cloud height is used as an estimate of the forest height. The P_{90} was chosen as it is known to have a strong linear correlation to the measured forest height [51]. The point heights above ground are calculated using a Digital Terrain Model (DTM) in the L-EST reference coordinate system. Data from 2659 forest stands are used for the analysis. The stand polygon shapes are buffered 20 m inside for the Soomaa test site and 15 m inside for the Peipsiveere test site to avoid the influence of the borderline errors and to take into account the sliding window footprint on the ground in coherence magnitude calculations. For each stand, ALS point clouds are then extracted and processed using FUSION/LDV freeware [52].

Table 1. The list of bistatic TanDEM-X stripmap acquisitions over the Soomaa test site. HoA is the Height of Ambiguity.

ID	Date	Incidence Angle (°)	HoA (m)	Minimum Ground Temperature (°C)	Temperature (°C)	Precipitation (mm)	Polarization	Water Level (cm)	Orbit	Resolution Ground Azimuth/Range (m)	Pixel Spacing Ground Azimuth/Range (m)
1	29 December 2010	44.6	41.4	−9.2	−6.8	0	HH	112	Ascending	3.30/2.52	1.99/1.94
2	1 August 2011	36.2	45.9	12.0	18.6	0	HH	46	Ascending	3.30/2.99	2.04/2.31
3	3 March 2012	23.4	44.7	−5.3	0.9	0	HH/VV	88	Ascending	6.60/2.96	2.35/2.29
4	8 March 2012	34.8	66.2	−22.9	−2.7	0	HH/VV	81	Ascending	6.60/2.06	2.85/1.59
5	14 March 2012	23.4	43.6	−5.5	−0.4	0	HH/VV	91	Ascending	6.60/2.96	2.35/2.29
6	25 March 2012	23.4	43.9	−3.5	0.9	9.9	HH/VV	374	Ascending	6.60/2.96	2.35/2.29
7	5 April 2012	23.4	16.2	−8.4	4.6	0	HH/VV	258	Ascending	6.60/2.97	2.35/2.30
8	5 April 2012	18.2	41.8	−8.4	−3.7	0	HH/VV	271	Descending	6.60/3.76	2.8/2.94
9	15 April 2012	45.2	30.8	−2	10.8	0	HH	147	Ascending	3.30/2.49	2.01/1.92
10	02 May 2012	34.8	24.7	−2.2	13.4	0	HH/VV	122	Ascending	6.60/2.06	2.85/1.59
11	18 May 2012	43.4	32.7	6.5	12.3	11	HH	81	Ascending	3.30/2.57	1.85/1.98
12	30 May 2012	23.4	18.5	6.6	9.1	20.6	HH/VV	57	Ascending	6.60/2.97	2.35/2.31
13	3 October 2012	34.8	33.7	5.6	10.2	0	HH/VV	88	Ascending	6.60/2.06	2.85/1.59
14	11 November 2012	23.3	19.7	−0.2	5.1	0	HH/VV	234	Ascending	6.60/2.97	2.35/2.30
15	16 November 2012	34.8	31.8	0.6	5.5	0	HH/VV	174	Ascending	6.60/2.06	2.85/1.59

Table 2. The list of bistatic TanDEM-X stripmap acquisitions over the Peipsiveere test site.

ID	Date	Incidence Angle (°)	HoA (m)	Minimum Ground Temperature (°C)	Temperature (°C)	Precipitation (mm)	Polarization	Orbit	Resolution Ground Azimuth/Range (m)	Pixel Spacing Ground Azimuth/Range (m)
16	4 January 2011	44.6	41.6	-13.4	-5.2	2.2	HH	Asc	3.30/2.51	1.99/1.94
17	9 September 2011	36.2	48.2	7.3	13.7	0.8	HH	Asc	3.30/2.99	2.20/2.31
18	30 March 2012	45.2	30.1	0.0	1.6	3.1	HH	Asc	3.30/2.49	2.01/1.92
19	5 November 2012	43.4	33.6	1.6	2.7	12.6	HH	Asc	3.30/2.57	1.85/1.98

5. Data Processing

The processing steps of the TanDEM-X Coregistered Single look Slant range Complex (CoSSC) product include coherence calculation according to (1) with a sliding window of (azimuth×range) and orthorectification of the coherence product (range Doppler terrain correction and geocoding) using satellite orbital information and Ground Control Points (GCP) from the image metadata. SRTM DEM is used in connection with the orthorectification.

For the Soomaa test site, coherence values are calculated for CoSSC images according to (1) using window sizes (azimuth × range) of 12 × 21, 13 × 14 and 17 × 18 pixels. In the Peipsiveere area, the window sizes are 12 × 13 and 13 × 14 pixels. The coherence calculation window size projected to the ground is approximately squared, with the length of its shortest edge starting from 25 m and ranging to 45 m for the largest window. The use of a relatively large averaging window during coherence calculation guarantees that the coherence overestimation bias is always less than 0.02 [53] and, thus, insignificant.

Further, coherence magnitude images are imported into a GIS program and converted to the same reference coordinate system as the previously-calculated ALS measured forest height data and the stand borders from the forest inventory database. Forest stands are divided into three groups by the dominant tree species, and statistics were calculated for each stand, resulting in a corresponding mean coherence magnitude and mean ALS forest height.

In order to provide representative and less biased estimates of coherence and heights in model fitting, the coherence data are analyzed stand-wise using a stand border map from ancillary data. The features of the stand border map are buffered 20 m inside for the Soomaa test site and 15 m inside for the Peipsiveere test site, with the purpose of avoiding border effects during the coherence calculation. The buffer distance size is approximately half of the size of the coherence image pixel size. The values of coherence and stand height pixels are then averaged inside the buffered polygons for the stand-wise estimates.

Additional criteria for the selection of the forest stands is based on the size and composition of the main tree layer. From the remaining polygons, only stands larger than one hectare are included in the analysis. Furthermore, only homogeneous stands with one tree layer and no understory layer are selected with the requirement that the proportion of the dominant tree species in the main tree layer is higher than 75%.

From the ALS data, mean forest height is calculated for every forest stand using the 90 percentile (P_{90}) height above the ground values of all of the echoes. The ALS data were acquired during 2010, while TanDEM-X scenes were acquired during 2010–2012; this factor can potentially introduce minor height differences during the model fitting. As the growth speed of forest depends on many environmental variables, such as the age of the forest, site type and water access, the corresponding change in stand height (different also for every scene) is neglected.

The pre-selected forest stands define the buffered polygons in which the coherence and ALS data are averaged and compared to each other, allowing one to calculate statistics for each forest stand. Figure 3 shows the TanDEM-X coherence magnitude image with the corresponding LiDAR-derived forest stand height map.

Fitting the Models to Measurements and Estimating Model Parameters

In the following section, three semi-empirical models (13), (14) and (15), along with the RVoG model (6) and (3) are compared using experimental data in order to evaluate their performance and to give estimates of the parameters of the models. The analysis is done by comparing stand-wise coherence magnitude measurements to the ALS measured stand average forest height data for every interferometric coherence image. Every coherence magnitude image contains a varying number of forest stands and has different imaging parameters. We assume that during the same acquisition, forests with a similar species composition have comparable attenuation and ground reflectivity properties and, therefore, can be described with the same model parameter.

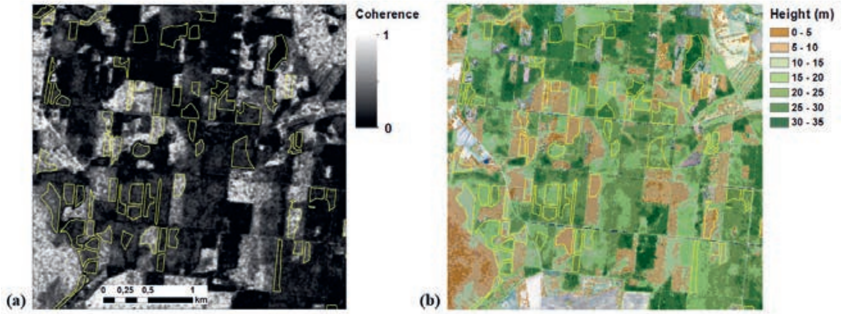

Figure 3. The TanDEM-X coherence image from 4 January 2011 (**a**) and corresponding LiDAR P_{90} forest height image from 29 June 2010 (**b**) show the selected forest stands (yellow) on the Peipsiveere test site over a 3.5 × 3.5 km area with center coordinates of 58°15′53.1″N, 27°23′10.8″E.

Clearly, such an assumption works best only for relatively homogeneous forests. Here, we use forest dominant species to assure forest similarity.

A map of forest species is the most common and often the only a priori information available, thus also suitable for the operational scenarios. Therefore, three dominant tree species (pine-dominated, spruce-dominated and deciduous forests) are analyzed separately in the study areas. All four presented models are fitted to the data in order to find the best parameter values and the goodness of fit. The model-fitting is performed separately for every scene and dominant species class. Parameter values are found by using an unconstrained non-linear optimization (Nelder–Mead method) to seek the minimum difference between the forward modeled coherence magnitude and the ALS forest height in the least squares sense. The goodness of fit is calculated as the root-mean-square deviation between the measured coherence magnitude and modeled coherence for the current subset as:

$$RMSD = \sqrt{\frac{\sum_{i=1}^{N}\left(x_i - x_i^{meas}\right)^2}{N}} \tag{16}$$

where x_i and x_i^{meas} are the modeled and measured coherence magnitudes for the i-th forest stand and N is the number of examined stands (either whole scene or specific forest type).

6. Experimental Results

In Figure 4, an overview of the entire multitemporal dataset is presented as a relation between the coherence magnitude and ALS forest height. The dataset comprises 3787 forest stands on 19 different image pairs acquired over two years. The left image shows the initial relation between forest stand heights and coherences, and on the right side, the same relation corrected with HoA (9) is shown. The benefit of using h/HoA as an argument is apparent, as the the variability caused by different baselines is mostly eliminated. For comparison, all three proposed semi-empirical models are presented on top of the data. Here, for simplicity, only one RVoG line is shown, while in reality, RVoG has slightly different curves for every baseline. As can be seen, at the general level, all models provide a reasonably good agreement with the majority of the measurements. However, it can be noted that the linear and sinc models cannot account for the ground contribution and assume zero coherence on the ground. On the other hand, it is remarkable how closely most of the measurements are located to a single line, taking into account that the graph covers all seasonal differences of three different forest types and several baseline configurations. In the following, a more detailed comparison between the models and data is provided scene by scene.

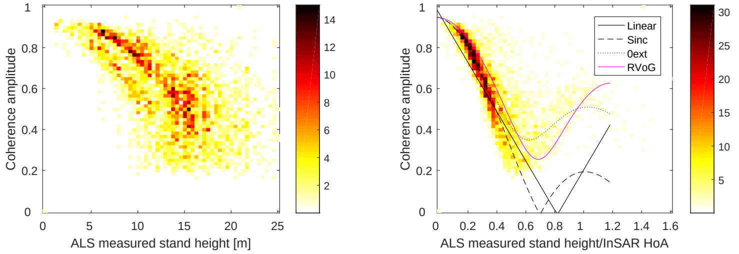

(**a**) (**b**)

Figure 4. TanDEM-X coherence against Airborne LiDAR Scanned (ALS) forest height for the entire dataset (19 TDX image pairs and 3787 forest stands). The colors represent how many coherence-stand height pairs fall into the value range. On the left (**a**), the coherence magnitude is compared to forest stand height, and on the right (**b**), the coherence magnitude is compered to ALS forest height divided by HoA (9) values.

6.1. Model Performance across Different Scenes

Relationships between the ALS measured stand height and coherence magnitude estimates are presented in Figure 5 for individual interferometric scenes and dominant tree species, along with the results of fitting the four proposed coherence models to the data. Only a selection of five representative images (out of 19 scenes in total) are shown in the figure.

All forest scenes generally exhibit a similar behavior with respect to the measured coherence in the h/HoA coordinates. Furthermore, all four models show agreement with the data, especially when the coherence is in the range between 0.4 and 0.9. In some cases, a very good correlation can be observed (particularly the 4 January 2011 and 3–25 March 2012 scenes) down to as low a coherence as 0.2.

The dominant species of the forest has an effect on the model parameters. For example, the scene acquired on 30 March 2012 shows that deciduous forest had clearly different extinction properties compared to coniferous forests. On the other hand, it appears that differences in between acquisition dates are larger than differences between tree species.

One notable feature that can be observed is that the negative correlation between forest height and coherence magnitude can turn into a positive correlation when the stand height is close to HoA (or even exceeds the HoA value), as for example seen on the 5 April 2012 or 30 March 2012 scene. This indicates that potential inversion based on the proposed models might still be possible even when the forest height exceeded HoA. However, errors are large, and potential inversion could lead to ambiguous results.

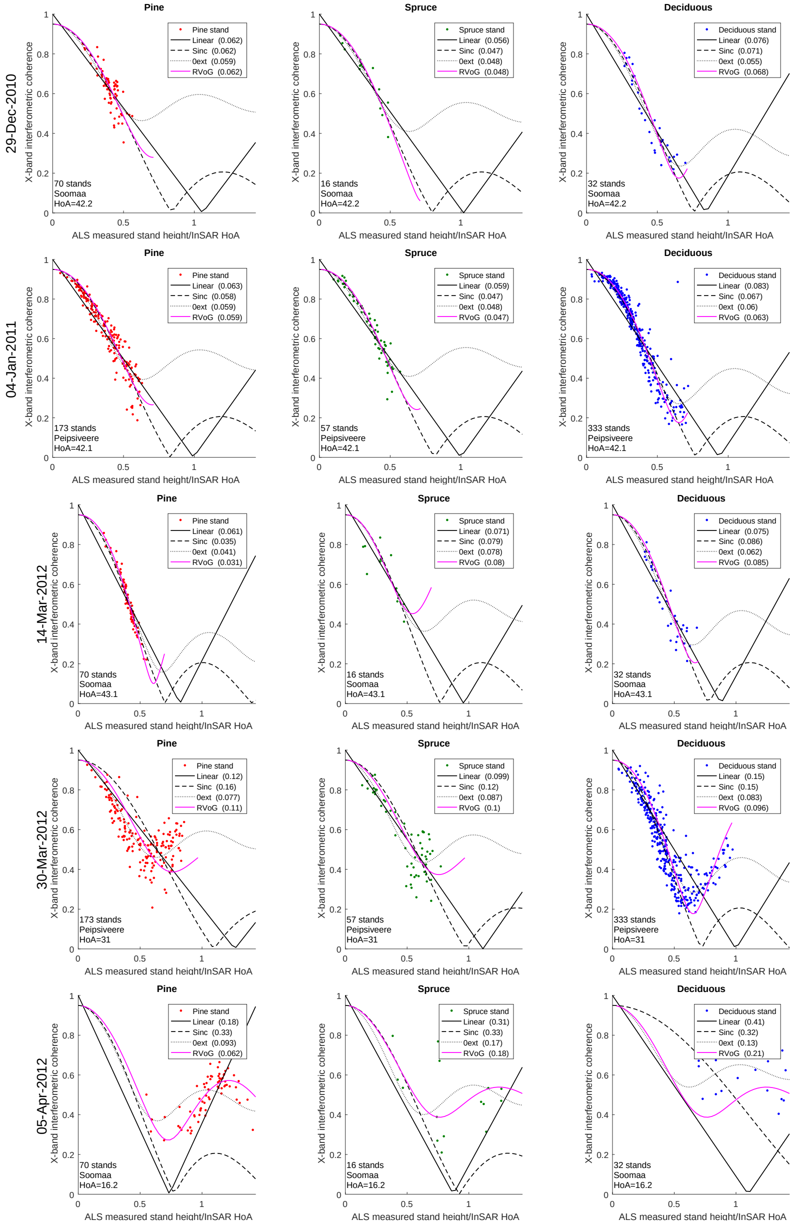

Figure 5. Four different models fitted to coherence and Airborne LiDAR Scanning (ALS) values for different TanDEM-X InSAR scenes. The fitting is performed separately for dominant tree species (>75% dominance); the first column presents pine stands (red), the second spruce stands (green) and the third deciduous stands (blue). Four different models (13), (14), (15) and (3) are presented as described in the legend. The goodness of fit parameter (RMSD) is also given within the brackets. The forest site and the HoA value for the scene is also given in the left corner of the axes.

The different models mostly agree in the region of $0.2 < h/HoA < 0.6$. However, it can be clearly seen that in the case of high coherence magnitude values (>0.9), the linear model is not adequate and fails to describe the data, while all other models agree well with each other and with the data. The differences between the sinc model and the RVoG model become evident in the case of low coherence values where RVoG and the *0ext* model adapt well to variations in the attenuation and ground reflection strength. A good compromise between the RVoG model and the sinc model appears to be the *0ext* model, which is a single parameter model like the sinc model, but allows flexibility close to that of RVoG. While the RVoG model adapts clearly best for all of the cases, this might have no importance in the operational scenarios where model parameters are unknown and the model flexibility hampers the potential inversion process. Therefore, for an operational height retrieval scenario, the linear model and the *0ext* model might give the best results, as the *0ext* model is more stable for small changes than RVoG, which has very high sensitivity for some combinations of ground to volume ratio and extinction.

According to RVoG, stands with high extinction and/or very strong ground contribution should occupy the region in the plot with high h/HoA and high coherence magnitude values. However, there are only a few such data points in our dataset, and presumably, such parameter combinations are not common for hemiboreal forest in the case of the X-band.

6.2. Goodness of Fit for Different Models and Tree Species

Different forest stands are likely to have slightly different extinction and ground reflectivity values, partially explaining fit error and scatter in the data, as a single model explains only the variation of heights between different forest stands. The variations in the ground contribution tend to increase the coherence magnitude and scatter the data towards the “tail” of RVoG. In other words, the coherence magnitude for a certain forest height can be significantly higher than expected, but very seldom lower than a certain limit. Therefore, when solving an inverse problem, it should be taken into account that the coherence model errors are asymmetric and tend to scatter towards higher coherence magnitude values.

Figure 6 illustrates the goodness of fit for three forest types across all stands and InSAR scenes for the examined models using the RMSD measure where the *0ext* model shows the best performance. Every stand is accounted in the histograms as a separate data point despite the fact that stands from the same scene have identical values for model parameters. As can be seen in Figure 6 (top row), the linear model has higher minimal error, but agrees rather well with a variety of the data. It cannot describe data well in the case of low coherence magnitude values and also has a significant deviation for coherence values above 0.9 (see Figure 5). The biggest drawback of using the linear model is that it cannot describe the increase of coherence magnitude (in response to increasing h/HoA) upon reaching intermediate values, like in the case of the 30 March 2012 scene (the “tail” scenario).

The same problem hampers the performance of the sinc model, which seems to offer slightly better performance than the linear model when the coherence is relatively high, but conditions present on the 30 March 2012 scene are problematic to describe. The sinc model has the poorest fit with the data in the region where stand height is closer to the height of ambiguity.

Based on the goodness of fit, the best performance is provided by the *0ext* model and RVoG. On average, the *0ext* model performs similarly to or even better than RVoG. A possible explanation is related to the high robustness of the *0ext* model. In cases where the RVoG parameters take extreme values to fit the coherence magnitude points in the low coherence region, the *0ext* model behaves in a more robust way. On the other hand, RVoG provides the best fit for scenarios when coherence values start to increase with increasing h/HoA (e.g., the 30 March 2012 scene), something that is not captured by other models.

The pine-dominated stands show the best agreement with the elaborated models. This is probably due to the homogeneity and similarity between the stands. Therefore, the pine stands agree best with the general assumptions made about the similarity between the stands on one image.

6.3. Goodness of Fit for Different Baselines

During the analysis, it was noted that the RMSD values are correlated between the different models, probably indicating the limitations of the assumption of similarity between stands from the same stratum. When the extinction values or ground contribution of the stands are in reality very different, a single model line cannot fit all of the points.

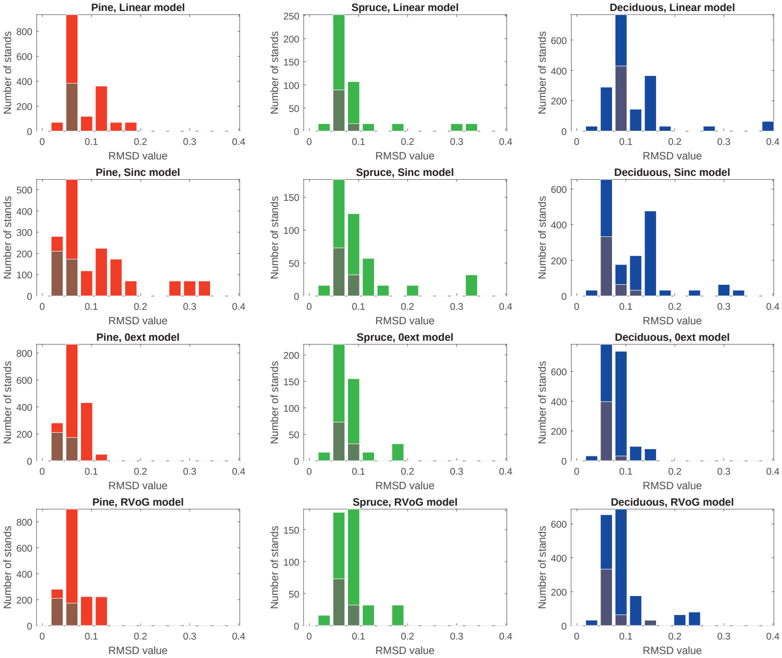

Figure 6. Goodness of fit for the four models: linear (13), sinc (14), *0ext* (15) and RVoG (3) and for three different forest types. On the histogram x-axis is the Root Mean Square Difference (RMSD) between measured coherence magnitude and model predicted coherence. Models use ALS-measured forest stand height as an argument. The darker bars depict the same histograms for a subset of scenes with HoA approximately twice as large as the highest stand height (4 January 2011, 3 March 2012, 8 March 2012, 14 March 2012 and 25 March 2012).

The dependence of the model fitting error on HoA is shown in Figure 7. The HoA appears to be one of the main parameters influencing the goodness of fit. There is a strong dependence between the linear and sinc model fitting error and HoA, which is caused mainly by the fact that these models are not able to adapt to the “tail” scenario (see Section 6.2). A similar dependence is visible for the more complex models, but to a lesser extent. One should keep in mind that the RMSD of the coherence magnitude model fit does not directly describe the error of the stand height accuracy, as both depend on HoA in a similar way. Therefore, the most accurate forest height predictions would be possible in cases where HoA is small enough to enable large coherence dynamics, but large enough to avoid the effects caused by true height being close to the HoA. The scenes with HoA around two-times higher than the stand height appear to be an optimal choice for forest height inversion. This is in good agreement with, e.g., [42] where it was observed that for Norway spruce-dominated forest with maximum tree heights of about 30 m, the optimum HoA is in the range of 20–50 m.

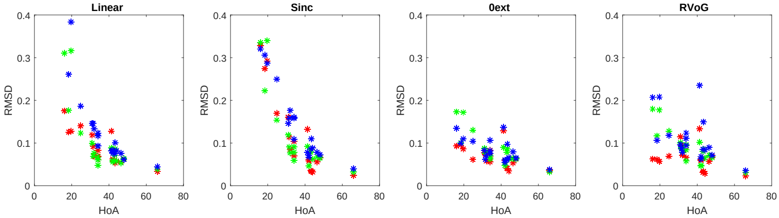

Figure 7. Dependence of RMSD of coherence model fit on HoA. Red marks denote pine, green spruce and blue deciduous stands.

6.4. Goodness of Fit for Winter Scenes

In Figure 6, the darker bars in all plots depict a subset of the data with frozen conditions. The subset comprises five scenes (4 January 2011, 3 March 2012, 8 March 2012, 14 March 2012, 25 March 2012), where the temperature has been significantly below the freezing point throughout the day. For all of those images, the HoA is approximately two-times higher than the highest stand height. Those conditions seem to give the best fit with models and create also the most favorable conditions for model inversion. It is notable that these scenes give a similar error level throughout all of the models, including the simple linear model. These results indicate the potential feasibility for forest height retrieval using single-pol X-band data and simple models given certain acquisition conditions. This is supported by the results from [42], where, based on the evaluation of InSAR height dynamics within the forest canopy, scenes acquired either only in frozen or only in unfrozen conditions are recommended for forest parameter estimation.

6.5. Parameter Range for Different Models

Figure 8 illustrates the species-wise dynamic range of parameters that the chosen models take across all InSAR scenes. Every stand is again counted as one data point in the histogram. The best fitting winter scenes are highlighted with darker bars. In general, differences between tree species are small. Larger variability and a smaller sample of spruce-dominated and deciduous stands has led to a wider variability in most of the parameters, respectively.

It should be taken into account that in the case of a poor fit, the model parameters tend to find middle ground and do not tell much about the target. Therefore, it is interesting to look at the results from the winter scenes, highlighted with darker bars. These describe parameter values for cases where the noise is the smallest. Interestingly, the parameters for pine stands show different regions where the model fit is good, indicating that the forest attenuation properties and/or ground contribution are clearly different for different acquisition dates.

From the linear model, it is easy to demonstrate the influence of the chosen parameter C_{lin} value on height prediction accuracy. With coherence magnitude around $\gamma = 0.5$, a variation of C_{lin} between 1.4 and 1.7 causes a difference in the predicted forest height in the order of magnitude $HoA/10$. This means that, given optimal acquisition conditions, forest stand height could be derived with an accuracy of a few meters even with fixed parameter values.

The RVoG parameter σ is also converted to actual extinction coefficient values by taking into account the incidence angle and presenting the value in dB/m (see Figure 8, last row). In general, the result is in agreement with values reported in the literature [31,54]. The extinction of the volume seems to be mostly less than 0.5 dB/m. However, it is difficult to explain why pine and deciduous forest seem to expose higher extinction than spruce dominated forests, which are usually denser. This might be caused by generally higher variability among spruce and deciduous stands, which also means that the assumption about the similarity of the attenuation properties is less valid.

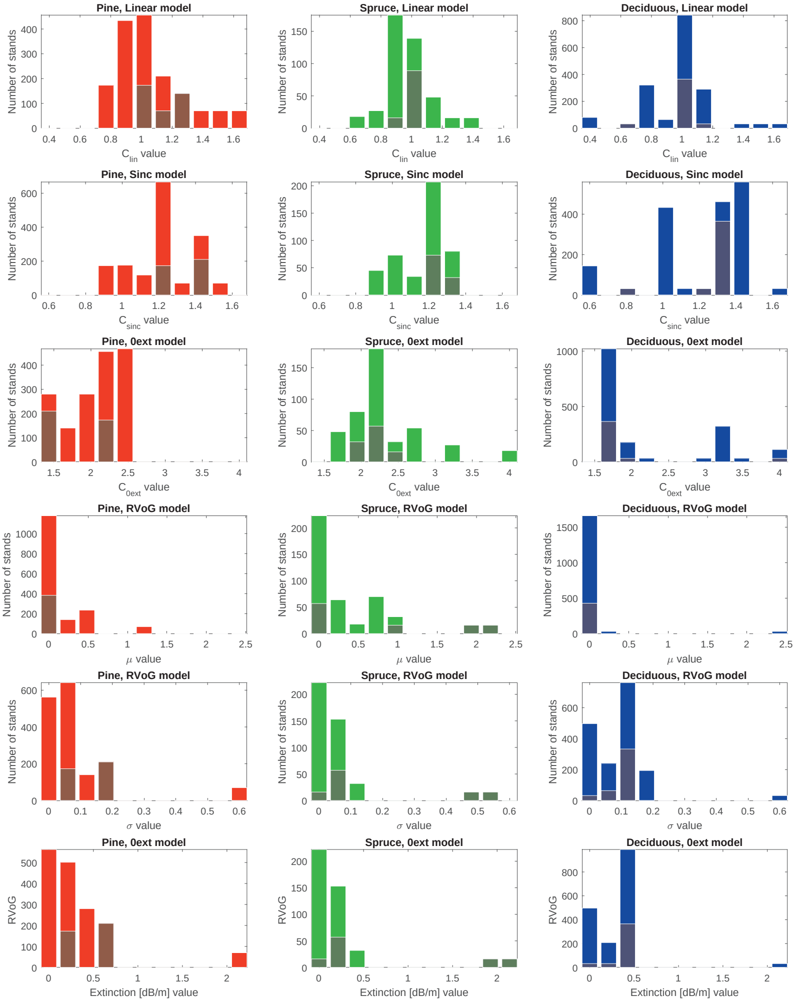

Figure 8. Parameters fitted for the chosen models. The darker bars depict histograms for a subset of scenes: 4 January 2011, 3 March 2012, 8 March 2012, 14 March 2012 and 25 March 2012. For these scenes, HoA was approximately twice as large as the highest stand height.

6.6. Similarities between the Models and Parameters

The presented models share common features, and four most significant inter-dependencies between the parameters of presented models are depicted in Figure 9. As can be seen from the panel on the left, the linear model and the simple sinc model parameters are in linear relation, as both parameters describe the steepness of the function. When comparing the model parameters with the RVoG model, it appears that all of the parameters are mainly related to the extinction parameter of the RVoG model. This indicates that in the RVoG model, the extinction parameter is perhaps more significant than the ground-to-volume ratio.

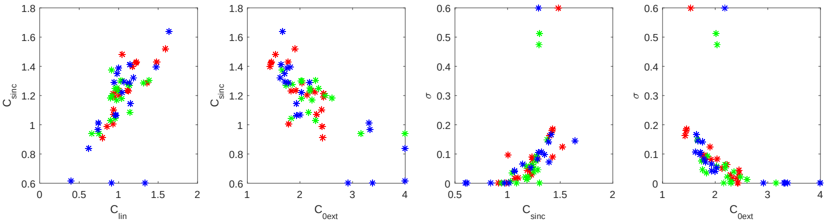

Figure 9. Interdependencies of the model parameters. Red marks denote pine, green spruce and blue deciduous stands.

7. Discussion

All four models perform well in describing the relationship between forest height and interferometric coherence magnitude. A single-parameter linear model shows a surprisingly balanced performance throughout the different conditions and imaging geometries. However, the linear model has a clear bias in the high coherence areas. In this region, the semi-empirical sinc model, on the other hand, provides good agreement with the data. However, both the linear and sinc model fail in describing the low coherence areas when stand height is close to the height of ambiguity. The best flexibility is provided by the two-parameter RVoG model, but unfortunately, two exponential parameters make the model rather unstable. The best compromise is provided by the empirically-parametrized zero extinction model, derived from RVoG.

Our analysis of the model fitting experiments supports the idea about the similarity of the electrophysical and ecological parameters of stands (e.g., extinction, tree density) on the same image that belong to the same tree species. This is demonstrated by the fact that even a large amount of different forest stands agree with the same empirical model curve, defined by a single empirical parameter. At the same time, this empirical parameter might slightly vary from scene to scene. This implies that variation between the stands that belong to the same forest type can be much smaller than the variation between the same stands acquired on different dates. The best agreement with the models was achieved in cold imaging conditions, indicating that in cold conditions, the forest stands' electrophysical parameters are probably most similar. This result indicates that the auxiliary information of tree species should be incorporated into routine forest height estimation whenever possible.

The work also indicates that in cold winter conditions, the assumption of similar extinction and ground reflection properties among similar forest types holds best and might be used for estimating forest height or forest extinction properties via model inversion. The results also show that when used for the purpose of forest height retrieval, the optimal height of ambiguity of the interferometric system should be around twice as large as the expected maximal forest height. It is observed, specifically for RVoG and sub-zero winter scenes, that decreasing the height of ambiguity does not increase the fit error, but rather introduces better dynamics for model inversion. This is expected to lead to better height retrieval accuracies. On the other hand, when the height of ambiguity of the interferometric system is in the order of the maximal stand height, models do not perform very well, and variations in the extinction properties introduce significant differences. Furthermore wet conditions introduce large variations, and model fitting by assuming similarity between the stands of the same forest type gives poor results.

This work also shows that both positive and negative correlation between forest height and coherence are possible and can also be described by the models. The positive correlation is observed in the areas where stand heights approached the height of ambiguity, within the so-called "tail" region of the model.

A set of models described in this work can be further used for predicting forest tree height and other relevant forest parameters, both on the stand level and the grid level.

8. Conclusions and Future Work

In this paper, space-borne interferometric X-band SAR coherence data and ALS-measured forest stand heights are used for comparing four different forest coherence models linking forest height and coherence magnitude. In addition to the random volume over ground model, three semi-empirical models are derived requiring only one fitting parameter: a simple linear model, a sinc model and a zero extinction *0ext* model. Moreover, it is shown that instead of the forest height, the height relative to the height of ambiguity should be used as a parameter in the model fitting. Using such relative forest height as an argument simplifies the models and provides a common basis for the assessment of different models and approaches despite differences in the imaging geometry.

Four models are compared to each other in the proposed framework and validated against a large dataset of coherence magnitude and ALS data over hemiboreal forests in Estonia. Both positive and negative correlation between forest height and coherence are captured and can also be described by the models. The positive correlation is observed in the areas where stand heights approached the height of ambiguity, within the so-called "tail" region of the model.

In addition to the models, the variation range for empirical model parameters is also given for hemiboreal forest, paving the road towards forest stand height maps derived from InSAR coherence measurements. Overall, these models establish the basis for a simple semi-empirical modeling approach that is capable of successfully describing the dynamics of InSAR coherence observed over boreal and hemiboreal forests. Further work will concentrate on actual forest height inversion using the proposed set of models.

The future work will concentrate on the application of the proposed models for tree height retrieval and potentially forest stem volume estimation taking into account species-specific allometric approaches. Further developments will consider producing estimates on the grid level rather than the stand-wise approach, as stand information might not be available for large-scale operational applications.

Acknowledgments: This work has been carried out under an ESA Contract (4000109690/13/NL/KML) for the PECS (Plan for European Cooperating States) and funded through the Government of Estonia. The authors would like to thank the project partners, European Space Agency, Reach-U and Tartu Observatory, for financial and technical support. Aire Olesk acknowledges the support of the European Social Fund's Doctoral Studies and Internationalisation Programme DoRa, carried out by Foundation Archimedes. Oleg Antropov acknowledges the support from the Electric Brain project funded by the Finnish Funding Agency for Technology and Innovation. The forest inventory data were provided by the Estonian Environment Information Centre and LiDAR data by the Estonian Land Board. The authors would like to thank DLR for the TanDEM-X imagery used in the study under science proposals NTI_INSA1194 and NTI_POLI2174. The authors would also like to acknowledge Martin Valgur from Reach-U for his contribution in the software development, Mait Lang from Estonian University of Life Sciences and Tartu Observatory for forest characteristics related discussions and Richard Knowelden for proofreading the manuscript.

Author Contributions: Aire Olesk, Jaan Praks and Kaupo Voormansik conceived of and designed the experiments. Aire Olesk and Tauri Arumäe prepared and processed the data. Jaan Praks and Oleg Antropov performed the experiments. Jaan Praks, Aire Olesk and Oleg Antropov wrote the paper. all authors analyzed the results and revised the paper.

Conflicts of Interest: The authors declare no conflict of interest.

Abbreviations

The following abbreviations are used in this manuscript:

SAR: Synthetic Aperture Radar
TanDEM-X: TerraSAR-X add-on for Digital Elevation Measurements
InSAR: Interferometric SAR
CoSSC: Coregistered Single look Slant range Complex

SRTM: Shuttle Radar Topography Mission
GCP: Ground Control Points
RVoG: Random Volume over Ground
AGB: Above Ground Biomass
LiDAR: Light Detection And Ranging
DEM: Digital Elevation Model
ENL: Equivalent Number of Looks
DTM: Digital Terrain Model
HoA: Height of Ambiguity
SLC: Single Look Complex
SM: Stripmap Mode
HH: Horizontal polarization transmit and Horizontal polarization receive
VV: Vertical polarization transmit and Vertical polarization receive
ALS: Airborne LiDAR Scanning
L-EST: (LAMBERT-EST) Lambert Conformal Conic Projection-Estonian Coordinate System
RMSD: Root Mean Square Deviation

References

1. Food and Agriculture Organization of the United Nations (FAO). Assessment of the Status of the Development of the Standards for Terrestrial Essential Climate Variables: Biomass (T12). Available online: http://www.fao.org/gtos/doc/ecvs/t12/t12.pdf (accessed on 24 April 2016).
2. Koch, B. Status and future of laser scanning, synthetic aperture radar and hyperspectral remote sensing data for forest biomass assessment. *ISPRS J. Photogramm. Remote Sens.* **2010**, *65*, 581–590.
3. Gonzalez, P.; Asner, G.P.; Battles, J.J.; Lefsky, M.A.; Waring, K.M.; Palace, M. Forest carbon densities and uncertainties from Lidar, QuickBird, and field measurements in California. *Remote Sens. Environ.* **2010**, *114*, 1561–1575.
4. Mitchard, E.T.; Saatchi, S.S.; Baccini, A.; Asner, G.P.; Goetz, S.J.; Harris, N.L.; Brown, S. Uncertainty in the spatial distribution of tropical forest biomass: A comparison of pan-tropical maps. *Carbon Balanc. Manag.* **2013**, *8*, 10.
5. Lu, D.; Chen, Q.; Wang, G.; Liu, L.; Li, G.; Moran, E. A survey of remote sensing-based aboveground biomass estimation methods in forest ecosystems. *Int. J. Digit. Earth* **2014**, *9*, 1–43.
6. Sinha, S.; Jeganathan, C.; Sharma, L.; Nathawat, M. A review of radar remote sensing for biomass estimation. *Int. J. Environ. Sci. Technol.* **2015**, *12*, 1779–1792.
7. Kaasalainen, S.; Holopainen, M.; Karjalainen, M.; Vastaranta, M.; Kankare, V.; Karila, K.; Osmanoglu, B. Combining lidar and synthetic aperture radar data to estimate forest biomass: Status and prospects. *Forests* **2015**, *6*, 252–270.
8. Imhoff, M.L. Radar backscatter and biomass saturation: Ramifications for global biomass inventory. *IEEE Trans. Geosci. Remote Sens.* **1995**, *33*, 511–518.
9. Le Toan, T.; Beaudoin, A.; Riom, J.; Guyon, D. Relating forest biomass to SAR data. *IEEE Trans. Geosci. Remote Sens.* **1992**, *30*, 403–411.
10. Ranson, K.J.; Sun, G. Mapping biomass of a northern forest using multifrequency SAR data. *IEEE Trans. Geosci. Remote Sens.* **1994**, *32*, 388–396.
11. Englhart, S.; Keuck, V.; Siegert, F. Aboveground biomass retrieval in tropical forests—The potential of combined X- and L-band {SAR} data use. *Remote Sens. Environ.* **2011**, *115*, 1260–1271.
12. Vastaranta, M.; Holopainen, M.; Karjalainen, M.; Kankare, V.; Hyyppä, J.; Kaasalainen, S. TerraSAR-X stereo radargrammetry and airborne scanning LiDAR height metrics in imputation of forest aboveground biomass and stem volume. *IEEE Trans. Geosci. Remote Sens.* **2014**, *52*, 1197–1204.
13. Persson, H.; Fransson, J.E. Forest variable estimation using radargrammetric processing of TerraSAR-X images in boreal forests. *Remote Sens.* **2014**, *6*, 2084–2107.
14. Solberg, S.; Riegler, G.; Nonin, P. Estimating forest biomass from TerraSAR-X stripmap radargrammetry. *IEEE Trans. Geosci. Remote Sens.* **2015**, *53*, 154–161.

15. Caicoya, A.T.; Kugler, F.; Hajnsek, I.; Papathanassiou, K. Boreal forest biomass classification with TanDEM-X. In Proceedings of the 2012 IEEE International Geoscience and Remote Sensing Symposium (IGARSS), Munich, Germany, 22–27 July 2012; pp. 3439–3442.
16. Askne, J.I.; Fransson, J.E.; Santoro, M.; Soja, M.J.; Ulander, L.M. Model-Based biomass estimation of a hemi-boreal forest from multitemporal TanDEM-X acquisitions. *Remote Sens.* **2013**, *5*, 5574–5597.
17. Askne, J.I.; Santoro, M. On the estimation of boreal forest biomass from TanDEM-X Data without training samples. *IEEE Geosci. Remote Sens. Lett.* **2015**, *12*, 771–775.
18. Soja, M.J.; Persson, H.J.; Ulander, L.M. Estimation of forest biomass from two-level model inversion of single-pass InSAR data. *IEEE Trans. Geosci. Remote Sens.* **2015**, *53*, 5083–5099.
19. Abdullahi, S.; Kugler, F.; Pretzsch, H. Prediction of stem volume in complex temperate forest stands using TanDEM-X SAR data. *Remote Sens. Environ.* **2016**, *174*, 197–211.
20. Soja, M.J.; Persson, H.; Ulander, L.M. Estimation of forest height and canopy density from a single InSAR correlation coefficient. *IEEE Geosci. Remote Sens. Lett.* **2015**, *12*, 646–650.
21. Nabuurs, G.; Masera, O.; Andrasko, K.; Benitez-Ponce, P.; Boer, R.; Dutschke, M.; Elsiddig, E.; Ford-Robertson, J.; Frumhoff, P.; Karjalainen, T.; et al. *Climate Change 2007: Mitigation. Contribution of Working Group III to the Fourth Assessment Report of the Intergovernmental Panel on Climate Change*; Metz, B., Davidson, O., Bosch, P., Dave, R., Meyer, L.A., Eds.; Cambridge University Press: Cambridge, UK; New York, NY, USA, 2007.
22. Solberg, S.; Næsset, E.; Gobakken, T.; Bollandsås, O.M. Forest biomass change estimated from height change in interferometric SAR height models. *Carbon Balanc. Manag.* **2014**, *9*, 5.
23. Karila, K.; Vastaranta, M.; Karjalainen, M.; Kaasalainen, S. Tandem-X interferometry in the prediction of forest inventory attributes in managed boreal forests. *Remote Sens. Environ.* **2015**, *159*, 259–268.
24. Cloude, S. *Polarisation: Applications in Remote Sensing*; Oxford University Press: Oxford, UK, 2009.
25. Treuhaft, R.; Gonçalves, F.; dos Santos, J.R.; Keller, M.; Palace, M.; Madsen, S.N.; Sullivan, F.; Graça, P.M. Tropical-forest biomass estimation at X-band from the spaceborne TanDEM-X interferometer. *IEEE Geosci. Remote Sens. Lett.* **2015**, *12*, 239–243.
26. Schlund, M.; von Poncet, F.; Kuntz, S.; Schmullius, C.; Hoekman, D.H. TanDEM-X data for aboveground biomass retrieval in a tropical peat swamp forest. *Remote Sens. Environ.* **2015**, *158*, 255–266.
27. Solberg, S.; Astrup, R.; Breidenbach, J.; Nilsen, B.; Weydahl, D. Monitoring spruce volume and biomass with InSAR data from TanDEM-X. *Remote Sens. Environ.* **2013**, *139*, 60–67.
28. Solberg, S.; Astrup, R.; Gobakken, T.; Næsset, E.; Weydahl, D.J. Estimating spruce and pine biomass with interferometric X-band SAR. *Remote Sens. Environ.* **2010**, *114*, 2353–2360.
29. Cloude, S.R.; Chen, H.; Goodenough, D.G. Forest height estimation and validation using Tandem-X polinsar. In Proceedings of the 2013 IEEE International Geoscience and Remote Sensing Symposium (IGARSS), Melbourne, Australia, 21–26 July 2013; pp. 1889–1892.
30. Praks, J.; Hallikainen, M.; Antropov, O.; Molina, D. Boreal forest tree height estimation from interferometric TanDEM-X images. In Proceedings of 2012 IEEE International Geoscience and Remote Sensing Symposium (IGARSS), Munich, Germany, 22–27 September 2012; pp. 1262–1265.
31. Praks, J.; Antropov, O.; Hallikainen, M.T. LIDAR-aided SAR interferometry studies in boreal forest: Scattering phase center and extinction coefficient at X-and L-band. *IEEE Trans. Geosci. Remote Sens.* **2012**, *50*, 3831–3843.
32. Lee, S.K.; Fatoyinbo, T.E. TanDEM-X Pol-InSAR inversion for mangrove canopy height estimation. *IEEE J. Sel. Top. Appl. Earth Obs. Remote Sens.* **2015**, *8*, 3608–3618.
33. Hajnsek, I.; Kugler, F.; Lee, S.K.; Papathanassiou, K.P. Tropical-Forest-Parameter estimation by means of Pol-InSAR: The INDREX-II campaign. *IEEE Trans. Geosci. Remote Sens.* **2009**, *47*, 481–493.
34. Kugler, F.; Schulze, D.; Hajnsek, I.; Pretzsch, H.; Papathanassiou, K.P. TanDEM-X Pol-InSAR performance for forest height estimation. *IEEE Trans. Geosci. Remote Sens.* **2014**, *52*, 6404–6422.
35. Krieger, G.; Moreira, A.; Fiedler, H.; Hajnsek, I.; Werner, M.; Younis, M.; Zink, M. TanDEM-X: A satellite formation for high-resolution SAR interferometry. *IEEE Trans. Geosci. Remote Sens.* **2007**, *45*, 3317–3341.
36. Treuhaft, R.N.; Madsen, S.N.; Moghaddam, M.; Zyl, J.J. Vegetation characteristics and underlying topography from interferometric radar. *Radio Sci.* **1996**, *31*, 1449–1485.
37. Cloude, S.; Papathanassiou, K. Three-Stage inversion process for polarimetric SAR interferometry. *IEE Proc. Radar Sonar Navig.* **2003**, *150*, 125–134.

38. Treuhaft, R.N.; Siqueira, P.R. The calculated performance of forest structure and biomass estimates from interferometric radar. *Waves Random Complex Mediu.* **2004**, *14*, S345–S358.
39. Askne, J.I.H.; Dammert, P.B.G.; Ulander, L.M.H.; Smith, G. C-band repeat-pass interferometric SAR observations of the forest. *IEEE Trans. Geosci. Remote Sens.* **1997**, *35*, 25–35.
40. Praks, J.; Kugler, F.; Papathanassiou, K.P.; Hajnsek, I.; Hallikainen, M. Height estimation of boreal forest: Interferometric model-based inversion at L-and X-band versus HUTSCAT profiling scatterometer. *IEEE Geosci. Remote Sens. Lett.* **2007**, *4*, 466–470.
41. Praks, J.; Demirpolat, C.; Antropov, O.; Hallikainen, M. On forest height retrieval from spaceborne X-band interferometric SAR images under variable seasonal conditions. In Proceedings of the XXXIII Finnish URSI Convention on Radio Science and SMARAD Seminar, Otaniemi, Finland, 24–25 April 2013; pp. 115–118.
42. Solberg, S.; Weydahl, D.J.; Astrup, R. Temporal stability of X-band single-pass InSAR heights in a spruce forest: Effects of acquisition properties and season. *IEEE Trans. Geosci. Remote Sens.* **2015**, *53*, 1607–1614.
43. Olesk, A.; Voormansik, K.; Tamm, T.; Noorma, M.; Praks, J. Seasonal effects on the estimation of height of boreal and deciduous forests from interferometric TanDEM-X coherence data. In Proceedings of the 2015 SPIE Remote Sensing. International Society for Optics and Photonics, Toulouse, France, 21–24 September 2015.
44. Olesk, A.; Voormansik, K.; Vain, A.; Noorma, M.; Praks, J. Seasonal differences in forest height estimation from interferometric TanDEM-X coherence data. *IEEE J. Sel. Top. Appl. Earth Obs. Remote Sens.* **2015**, *8*, 5565–5572.
45. Kugler, F.; Lee, S.K.; Hajnsek, I.; Papathanassiou, K.P. Forest height estimation by means of Pol-InSAR data inversion: The role of the vertical wavenumber. *IEEE Trans. Geosci. Remote Sens.* **2015**, *53*, 5294–5311.
46. Estonian Environment Agency (EEIC). Available online: http://www.keskkonnaagentuur.ee/ (accessed on 20 April 2016).
47. Riigi Teataja. Available online: https://www.riigiteataja.ee/akt/MS (accessed on 23 April 2016).
48. Voormansik, K.; Praks, J.; Antropov, O.; Jagomagi, J.; Zalite, K. Flood mapping with TerraSAR-X in forested regions in Estonia. *IEEE J. Sel. Top. Appl. Earth Obs. Remote Sens.* **2014**, *7*, 562–577.
49. Zalite, K.; Voormansik, K.; Olesk, A.; Noorma, M.; Reinart, A. Effects of inundated vegetation on X-band HH–VV backscatter and phase difference. *IEEE J. Sel. Top. Appl. Earth Obs. Remote Sens.* **2014**, *7*, 1402–1406.
50. Estonian Meteorological and Hydrological Institute. Available online: http://www.emhi.ee/ (accessed on 24 April 2016).
51. Lang, M.; Arumäe, T.; Anniste, J. Estimation of main forest inventory variables from spectral and airborne lidar data in Aegviidu test site, Estonia. *For. Stud./Metsanduslikud Uurim.* **2012**, *56*, 27–41.
52. McGaughey, R. FUSION/LDV: Software for LIDAR Data Analysis and Visualization. Version 3.42. Available online: http://forsys.cfr.washington.edu/fusion/FUSION_manual.pdf (accessed on 21 March 2015).
53. Hoen, E.W. A Correlation-Based Approach to Modeling Interferometric Radar Observations of the Greenland Ice Sheet. Ph.D. Thesis, Stanford University, CA, USA, 2001.
54. Praks, J.; Hallikainen, M.; Kugler, F.; Papathanassiou, K.P. X-band extinction in boreal forest: Estimation by using E-SAR POLInSAR and HUTSCAT. In Proceedings of the 2007 IEEE International Geoscience and Remote Sensing Symposium, Barcelona, Spain, 23–27 July 2007; pp. 1128–1131.

V

Arumäe, T., Lang, M. 2016. ALS-based wood volume models of forest stands and comparison with forest inventory data. Forestry Studies, 64, 5–16.

Forestry Studies | Metsanduslikud Uurimused, Vol. 64, Pages 5–16

DE GRUYTER
OPEN

Aerolidarilt puistu tüvemahu hindamise mudelid ning võrdlus takseeritud tagavaraga

Tauri Arumäe[1,2*] **ja Mait Lang**[1,3]

Arumäe, T., Lang, M. 2016. ALS-based wood volume models of forest stands and comparison with forest inventory data. – Forestry Studies | Metsanduslikud Uurimused 64, 5–16. ISSN 1406-9954. Journal homepage: http://mi.emu.ee/forestry.studies

Abstract. Airborne laser scanning (ALS) based standing wood volume models were analysed in two contrasting test sites with different forest types in Estonia. In Aegviidu test site main tree species are Scots pine and Norway spruce and Laeva test site is mainly dominated by deciduous species. ALS data measurements were carried out for Aegviidu in 2008 and for Laeva in 2013. Approximately 450 sample plots were established additionally to the forest inventory dataset in both test sites. Exclusive to the sample plots, 46 stands were measured in 2012 in Aegviidu for stand-level model. The sample plot-based model standard error in Aegviidu was S_e = 59.8 m^3/ha (22%) and in Laeva S_e = 69.2 m^3/ha (29%). The stand-level model based on 46 measured stands from Aegviidu had S_e = 38.4 m^3/ha. Based on the models a cross-validation between the two test sites was carried out and systematic differences between the two test sites were found. The reasons are related to differences in optical properties of trees, crown shapes, flight configuration and canopy cover even though the sample plot-based models included ALS-based canopy cover variable. The ALS-based wood volume estimate was also compared to forest inventory (FI) data and systematically larger estimates compared to FI dataset in both test sites were found. This average systematic error increased substantially (by 100 m^3/ha) for stands with wood volume over 250 m^3/ha. It was also detected that a model developed on small point clouds drawn for sample plots may produce systematic errors when applied to stand-level point clouds.

Key words: airborne lidar data, standing wood volume, forest inventory data, point cloud size.

Authors' addresses: [1]Institute of Forestry and Rural Engineering, Estonian University of Life Sciences, Kreutzwaldi 5, 51014 Tartu, Estonia; [2]State Forest Management Centre, 10149, Toompuiestee 24, Tallinn; [3]Tartu Observatory, 61602 Tõravere, Tartumaa, Estonia; *e-mail: tauri.arumae@rmk.ee

Sissejuhatus

Aerolidari (ALS) andmed on laialdast kasutust leidnud praktilises metsanduses – nii saab ALS andmetelt hinnata metsade puidu tagavara (Næsset, 2002; Salas *et al.*, 2010; Bouvier *et al.*, 2015), kõrgust (Næsset, 1997; Næsset & Bjerknes, 2001), võraalguse kõrgust (Arumäe & Lang, 2013) ja seeläbi planeerida majandustegevust. ALS-mõõdistamisega Eestis alustas Maa-amet aastal 2008. Kogu ala mõõdistatakse regulaarselt nelja-aastase tsükliga, mis tähendab, et aastaks 2015 oli kogu riik kaetud korduvate laserandmetega (LiDAR kõrguspunktid, 2015).

Üksiku puu tagavara all mõistetakse enamasti puu tüve mahtu koos koorega, juurekaelast ladvani, ilma okste mahuta (Krigul, 1972; Vaus, 2005). Puistu tagavara (*M*) on defineeritud kui kõigi elusate, üle 1,3 meetri kõrguste puude mahtude summa. Puistu tagavara on üks olulisemaid metsa struktuuri kirjeldavaid tunnuseid metsade

DOI: 10.1515/fsmu-2016-0001

majandamise planeerimisel, majandusliku väärtuse hindamisel ning on otseselt kasutatav taimestikku seotud süsiniku hindamiseks (Neumann *et al.*, 2016). Puutüve mahu arvutamiseks kasutatakse erinevaid mudeleid, mille hinnangud ei lange alati kokku (Krigul, 1972; Ozolinš, 2002; Padari *et al.*, 2009). Kõige lihtsamal juhul võiks puutüve ette kujutada koonusena, mille mahu saab arvutada tüve rinnasläbimõõdu (*d*) ja kõrguse (*h*) järgi. Siiski erineb puu tüvi koonusest üsna palju ja seetõttu kasutatakse funktsioone, mis reaalsete puude tüve kuju paremini lähendavad (Ozolinš, 2002; Metsa korraldamise…, 2009). Puistu tüvemahu ehk puidu tagavara hindamine ALS punktipilvest põhineb selle pilve punktide meetrikute (Næsset, 1997; Lang *et al.*, 2012; Maack *et al.*, 2016) ja metsas mõõdetud proovitükkidelt saadud puistu takseertunnuste seostel. Punktipilve meetrikutele (peegelduste kõrgusjaotuse protsentiilid, peegelduste suhteline vertikaalne jaotus jm) ning proovitükkidel mõõdetud puistu takseertunnustele tuginedes koostatakse mudelid, mida saab lausaliselt punktipilvel rakendada.

Aerolidari andmestik annab meile võimaluse uuendada kunagi kutseliste taksaatorite koostatud ja andmebaasidesse salvestatud takseerkirjeldusi, mis on olnud metsade majandamiskava aluseks. Metsamajanduskava aluseks olevaid andmeid kontrollivad Keskkonnaagentuuri audiitorid (Metsaressursi arvestuse…, 2016) ja seejärel kantakse takseerkirjeldused Metsaressursi arvestuse riikliku registri andmebaasi (edaspidi Metsaregister; Metsaressursi arvestuse…, 2016). Kui andmed on registrisse lisatud, siis tavaliselt ei uuendata kirjeid peale planeeritud majandusotsuste teostamist, vaid alles peale järgmiste metsamajandamiskava koostamist. Keskmine vanus Metsaregistri kirjetel on viis aastat (Pärt, 2010), lisaks on takseerandmetes vigadega kirjeid. Aerolidari andmed uuenevad Maa-ameti lennuplaanide järgi iga 4...5 aasta järel (LiDAR kõrguspunktid, 2015), mistõttu tagab see palju ajakohasema ülevaate meie metsaressurssidest.

Statistilise metsainventuuri (SMI) raames on selgunud, et Metsaregistris olevate takseeritud eraldiste tagavara on süstemaatiliselt alla hinnatud, võrrelduna SMI andmetega (Pärt, 2010). SMI käigus mõõdetakse Eestis aastas metsamaal umbes 2300 proovitükki (Adermann, 2010), eesmärgiga saada Eesti metsadest ja maakasutusest üldine ülevaade. SMI ja takseerimise tulemusel saadud puidu tagavara hinnangute süstemaatilise erinevuse põhjuseks on erinev metoodika – kui proovitükkidel põhinev SMI andmestik saadakse instrumentaalse mõõtmisega, siis takseerimisel tuginevad väljaõppinud taksaatorid võimalusel varasematele takseerandmetele ja silmamõõdulisele hinnangule (Raudsaar *et al.*, 2014). Varasemate takseerandmete kasutamine mõjutab aga paratamatult taksaatorit tema hinnangutes ja tulemus võib olla nihutatud (Raudsaar *et al.*, 2014). Võrreldes proovitükkide mõõtmisega kasutavad taksaatorid mõõteriistadest vajadusel vaid Bitterlichi relaskoopi rinnaspindala hindamiseks ja kõrgusmõõtjat, et mõnel mudelpuul mõõta kõrgus. Lisaks mõõdetakse mõnel mudelpuul rinnasdiameeter, millega üldjuhul mõõtmised piirduvad. Kuna ALS-andmetel põhinevad mahumudelid on lähendatud SMI-sarnase mõõtmismetoodikaga tehtud proovitükkidelt, siis võib eeldada Metsaregistri ja ALS-andmetel põhinevates tagavarade hinnangutes samuti süstemaatilisi erinevusi.

Uurimuse eesmärgiks on anda ülevaade aerolidari andmetel põhinevatest puistu tüvemahu hindamise mudelitest ning võimalikest probleemidest nende kasutamisel. Analüüsis võrreldi omavahel kahe erineva katseala, Laeva ja Aegviidu proovitükkide andmetel koostatud mudeleid ja rakendati neid mudeleid ka eraldiste kaupa ning võrreldi tulemusi Metsaregistris olevate puistute takseerimisel saadud tüvemahu hinnangutega.

Materjal ja metoodika

Katsealad

Antud uurimuses on kasutatud kahe katseala andmeid – Aegviidu (EPSG:3301, 6572701 N; 587333 E) ja Laeva (EPSG:3301, 6490854 N; 642472 E). Aegviidu katseala (joonis 1) rajati aastal 2008 (Anniste & Viilup, 2011). Katsealade suuruseks valiti 15 × 15 km. Aegviidus oli takseerandmetega kaetud 76% alast ning domineerivaks puuliigiks oli harilik mänd (*Pinus sylvestris* L.). Kokku mõõdeti Aegviidu katsealal 452 ringproovitükki, raadiusega 8–15 meetrit. Laeva katseala (Lang *et al.*, 2014) rajati 2013. aastal sarnaselt Aegviiduga. Laeva katseala pindalast 52% on takseerandmetega mets ja domineerivateks puuliikideks on arukask (*Betula pendula* Roth) ning harilik haab (*Populus tremula* L.). Laeva katsealal mõõdeti 405 proovitükki. Mõlemal katsealal rajati proovitükid eraldise homogeensesse ossa, mis kirjeldaks eraldise keskmist kõige paremini. Proovitükid jagati puistutesse testala puistute liigilise koosseisu jagunemisega võrdeliselt.

Joonis 1. Laeva ja Aegviidu katsealad.
Figure 1. Laeva and Aegviidu test sites.

Lisaks 452 ringproovitükile tehti Aegviidu katsealal 2012. aastal uued mõõtmised eraldisepõhiseks analüüsiks. Valimis oli 46 eraldist, igasse eraldisse rajati 8...12 ringproovitükki sõltuvalt eraldise pindalast. Proovitükid olid raadiusega 8...15 meetrit lähtudes Bitterlichi lihtrelaskoobi loendist. Proovitükid olid paigutatud vähemalt 50-meetriste piki- ja külgvahedega määratud käigujoontele. Hiljem arvutati proovitükkide keskmistena eraldiste tagavarade hinnangud, mida kasutati eraldiste piiride järgi välja lõigatud punktipilvel põhineva mudeli lähendamiseks.

Aerolidari andmed

ALS-mõõtmised katsealadel tegi Maa-amet laserskanneriga Leica ALS50-II. Aegviidu katseala skaneeriti 2008. aasta suvel (lennukuupäevad: 11.07, 27.07, 01.09). Andmetihedus laserandmetel oli 0,45 peegeldust/m^2, lennukõrgus oli 2400 m, proovitükkide esimeste peegelduste ja kõikide peegelduste suhtearv oli 0,71. Laeva katsealal lennati suvel 2013 (13.07) ja andmetihedus oli 2,0 peegeldust/m^2, lennukõrgus oli 1550 m, proovitükkide esimeste ja kõigi peegelduste suhtearv oli 0,78.

Aerolidari andmete töötlemiseks kasutati vabavara FUSION (McGaughey, 2014). Laserandmetest filtreeriti esmalt maapinnalähedased peegeldused, kasutades FUSIONi moodulit GroundFilter ning koostati mooduliga GridSurfaceCreate maapinna kõrgusmudel (DTM – *digital terrain model*). Seejärel lahutati DTM peegelduste üldisest punktipilvest ClipData mooduliga. Maapinna kõrguse suhtes normeeritud punktipilvest lõigati metsaeraldiste piiride või proovitüki tsentrite koordinaatide ning raadiuse järgi peegelduste andmestikud (moodul PolyClipData). Eraldatud pilvedele arvutati pilve kirjeldavad meetrikud mooduliga CloudMetrics. Aegviidus mõõdetud 46 eraldise piirid puhverdati 10 meetrit sisse välistamaks tulemustes piirivigu.

Puistu tagavara (*M*) hindamiseks aerolidari andmetest kasutati puistu kõrgusel

(H), rinnaspindalal (G) ja vormiarvul (F) põhineva tüvemahu hindamise valemi (Krigul, 1972)

$$M = G \times H \times F \tag{1}$$

analoogi varasemast uuringust (Lang *et al.*, 2012)

$$M_{ALS} = (a \times P_{80}{}^{b} + c \times P_{25})\, K^{d}, \tag{2}$$

kus P_{80} – lidari peegelduste kõrgusjaotuse 80-protsentiil;
P_{25} – lidari peegelduste kõrgusjaotuse alumine kvartiil;
K – katvuse hinnang (Lang, 2010) arvutatuna 1,3 meetri kõrgusel referentsnivool;
a,b,c,d – katseala proovitükkidelt lähendatud mudeli parameetrid.

Võrreldes Lang *et al.* (2012) uurimusega, täpsustati Aegviidu puistute kõrguskõveraid proovitükkidel, mistõttu lähendati ka uued parameetrid tüvemahu mudelile (2). Parameetrite lähendamiseks kasutati tarkvara R programmi nls (R Core Team, 2014).

Mahumudeli vigade analüüsiks võrreldi esmalt 46 Aegviidu eraldise aerolidari andmetest hinnatud metsa kõrgust (H_{ALS}) ja mõõdetud metsa kõrgust, kuna punktipilve kõrgusjaotuse ülemised protsentiilid on mahumudelis (2) kõige olulisema kaaluga. H_{ALS} arvutamiseks kasutati P_{80} analoogselt Lang *et al.* (2012) uurimusele ja metsa kõrgus ALS-andmetelt arvutati valemiga

$$H_{ALS} = a \times P_{80} + b. \tag{3}$$

Aegviidu uuendatud proovitükkide andmete põhjal lähendati puistu kõrguse mudelile (3) samuti uued parameetrid a = 0,99 (S_{e_a} = 0,02) ja b = 1,11 (S_{e_b} = 0,27) ning saadi mudel determinatsioonikordajaga R^2 = 0,94 ja lähendi jääkveaga S_e = 1,53 m. Võrdlusandmetena kasutatud 46 eraldise mõõdetud kõrgused arvutati 2012. aastast kasvumudelitega (formis.emu.ee, mudel 9; Kiviste, 1999) 2008 aastasse, mil tehti lidarmõõdistus.

Takseerandmestik

Metsaregistri andmestik Laeva katsealale pärineb aastast 2013 ning Aegviidu katsealale aastast 2011. Mõlemal katsealal korrigeeriti puistute tagavara lasermõõdistuse aastasse juurdekasvu mudeliga (formis.emu.ee, mudel 179; Metsa korraldamise juhend, 2006). Keskmine aastane tüvepuidu juurdekasv Laeva eraldistel oli 5,9 m^3/ha/a ja Aegviidus 5,1 m^3/ha/a. Aegviidu katseala takseerandmestikus oli kokku 11631 eraldise kirjet ning Laeva katseala jaoks olid 4549 eraldise andmed. Eraldise tagavara (M_{Mreg}), mida võrreldi M_{ALS}-ga, arvutati I ja II rinde mahtude summana.

Andmetest eemaldati enne võrdlust ilmselgete vastuolude ja vigadega kirjed (piiriveast tingitud erinevused, vananenud andmed, osaliselt uuendamata vms), kus erinevused takseeritud tüvemahu ja ALS-põhise hinnangu vahel olid väga suured (Aegviidus *ca* 1000 kirjet, Laeva katsealal *ca* 300 eraldise kirjet).

Veahinnangud

Keskmine hinnangu viga (*MEE*) on arvutatud valemiga

$$MEE = \sum(X - Y)/N, \tag{4}$$

kus X on argument, Y on funktsioontunnus ja N on valimi maht.

Ruutkeskmine viga (*RMSE*) on arvutatud valemiga

$$RMSE = \sqrt{\sum(X - Y)^2 / N,} \tag{5}$$

kus X on argument, Y on funktsioontunnus ja N on valimi maht.

Eraldi katsena mõlemal testalal koostati mudelite valideerimiseks 1000 mudelit võttes iga mudeli koostamiseks juhuslikult umbes pooled proovitükkidest. Mudelit valideeriti iga kord samal katsealal valimist välja jäänud proovitükkidel. Igale uuele mudelile arvutati hinnangu keskmine viga ja ruutviga ja kõikide katsete põhjal saadi vigade 95%-lised usalduspiirid.

Tulemused

ALS-mudelid tagavara hindamiseks

Aegviidu ja Laeva katsealal hinnati proovitükkide põhjal mudelile (2) parameetrid ja saadi vastavalt mudelid M_{ALS_Aegv} ja M_{ALS_Laeva} (tabel 1). Aegviidus mõõdetud 46 eraldisele lähendati eraldi mahumudeli (2) parameetrid ja saadi mudel M_{ALS46}.

Tüvemahu mudelite mõju tagavara hinnangule

Aegviidu katseala takseeritud tüvemahu (M_{Mreg_Aegv}) ja aerolaserskaneerimise andmetelt arvutatud tüvemahu (M_{ALS_Aegv}) võrdlusest (joonis 2a) selgus, et takseeritud mahud on süstemaatiliselt alla hinnatud ja alates puistute tüvemahust 250 m^3/ha see vahe suureneb. Keskmine M_{Mreg_Aegv} ja M_{ALS_Aegv} erinevus alla 250 m^3/ha tagavaraga eraldistes oli 29 m^3/ha ja üle 250 m^3/ha tagavaraga eraldistes 158 m^3/ha. Ka Laeva puistute takseeritud tagavara (M_{Mreg_Laeva}) oli võrreldes ALS-andmetelt arvutatuga (M_{ALS_Laeva}) süstemaatiliselt väiksem (joonis 2b). Laeva katsealal olid erinevused vastavalt alla ja üle 250 m^3/ha tüvemahuga eraldistes 18 m^3/ha ja 116 m^3/ha. Sarnast

Tabel 1. Aegviidu ja Laeva puistute ALS-põhise mahumudeli (2) parameetrid ja standardvead (S_e).

Table 1. Parameters and standard errors (S_e) of wood volume model (2) for Aegviidu and Laeva test sites.

Katseala / *Test site*	Mudel / *Model*	S_e, m^3/ha^{-1}	Parameetrid / *Parameters*							
			a	S_e	*b*	S_e	*c*	S_e	*d*	S_e
Aegviidu	M_{ALS_Aegv}	59,8	3,48	0,96	1,55	0,08	9,22	1,76	1,08	0,07
Laeva	M_{ALS_Laeva}	69,2	0,58	0,26	1,91	0,12	9,06	1,27	*0,17*	0,12
Aegviidu 46 eraldist	M_{ALS46}	38,4	*2,10*	1,35	1,71	0,18	*3,99*	4,41	0,91	0,20

* Kursiivis toodud parameetrid on statistiliselt mitteolulised ($p > 0,05$).

** Parameters in italic are not statistically significant ($p > 0.05$).*

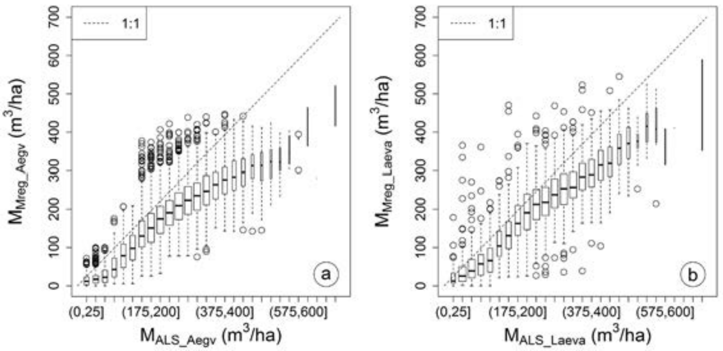

Joonis 2. Karpdiagrammidel ilmneb nii Aegviidu (a) kui Laeva (b) metsade takseeritud tagavara (M_{Mreg_Aegv}, M_{Mreg_Laeva}) süstemaatiline erinevus ALS-põhiselt hinnatud puistute tüvemahust (M_{ALS_Aegv}, M_{ALS_Laeva}).

Figure 2. There is a systematic difference of Aegviidu (a) and Laeva (b) forest management inventory database stand volume (M_{Mreg_Aegv}, M_{Mreg_Laeva}) from ALS-based stand volume estimates (M_{ALS_Aegv}, M_{ALS_Laeva}).

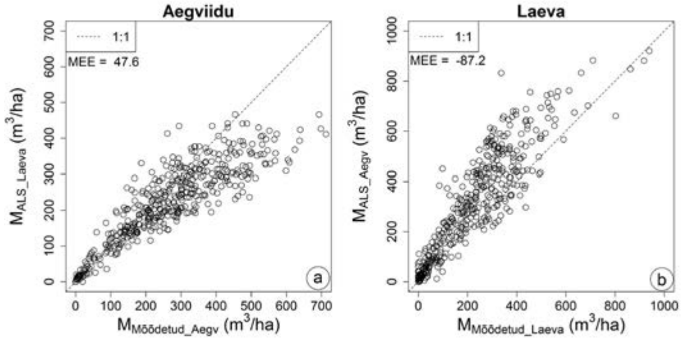

Joonis 3. Mudelite (M_{ALS_Laeva}, M_{ALS_Aegv}) ristvalideerimine Aegviidu (a) ja Laeva (b) katseala proovitükkidel mõõdetud tüvemahu andmetel ($M_{Mõõdetud\_Aegv}$, $M_{Mõõdetud\_Laeva}$).

Figure 3. Cross-validation of Aegviidu (a) and Laeva (b) models (M_{ALS_Laeva}, M_{ALS_Aegv}) using measured standing wood volume from sample plots ($M_{Mõõdetud\_Aegv}$, $M_{Mõõdetud\_Laeva}$).

süstemaatilist erinevust võrreldes Metsaregistri andmetega on käsitlenud ka Lang *et al*. (2014) ja Raudsaar *et al*. (2014).

Selgitamaks mahumudeli rakendatavust väljaspool katseala, ristvalideeriti Aegviidu ja Laeva ALS-põhiseid tagavara mudeleid. Selgus, et Aegviidus mõõdetud proovitükkide tagavarad ($M_{Mõõdetud\_Aegv}$) on neile Laeva mudeliga (M_{ALS_Laeva}) arvutatust süstemaatiliselt suuremad (MEE = 47 m³/ha) ja keskmine ruutviga ($RMSE$) on 92 m³/ha (joonis 3a). Võrdluseks sama katseala piires koostatud ja rakendatud ALS-põhised tagavara mudelite veahinnangute 95%-lised usalduspiirid olid $55 \leq RMSE \leq 66$ m³/ha ja $-11 \leq MEE \leq 11$ m³/ha. Laeva katsealal mõõdetud proovitükkide tagavarad ($M_{Mõõdetud\_Laeva}$) olid süstemaatiliselt väiksemad (MEE = –87 m³/ha ja $RMSE$ = 128 m³/ha) neile Aegviidu mudeliga (M_{ALS_Aegv}) saadud hinnangutest. Võrdluseks sama katseala piires koostatud ja rakendatud ALS-põhised tagavara mudelite veahinnangute 95%-lised usalduspiirid olid $65 \leq RMSE \leq 78$ m³/ha ja $-12 \leq MEE \leq 13$ m³/ha.

Nii nagu ainult proovitükkidele tugineva mudeli puhul, olid Aegviidus mõõdetud 46 eraldise tagavarad (M_{Er46}) suuremad eraldise takseeritud tagavarast (M_{Mreg}) (MEE=44,3 m³/ha). Kui neile 46 eraldisele arvutati tüvemaht mudeliga M_{ALS_Aegv}, siis saadi süstemaatiliselt suurem hinnang võrreldes mõõdetuga (MEE = –30,3 m³/ha) (joonis 4b). Rakendades aga nende 46 eraldiste piires tehtud punktipilve väljavõtetel koostatud mudelit Aegviidu katseala kõikidel proovitükkidel, saadi vastupidine süstemaatiline tüvemahu hinnangu nihe.

Tüvemahu hindamisel võib süstemaatiline viga tekkida, kui metsa kõrgus on ühesuunaliselt ja pidevalt alla või üle hinnatud. Aegviidu katsealal 46 puistu kõrgus (H_{Prt46}) on aga tugevas korrelatsioonis ($R^2 > 0,95$) aerolidarilt saadud metsa kõrguse hinnanguga (H_{ALS}) ja kahe hinnangu kooskõla kinnitab ka üsna väike MEE = 0,4 meetrit (joonis 4c).

Arutelu

Uurimuse tulemustest selgus, et proovitükkide lasermõõdistuse andmetel põhinevad tüvemahu mudelid annavad sarnaselt SMI tulemustega Metsaregistri takseerandmetes olevast tüvemahust süstemaatiliselt suuremaid hinnanguid. Põhjused on paljuski samad, kuid aerolidari andmete

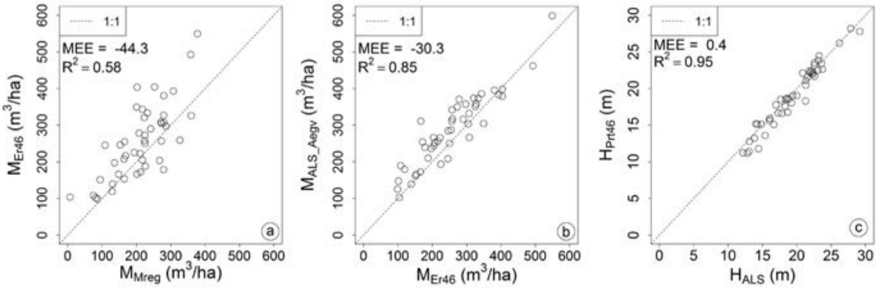

Joonis 4. Aegviidu 46 eraldise andmetel tehtud võrdlused: a) mõõdetud (M_{Er46}) ja takseeritud tagavara (M_{Mreg}); b) ALS-põhine mudel M_{ALS_Aegv} (tabel 1) ja mõõdetud tagavara (M_{Er46}); c) eraldistel mõõdetud kõrgus (H_{Prt46}) ja ALS-põhine puistu kõrgus (H_{ALS}).

Figure 4. Aegviidu 46 stands: a) measured (M_{Er46}) and forest inventory database (M_{Mreg}) wood volume; b) ALS-based (Table 1) (M_{ALS_Aegv}) and measured wood volume (M_{Er46}); c) measured stand height (H_{Prt46}) and predicted stand height (H_{ALS}) with test site model.

kasutamisel tuleb arvesse võtta veel muidki võimalikke veaallikaid.

Esimene võimalik veaallikas on mudelite koostamiseks kasutatud proovitükkide asukohatäpsus. Siiski on põhjust arvata, et proovitükile tema raadiuse ja tsentri asukoha koordinaatide järgi eraldatud aerolidari punktipilve asukohaviga on juhuslikku laadi ning tõenäoliselt selle vea tulemusel muutuvad mudelite lähendite jääkhälbed suuremaks ja hinnangutes olulisi süstemaatilisi vigu ei teki. Kui võtta lisaks arvesse eeskiri, millest lähtuvalt paigutati kõik mõõdetud proovitükid eraldise homogeensesse ossa ja piirist oluliselt sissepoole, siis tsentri asukoha 5...10 meetrise vea korral kõrgushinnangud oluliselt ei varieeru (Lang *et al.*, 2012).

Teine veaallikas on proovitükkide punktipilvede põhjal arvutatud peegelduste kõrgusjaotuse protsentiilide ja katvuse hinnangute võimalik süstemaatiline erinevus võrreldes suurte punktipilvede samade meetrikutega. Varasemas uuringus rakendasid Arumäe & Lang (2016) proovitükkidelt lähendatud metsa kõrgusmudelit 50 ha suurustele punktipilvedele ning tulemustest selgus, et see põhjustab kõrgushinnangutes süstemaatilise erinevuse. Peamiseks põhjuseks toodi suure punktipilve heterogeensus –50 ha suurusega punktipilve jääb nii lagedaid alasid kui 30-meetrise kõrgusega metsi, ning kõrgusprotsentiili abil selle pilve kirjeldamine ei pruugi olla kõige parem lahendus. Punktipilve suuruse mõju tuli ilmsiks ka antud uurimuses (joonis 4b). Lisaks punktipilve suurusele avaldab arvatavasti mõju ka erinev mõõtmismetoodika proovitükil ja eraldisel. Kui kogu testala mudeli koostamiseks rajatud proovitükid paigutati eraldise sisse, homogeensesse ossa, siis Aegviidu 46 eraldises paigutati proovitükid kindla vahemaa järgi, olenemata asukoha homogeensusest. Seejärel arvutati mõõdetud proovitükkide pealt eraldiste keskmised takseertunnused. Kui aga proovitükid paigutada metsa nii, et välditakse häile, siis võibki mudelisse tekkida positiivne viga tüvemahu ennustamisel. Seega tuleks suurtele aladele läheneda pigem rastripõhiselt, kus igale väiksele pikslile saab takseertunnuseid arvutada väikse pilve mudeliga, sest väiksematel punktipilve väljavõtetel kajastub metsa heterogeensus täpsemalt.

Mudelite eraldiste kaupa rakendamisel mõjutavad tulemust piirivead. Teadaolevalt võivad eraldiste piirivead olla kuni 10 meetrit ning näiteks paari meetri kõrguse noorendiku kõrval olevad kõrged puud võivad tekitada aerolidari andmetelt kõrguse hindamisel positiivse vea. Sarnaselt mõjuvad noorendikesse jäetud üksikud seemne- ja säilikpuud. Niisamuti võivad piiri- ja asukohavead väikese pindalaga või väga kitsaste ja ebakorrapäraste eraldiste kõrgushinnangut süstemaatiliselt kahandada, kui kõrval peaks olema lage ala. Kuna aerolidari mahumudelis (2) on kõige olulisema kaaluga P_{80} ehk 80-kõrgusprotsentiil, siis on metoodika tundlik kõrgushinnangu vigadele (ühe meetrine kõrguse ülehindamine tähendab hektaritagavara hinnangu kasvu mudeliga M_{ALS_Aegv} 25 kuupmeetri võrra). Punktipilve kõrgusjaotuse hinnangut mõjutab kaudselt ka puistu tihedus ja sellest tulenev võrastiku katvus. Näiteks kui sajast aerolidari peegeldusest kümme pärinevad piirivea tõttu naabereraldise kõrgematelt puudelt, siis P_{80} sellest tõenäoliselt ei muutu, kuid P_{90} puhul saavad just need kümme punkti määravaks. Katvuse hinnanguid mõjutavad aga ka peegelduste valik (Lang 2010), skaneerimisnurk (Korhonen *et al*., 2011) ja impulsi jagunemine. Katvuse stabiilse hinnangu saamine eeldab vähemalt 300 punkti proovitüki kohta (Rautiainen *et al*., 2005), mis standardse Maa-ameti ALS andmetiheduse juures nõuaks vähemalt 25 m suuruse piksli kasutamist. Samas suuremate pikslite puhul tekivad puistute servades piirivigade probleemid. Metsakorralduse tarbeks tehtavate ortofotode saamiseks lennatakse kõrgemalt, punkte on seetõttu hõredamalt (*ca* 0,2 peegeldust/m^2) ja seega puistupõhine lähenemine on õigustatud.

Kõrgushinnangute võrdluse katses 46 eraldisel selgus aga, et mõõdetud ja aerolidarilt hinnatud kõrgused on omavahel tugevas korrelatsioonis (joonis 4c) ja arvutatud keskmine H_{ALS} oli keskmiselt ainult 0,4 meetrit mõõdetust kõrgem. See muudab kõrguse hinnangutest tingitud suure süstemaatilise vea vähetõenäoliseks. Lisaks on aerolidaril põhinevasse puistu tüvemahu mudelisse (2) lisatud võrastiku katvuse hinnang (*K*), mille eesmärgiks on puistu tihedusega arvestamine. Kuigi Laeva katsealal selgus, et katvus on mudelis vähe-oluline (tabel 1), ei ole katvuse mudelist välja jätmine mudeli loogikast lähtuvalt põhjendatud. Mudeli standardviga katvuse välja jätmisel oluliselt ei muutunud ning on alust arvata, et see aitab ka piirivigadest tingitud puistute kõrgushinnangute vigu vähendada.

Kahe katseala mudelite ristvalideerimisel selgus, et lehtpuu- ja okaspuumetsade jaoks ei sobi ühiseks mudeliks ei Laeva ega Aegviidu andmetel lähendatud mudel. Kui katseala siseselt olid mudeli valideerimisel veahinnanguid väikesed, siis teisele katsealale rakendades veahinnangud suurenesid oluliselt. Põhjusena võib eelkõige välja tuua Laeva tihedad metsad, kus proovtükkidel arvutatud ALS-põhine keskmine võrastiku katvus oli 77%, aga Aegviidus oli keskmine ALS-põhine katvuse hinnang 66% ja erinevus on statistiliselt oluline (p < 0,001). Katvuse hinnangu küllastumisest tingituna on mudelis M_{ALS_Laeva} katvuse hinnang statistiliselt ebaoluline võrrelduna Aegviidu metsadega (tabel 1). Niisamuti on erinevatel liikidel erineva kujuga võrad, mis muudavad peegelduse tekkimist (Næsset, 2002). Seega oleks ALS andmetele tugineva tüvemahumudeli rakendamisel eelnevalt teada vaadeldava puistu liigilist koosseisu. Liigilise kooseisu määramist multispektraalsetelt satelliidipiltidelt näitasid Lang *et al.* (2014). Katvuse ja muude meetrikute hinnanguid võivad mõjutada nii puistute erinev keskmine peegeldustegur, mis skanneri Leica ALS50-II laserimpulsi lainepikkusel (1064 nm) on okasmetsas 0,15...0,20 ja lehtmetsas 0,30 (Kuusk *et al*., 2013). Niisamuti mõjutab meetrikuid lennukõrgus, mis määrab impulsi suuruse maapeal (*footprint*) (Nicholas *et al*., 2006). Lisaks kasutatakse ALS-mõõdistustel skanneri seadistustes automaatset tundlikkuse kontrolli (*automatic gain control* – AGC) (Vain *et al*., 2010; Korpela *et al*., 2013), mille mõju metsa jaoks saadud ALS-meetrikutele pole praktiliselt uuritud.

Omaette probleem on takseerandmete ja lasermõõdistamiste ajaline kokkusobivus. Takseerandmetes olev tüvemaht ennustati mahu juurdekasvu mudeli abil lasermõõdistamise aastasse, arvestades puistute inventeerimiskuupäevi. Selle tulemusel takseerandmetes oleva tüvemahu hinnangu ja aerolidari andmetelt saadud tüvemahu keskmine erinevus (*MEE*) kahanes 25 m^3/ha. Võib muidugi kahtlustada, et ka tüvemahu juurdekasvu mudel hindab mahu juurdekasvu alla. Siiski on näiteks Aegviidu 46 täpsemalt mõõdetud eraldise jaoks arvutatud juurdekasv 6,0 m^3/ha/a isegi veidi suurem kui Raudsaar *et al*. (2014) avaldatud Eesti puistute keskmine (5,2 m^3/ha/a).

Päris kõrvale ei saa jätta ka võimalust, et aerolidari andmete aluseks olevate proovitükkide mõõtmistes esinevad vead, mille tagajärjel saadakse süstemaatiliselt suurem tüvemahu hinnang, mis omakorda kandub edasi mudelisse. Selliseid probleeme tekitavad vead võivad olla näiteks vale tüveläbimõõdu mõõtmise kõrgus, vead puistu kõrguskõveras või proovitüki piiripealsete puude kaasamises. Laeva ja Aegviidu katseala proovitükke mõõtsid paljud erinevad mõõtjad ja samasuunalise vea tekkimine on vähetõenäoline.

Käesolevas uurimuses välja töötatud mudelid sobivad eelkõige kasutamiseks Laeva ja Aegviiduga piirkonnaga sarnastes metsades ning Maa-ameti suvistel lendudel tehtud mõõtmisandmetel, kuna kevadistel topograafilistel lendudel on lehtpuumetsadel oluliselt teistsugused peegeldusomadused. Niisamuti võib oletada, et mudelid võivad anda süstemaatilise veaga prognoosi Lääne-Eestis, kus metsadel on oluliselt teistsugune vormiarv (Padari, 1993).

Kokkuvõte

Töö tulemustest lähtuvalt saab teha kolm järgmist järeldust.

- Metsaregistris esitatud metsa tagavara on süstemaatiliselt alla hinnatud, võrreldes aerolidari andmetelt arvutatud tagavaraga. Allahindamine kasvab oluliselt eraldistes, kus tagavara on 250 m^3/ha või enam. Peamiste põhjustena on välja toodud takseerimisandmete silmamõõduline hindamine ning aerolidari andmete puhul proovitükkide põhiste mudelite rakendamine suurematele aladele.
- Väikestelt lidari punktipilvedelt saadud mudelid võivad eraldiste kaupa tehtud punktipilve väljavõtetele rakendades anda süstemaatilise veaga hinnanguid.
- ALS-andmetelt tuletatud metsa tagavara mudelid on soovitav kasutada lokaalselt või sarnastele metsatüüpidele. Antud uurimuses leiti Laeva lehtpuupuistute ja Aegviidu okaspuupuistute vahel olulised erinevused metsade võrastike katvuses (Laeva metsade keskmine katvus oli 11% suurem), mistõttu mudelite ristvalideerimisel ilmnesid ka olulised metsa tagavara hinnangu erinevused.

Tänuavaldused. Aegviidu ja Laeva katseala andmete kogumist toetas Riigimetsa Majandamise Keskus. Andmeanalüüsi toetas Haridusministeeriumi institutsionaalne uurimustoetus IUT21-4. Autorid tänavad kolme anonüümset retsensenti kasulike märkuste eest. Tänud Lauri Korhonenile ingliskeelse teksti kommenteerimise eest.

Kasutatud kirjandus

Adermann, V. 2010. Estonia (National forest inventory report). – Tomppo, E., Gschwantner, T., Lawrence, M., McRoberts, R.E. (eds.). National forest inventories: pathways for common reporting (NFI reports section). Heidelberg, Springer, 171–184.

Anniste, J., Viilup, Ü. 2011. Determination of forest characteristics with the laser scanning. (Metsa takseertunnuste määramisest laserskanneerimise abil). – Artiklid ja uurimused. Luua Metsanduskool, 10, 38–53. (In Estonian).

Arumäe, T., Lang, M. 2013. A simple model to estimate forest canopy base height from airborne lidar data. (Puistu esimese rinde võrastiku alguse kõrguse hindamine lennukilidari mõõdistusandmete järgi). – Forestry Studies / Metsanduslikud Uurimused, 58, 46–56.

Arumäe, T., Lang, M. 2016. A validation of coarse scale global vegetation height map for biomass estimation in hemiboreal forests in Estonia. – Baltic Forestry, 22(2). (In press).

Bouvier, M., Durrieu, S., Fournier, R.A., Renaud, J.P. 2015. Generalizing predictive models of forest inventory attributes using an area-based approach with airborne LiDAR data. – Remote Sensing of Environment, 156, 322–334.

Kiviste, A. 1999. Estonian forest growth models. (Eesti puistute kasvumudelitest). – Transactions of the Faculty of Forestry, Estonian Agricultural University, Continuous Forest Management Planning. (EPMÜ Metsandusteadukonna toimetised, Pidev metsa korraldus), 32, 28–36. (In Estonian).

Korhonen, L., Korpela, I., Heiskanen, J., Maltamo, M. 2011. Airborne discrete-return LIDAR data in the estimation of vertical canopy cover, angular canopy closure and leaf area index. – Remote Sensing of Environment, 115, 1065–1080.

Korpela, I., Hovi, A., Korhonen, L. 2013. Backscattering of individual LiDAR pulses from forest canopies explained by photogrammetrically derived vegetation structure. – ISPRS Journal of Photogrammetry and Remote Sensing, 83, 81–93.

Krigul, T. 1972. Forest mensuration. (Metsatakseerimine). Tallinn, Valgus. 348 pp. (In Estonian).

Kuusk, A., Lang, M., Kuusk, J. 2013. Database of optical and structural data for the validation of forest radiative transfer models. – Kokhanovsky, A. (ed.). Light Scattering Reviews, 7, Berlin, Heidelberg, Springer, 109–148.

Lang, M. 2010. Estimation of crown and canopy cover from airborne lidar data. (Metsa katvuse ja liituse hindamine lennukilt laserskanneriga). – Forestry Studies / Metsanduslikud Uurimused, 52, 5–17. (In Estonian with English summary).

Lang, M., Arumäe, T., Anniste, J. 2012. Estimation of main forest inventory variables from spectral and airborne lidar data in Aegviidu test site, Estonia. (Lennukilidari ja spektraalse kaugseireandmestiku kasutamine metsa peamiste takseertunnuste hindamiseks Aegviidu katsealal). – Forestry Studies / Metsanduslikud Uurimused, 56, 27–41. (In Estonian with English summary).

Lang, M., Arumäe, T., Lükk, T., Sims, A. 2014. Estimation of standing wood volume and species composition in managed nemoral multi-layer mixed forests by using nearest neighbour classifier, multispectral satellite images and airborne lidar data. – Forestry Studies / Metsanduslikud Uurimused, 61, 47–68.

LiDAR kõrguspunktid. 2015. (LiDAR heightpoints). [WWW document]. – URL http://geoportaal.maaamet.ee/est/Andmed-ja-kaardid/Topograafilised-andmed/Korgusandmed/LiDAR-korguspunktid-p499.html [Accessed 15 March 2016]. (In Estonian).

Maack, J., Lingenfelder, M., Weinacker, H., Koch, B. 2016. Modelling the standing timber volume of Baden-Württemberg – A large-scale approach using a fusion of Landsat, airborne LiDAR and National Forest Inventory data. – International Journal of Applied Earth Observation and Geoinformation, 49, 107–116.

McGaughey, R.J. 2014. FUSION/LDV: Software for LIDAR data analysis and visualization. March 2014 – FUSION, version 3.42. United States Department of Agriculture Forest Service Pacific Northwest Research Station.

Metsa korraldamise juhend. 2009. (Forest management guide). Riigi Teataja, RT I, 24.11.2015, 6. (In Estonian).

Metsaressursi arvestuse riikliku registri põhimäärus. 2016. (State register for accounting of forest resource). Riigi Teataja, RT I, 12.01.2016, 2. (In Estonian).

Næsset, E. 1997. Determination of mean tree height of forest stands using airborne laser scanner data. – ISPRS Journal of Photogrammetry & Remote Sensing, 52, 49–56.

Næsset, E. 2002. Predicting forest stand characteristics with airborne scanning laser using a practical two-stage procedure and field data. – Remote Sensing of Environment, 80, 88–99.

Næsset, E., Bjerknes, K.O. 2001. Estimating tree heights and number of stems in young forest stands using airborne laser scanner data. – Remote Sensing of Environment, 78, 328–340.

Neumann, M., Moreno, A., Mues, V., Härkönen, S., Mura, M., Bouriaud, O., Lang, M., Achten, W.M.J., Thivolle-Cazat, A., Bronisz, K., Merganič, J., Decuyper, M., Alberdi, I., Astrup, R., Mohren, F., Hasenauer, H. 2016. Comparison of carbon estimation methods for European forests. – Forest Ecology and Management, 361, 397–420.

Nicholas, R.G., Nichoals, C.C., Culvenor, D.C. 2006. Assessment of forest structure with airborne LiDAR and the effects of platform altitude. – Remote Sensing of Environment, 103, 140–152.

Ozolinš, R. 2002. Forest stand assortment structure analysis using mathematical modelling. – Forestry Studies / Metsanduslikud Uurimused, 37, 33–42.

Padari, A. 1993. Relationship between distance from sea and stand variables of Scots pine in Hiiumaa. (Hiiumaa männikute takseertunnuste sõltuvusest mere kaugusest). BSc Thesis, Estonian Agricultural University. (In Estonian).
Padari, A., Muiste, P., Mitt, R., Pärn, L. 2009. Estimation of Estonian wood fuel resources. – Baltic Forestry, 15, 77–85.
Pärt, E. 2010. Overview of Estonian forests. (Ülevaade: Eesti metsavarud). [WWW document]. – URL http://www.envir.ee/sites/default/files/elfinder/article_files/eestimetsavarud2.pdf [Accessed 15 March 2016]. (In Estonian).
R Core Team. 2014. R: a language and environment for statistical computing. R Foundation for Statistical Computing, Vienna, Austria. ISBN 3-900051-07-0. [WWW document]. – URL http://www.rproject.org [Accessed 15 March 2016].
Raudsaar, M., Pärt, E., Adermann, V. 2014. Overview of Estonian forests. (Ülevaade Eesti metsavarudest). – Keskkonnaagentuur (ed.). Aastaraamat Mets 2013. (Yearbook Forest 2013). Tartu, OÜ Paar, 1–2. (In Estonian).
Rautiainen, M., Stenberg, P., Nilson, T. 2005. Estimating canopy cover in scots pine stands. – Silva Fennica, 39, 137–142.
Salas, C., Ene, L., Gregoire, T.G., Næsset, E., Gobakken, T. 2010. Modelling tree diameter from airborne laser scanning derived variables: a comparison of spatial statistical models. – Remote Sensing of Environment, 114, 1277–1285.
Vain. A., Yu, W., Kaasalainen, S., Hyyppä, J. 2010. Correcting airborne laser scanning intensity data for automatic gain control effect. – IEEE Geoscience and Remote Sensing Letters, 7, 511–514.
Vaus, M. 2005. Forest mensuration. (Metsatakseerimine). Tartu, OÜ Halo Kirjastus. 178 pp. (In Estonian).

ALS-based wood volume models of forest stands and comparison with forest inventory data

Tauri Arumäe and Mait Lang

Summary

Airborne lidar (ALS) measurements have been carried out by Estonian Land Board regularly since 2008 in leaf-off conditions and during full-leaf conditions in summer. ALS measurements are widely used for digital terrain modelling, and in forestry for stand height, standing wood volume and canopy cover estimation (Næsset, 1997; Næsset & Bjerknes, 2001; Næsset, 2002; Salas *et al*., 2010; Bouvier *et al*., 2015). In this study ALS-based standing volume model (2) (Lang *et al*., 2012) was evaluated in two test sites (Figure 1) and the wood volume estimates were compared to data from forest inventory database. The two test sites represent two different contrasting forest types – Aegviidu (Anniste & Viilup, 2011) is dominated by coniferous forests and Laeva (Lang *et al*., 2014) is dominated by deciduous forests.

Three sets of parameters (Table 1) for the model (2) were estimated by using sample plot data from Aegviidu (M_{ALS_Aegv}), sample plot data from Laeva (M_{ALS_Laeva}) and data from 46 stands in Aegviidu (M_{ALS46}). For estimating variability of the models M_{ALS_Laeva} and M_{ALS_Aegv} at test site-level we created 1000 models, each based on approximately 50% of randomly selected sample plots. The estimated parameters for each model were validated on the remaining sample plots. The 95% confidence intervals of *MEE* (4) and *RMSE* (5) were calculated for the 1000 models.

The sample plot-based model estimated systematically larger wood volume for forest stands compared to forest inventory data. Similar difference of wood volume estimates between forest inventory data and National Forest Inventory (NFI) data is reported by Adermann (2010). The differences are caused by the applied methodology in sample plot measurements and forest inventory. The mean error of estimate (*MEE*) increased by about 100 m^3/ha in stands with standing volume estimates greater than > 250 m^3/ha in both test sites (Figure 2).

Cross-validation of the models from Laeva and Aegviidu (Figure 3) showed an increase in *MEE* and *RMSE* when the models were applied to the different type of forests, not present in the model data. The model M_{ALS_Laeva} gave on Aegviidu plots *MEE* = 47 m^3/ha and *RMSE*=92 m^3/ha (Figure 3a), while the random 1000 models showed much smaller *RMSE* (55...66 m^3/ha) and *MEE* (−11...11 m^3/ha). Similar results (Figure 3b) were found by applying the Aegviidu model M_{ALS_Aegv} to Laeva test plots and comparing it to the measured standing volume $M_{Mõõdetud\_Laeva}$ (*MEE* = −87 m^3/ha and *RMSE* = 128 m^3/ha).

The cross-validation results can partially be explained by the differences in forest types (optical properties in near infra-red spectral region) and canopy cover estimates (*K*) – in coniferous forests in Aegviidu the mean *K* was 66% and in Laeva deciduous forest it was 77%. In Laeva model (Table 1), the parameter of *K* was statistically insignificant, however, canopy cover estimate is crucial for correcting M_{ALS} estimates in sparse stands and therefore *K* was included into the model.

The study also showed that the ALS point cloud size has an influence to the wood volume estimates. Models that were developed on small plots (10...15 m) systematically (*MEE* 30 m^3/ha) overestimated the wood volume when applied to point clouds extracted for forest stands (Figure 4b). Similar effect of point cloud size on stand height estimations was shown by Arumäe & Lang (2016). However, the systematic difference is more likely related to the approach used to establish sample plots in forest when whole test site or a stand was described. The small circular plots were positioned in a homogeneous area in the stand, whereas the 46 stands were characterized by using randomly placed plots.

The model (2) parameters estimated in this study should only be used for forests similar to Aegviidu and Laeva test sites and using ALS-measurements carried out after final leaf unfolding phenophase.

Received March 24, 2016, revised May 24, 2016, accepted June 17, 2016

VI

Lang, M., **Arumäe, T.**, Laarmann, D., Kiviste, A. 2017. Estimation of change in forest height growth. Forestry Studies, 67, 5−16.

Forestry Studies | Metsanduslikud Uurimused, Vol. 67, Pages 5–16

DE GRUYTER
OPEN

Puistute kõrguskasvu muutuse hindamine

Mait Lang[1,2,*], Tauri Arumäe[2], Diana Laarmann[2] ja
Andres Kiviste[2]

Lang, M., Arumäe, T., Laarmann, D., Kiviste, A. 2017. Estimation of change in forest height growth. – Forestry Studies | Metsanduslikud Uurimused 67, 5–16. ISSN 1406-9954. Journal homepage: http://mi.emu.ee/forestry.studies

Abstract. Forest height increment rate is related to the forest growth conditions. Databases of previous forest inventories contain information about forest height-age relationship on large number of forest stands while repeated measurements of permanent sample plots provide an excellent reference for comparison. Repeated airborne laser scanning of forest stands is an additional source for the estimation of change in forest structure. In this study, height growth of middle-aged and older forest stands for about 10 year period was compared to an algebraic difference model on permanent sample plots (66) and for a sample of forest stands with repeated airborne laser scanning data (61). The model was based on a large dataset of forest inventory records from the period of 1984–1993. Statistically significant increased forest height growth was found in permanent sample plots based on tree height measurements (9 cm/yr^{-1}) as well in stands with repeated laser scanning data (4.5 cm/yr^{-1}) in South-East Estonia compared to the algebraic difference model. The difference between the two data sets was explained by their mean age and site class, but the increased forest height growth compared to the old forest inventory data indicates improved growth conditions of forests in the test area. The results hint also that empirical data-based forest growth models need to be updated to avoid biased growth estimates.

Key words: laser scanning, change detection, permanent sample plots, historical forest data, forest growth models.

Authors' addresses: [1]Tartu Observatory, 61602 Tõravere, Tartu County, Estonia; [2]Institute of Forestry and Rural Engineering, Estonian University of Life Sciences, Kreutzwaldi 5, 51014 Tartu, Estonia; *e-mail: mait.lang@to.ee

Sissejuhatus

Metsamajanduslike otsuste kavandamine põhineb andmetel ja mudelitel. Metsa kasvu seaduspärasusi kirjeldavate mudelite aluseks olevad mõõtmisandmed jätavad neisse mudelitesse oma jälje. Kui puistute kasvu mõjutavad keskkonnatingimused muutuvad, siis võib varasemate empiiriliste vaatlusandmete põhjal lähendatud mudeli parameetreid kasutades saada süstemaatilise veaga hinnangu (Kiviste, 1999).

Esimene avaldus metsa kasvu kiirenemisest Eestis ilmnes metsakorralduse takseerkirjelduste andmeil kasvukohatüübiti koostatud kõrguse vanuseridade võrdlemise tulemusel (Nilson & Kiviste, 1984). Samal aastal avaldati hüpotees metsa kasvu kiirenemisest ka Soome reservaatmetsadest võetud puursüdamike analüüsi põhjal (Hari *et al.*, 1984). Järgneva aastakümne jooksul avaldati mitmeid uurimusi muutustest metsa kasvus erinevates Euroopa maades (Spiecker *et al.*, 1996). Eestis võrreldi sõjajärgse (1950-ndate) ja 1990-ndate metsakorralduste andmeid puistute kaupa, millest selgus, et kõrgusindeks H50 oli 40-aastase perioodi jooksul suurenenud sõltuvalt puuliigist ja kasvukohast 2–3 meetrit (Kiviste, 1999). Lisaks metsakorralduse andmetele on puude kõrguskasvu muutust uuritud ka samas kasvukohas erineva vanusega puude kõrguse kasvukäikude võrdlemise teel (Metslaid *et al.*, 2011). Kuigi metsa kasvu kiirenemise kohta viimastel

DOI: 10.1515/fsmu-2017-0009

aastakümnetel on avaldatud arvestataval hulgal tõendeid, ei ole uurijate hulgas ühist seisukohta selle põhjuste osas: metsa kasvu kiirenemise põhjuseks on peetud süsihappegaasi kontsentratsiooni suurenemist atmosfääris, õhusaastest tingitud metsamulla viljakuse suurenemist, metsakuivenduse pikaajalist mõju, aga ka intensiivset metsamajandamist (hooldusraied, metsaselektsioon) (Nilson *et al.*, 1999). Puistu kõrguse kasv võib olla ka negatiivne, kui puude suremusest tingituna puistu laguneb või hoopis hävib tulekahju või tormi tõttu täielikult, mis on näiteks ürgmetsades häiringurežiimi normaalne osa (Mathiesen, 1940).

Puude kõrguste mõõtmiseks ja puistu kõrguse hindamiseks on järjest rohkem kasutusele võetud lennukitelt tehtav laserskaneerimine (lidarmõõdistus). Yu *et al.* (2006) kasutasid suure punktitihedusega skaneerimise andmeid üksikpuude kõrguskasvude mõõtmiseks ja leidsid, et peegelduste kõrgusjaotuste ülemised protsentiilid sobisid selleks hästi. Rutiinse topograafilise kaardistamise jaoks valitakse tavaliselt selline lennukõrgus ja skanneri seadistus, mille korral laserimpulss valgustab maapinna lähedal umbes 0,5 m läbimõõduga ala. Skanner registreerib kohad, kus laserkiire tagasipeegeldumine on kõige tugevam ja nii tekib kolmemõõtmeline punktipilv, milles kajastub nii maapind kui ka seda kattev laserimpulsi jaoks üldiselt poolläbilaskev puistu võrastiku struktuur. Peegelduste kõrgusjaotuse määrab peamiselt taimkatte lehepinnaindeks (Magnussen & Boudewyn, 1998). Korduvalt sama puistut mõõtes saame hinnata võrastikus toimunud muutusi.

Käesolevas uuringus võrreldi puistu kõrguse diferentsmudeliga (Kiviste, 1997) prognoositud kõrguse kasvu 1) Järvselja puistute korduva lidarmõõdistuse põhjal saadud kõrguse kasvuga ja 2) metsa kasvukäigu püsiproovitükkidel (Kiviste *et al.*, 2015) tehtud mõõtmistega. Eesmärgiks oli selgitada, kas puistute kõrguse kasv praegu ja ajavahemikul 1984–1993 on sarnane või on võimalik tuvastada süstemaatilisi erinevusi kasvu kiiruses.

Materjal and meetodika

Järvselja katseala metsaeraldiste andmed

Esimene vaatlusandmestik (tabel 1) puistute kõrguse kohta võeti Järvselja metsakorralduse andmebaasist. Järvselja puistute andmed on saadud tavalise lausmetsakorralduse meetodiga (Metsakorralduse, 2017). Metsa takseerimisel puistud piiritletakse, hinnatakse puistu koosseis ja mõõdetakse puistuelementide rinnaspindala. Puistuelementide kõrguse hindamiseks kasutatakse välitöödel üksikpuude mõõtmisandmeid. Puistuelemendi kõrguseks takseerandmetes on rinnaspindala järgi keskmise puu kõrgus (Lorey kõrgus, vt. Krigul, 1972). Takseerandmetes on ka eraldisele määratud kasvukohatüübi kood ja puistu vanus. Käesolevas uuringus kasutati 2011. aastal välja antud metsakorralduse andmebaasi.

Tabel 1. Järvseljal mõõdetud puistute üldiseloomustus (puuliikide koodide selgitused on lisas 1).

Table 1. General characteristics of Järvselja forest stands used in this study. Smaller site class values indicate fertile soils. Species codes are given in the Appendix 1.

Peapuuliik *Main species*	Boniteediklass *Site class*	Puistu vanus *Stand age*		Arv *Count*
		Minimum	*Maximum*	
HB	0	70	85	2
KS	0	50	100	3
KU	0	26	61	4
MA	0	75	75	1
KS	1	16	90	15
KU	1	34	78	6
LM	1	30	33	3
MA	1	115	115	1
KS	2	10	45	6
KU	2	37	200	3
MA	2	70	70	1
PN	2	90	105	2
KS	3	125	125	1
KU	3	125	125	1
LM	3	10	150	2
MA	3	115	115	1
KS	4	25	25	1
MA	4	130	190	5
MA	5	120	145	3

Metsa kasvukäigu püsiproovitükkide võrgustiku kordusmõõtmise andmed

Teine puistute kõrguse kasvu empiiriline andmestik pärines Eestit katva metsa kasvukäigu püsiproovitükkide võrgustiku (Kiviste *et al.*, 2015) andmebaasist. Analüüsimiseks võeti Järvseljast kuni 50 km kaugusel asuvate proovitükkide kaks 10-aastase vahega tehtud kordusmõõtmist, mille viimane mõõtmine oli aastail 2012–2016 (joonis 1). Neile tingimustele vastavaid mõõtmispaare ehk proovitükke oli 66, mille esimese mõõtmise üldandmed on esitatud tabelis 2. Nende puistute keskmine boniteet on 1,0. Neist 15 proovitükil oli kahe kordusmõõtmise vahel toimunud harvendusraie, mille käigus oli vähemalt 20% puudest välja raiutud. Puistu kõrguseks võeti esimese rinde puuliikide kõrguste rinnaspindala järgi kaalutud keskmine kõrgus.

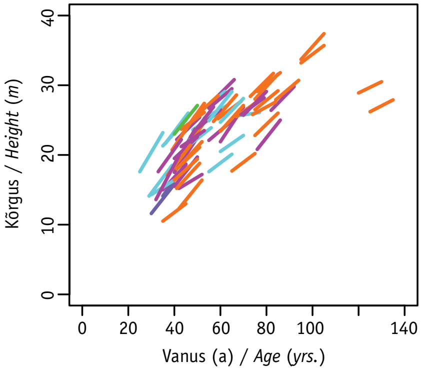

Joonis 1. Puistu I rinde keskmise kõrguse muutumine kümne aasta jooksul püsiproovitükkide kordusmõõtmiste andmeil. Värvid peapuuliikidele on vastavalt metsakorralduse juhendile.

Figure 1. Stand height growth of first layer during 10 years measured in the sample plots of the Estonian Network of Forest Research. Line colours correspond to dominating tree species.

Tabel 2. Metsa kasvukäigu proovitükkide võrgustiku puistute valimi üldiseloomustus (puuliikide koodide selgitused on lisas 1).

Table 2. General characteristics of sample plots of the Estonian Network of Forest Research Plots used in this study. Smaller site class values indicate fertile soils. Species codes are given in appendix 1.

Peapuuliik *Main species*	Boniteediklass *Site class*	Puistu vanus *Stand age* *Minimum*	*Maximum*	Arv *Count*
HB	0	40	40	1
KS	0	25	53	5
KS	1	29	67	8
KS	2	60	60	1
KS	3	55	55	1
KU	0	33	56	8
KU	1	32	82	9
KU	2	40	76	3
LM	2	35	35	1
LM	3	30	30	1
MA	0	39	95	8
MA	1	37	84	13
MA	2	41	125	4
MA	3	35	65	3

Puistute kõrguse kasvu hindamine lidarmõõdistuse andmete põhjal SA Järvselja Õppe- ja katsemetskonna alal

Käesolevas katses kasutatakse kahe tavalisest suurema punktitihedusega lidarmõõdistuse andmeid. Lasermõõtmised tegi Eesti Maa-amet 30. juulil 2009 skanneriga Leica ALS50-II ja 16. juunil 2017 skanneriga Riegl VQ-1560i (Riegl, 2017). Mõlemal aastal kasutas Eesti Maa-amet kõrguste esitamiseks Kroonlinna nullpunkti. Mõlemad skannerid töötavad spektri lähiinfrapunases osas 1064 nm lainepikkuse juures. Laserkiire hajumisnurk on 1/e^2 energia kriteeriumi järgi skanneril Leica ALS50-II 0,22 milliradiaani ja skanneril Riegl VQ-1560i ≤ 0,25 milliradiaani. Mõõtmiste põhieesmärgiks oli saada andmestik kolme Järvseljal asuva rahvusvahelise kiirguslevimudelite võrdluskatses kasutatud puistu kohta (Kuusk *et al.*, 2013), aga skaneeritud alale jäi ka teisi puistuid. Skannerite seadistusest ja lennukõrgusest (500 m ja 300 m) tulenevalt oli keskmine punktitihedus 2009. aastal 23,7 p/m^{-2} ja 161,3 p/m^{-2} 2017. aastal. Skaneerimisnurk ulatus 30 kraadini ja ühe impulsiga valgustatud ala läbimõõt (hetkevaateväli) oli maapinnal 2009. aastal 10–11 cm ja veidi üle 7 cm 2017. aastal.

Lasermõõdistuse andmetest lõigati iga puistu piiride järgi välja tükid. Puistutes, kus 2009. aastal ja 2017. aastal oli skaneeritud erineva suurusega ala, võeti peegeldused mõlema aasta mõõdistuse ühiselt alalt. Andmetöötluseks kasutati pakettide LAStools (Isenburg, 2017) ja FUSION (McGaughey, 2016) vahendeid. Servade mõju vähendamiseks jäeti peegelduste andmetest välja 10 m laiune puhverala puistute piiride lähedalt. Kahe mõõtmise ühisel alal leidus 61 üle 10-aastast puistut, kus oli vähemalt 0,1 ha suurune ala mõõdetud ja kahe laserskaneerimise vahelisel ajal polnud toimunud raieid ning puistu kõrgus eraldise siseselt oluliselt ei varieerunud. Nende puistute keskmine boniteediklass on 1,8.

Laserskaneerimise puhul mõõdetakse puistu kõrgust maapinna suhtes. Laserimpulsi peegelduste andmete kasutamisel kanduvad maapinna kõrguse vead seega edasi ka puistu kõrguse andmetesse. Maapinna kirjeldamiseks saab konstrueerida digitaalse kõrgusmudeli, aga kuna Järvselja puistutes on reljeefi muutused väikesed ja analüüsimiseks kasutati puistu ala kohta keskmistatud pilvemeetrikuid, siis uuriti peegelduste kõrgusjaotuse alumiste protsentiilide (H_{P01} ja H_{P05}) sobivust maapinna kõrguse hindamiseks. Eristades ainult esimesed või kõik peegeldused kaheks vaatlusandmestikuks saadi 2009. ja 2017. aasta lasermõõdistuse põhjal, et 2017. aastal on peegelduste kõrgusjaotuste maapinnalähedased protsentiilid keskmiselt 7–9 cm kõrgemal (tabel 3). Esimeste peegelduste kõrgusjaotuse 5-protsentiilide seos oli nõrgem nelja tiheda puistu tõttu, kus 2009. aastal maapinna lähedalt esimesi peegeldusi ei tekkinud. Puistute kõrguse arvutamiseks valiti maapinna kõrguste jaoks kõikidel peegeldustel põhinev H_{P01_k}, mille konkreetne väärtus määrati iga puistu alalt eraldatud punktiparvest.

Lidarmõõdistuse andmete alusel puistu kõrguse hindamisel tuleb teha nii peegelduste kui ka kõrgusjaotuse protsentiili valik. Üldiselt on osutunud otstarbekaks kasutada puistu kõrguse hindamiseks mõnda peegelduste kõrgusjaotuste ülemistest protsentiilidest (joonis 2). Erinevates skannerites kasutatavad peegelduskoha tuvastamise algoritmid ja erinevad mõõtmistingimused mõjutavad ühe impulsi kohta tekkivate peegelduste arvu ja peegelduste kõrgusjaotust. Näiteks Leica ALS50-II registreerib ühe impulsi kohta peegeldusi

Tabel 3. Peegelduste valik maapinna kõrguse määramiseks Järvselja 2009. ja 2017. aasta lasermõõdistuse andmetest. Statistiliselt mitteolulised parameetrid on kursiivis. S_e on mudeli jääkviga.

Table 3. Selection of point cloud metrics for the ground surface level estimation in Järvselja for years 2009 and 2017 and linear regression model (y=ax+b) between observations of the years. S_e is the model residual standard error. Statistically insignificant parameters are in italics.

Punktipilve meetrik / *Point cloud metric*	Väärtus (m) / *Value (m)*, *Aasta / Year*		Lineaarseose parameetrid / *Linear model parameters*			
	2009	2017	*a*	*b*	S_e	R^2
H_{P01_k}	33.94	34.03	*0.115*	0.565	0.08	0.998
H_{P01_1}	34.06	34.14	*0.120*	0.817	0.21	0.986
H_{P05_k}	34.22	34.29	*-0.170*	0.650	0.16	0.993
H_{P05_1}	35.40	34.91	*16.63*	0.0001	1.60	0.467

minimaalselt 3,5 m vahekauguselt (Leica, 2009), kuid Riegl VQ-1560i puhul on see piirang tõenäoliselt oluliselt väiksem (Erkko Grünthal, Eesti Maa-amet, Mustamäe tee 51, Tallinn). Ka ühe impulsi kohta registreeritavate peegelduste arv on skanneril Riegl VQ-1560i suurem võrreldes skanneriga Leica ALS50-II. Kõikidest peegeldustest moodustasid esimesed 2009. aastal 79% ja 2017. aastal 56%, teiste peegelduste osakaal oli vastavalt 19% ja 31%. Kuna esimesest peegeldusest järgmiste registreerimise metoodika oli skanneritel erinev (mida näitas ka teiste peegelduste osakaal), siis võeti puistu kõrguse mõõtmiseks andmestikust ainult laserimpulsi esimesed peegeldused. Puistute kõrguskasvu hindamiseks analüüsiti esimeste peegelduste kõrgusjaotuse 80-, 90-, 95- ja 99-protsentiilide väärtusi 2009. ja 2017. aastal. Peegelduste kõrgusjaotuse ülemised protsentiilid on osutunud sobivateks tunnusteks Eestis metsa kõrguse hindamisel (Lang *et al.*, 2012).

Puistu kõrguse diferentsmudel

Teise Maailmasõja järgsetel aastatel kasutati Eesti metsanduses puistu kõrguse prognoosimiseks peamiselt Orlovi boniteerimistabeleid. Pärast elektronarvutite kasutuselevõttu metsakorralduses 1970-ndatel aastatel tekkis võimalus takseerkirjelduste massiliseks töötlemiseks regressioonanalüüsi vahendusel (Tappo, 1982), kusjuures rühmitamise aluseks olid ikkagi boniteet ja peapuuliik. Orlovi boniteerimismudeli eeldusest vabanemiseks koostati Eesti riigimetsa 1984–1993.a. andmete põhjal puistute vanuseread kasvukohatüüpide ja peapuuliikide järgi (Kiviste, 1995). Ridade koostamisel kõrvaldati erindid ja edasises analüüsis kasutati vaid puistute andmeid latieast raievanuseni. Koostatud ridu on modelleeritud mitmel meetodil, millest on enim kasutamist leidnud algebraline diferentsmudel kujul

$$H_{pr} = f\,(A_1, H_1, A, OHOR, PE, TEKE) \qquad (1)$$

kus prognoositav kõrgus (H_{pr}) vanuses A arvutatakse lähtuvalt teadaolevast kõrgusest H_1 vanuses A_1, kasvukohatüübi mulla kõduhorisondi tüsedusest OHOR, enamuspuuliigist PE ja puistu tekkeviisist TEKE, mis võib olla, kas looduslik või kultuur (Kiviste, 1997). Kõrguse diferentsmudeli kasutajafunktsioon enamlevinud modelleerimiskeskkondade jaoks (R, FoxPro, Excel, OpenOffice) on allalaaditav infosüsteemist FORMIS (https://formis.emu.ee; ID = 9).

Andmeanalüüs

Järvselja puistute kõrguskasvu analüüsimiseks kasutati puistu esimese rinde keskmist kõrgust, mis saadi puistuelementide kõrguste rinnaspindalaga kaalutud keskmisena. Järvselja puistute kõrguse kasvu hindamiseks kahe lasermõõdistuse vahele jäävas ajavahemikus prognoositi puistutele kõrgus H_{pr} diferentsvõrrandiga (1) võttes aluseks 2011. aasta metsakorralduse andmetes oleva puistute inventeerimise aasta ja takseerandmed. Puistute kõrgus prognoositi nii 2009. kui ka 2017. aastasse ja edasi kasutati analüüsis nende kahe seisundi vahet võrdluseks lidarmõõdistuse andmetest arvutatud puistu kõrguse kasvule.

Valimisse sattunud puistu kasvukäigu proovitükkide esimese mõõtmise andmeil (enamuspuuliik, kasvukohatüüp, esimese rinde vanus ja kõrgus) arvutati diferentsvõrrandiga (1) puistu kõrguse prognoos 10 aastat edasi (H_{pr}) ning teisel mõõtmisel saadud puistu kõrguse ja prognoositud kõrguse vahe. Puistu tekkeviisiks võeti looduslik. Puistu kõrgus arvutati esimese rinde puuliikide kõrguste rinnaspindalaga kaalutud keskmisena. Kõrguskõveraks võeti Kiviste *et al.* (2003) üheparameetriline mudel, mille uuendatud parameetritega variant on allalaaditav metsanduslike mudelite infosüsteemist FORMIS (ID = 82). Puistu kõrguse ja prognoositud kõrguse keskmist vahet hinnati t-testiga ning vahet mõjutavaid faktoreid lineaarmeetodite protseduuri kasutades.

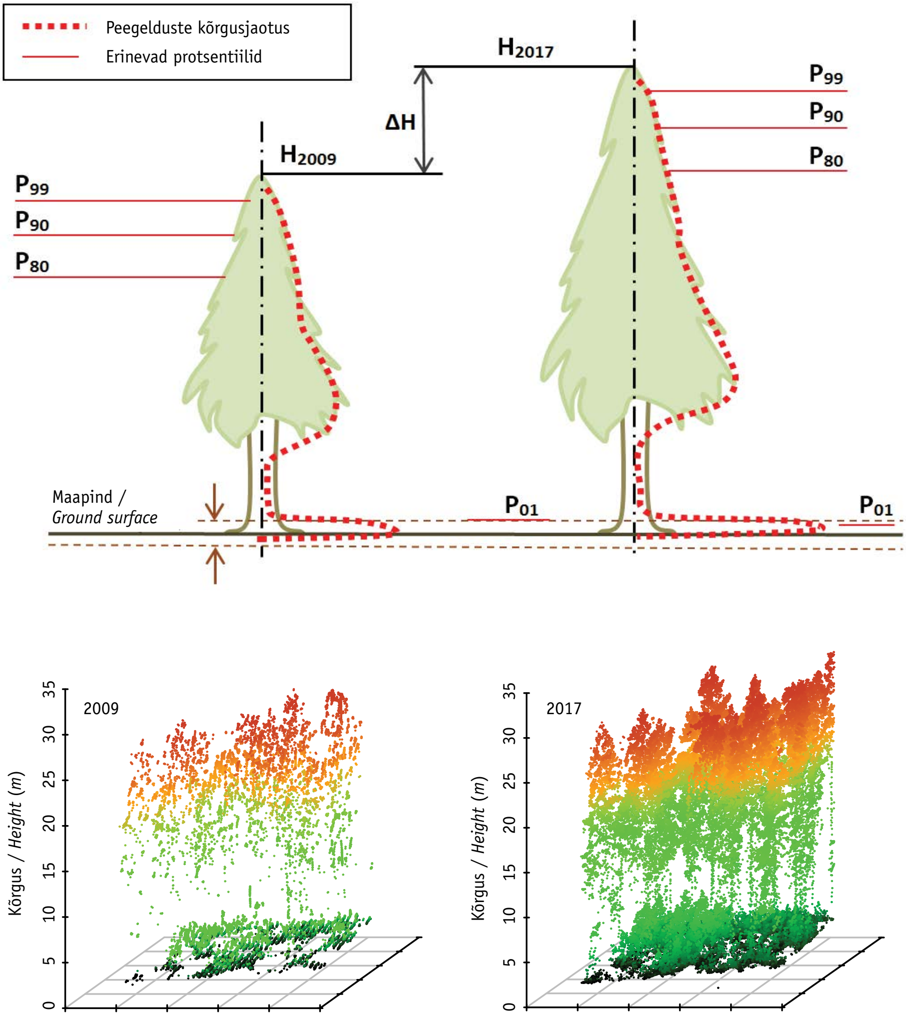

Joonis 2. Laserimpulsi peegelduste kõrgusjaotuse ülemised protsentiilid (P*), kõrguskasv ja näide 2009. ja 2017. aasta punktipilvest.

Figure 2. An approximate position of lidar point cloud height distribution percentiles (P) and examples of lidar data from 2009 and 2017 measurements.*

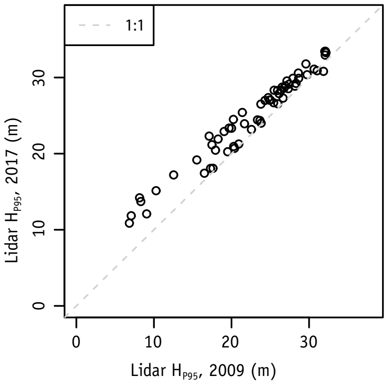

Joonis 3. Järvselja puistute 2009. aasta ja 2017. aasta lidarmõõdistusel saadud peegelduste kõrgusjaotuse 95-protsentiilid (HP95).

Figure 3. Forest height growth during the period 2009–2017 based on the 95th percentile of lidar pulse return height distribution.

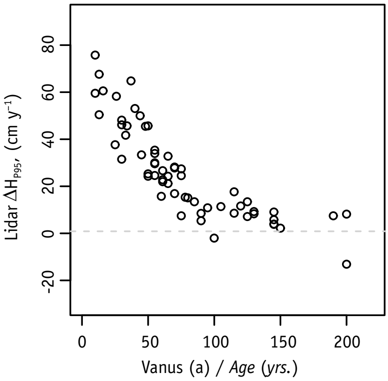

Joonis 4. Lasermõõdistusega saadud metsa kõrguskasvu hinnang ajavahemikus 2009–2017 sõltuvalt puistu vanusest.

Figure 4. Stand age dependence of airborne lidar measurements-based forest height growth estimate. The observation period ranges from 2009 to 2017.

Tulemused

Lasermõõdistuse andmetest arvutatud peegelduste kõrgusjaotuste ülemiste protsentiilide puhul ilmnes selgelt kõrguse kasv (*t-test*, $p < 0{,}01$). Noortes puistutes oli kõrguskasv suurem kui vanemates puistutes. Vanades või väheviljakatel muldadel kasvavatel metsadel oli kõrguskasv väike või isegi mõnikord negatiivne - suuremad puud surevad ja puistu laguneb (joonised 3, 4).

Kõik kasutatud kõrgusjaotuse ülemised protsentiilid v.a H_{P80} kasvasid keskmiselt kiiremini kui puistu kõrguse diferentsmudeliga ennustatud puistu kõrguse muutus ajavahemikus 2009–2017 (*t-test*, $p < 0{,}05$). Puistute kõrgus 8-aastase perioodi lõpus oli lidarmõõdistuse andmetel sõltuvalt vaadeldavast kõrgusjaotuse protsentiilist 0,38–0,48 m (standardviga < 0,1 m) suurem kui diferentsvõrrandiga prognoositud. H_{P80} puhul keskmiselt erinevust diferentsvõrrandiga prognoositud kõrguse kasvust ei saanud statistiliselt usaldusväärselt tõestada, kuigi hajuvusdiagramm oli üldiselt sarnane kõrgemate protsentiilide seosele (joonis 5). Kõrgusjaotuse madalamate

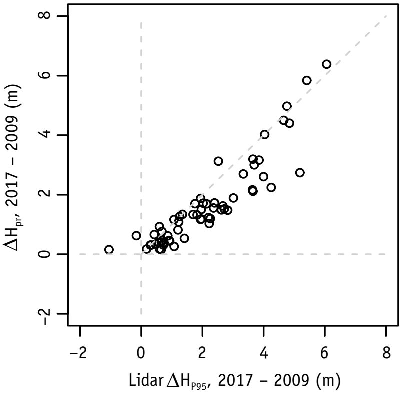

Joonis 5. Järvselja puistute korduval lasermõõdistusel (HP95) ja puistu kõrguse diferentsmudeliga (1) saadud metsa kõrguse Hpr kasvu võrdlus ajavahemikus 2009–2017.

Figure 5. Lidar measurements indicate greater height increment compared to old inventory data-based algebraic difference model (1) prediction Hpr.

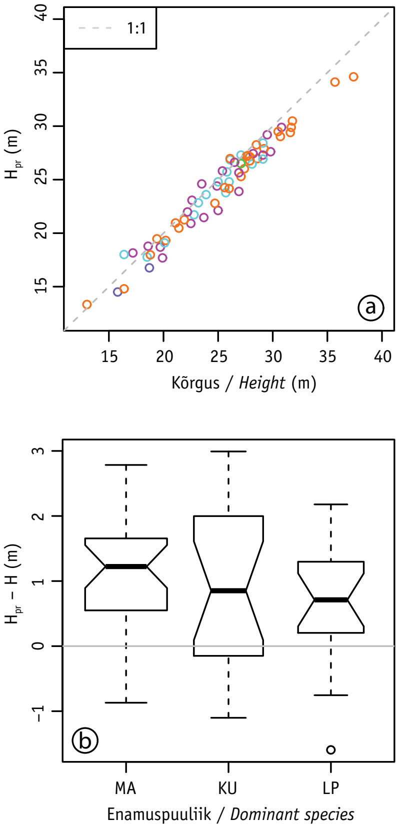

Joonis 6. (a) Püsiproovitükkidelt mõõdetud ja diferentsmudeliga prognoositud puistu kõrgused (värvid peapuuliikidele on vastavalt metsakorralduse juhendile). b) 10-aastase perioodi kõrguskasvu erinevus diferentsmudeli prognoosist karpdiagrammidena peapuuliikide järgi.

Figure 6. (a) Measurements in permanent sample plots indicate greater height increment during the last ten year period compared to old inventory data-based algebraic difference model prediction Hpr (colours correspond to tree species). (b) The increased height increment is present all stands dominated with pine (MA), spruce (KU) and deciduous broadleaf tree species (LP).

protsentiilide väärtuseid mõjutab puistu võrastiku liituse ja katvuse muutus, mis tuleneb puude võraraadiuste kasvust või alameetodil tehtud harvendusraietest. Testist jäeti välja lagunev, surevate puudega 200 aasta vanune kuusik, mille puhul lidarmõõdistuse andmetes esines kõikide ülemiste kõrgusprotsentiilide kahanemine. Ainult valimi kõige nooremates puistutes kaldus puistu kõrguse diferentsmudel prognoosima suuremat kõrguse kasvu kui ilmnes lasermõõdistuse andmetest.

Metsa kasvukäigu proovitükkidel kasvavate puistute kõrgus 10 aasta möödumisel osutus keskmiselt 0,92 m (standardviga 0,12 m) võrra suuremaks kui diferentsvõrrandiga prognoositud (joonis 6). Proovitükkide kõrguse ja prognoosi erinevus sõltus eelkõige puistu vanusest, aga ka harvendusraietest, mille mõju oli 0,54 m (standardviga 0,3 m).

Arutelu

Nii Järvselja puistute laserskaneerimise andmete põhjal kui ka Järvselja ümbrusse jäävatel metsa kasvukäigu püsiproovitükkidel tehtud mõõtmiste kohaselt kasvab puistute kõrgus üldiselt kiiremini kui prognoosib Eesti puistute ajavahemiku 1984–1993 takseerkirjeldustele tuginev Kiviste (1997) diferentsmudel. Lidariga tehtud kordusmõõdistuse andmete põhjal puistute kõrguskasvu hindamisel on oluline maapinna kõrguse täpne määramine. Peegelduste kõrgusjaotuse 1-protsentiilide erinevus oli kahe mõõdistuse andmete puhul ülemiste protsentiilide kasvuga (u 2 m) võrreldes tühine. Puistu kõrguse kasvu hindamiseks kasutatavad peegelduste kõrgusjaotuse ülemiste protsentiilide väärtused võivad olla mõjutatud impulsiga valgustatud ala suurusest ja skaneerimise tulemuseks saadud punktipilve tihedusest. Suurema hetkevaatevälja ja madalama punktitiheduse korral ei kajastu andmestikus puude ladvad vaid pigem võrade ülemised oksad. Käesolevas uurimuses kasutati suure punktitihedusega ja väikese hetkevaateväljaga (7–10 cm) skaneerimisandmeid, mis jäädvustavad puuvõrade ülaosa struktuuri üsna hästi. Laserimpulsi peegelduste kõrgusjaotuse ülemiste protsentiile asukohti mõjutab ka puuvõrade kuju ja lehemassi jaotus võras. Kui näiteks puude võrad muutuvad vananedes ülaosas laiemaks või lehtpuudel isegi üsna lamedaks, siis tekib rohkem peegeldusi kõrgemalt ning laserskaneerimise andmetest saadud puistu kõrguse hinnang kasvab rohkem kui ladva järgi mõõdetuna. Kantola & Mäkelä (2004) märgivad aga, et harilikul männil võra kuju vanusega oluliselt ei muutu ning kuusikutes võtab oluliste muutuste ilmnemine vähemalt 40 a. Ka Yu *et al.* (2006) näitasid, et lidarmõõdistusega ja maapealsete mõõtmistega saadud puude kõrguskasvude hinnangud on üsna hästi kooskõlas. Seega võib lidarmõõdistuse andmete põhjal saadud puistute kõrguse muudu hinnangut pidada usaldusväärseks.

Nii Järvselja puistute kõrguskasv lidarmõõtmiste alusel kui ka metsa kasvukäigu proovitükkidel tehtud puude kõrguste mõõtmiste järgi saadud kõrguskasv oli suurem kui diferentsvõrrandiga prognoositud. Lidarmõõdistusel põhinev Järvselja puistute kõrguskasv oli küll metsa kasvukäigu proovitükkidel olevate puistute kõrguskasvust oluliselt väiksem, kuid ka Järvselja puistute valimi keskmine boniteet oli keskmiselt poole klassi võrra madalam. Ka oli Järvselja puistute valimi keskmine vanus suurem ehk 2009. aastal 66 aastat võrreldes metsa kasvukäigu proovitükkidel kasvavatel puistute vanusega 54 aastat perioodi alguses.

Esmapilgul võiks järeldada, et Kiviste (1997) mudel ei sobi puistu kõrgusekasvu prognoosimiseks, sest samadel puistutel mõõdetud kõrguse kasv kümnekonna aasta jooksul ületas mudeliga prognoositu (seda nii püsiproovitükkide kui ka lidarmõõtmise andmeil). Seda, et mudel intensiivsel kasvuperioodil puistu kõrguskasvu alla hindab, on tõdetud ka metsakorralduse praktikas (Enn Pärt, kirjavahetus, 17.01.2018). Samas lähendas antud mudel 1984–1993. aastate metsakorralduse takseerkirjelduste andmeil koostatud metsatüüpide aegridu piisava täpsusega (Kiviste, 1997). Selle mudeli kuju oli üsna heas kooskõlas ka hilisemate metsakorralduste andmeil koostatud metsatüüpide aegridadega, ehkki mudeli asümptoodiparameetri hinnangud hilisematel andmetel olid mõnevõrra suuremad (metsatüüpide keskmised boniteedid paranesid). Selline olukord, kus puistute kordusmõõtmiste andmeil koostatud kasvukäik erineb erivanuseliste puistute üksikmõõtmiste andmeil koostatud aegreast, saab tekkida siis, kui puistu kasvukäik (kasvutingimused) ajas muutub. Mudelarvutuslikus katses, kus imiteeriti puistu kõrgusindeksi H_{50} pidevat suurenemist 4 cm aastas, tekkis praegusele väga sarnane olukord (Nilson & Kiviste, 1986; Kiviste, 1999), kus erivanuseliste puistute andmeil koostatud kõrguse aegrida oli samamoodi kumeram kui puistu tegelik kasvukäik. Enam-vähem samasugused tulemused saadi ka siis, kui Kiviste (1997) mudeli asemel kasutati Orlovi boniteerimistabelite lähendmudelit (Kiviste, 1999).

Metsa kasvu modelleerimine ajas muutuvate kasvutingimuse korral on tunduvalt keerulisem kui traditsiooniline puistu kasvukäigu modelleerimine (vaikimisi) kasvutingimuste konstantsust eeldades. Metsa kasvu kiirenemist Eestis võib põhjustada intensiivne metsamajandamine (metsauuendamise materjali kvaliteedi tõstmine, noorendike hooldamine, harvendusraied, kuivenduse pikaajaline mõju jne), aga ka üldine keskkonna muutumine (süsihappegaasi kontsentratsiooni suurenemine atmosfääris ja sellest tingitud soojenemine, õhusaaste toimimine metsamulla väetisena).

Puistu kasvukäigu edasisel modelleerimisel tuleb ilmselt loobuda metsakorralduse keskmiste takseertunnuste aegridade kasutamisest algandmetena ja selle asemel kasutada puistute kordusmõõtmiste andmeid (metsakorralduse takseerkirjeldustest, püsiproovitükkidelt või lidarmõõtmistest). Kõrguskasvu muutuse täpsemaks analüüsiks oleks vajalik puistu kõrgusena keskmise kõrguse asemel ülakõrguse kasutuselevõtmine. Ülakõrgus ei ole nii tundlik hooldusraietele kui keskmine kõrgus, mistõttu see sobiks kasvutingimuste kirjeldamiseks paremini kui keskmine kõrgus. Hetkel mõjutavad kõik eelpool loetletud potentsiaalsed mõjufaktorid kõrguskasvu positiivses suunas, kuid edaspidi võib olukord muutuda. Seetõttu tuleb jätkuvalt koguda andmeid metsa kohta, eelkõige muidugi jätkata mõõtmisi püsiproovitükkidel, aga vähemtähtis ei ole ka varasemate metsakorralduse takseerkirjelduste, kaugseire ja muu metsainfo säilitamine edasiseks töötlemiseks sobival kujul.

Tänuavaldused. Uurimus on osa Eesti Teadusagentuuri finantseeritavast projektist IUT21-4. Autorid tänavad Eesti Maa-ametit testlendude andmete kasutamisvõimaluse eest. Mait Metsur ja Erkko Grünthal Eesti Maa-ametist selgitasid Riegl-i laserskanneri tehnilisi eripärasid. Metsa kasvukäigu uuringute proovitükkide võrgustiku rajamist toetas Riigimetsa Majandamise Keskus ja kordusmõõtmiste korraldamist SA Keskkonnainvesteeringute Keskus. Autorid tänavad retsensente abistavate märkuste eest. Täname Enn Pärti kasulike tähelepanekute eest.

Lisa 1. Tabel A1. Puuliikide koodid.

Appendix 1. Table A1. Tree species codes.

Puuliigi kood / *Tree species code*	Puuliik *Species name*
HB	Harilik haab (*Populus tremula* L.)
KS	Arukask, sookask (*Betula pendula* Roth, *Betula pubescens* Ehrh.)
KU	Harilik kuusk (*Picea abies* (L.) Karst.)
LM	Sanglepp (*Alnus glutinosa* (L.) Gaertn.)
MA	Harilik mänd (*Pinus sylvestris* L.)
PN	Harilik pärn (*Tilia cordata* Mill.)

Kasutatud kirjandus

Hari, P., Arovaara, H., Raunemaa, T., Hautojärvi, A. 1984. Forest growth and effect of energy production: a method of detecting trends in the growth potential of trees. – Canadian Journal of Forest Research, 14, 437–440.

Isenburg, M. 2017. LAStools - efficient LiDAR processing software. [WWW document]. – URL http://rapidlasso.com/LAStools [Downloaded 17 October 2017, unlicensed].

Kantola, A., Mäkelä, A. 2004. Crown development in Norway spruce (*Picea abies* (L.) Karst.). – Trees 18, 408–421.

Kiviste, A. 1995. An analysis of main forest inventory variables in the Estonian state forests. (Eesti riigimetsa puistute kõrguse, diameetri ja tagavara sõltuvus puistu vanusest ja kasvukohatingimustest 1984.–1993. a. metsakorralduse takseerkirjelduste andmeil). – EPMÜ teadustööde kogumik, 181, 132–148. Tartu, Eesti Põllumajandusülikool. (In Estonian).

Kiviste, A. 1997. An algebraic difference model for the forest growth simulation in Estonia (Eesti riigimetsa puistute kõrguse, diameetri ja tagavara vanuseridade diferentsmudel 1984.–1993. a. metsakorralduse takseerkirjelduste andmeil). – EPMÜ teadustööde kogumik 189, 63−75. Tartu, Eesti Põllumajandusülikool. (In Estonian).

Kiviste, A. 1999. Site index change in the 1959s–1990s according to Estonian forest inventory data. – Causes and consequences of accelerating tree growth in Europe. EFI Proceedings, 27, 87–100.

Kiviste, A., Hordo, M., Kangur, A., Kardakov, A., Laarmann, D., Lilleleht, A., Metslaid, S., Sims, A., Korjus, H. 2015. Monitoring and modeling of forest ecosystems: the Estonian Network of Forest Research Plots. – Forestry Studies / Metsanduslikud Uurimused, 62, 26–38.

Kiviste, A., Nilson, A., Hordo, M., Merenäkk, M. 2003. Diameter distribution models and height-diameter equations for Estonian forests. – Amaro, A., Reed, D., Soares, P. (eds.). Modelling forest systems. CAB International, 169−179.

Krigul, T. 1972. Forest mensuration. (Metsatakseerimine). Tallinn, Valgus, 108–109. (In Estonian)

Kuusk, A., Lang, M., Kuusk, J. 2013. Database of optical and structural data for the validation of forest radiative transfer models. – Kokhanovsky, A.A. (ed.). Radiative Transfer and Optical Properties of Atmosphere and Underlying Surface. Light Scattering Reviews, 7, Springer, 109–148.

Lang, M., Arumäe, T., Anniste, J. 2012. Estimation of main forest inventory variables from spectral and airborne lidar data in Aegviidu test site, Estonia. – Forestry Studies / Metsanduslikud Uurimused, 56, 27–41.

Leica. 2009. Leica ALS50-II airborne laser scanner product specifications. Leica Geosystems AG Heerbrugg, Switzerland.

Magnussen, S., Boudewyn, P. 1998. Derivations of stand heights from airborne laser scanner data

with canopy-based quantile estimators. – Canadian Journal of Forest Research, 28, 1016–1031.
Mathiesen, A. 1940. Virgin forest and its aspect. (Ürgmetsast ja selle ilmest). R. Tohver, Tallinn. (In Estonian).
McGaughey, R.J. 2016. FUSION/LDV: Software for LIDAR data analysis and visualization. October 2016 – FUSION Version 3.60+. Pacific Northwest Research Station, United States Department of Agriculture Forest Service.
Metsakorralduse. 2017. Forest inventory act. (Metsa korraldamise juhend). – RT I, 22.02. 2017, 11. (In Estonian).
Metslaid, S., Sims, A., Kangur, A., Hordo, M., Jõgiste, K., Kiviste, A., Hari, P. 2011. Growth patterns from different forest generations of Scots pine in Estonia. − Journal of Forest Research, 16(3) 237−243.
Nilson, A., Kiviste, A. 1984. Männikute „kasvukäigu“ mudel tüpiseerimata kasvutingimuste järgi. – EPA teadusliku tööde kogumik, 151, 50−59. (In Estonian)
Nilson, A., Kiviste, A. 1986. Reflection of environmental changes in models of forest growth composed using different methods. In: Monitoring of forest ecosystems. Abstracts of scientific conference. Kaunas, 05–06.06.1986. Kaunas–Academy. p. 336–337. (In Russian).
Nilson, A., Kiviste, A., Korjus, H., Mihkelson, S., Etverk, I., Oja, T. 1999. Impact of recent and future climate change on Estonian forestry and adaptation tools. – Climate Research, 12, 205−214.
Riegl. 2017. Dual channel waveform processing airborne LiDAR scanning system for high-point density and ultra wide area mapping: Riegl VQ-1560i datasheet. [WWW document]. – URL http://www.riegl.com/nc/products/airborne-scanning/produktdetail/product/scanner/55/ [Accessed 03 November 2017].
Spiecker, H., Mielikäinen, K., Kohl M., Skovsgaard, J. (eds). 1996. Growth trends in European forests: studies from 12 countries. Springer, Berlin.
Tappo, E. 1982. Mean characteristics of forest stands in Estonia by dominant species, site fertility and age. (Eesti NSV puistute keskmised takseertunnused puistu enamuspuuliigi, boniteedi ja vanuse järgi). Tallinn, Eesti NSV Põllumajandusministeeriumi Informatsiooni ja Juurutamise Valitsus. 72 pp. (In Estonian).
Yu, X., Hyyppä, J., Kukko, A., Maltamo, M., Kaartinen, H. 2006. Change detection techniques for canopy height growth measurements using airborne laser scanner data. – Photogrammetric Engineering and Remote Sensing, 72, 1339–1348.

Estimation of change in forest height growth

Mait Lang, Tauri Arumäe, Diana Laarmann and Andres Kiviste

Summary

First signs of increased forest growth rate in Estonia were found by Nilson & Kiviste (1984) who analysed stand height dependence on age using forest inventory database records. In the same year Hari *et al.* (1984) published a hypothesis about increased forest growth rate based on increment cores taken from strictly protected forests. During following decade several publications about changes in forest growth were published (Spiecker *et al.*, 1996). However, there is still a question whether the increase in forest growth rate continues or has it reached its asymptote. In this study, height growth of middle-aged and older hemiboreal forests was analysed.

The empirical data was obtained from 61 forests stands (Table 1) with repeated airborne laser scanning data located in Järvselja, South-East Estonia and secondly from 66 permanent sample plots (Table 2) belonging to the Estonian Network of Forest Research Plots (Kiviste *et al.*, 2015) and located within 50 km range from Järvselja. The airborne laser scanning of Järvselja forest stands was carried out in 30.07.2009 for the Radiative transfer Model Intercomparison (RAMI) experiment (Kuusk *et al.*, 2013) and was repeated in 16.06.2017 by Estonian Land Board using Leica ALS50-II and Riegl VQ-1560i scanners. Mean point density was in 2009 23.7 p/m^{-2} and 161.3 p/m^{-2} in year 2017 (Figure 2). For each forest stand point heights were normalized using 1th percentile of point cloud height distribution which was strongly correlated between the 2007 and 2017 flights (Table 2). Lidar data were processed using LAStools (Isenburg, 2017) and FUSION (McGaughey, 2016). From the normalized to ground level point cloud for each stand 80th, 90th, 95th and 99th percentiles for first returns were extracted. For the permanent sample plots, first (upper) tree layer mean height was calculated using height curve fitted on sample tree measurements and basal area of trees was used for weight. Repeated measurements from each sample plot with 10 year interval were used for height growth calculation. For Järvselja forest stands and for permanent sample plots an old inventory data-based algebraic difference model (1) (Kiviste, 1995; 1997) was used to predict height (H_{pr}) for selected age (A) of each forest stand. The selected stand ages corresponded to the years of lidar measurements or the last measurement on permanent sample plots. The model additional parameters are known height H_1 at age A_1, soil organic layer thickness OHOR, stand origin (natural or cultivated) and dominant species. The model (1) is based on the 1984–1993 forest inventory data of Estonian State forests and represents forest growth conditions for the period in Estonia.

All the upper percentiles of lidar point cloud height distribution increased in all forest stands in Järvselja except in one old Silver birch stand and in one 200-years old Norway spruce stand where many tall trees were dead since 2009 (Figure 3). The increment in point cloud upper percentiles was greater in younger stands (Figure 4). In average, the increment in point cloud upper percentile values was 0.38–0.48 m greater (standard error < 0.1 m) than the height growth predicted with the model (1) (Figure 5) for the stands. Similar but even greater difference (0.92 m, standard error 0.12 m) was observed in permanent sample plots (Figure 6) between measurements and the model prediction. This can be well explained by the mean age (54 years) of the forest which was 12 years less than age of Järvselja stands and also the mean site fertility in permanent sample plots was significantly greater.

The difference between the two data sets was explained by their mean age and site class, but the increased forest height growth compared to the old forest inventory data indicates improved growth conditions of forests in the test area. The results hint also that empirical data-based forest growth models need to be update to avoid biased growth estimates. It is also important to continue tree measurements on the Estonian Network of Forest Research Plots (Kiviste *et al.*, 2015), while such time series are very valuable for detecting future trends in forest growth.

Received November 15, 2017, revised January 15, 2017, accepted January 29, 2018

VII

Arumäe, T., Lang, M. 2018. Estimation of canopy cover in dense mixed-species forests using airborne lidar data. European Journal of Remote Sensing, 51(1), 132−141.

European Journal of Remote Sensing

ISSN: (Print) 2279-7254 (Online) Journal homepage: http://www.tandfonline.com/loi/tejr20

Estimation of canopy cover in dense mixed-species forests using airborne lidar data

Tauri Arumäe & Mait Lang

To cite this article: Tauri Arumäe & Mait Lang (2018) Estimation of canopy cover in dense mixed-species forests using airborne lidar data, European Journal of Remote Sensing, 51:1, 132-141, DOI: 10.1080/22797254.2017.1411169

To link to this article: https://doi.org/10.1080/22797254.2017.1411169

EUROPEAN JOURNAL OF REMOTE SENSING, 2017
VOL. 51, NO. 1, 132–141
https://doi.org/10.1080/22797254.2017.1411169

Taylor & Francis
Taylor & Francis Group

Estimation of canopy cover in dense mixed-species forests using airborne lidar data

Tauri Arumäe[a,b] and Mait Lang[a,c]

[a]Institute of Forestry and Rural Engineering, Estonian University of Life Sciences, Tartu, Estonia; [b]Forest survey management division, State Forest Management Centre, Tallinn, Estonia; [c]Department of Remote Sensing, Tartu Observatory, Tõravere, Tartumaa, Estonia

ABSTRACT

Airborne laser scanning (ALS) data and digital hemispherical photos (DHP) from 93 sample plots in Laeva test site, Estonia, were used to study effects of phenology and scan angle on the ALS-based canopy cover (CC_{ALS}) estimates. The relative share of first returns ($P_{1/A}$) for 6185 forest stands was analysed. The CC_{ALS} was calculated using different height thresholds and echoes, and was compared with the CC estimates based on DHP (CC_{DHP}) and crown model (CC_{RCrown}). The first of many echoes-based canopy cover estimate ($CC_{ALS,1.3\_1}$) saturated at values greater than 80%. The strongest correlation of CC_{DHP} was found with $CC_{ALS,1.3\_A}$ using all echoes and a 1.3 m height break (R^2 = 0.81, $RMSE$ = 11.8%). Correcting the estimate for view nadir angle did not improve the correlation of $CC_{ALS,1.3\_A}$ with CC_{DHP}. The CC_{RCrown} had a weak correlation ($R^2 < 0.25$) with CC_{ALS} and with CC_{DHP}. The $P_{1/A}$ was not influenced by tree species composition, but by phenology, stand relative density and forest height; however, CC_{ALS} was not dependent on stand height. Foliage phenology had a substantial effect on CC_{ALS} and CC_{DHP}. In dense mixed-species forests, we recommend to use all returns for canopy cover estimation.

ARTICLE HISTORY
Received 9 February 2017
Revised 30 June 2017
Accepted 25 November 2017

KEYWORDS
Airborne lidar data; canopy cover; tree crown models; live crown base height; phenology

Introduction

Airborne laser scanning (ALS) has become a widely used remote sensing method for assessing forest structure variables in operational forestry (Andersen, McGaughey & Reutebuch, 2005). The main applications of ALS are forest height map construction (Arumäe & Lang, 2016a; Næsset, 1997a), wood volume and biomass estimation (Bouvier, Durrieu, Fournier, & Renaud, 2015; Ferraz et al., 2016; Guerra-Hernández et al., 2016; Næsset, 1997b; Patenaude et al., 2004, Popescu, Zhao, Neuenschwander, & Lin, 2011), carbon stock monitoring (Bright, Hicke, & Hudak, 2012) and biodiversity mapping (Müller & Vierling, 2014; Smith, Anderson, & Fladeland, 2008). Vertical canopy cover (CC) is the key factor for most of these estimates and when combined with other forest structure parameters it is used for leaf-area index (LAI) mapping (Korhonen & Morsdorf, 2014; Solberg et al., 2009) or could be used for planning of thinnings in forest management (Vastaranta et al., 2011). Forest canopy structure is additionally described with mean tree height (*H*), crown length and the ratio of crown length to *H*, crown cover, effective CC and angular canopy closure. Distinguishing between different CC estimates is essential for forest structure studies (Jennings, Brown, & Sheil, 1999; Korhonen, Korpela, Heiskanen, & Maltamo, 2011). The CC, as defined by Jennings et al. (1999) and as used in this study, is the share of ground covered by the vertical projection of the canopy and is commonly expressed as a percentage. The simplest method for measuring vertical CC is using the Cajanus tube (Korhonen, Korhonen, Rautiainen, & Stenberg, 2006; Rautiainen, Stenberg, & Nilson, 2005). Canopy closure, on the other hand, is defined as the proportion of the sky hemisphere obscured by the vegetation canopy when viewed from a single point (Jennings et al., 1999). Canopy closure can be estimated from digital hemispherical photos (DHP) or measured using the LAI-2000 plant canopy analyser (Jonckheere, Nackaerts, Muys, & Coppin, 2005).

The CC and crown cover (ratio of the total area of crown vertical projections divided by the sampling area) are also estimated using crown radius models and stand density (Spurr, 1948). Tree crown radius is commonly estimated using stem diameter at breast height (Davies & Pommerening, 2008; Spurr, 1948) and can be used for tree competition assessment (Purves, Lichstein, & Pacala, 2007). The relationship between stem diameter at breast height, tree crown radius and CC can be used to estimate the mean tree size from ALS data (Ferraz, Saatchi, Mallet, & Meyer, 2016). However, crown radius models may yield different crown cover estimates, depending on the definition of tree crowns, tree species and age (Kandare, Ørka, Dalponte, Næsset, & Gobakken, 2017).

CONTACT Tauri Arumäe tauri.arumae@rmk.ee Institute of Forestry and Rural Engineering, Estonian University of Life Sciences, Kreutzwaldi 5, Tartu 51014, Estonia

Commonly, tree crowns are modelled as solid geometrical shapes – a cone, ellipsoid (Kuusk & Nilson, 2000) or convex irregular polygon (Mongus & Žalik, 2015). If gaps in the tree crown are accounted, then the result is an effective CC estimate (Duncanson, Cook, Hurtt, & Dubayah, 2014).

A DHP records all the radiation penetrating through tree crown or plant canopy, taking into account all the gaps inside the tree crowns, and the share of sky pixels in the total number of pixels is the effective canopy closure. For the conversion of canopy closure into CC, the view zenith angle should not exceed 20° (Korhonen, Korpela, Heiskanen & Maltamo, 2011) and the estimates should be corrected for within-crown gap fraction (Nilson & Kuusk, 2004). The sources of uncertainties in the ALS data-based estimates of CC (CC_{ALS}) are related to the scanning setup where the view nadir angle (VNA) is usually in the range of $0° \leq VNA \leq 30°$ and the angular dependence of the observations is characteristic of canopy closure. There are no clear rules of how to account for within-crown gaps. The pulse footprint of the scanners is commonly larger than gaps inside crowns. For example, Leica ALS50-II at a 2400-m flight altitude and beam divergence of 0.22 mrad (Leica, 2007) has a pulse footprint of about 50 cm in diameter. The canopy itself is also semi-transparent on near-infrared (NIR) wavelengths used in most of the topographic mapping oriented ALS devices, so defining crown gaps is problematic. A laser scanner can also retrieve echoes from overlapping crowns, which would allow estimating crown cover, when the overlapping areas of the crowns are taken into account separately.

The most common method for the CC_{ALS} estimation is using a height break or threshold and calculating the share of the first and first of many echoes above the height break in the total number of echoes (Korhonen, Korpela, Heiskanen & Maltamo, 2011). The threshold is commonly set at a few metres above the ground corresponding to the live crown base height (Smith et al., 2009). However, it is found that the CC_{ALS} estimate based on the first and first of many echoes using the, e.g. Leica ALS50-II scanner will result in the CC_{ALS} estimate saturation, especially in dense deciduous forests (Lang, 2010; Lang, Arumäe, & Anniste, 2012). The CC_{ALS} is influenced also by scanning parameters (Keränen, Maltamo, & Packalen, 2016) and the ratio of the first echo count to all echoes ($P_{1/A}$) which characterizes pulse splitting and is affected by phenology stages, especially for deciduous forests (Wasser, Day, Chasmer, & Taylor, 2013). In NIR spectral region, broadleaved deciduous tree species have a higher reflectance than needle leaf species (Kuusk, Lang, & Kuusk, 2013) which can also influence the $P_{1/A}$. As a result, CC is at best estimated from ALS data with a root mean square error of 10% (Ferraz et al., 2015). Similar results are shown for canopy closure estimates (Moeser, Roubinek, Schleppi, Morsdorf, & Jonas, 2014). In practical applications where CC_{ALS} or its analogues are used for ALS-based wood volume models (Arumäe & Lang, 2016b; Bouvier et al., 2015) an error of 10% in CC_{ALS} causes about a 15% difference in predicted wood volume.

The aim of this study was to test different CC_{ALS} estimation methods in dense deciduous broadleaf-dominated hemi-boreal forests stands. The ALS data were from two phenological phases – before bud swelling with leaves off (bBS) and after the final leaf unfolding stage (aFLU) with leaves fully developed. CC estimates from DHP (CC_{DHP}) were chosen as the reference for other methods. Additional tests were carried out using CC estimates based on tree position data and the crown radius model (CC_{RCrown}). The influence of scan angle, $P_{1/A}$ and plot location on the CC_{ALS} estimates was investigated.

Materials and methods

Study site

The 15 × 15 km test site is located in south-eastern Estonia, near Laeva (Lang, Arumäe, Lükk, & Sims, 2014). The terrain is rather flat. Half of the area is covered by forests. The forests are of mixed species and multi-layer structure is common, with a dense understory layer of *Padus avium* Mill. and *Corylus avellana* L. Dominant tree species are silver birch (*Betula pendula* Roth), Norway spruce (*Picea abies* L.), trembling aspen (*Populus tremula* L.), black alder (*Alnus glutinosa* L.) and Norway spruce in the lower layer. The most common site types are the *Aegopodium* and *Filipendula* (Lõhmus, 2004) and based on FAO-UNESCO, the soil types are mainly fertile *Calci Eutric Gleysols* and *Eutri Histic Gleysols*. The forest height can reach up to 37 m (typical height in mature forests is 25–30 m) and the basal area is up to 40 m^2/ha according to forest inventory (FI) data.

The first dataset in the tests was FI data for 6185 stands. The FI data were used for studying the influence of deciduous species fraction on $P_{1/A}$. The majority of the stands were inventoried in 2013. The average stand size was 2.0 ha and dominating tree species are silver birch and trembling aspen with a common second layer of Norway spruces. The second dataset was based on 93 sample plots extracted from the Estonian Network of Forest Research (ENFR) database (Kiviste et al., 2015). According to Kiviste et al. (2015) all the trees on these plots were calipered, tree positions were mapped and model trees were selected for crown base height and height measurements. The rest of the tree heights were estimated using diameter-height models based on sample tree measurements. Dominating tree species in the ENFR plots are silver birch and trembling aspen, with an average age of 59 years for silver birch and 65 years for trembling aspen. The average height of the forests was 23 m and basal area average was 25 m^2/ha. The average relative density (also known as stand stocking index) was 81%.

ALS data

The ALS data were collected in spring (06 May 2013) and summer (13 July 2013) by the Estonian Land Board using the scanner Leica ALS50-II. The ALS point density for bBS was 0.5 points/m^2, the flight altitude was 2400 m and ALS pulse footprint diameter on the ground was 50 cm. Point density for aFLU dataset was 2 points/m^2, flight altitude 1800 m and pulse footprint diameter on the ground was 40 cm in diameter. The bBS and aFLU datasets were combined in one analysis to increase the range of CC_{ALS} and to use the bBS data as a substitute for possible defoliation effects. The VNA did not exceed 28°. The ALS data were processed using FUSION/LDV freeware (McGaughey, 2014).

The CC_{ALS} was calculated using different height breaks (z) with a 1-m step starting from 1.3 m and ending at the live crown base height (H_{LCB}) to reduce the forest understory vegetation influence. The CC_{ALS} was calculated as follows:

$$CC_{ALS,z\_E} = \frac{100 \cdot P_E(h_p > z)}{P_E} \tag{1}$$

where

P – the number of echoes,
h_p – the pulse return height from the ground,
E – selection of the first or first of many (“1”) or all (“A”) echoes.

The ALS-based live crown base height (H_{LCB_ALS}) was estimated with the model (2) taken from Arumäe and Lang (2013), where $H_{LCB\_ALS\_0}$ is calculated using point cloud height distribution mode value (H_{Mode}) and standard deviation (H_{Stdev}) excluding the points with $h_p \leq 1.3$ m.

$$H_{LCB\_ALS\_0} = H_{Mode} - \frac{H_{Stdev}}{2} \tag{2}$$

Correlation between the measured H_{LCB} and $H_{LCB\_ALS\_0}$ was strong (R^2 = 0.79). However, $H_{LCB\_ALS\_0}$ overestimated H_{LCB} on average by 6.8 m and therefore a linear correction model (3) was applied.

$$H_{LCB\_ALS} = 0.69 \cdot H_{LCB_{ALS_0}} - 1.3 \tag{3}$$

We tested also the influence of VNA correction on CC_{ALS} depending on the selection of echoes and ALS measurement geometry. To study the CC_{ALS} dependence on scanning angle, first 38 of the ENFR plots were selected where the scan angle was large (18–28°). The sample plots occurred on the overlapping area of scan swaths and, as the result of the flight plan, they were scanned from two opposite directions (*ALS_Left; ALS_Right*). The relationship between CC_{ALS_Left} and CC_{ALS_Right} was analysed before and after the VNA correction with the model by Korhonen and Morsdorf (2014)

$$CC_{ALS} = CC_{ALS,1.3\_1} - 0.0253 \cdot \theta_{scan} \cdot F_{max}, \tag{4}$$

where

$CC_{ALS,1.3\_1}$ – the CC estimate using the first or first of many echoes,
θ_{scan} – mean scan angle (°),
F_{max} – height of the highest echo above the digital terrain model (m).

In pulse splitting analysis, both canopy and ground returns were included to test the influence of tree species on $P_{1/A}$. The impact of foliage phenology on the occurrence of returns within the canopy and the corresponding $P_{1/A}$ was analysed in the ENFR plots including only the pulse returns with $h_p > 1.3$.

Digital hemispherical photographs

The DHP measurements were carried out in the summer of 2013. On 32 out of the 93 ENFR plots, DHP measurements were carried out also in spring at the time before bud swelling. Twelve photos per plot were taken following the VALERI protocol (Validation of Land European Remote Sensing Instruments, http://www.avignon.inra.fr/valeri/). Three sampling points were marked in all four cardinal points, with a 4-m distance between each sample. For hemispherical photos, we used a Nikon D5100 with the Sigma 4.5 mm F2.8 EX DC HSM Circular Fisheye lens and a Canon EOS 5D with the Sigma 8 mm 1:3.5 EX DG Fisheye lens. The HSP software (Lang, Kodar, & Arumäe, 2013) was used for DHP processing. The CC_{DHP} for each plot was then calculated as an average of CC estimates from 12 single photos. Pixels from the view zenith angle of less than 9° were used to measure CC (corresponds roughly to the first ring of LAI-2000).

Crown radius models

Two crown radius (R_{Crown}) models were initially tested – the first model was published by Jakobsons (1970) and is based on stem diameter at breast height (d). The second R_{Crown} model (model 14 from Lang, Nilson, Kuusk, Kiviste, & Hordo, 2007) is based on tree height and d. Using the calculated R_{Crown} values, the CC (CC_{RCrown}) estimate was calculated by merging all the crown shapes. The CC_{RCrown} using

Jakobsons (1970) model was 32–42% greater compared to the CC_{RCrown} calculated using model by Lang et al. (2007). Additionally, the average CC for all 93 plots with Jakobsons' (1970) R_{Crown} model was 50% greater than with the model by Nilson, Lang, Kuusk, Anniste, and Lükk (2000) that relates $CC = 100 \cdot (0.898T + 0.044)$ where T is stand relative density. Therefore, Jakobsons' (1970) model was abandoned.

Tree crown vertical projections on the ground can be represented as concentric rings of a particular radius in the case of equal spacing of the trees. In natural stands, however, distances between trees vary and, due to the competition for light, branches grow more likely towards open space. As a result, the overlaps between tree crown projections decrease and CC increases. Since tree positions in the ENFR plots were known, a model from Lang and Kurvits (2007) was used to adjust crown projections according to the neighbours of each tree, while the area of each crown projection was fixed to that of the circle with the predicted crown radius. This model was able to draw more realistic crown shapes, and a visual comparison of the adjusted crown projections with orthophotos showed a good agreement. For each sample plot, all crown projections were then merged into one polygon using QGIS to calculate the CC_{RCrown}. After the crown shape modification, CC increased (mean CC_{CRown} by 3% and the maximum difference was 16%) compared to the circular crown projections-based CC. We assumed that this also increases the correlation with CC_{ALS}. We did not apply edge correction (see, e.g., Lilleleht, Sims, & Pommerening, 2014) and a small underestimation of CC near a sample plot border is still possible. To study the edge effect, a 2-m wide buffer was excluded from outside the sample plots. The parts of crown projections within the decreased sample plot were then extracted and CC_{RCrown} was estimated again. The CC_{RCrown} estimates were compared with the aFLU CC_{ALS}.

Manipulation of plot centre location

To estimate the stability of CC_{ALS}, the centre positions of the 93 ENFR plots were randomly dislocated for 100 times within a radius of 10 m, which corresponds roughly to the estimated maximum error in the ENFR plot coordinate measurements. The $CC_{ALS,1.3\_A}$ was calculated for each dislocated point cloud sample and variation was analysed.

Error estimates

The mean error of estimate (*MEE*) was calculated as

$$\mathrm{MEE} = \Sigma(\mathrm{X} - \mathrm{Y})/\mathrm{N} \qquad (5)$$

and the root mean square error (*RMSE*) was calculated as

$$RMSE = \sqrt{\sum(X - Y)^2/N} \qquad (6)$$

where X is the argument, Y is the dependent variable and N is the number of observations.

Results

The shifting of the centre coordinate showed that the $CC_{ALS,1.3\_A}$ estimates are rather stable concerning errors in ALS point cloud sample locations. The standard error of $CC_{ALS,1.3\_A}$ for the 93 ENFR plots was 0.15% and the average interquartile range of $CC_{ALS,1.3\_A}$ was 2.2%. The largest range of $CC_{ALS,1.3\_A}$ estimates was 23%, nine sample plots had a $CC_{ALS,1.3\_A}$ range of larger than 10% and the average range of $CC_{ALS,1.3\_A}$ was 6.1%.

There was a substantial influence of phenology on the CC_{ALS} estimates. For bBS, the average $CC_{ALS,1.3\_A}$ of the ENFR plots was about 20% smaller compared to the average of aFLU conditions (Table 1).

The correlation of CC_{DHP} with the first echoes-based $CC_{ALS,1.3\_1}$ was weaker ($R^2 = 0.75$, $RMSE = 20.7\%$) than with $CC_{ALS,1.3\_A}$ ($R^2 = 0.81$, $RMSE = 11.8\%$; Figure 1, Table 1). When aFLU and bBS measurements were tested separately, the smallest *RMSE* was found for $CC_{ALS,1.3\_A}$ and CC_{DHP} of aFLU flight and the R^2 corresponded to a moderate correlation.

The change in correlation between $CC_{ALS,z}$ and CC_{DHP} when the height break was raised from $z = 1$ to $z = 5$ m was not significant. Raising the z even higher, up to 10 m, somewhat improved the predictive power of the first echoes, but the increase in R^2 was small. The $CC_{ALS,LCB}$, estimated at $z = H_{LCB\_ALS}$, had surprisingly only a weak correlation ($R^2 = 0.15$) with CC_{DHP} for aFLU dataset and no correlation for bBS measurements ($R^2 = 0$). This was most likely due to the ALS-based H_{LCB} model (2) not being able to predict the H_{LCB} for bBS dataset. The H_{Mode} for bBS data occurred near the minimum height threshold of 1.3 m following the mode value of the pulse return height distribution and the $CC_{ALS,LCB}$ was substantially overestimated. This was probably the result of a dense forest understory and second layer of spruces in many stands that caused pulse returns from below the upper tree layer and flattened the height distribution of pulse returns and changed the position of H_{Mode}. Using the measured H_{LCB}

Table 1. Relationships between CC_{DHP} and $CC_{ALS,1.3}$ depending on the phenophase and selection of pulse return.

	$CC_{1.3}$ using the first and first of many echoes (%)				$CC_{1.3}$ using all echoes (%)			
Phenophase[a]	Mean	*RMSE*	*MEE*	R^2	Mean	*RMSE*	*MEE*	R^2
bBS	74.0	34.8	−31.7	0.64	59.7	19.3	−17.3	0.62
aFLU	93.9	14.0	−11.9	0.32	83.5	7.4	−1.5	0.37
Combined	-	20.7	−17.1	0.75	-	11.8	−5.6	0.81

[a] bBS: before bud swelling; aFLU: after final leaf unfolding.

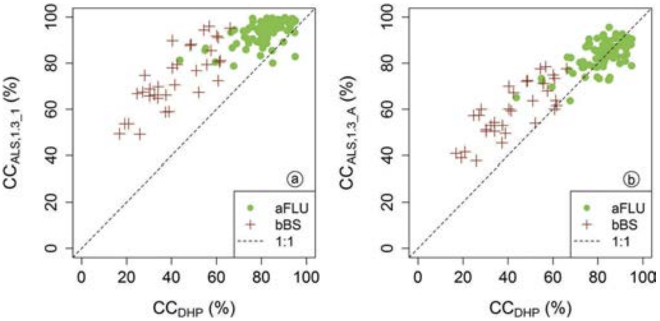

Figure 1. First echoes-based canopy cover (CC) calculated at 1.3-m height break $CC_{ALS,1.3\_1}$ saturates in dense forests in summer (aFLU) (a) compared to all echoes-based $CC_{ALS,1.3\_A}$ (b).

for z instead of the point cloud-based H_{LCB_ALS} improved the correlation of $CC_{ALS,LCB}$ with CC_{DHP} (R^2 = 0.22) when tested for aFLU dataset. We found also that CC_{DHP} was almost always smaller than CC_{ALS} (Table 1, Figure 1). Since the gap fraction estimation from DHP with the LinearRatio (Cescatti, 2007) method that is used in HSP software is an unbiased technique (Lang, Kodar & Arumäe, 2013, Lang et al., 2017), the CC_{ALS} is probably overestimated. However, in our study we did not correct CC_{DHP} for within the crown gap fraction which would increase aFLU CC_{DHP} by a few percentages and thus established a good correlation between the mean $CC_{ALS,1.3\_A}$ and CC_{DHP}.

The pulse splitting within the canopy showed also a difference between aFLU and bBS datasets. The pulses were splitting less (p-value < 0.01) and the share of the first returns increased using aFLU data ($P_{1/A}$ = 0.82) compared to the bBS dataset ($P_{1/A}$ = 0.76). This is also one of the reasons for the systematically overestimated CC_{ALS} for bBS data (Figure 1), since the number of returns from the canopy increased.

The comparison of $CC_{ALS,1.3\_1}$ in the ENFR plots that were scanned twice indicated that at a large VNA, the CC estimates for sample plots may vary substantially when calculated from repeated scans taken from different directions – the maximum differences ranged up to 8%. The VNA correction improved the $CC_{ALS,1.3\_1}$ estimation (Figure 2) precision as appeared from the analysis of overlapping scan swaths. The VNA correction also decreased CC_{ALS} by 13% on average, but the scatter between the repeated measurements remained considerable (Figure 2(b)). The VNA uncorrected dataset (Figure 2(a)) showed a slightly weaker correlation between CC_{ALS_Left} and CC_{ALS_Right} (R^2 = 0.81, $RMSE$ = 4.2%) compared to the VNA corrected dataset (Figure 2(b); R^2 = 0.89; $RMSE$ = 3.8%); however, the change in R^2 was statistically insignificant when tested using Sheskin's (2000) statistical test.

The CC_{ALS} of all ENFR plots was then corrected for the VNA and compared to CC_{DHP} (Figure 3). The scan angle correction decreased the MEE of the relationship between $CC_{ALS,1.3\_1}$ and CC_{DHP} from −12.8 to −4.7; however, the change in R^2 was not significant according to the statistical test (Sheskin, 2000). The scan angle correction caused a systematic underestimation of $CC_{ALS,1.3\_A}$ compared to CC_{DHP} with MEE increasing from −2.8 to 5.3, but the increase in R^2 was again not statistically significant.

The percentage of deciduous tree species in the dominant layer of trees had no correlation with the first echo ratio $P_{1/A}$ (R^2 = 0) using the aFLU dataset. Whereas $P_{1/A}$ had a negative moderate correlation with stand relative density (R^2 = 0.35) and a moderate negative correlation with the ALS-based 80th height percentile (H_{P80}; R^2 = 0.56). The VNA had an influence on $P_{1/A}$. The share of pulses giving only a single echo increased with VNA ≥ 10° and the $P_{1/A}$ at VNA ≥ 16° was 2% larger compared to the near nadir $P_{1/A}$ (p-value < 0.01 based on 379 stands scanned at nadir and 420 stands scanned at VNA>16°).

In contrary to the expected relationship between CC_{ALS} and tree crown-based CC, the concentric ring-based CC_{RCrown} showed no correlation with CC_{DHP} or CC_{ALS}. The neighbourhood corrected CC_{RCrown} showed a weak correlation with CC_{DHP} (R^2 = 0.14) and also with $CC_{ALS,1.3\_A}$ (R^2 = 0.22) and $CC_{ALS,1.3\_1}$ (R^2 = 0.14). Our test with the excluded 2-m-wide buffer from outside the sample plots where the crown model may have lacked the influence of external competition did not show a marked increase in the correlations with other CC estimates. The 2-m buffer zone exclusion increased the average of CC_{RCrown} by 2.7% and increased the $R^2$of the CC_{RCrown} relationship with CC_{DHP} (R^2 = 0.18), $CC_{ALS,1.3\_A}$ (R^2 = 0.24) and $CC_{ALS,1.3\_1}$ (R^2 = 0.16), but statistically the influence

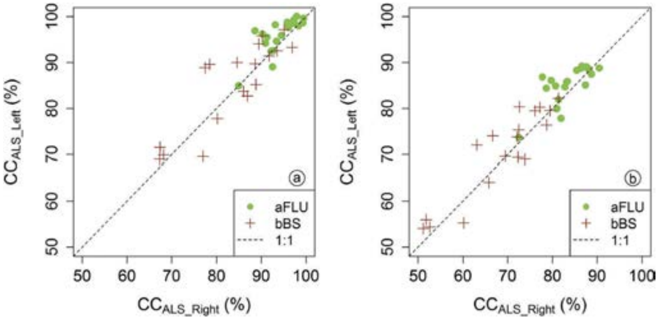

Figure 2. Comparison of CC_{ALS} estimated from the opposite direction flights using the first echoes (a) without VNA correction and (b) using Korhonen and Morsdorf's (2014) VNA correction model.

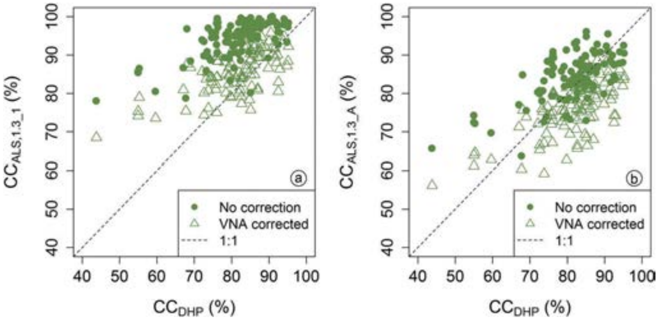

Figure 3. Influence of view nadir angle correction on $CC_{ALS,1.3}$ estimates using the first echoes (a) and using all echoes (b).

was insignificant (p-value > 0.05). The correlation of CC_{RCrown} with CC_{ALS} based on the measured H_{LCB} was weak (R^2 = 0.02), but the mean values of the two CC estimates (67.4% and 69.7%, correspondingly) were closer than CC_{RCrown} and $CC_{ALS,1.3\_A}$ (67.4% and 83.6%, correspondingly).

Discussion

The comparison of CC_{ALS} and CC_{DHP} in the best-case scenario had an *RMSE* of 11.8%, which is comparable to the results of similar studies (Ahmed, Franklin, Wulder, & White, 2015; Smith et al., 2009). The relatively large *RMSE* is most likely the result of measurement errors and comparison of different variables as CC. For example, DHP is measuring light that is penetrating the canopy and the tree crowns are accounted as semi-transparent, as opposed to the CC_{RCrown} which accounts crowns as solid shapes, but ALS-based measurements use the NIR spectral region where also foliage is semi-transparent. Also, the ALS observations are not points, but samples with an area defined usually by the laser beam divergence and flight altitude (Baltsavias, 1999). Sample plot position errors also propagate into CC_{ALS} and decrease the reliability of the CC estimates. Although we found that $CC_{ALS,1.3\_A}$ was usually not substantially influenced by the positioning errors of sample plots, this was probably due to the ENFR plots being well-positioned in homogeneous parts of forest stands. On the other hand, CC_{ALS} calculated for a sample plot using ALS point clouds from different flight paths had an uncertainty of up to 8% in CC units in the forests.

Somewhat surprisingly, there was only a weak correlation between CC_{RCrown} and $CC_{ALS,z}$. This is most likely because CC_{RCrown} and $CC_{ALS,z}$ are different by their definition or is because of the used R_{Crown} models, which were not able to predict accurately tree crown radius in the dense stands. One reason might be also the influence of understory trees, for which there was no data to calculate CC_{RCrown} estimates.

However, there was not much of an improvement in correlation when CC_{ALS} was estimated at measured H_{LCB} threshold to exclude the influence of understory vegetation. Only the mean value of CC_{RCrown} was in a better agreement with $CC_{ALS,LCB}$ compared to $CC_{ALS,1.3}$. The correlation of CC_{RCrown} with CC_{DHP} and $CC_{ALS,LCB}$ did not show a significant improvement after adjusting crown shapes, however, the CC_{RCrown} was estimated according to the competition of neighbouring trees. It is possible that the tree crown shapes vary in nature much more than predicted by the model, and in semi-naturally developed forests, tree stems are not strictly vertical due to competition during their growth. As a result, the CC can be much larger in many plots compared to the estimates based on the crown projections and assumed vertical stems at tree stump locations.

In the dense forests, the CC_{ALS} was estimated using the regular height break z = 1.3 m and saturated using the first or first of many echoes at CC greater than 80%, whereas the CC_{ALS,z_A} did not saturate. There was not much of an influence on CC_{ALS} from the increase in z until 10 m above the ground or until the H_{LCB} level was reached. Raising the threshold higher than 1.3 m did improve the predictive power of the first echoes, but overall, the relationship between CC_{ALS} and CC_{DHP} was still weak and the change in the determination coefficient was statistically insignificant. Using the ALS-based H_{LCB} as a threshold introduces additional errors in CC caused by the errors in H_{LCB_ALS} estimation. On the other hand, the lack of sensitivity of CC_{ALS} to the change in z is probably caused by the upper layer dense canopy in the forests (images can be found in the appendix in Lang et al., 2014), which captures most of the pulse energy and thus relatively fewer echoes from the lower layers down to the ground vegetation are triggered. On the other hand, there is a clear negative correlation between the leaf area index of upper and lower canopy layers in forests (Chianucci, Puletti, Venturi, Cutini, & Chiavetta, 2014; Kodar et al., 2011). In our test, DHPs were taken always at 1.3 m above the ground and a denser forest understory in the case of a smaller CC of the upper layer can explain the weak correlation between the values of CC_{ALS} calculated using H_{LCB} and CC_{DHP}.

In addition to the selection of pulse returns and discrimination threshold for the CC estimation, there are also sampling problems and issues related to the interaction between the lidar pulse and forest canopy. The laser scanners measure at various VNAs and this raises the question of representativity of higher-order echoes in the case of small sample plots in tall forests. With the VNA increase, the second and higher-order returns are displaced horizontally by $h_{diff} \times \tan(\mathrm{VNA})$, where h_{diff} is the vertical distance between the first and subsequent returns of the lidar pulse. For example, at VNA = 25° and h_{diff} = 21 m, the displacement in the horizontal direction is 9.8 m. Therefore when a pulse is sent out at a large VNA, the first echo is triggered from a plot or grid cell location and the following echoes would be received in a shifted location, but their occurrence is still determined by the part of the canopy that triggered the first echo. This makes the CC_{ALS} estimate dependent on the grouping of trees and sensitive to variation in forest height. However, there was a positive correlation between the VNA and canopy $P_{1/A}$ at larger scan angles (VNA>15°) meaning fewer returns per pulse at the view angles. The reasons for this may include the increase in footprint size at larger scanning angles (Heritage & Large, 2009; Korhonen, Korpela, Heiskanen & Maltamo, 2011) and the fact that at large scan angles the probability of seeing crown sides increases and so does the path length through the canopy. The increased path length within the forest canopy causes more scattering which flattens the distribution of the received energy leaving less chance for the scanner internal software to distinguish more than just the first return from emitted pulses.

Additionally to the VNA, the species composition is known to influence the point cloud height distribution and therefore the estimates of CC_{ALS} (Wasser, Day, Chasmer, & Taylor, 2013). The higher reflectance of deciduous broadleaf tree species in NIR should, in theory, result in a greater $P_{1/A}$ as the pulses are being split less due to a stronger signal from the top of the canopy. However, based on the 6185 forest stands, the fraction of broadleaf trees in the upper layer had no influence on $P_{1/A}$, but $P_{1/A}$ was influenced by the structural features of the forest – stand density and height. The correlation between $P_{1/A}$ and forest height is partially explained by the fact that the Leica ALS50-II scanner can register up to four echoes from a single pulse, with a minimum distance of greater than 3.5 m between the echoes. Therefore, the splitting of pulses can only occur in forests where the tree height exceeds the multiple value of the spacing distance. The $P_{1/A}$, and therefore CC_{ALS}, is also influenced by the scanner automatic gain control (AGC) (Vain, Yu, Kaasalainen, & Hyyppa, 2010) which regulates the intensity of the emitted pulses, but the effect was not studied in this research. Similarly to AGC, which regulates the emitted energy, the flight altitude and, in turn, the footprint size has an effect on echo registration (Gaveau & Hill, 2003). The increased pulse splitting found on ENFR plots during bBS compared to aFLU phenophase may also be one reason why all returns-based CC_{ALS} estimates were still systematically greater compared to CC_{DHP} in spring, while there was a good agreement in summer. Similarly to Straatsma and Middelkoop (2006) we found that there were fewer second or higher-order returns per pulse in summer triggered by the canopy compared to leafless conditions in spring. This is related to the higher NIR reflectance of the foliage compared to leafless branches, which creates a better-defined mode value into the distribution of returned photons. However, CC_{ALS} and CC_{DHP} both showed a consistent increase in CC in accordance with the foliage phenology. The phenology-driven change in CC_{ALS} may be an indicator of the share of deciduous species in the estimation of species composition in forest stands.

To account for the complex influence of the VNA on CC_{ALS} estimates, we applied the VNA correction model published by Korhonen and Morsdorf (2014). In general, there was a small increase in correlation between the CC_{ALS} and CC_{DHP} and a decrease in *RMSE*, but the improvement was statistically insignificant. The VNA correction of $CC_{ALS,1.3\_A}$ resulted in a systematically smaller estimate compared to CC_{DHP} and is therefore not recommended for $CC_{ALS,1.3\_A}$. This indicates that the VNA correction models for ALS-based CC estimates are dependent on the selection of pulse returns, since the model was originally constructed for the first returns of laser pulses. For future studies, a VNA correction model also for all returns-based CC_{ALS} should be developed.

Conclusion

We analysed discrete-return ALS data from dense deciduous broadleaf-dominated mixed forests for CC estimation using references obtained from tree crown models and DHP. The uncertainties in the ALS-based CC estimates due to the errors in sample plot location and sampling of point clouds from different scans at large VNAs are roughly in the same range and reach up to 8–10% in CC units in the stands. Correction of VNA effects systematically decreased CC estimates, but did not decrease variability and there was no improvement in the correlation with CC estimated from DHPs. A VNA effect correction model developed for the first returns yields biased CC values when applied to all returns-based CC estimates. There is not much of an influence on ALS-based CC estimates when selecting a threshold height from the range between 1.3 m above the ground and the level of the live crown base in the dense forests.

There was a good agreement between the CC estimated from ALS data and DHPs, while both estimates had only a weak correlation with the CC based on crown radius models. The weak correlation was probably related to the different meaning of the variables and failure of crown models to account for single tree crown plasticity in the dense forests. The increase in foliage density decreases the number of returns per pulse triggered from the forest canopy. This effect may be important for ALS-based defoliation estimates which will be thus less sensitive to an actual decrease in foliage density. In general, the number of returns per pulse in the aFLU phenophase ALS data was not dependent on the proportion of broadleaf trees but only on forest height and stand relative density. Finally, for the estimation of CC using ALS data in the dense forests, we recommend using the first returns and VNA effect correction or all returns without the correction.

Acknowledgments

The authors would like to thank the Estonian Land Board for the airborne lidar data. Data acquisition was financed by the Estonian State Forest Management Centre. Ave Kodar helped during field measurements. Data analysis was supported by the Ministry of Education and Research grant IUT21-4. The Estonian Network of Forest Research Plots was supported by the Estonian State Forest Management Centre and the Estonian Environmental Investment Centre. The authors are also thankful for the helpful comments from the anonymous reviewers.

Disclosure statement

No potential conflict of interest was reported by the authors.

References

Ahmed, O.S., Franklin, S.E., Wulder, M.A., & White, J.C. (2015). Characterizing stand-level forest canopy cover and height using Landsat time series, samples of airborne LiDAR, and the random forest algorithm. *ISPRS Journal of Photogrammetry and Remote Sensing*, *101*, 89–101. doi:10.1016/j.isprsjprs.2014.11.007

Andersen, H.-E., McGaughey, R.J., & Reutebuch, S.E. (2005). Estimating forest canopy fuel parameters using LIDAR data. *Remote Sensing of Environment*, *94*, 441–449. doi:10.1016/j.rse.2004.10.013

Arumäe, T., & Lang, M. (2013). A simple model to estimate forest canopy base height from airborne lidar data. *Forestry Studies*, *58*, 46–56. doi:10.2478/fsmu-2013-0005

Arumäe, T., & Lang, M. (2016a). A validation of coarse scale global vegetation height map for biomass estimation in hemiboreal forests in Estonia. *Baltic Forestry*, *22* (2), 275–282. Retrieved from https://www.balticforestry.mi.lt/bf/index.php?option=com_content&view=article&catid=14&id=455

Arumäe, T., & Lang, M. (2016b). ALS-based wood volume models of forest stands and comparison with forest inventory data. *Foresty Studies*, *64*, 5–16. doi:10.1515/fsmu-2016-0001

Baltsavias, E.P. (1999). Airborne laser scanning: Basic relations and formulas. *ISPRS Journal of Photogrammetry & Remote Sensing*, *54*, 199–214. doi:10.1016/S0924-2716(99)00015-5

Bouvier, M., Durrieu, S., Fournier, R.A., & Renaud, J.-P. (2015). Generalizing predictive models of forest inventory attributes using an area-based approach with airborne LiDAR data. *Remote Sensing of Environment*, *156*, 322–334. doi:10.1016/j.rse.2014.10.004

Bright, B.C., Hicke, J.A., & Hudak, A.T. (2012). Estimating aboveground carbon stocks of a forest affected by mountain pine beetle in Idaho using lidar and multispectral imagery. *Remote Sensing of Environment*, *124*, 270–281. doi:10.1016/j.rse.2012.05.016

Cescatti, A. (2007). Indirect estimates of canopy gap fraction based on the linear conversion of hemispherical photographs: Methodology and comparison with standard thresholding techniques. *Agricultural and Forest Meteorology*, *143*, 1–12. doi:10.1016/j.agrformet.2006.04.009

Chianucci, F., Puletti, N., Venturi, E., Cutini, A., & Chiavetta, U. (2014). Photographic assessment of overstory and understory leaf area index in beech forests under different management regimes in Central Italy. *Forestry Studies*, *61*, 27–34. doi:10.2478/fsmu-2014-0008

Davies, O., & Pommerening, A. (2008). The contribution of structural indices to the modelling of Sitka spruce (*Picea sitchensis*) and birch (*Betula* spp.) crowns. *Forest Ecology and Management*, *256*, 68–77. doi:10.1016/j.foreco.2008.03.052

Duncanson, L.I., Cook, B.D., Hurtt, G.C., & Dubayah, R.O. (2014). An efficient, multi-layered crown delineation algorithm for mapping individual tree structure across multiple ecosystems. *Remote Sensing of Environment*, *154*, 378–386. doi:10.1016/j.rse.2013.07.044

Ferraz, A., Mallet, C., Jacquemoud, S., Gonçalves, G.R., Tomé, M., Soares, P., … Bretar, F. (2015). Canopy density model: A new ALS-derived product to generate multilayer crown cover maps. *IEEE Transactions on Geoscience and Remote Sensing*, *53*, 6776–6790. doi:10.1109/TGRS.2015.2448056

Ferraz, A., Saatchi, S., Mallet, C., Jacquemoud, S., Gonçalves, G., Silva, C.A., … Pereira, L. (2016). Airborne lidar estimation of aboveground forest biomass in the absence of field inventory. *Remote Sensing*, *8*(8), 1–18. doi:10.3390/rs8080653

Ferraz, A., Saatchi, S., Mallet, C., & Meyer, V. (2016). Lidar detection of individual tree size in tropical forests. *Remote Sensing of Environment*, *183*, 318–333. doi:10.1016/j.rse.2016.05.028

Gaveau, D.L.A., & Hill, R.A. (2003). Quantifying canopy height underestimation by laser pulse penetration in small-footprint airborne laser scanning data. *Canadian Journal of Remote Sensing*, *29*, 650–657. doi:10.5589/m03-023

Guerra-Hernández, J., Görgens, E.B., García-Gutiérrez, J., Rodriguez, L.C.E., Tomé, M., & González-Ferreiro, E. (2016). Comparison of ALS based models for estimating aboveground biomass in three types of Mediterranean forest. *European Journal of Remote Sensing*, *49*, 185–204. doi:10.5721/EuJRS20164911

Heritage, G.L., & Large, A.R.G. (2009). Principles of 3D laser scanning. In G.L. Heritage & A.R.G. Large (Eds.), *Laser scanning for the environmental sciences* (pp. 21–34). Chichester: John Wiley & Sons.

Jakobsons, A. (1970). Sambandet mellan trädkronans diameter och andra trädfaktorer, främst brösthöjdsdiametern. [The correlation between the diameter of tree crown and ohter tree factors – Mainly the breastheight diameter]. *Research Notes*, *14*, 75. In Swedish with an English summary.

Jennings, S.B., Brown, N.D., & Sheil, D. (1999). Assessing forest canopies and understorey illumination: Canopy closure, canopy cover and other measures. *Forestry*, *72*, 59–74. doi:10.1093/forestry/72.1.59

Jonckheere, I., Nackaerts, K., Muys, B., & Coppin, P. (2005). Assessment of automatic gap fraction estimation of forests from digital hemispherical photography. *Agricultural and Forest Meteorology*, *132*, 96–114. doi:10.1016/j.agrformet.2005.06.003

Kandare, K., Ørka, H.O., Dalponte, M., Næsset, E., & Gobakken, T. (2017). Individual tree crown approach for predicting site index in boreal forests using airborne laser scanning and hyperspectral data. *International Journal of Applied Earth Observation and Geoinformation*, *60*, 72–82. doi:10.1016/j.jag.2017.04.008

Keränen, J., Maltamo, M., & Packalen, P. (2016). Effect of flying altitude, scanning angle and scanning mode on the accuracy of ALS based forest inventory. *International Journal of Applied Earth Observation and Geoinformation*, *52*, 349–360. doi:10.1016/j.jag.2016.07.005

Kiviste, A., Hordo, M., Kangur, A., Kardakov, A., Laarmann, D., Lilleleht, A., … Korjus, H. (2015). Monitoring and modelling of forest ecosystems: The Estonian Network of Forest Research Plots. *Forestry Studies*, *62*, 26–38. doi:10.1515/fsmu-2015-0003

Kodar, A., Lang, M., Arumäe, T., Eenmäe, A., Pisek, J., & Nilson, T. (2011). Leaf area index mapping with airborne lidar, satellite images and ground measurements in Järvselja VALERI test site. *Forestry Studies*, *55*, 11–32. doi:10.2478/v10132-011-0099-1

Korhonen, L., Korhonen, K.T., Rautiainen, M., & Stenberg, P. (2006). Estimation of forest canopy cover: A comparison of field measurement techniques. *Silva Fennica*, *40*, 577–588. doi:10.14214/sf.315

Korhonen, L., Korpela, I., Heiskanen, J., & Maltamo, M. (2011). Airborne discrete-return LIDAR data in the estimation of vertical canopy cover, angular canopy closure and leaf area index. *Remote Sensing of Environment*, *115*, 1065–1080. doi:10.1016/j.rse.2010.12.011

Korhonen, L., & Morsdorf, F. (2014). Estimation of canopy cover, gap fraction and leaf area index with airborne laser scanning. In *Forestry applications of airborne laser scanning: Concepts and case studies* (pp. 397–417). Dordrecht: Springer. doi:10.1007/978-94-017-8663-8

Kuusk, A., Lang, M., & Kuusk, J. (2013). Database of optical and structural data for the validation of forest radiative transfer models. In *Light scattering reviews* (Vol. *7*, pp. 109–148). Berlin, Heidelberg: Springer. doi:10.1007/978-3-642-21907-8

Kuusk, A., & Nilson, T. (2000). A directional multispectral forest reflectance model. *Remote Sensing of Environment*, *72*, 244–252. doi:10.1016/S0034-4257(99)00111-X

Lang, M. (2010). Estimation of crown and canopy cover from airborne lidar data. *Forestry Studies*, *52*, 5–17. doi:10.2478/v10132-011-0079-5

Lang, M., Arumäe, T., & Anniste, J. (2012). Estimation of main forest inventory variables from spectral and airborne lidar data in Aegviidu test site, Estonia. *Forestry Studies*, *56*, 27–41. doi:10.2478/v10132-012-0003-7

Lang, M., Arumäe, T., Lükk, T., & Sims, A. (2014). Estimation of standing wood volume and species composition in managed nemoral multi-layer mixed forests by using nearest neighbour classifier, multispectral satellite images and airborne lidar data. *Forestry Studies*, *61*, 47–68. doi:10.2478/fsmu-2014-0010

Lang, M., Kodar, A., & Arumäe, T. (2013). Restoration of above canopy reference hemispherical image from below canopy measurements for plant area index estimation in forests. *Forestry Studies*, *59*, 13–27. doi:10.2478/fsmu-2013-0008

Lang, M., & Kurvits, V. (2007). Restoration of tree crown shape for canopy cover estimation. *Forestry Studies*, *46*, 23–34. doi:10.2478/v10132-011-0079-5

Lang, M., Nilson, T., Kuusk, A., Kiviste, A., & Hordo, M. (2007). The performance of foliage mass and crown radius models in forming the input of a forest reflectance model: A test on forest growth sample plots and Landsat 7 ETM+ images. *Remote Sensing of Environment*, *110*, 445–457. doi:10.1016/j.rse.2006.11.030

Lang, M., Nilson, T., Kuusk, A., Pisek, J., Korhonen, L., & Uri, V. (2017). Digital photography for tracking the phenology of an evergreen conifer stand. *Agricultural and Forest Meteorology*, *246*, 15–21. In press. doi:10.1016/j.agrformet.2017.05.021

Leica. (2007). Leica ALS50-II airborne laser scanner product specifications. Retrieved from http://www.nts-info.com/inventory/images/ALS50-II.Ref.703.pdf

Lilleleht, A., Sims, A., & Pommerening, A. (2014). Spatial forest structure reconstruction as a strategy for mitigating edge-bias in circular monitoring plots. *Forest Ecology and Management*, *316*, 47–53. doi:10.1016/j.foreco.2013.08.039

Lõhmus, E. (2004). *Estonian site types* (pp. 80). Tartu: Eesti Loodusfoto.

McGaughey, R.J. (2014). *FUSION/LDV: Software for LIDAR data analysis and visualization. March 2014 – FUSION, version 3.42*. United States Department of Agriculture Forest Service Pacific Northwest Research Station. http://forsys.cfr.washington.edu/fusion/FUSION_manual.pdf

Moeser, D., Roubinek, J., Schleppi, P., Morsdorf, F., & Jonas, T. (2014). Canopy closure, LAI and radiation transfer from airborne LiDAR synthetic images. *Agricultural and Forest Meteorology*, *197*, 158–168. doi:10.1016/j.agrformet.2014.06.008

Mongus, D., & Žalik, B. (2015). An efficient approach to 3D single tree-crown delineation in LiDAR data. *ISPRS Journal of Photogrammetry and Remote Sensing*, *108*, 219–233. doi:10.1016/j.isprsjprs.2015.08.004

Müller, J., & Vierling, K. (2014). *Assessing biodiversity by airborne laser scanning* (pp. 357–374). Dordrecht: Springer. doi:10.1007/978-94-017-8663-8

Næsset, E. (1997a). Determination of mean tree height of forest stands using airborne laser scanner data. *ISPRS Journal of Photogrammetry & Remote Sensing*, *52*, 49–56. doi:10.1016/S0924-2716(97)83000-6

Næsset, E. (1997b). Estimating timber volume of forest stands using airborne laser scanner data. *Remote Sensing of Environment*, *61*, 246–253. doi:10.1016/S0034-4257(97)00041-2

Nilson, T., & Kuusk, A. (2004). Improved algorithm for estimating canopy indices from gap fraction data in forest canopies. *Agricultural and Forest Meteorology*, *124*, 157–169. doi:10.1016/j.agrformet.2004.01.008

Nilson, T., Lang, M., Kuusk, A., Anniste, J., & Lükk, T. (2000). Forest reflectance model as an interface between satellite images and forestry databases. In *Remote sensing and forest monitoring. IUFRO conference* (pp. 462–476). Luxembourg: Office for Official Publications of the European Communities.

Patenaude, G., Hill, R.A., Milne, R., Gaveau, D.L.A., Briggs, B.B.J., & Dawson, T.P. (2004). Quantifying forest above ground carbon content using LiDAR remote sensing. *Remote Sensing of Environment*, *93*, 368–380. doi:10.1016/j.rse.2004.07.016

Popescu, S.C., Zhao, K., Neuenschwander, A., & Lin, C. (2011). Satellite lidar vs. small footprint airborne lidar: Comparing the accuracy of aboveground biomass estimates and forest structure metrics at footprint level. *Remote Sensing of Environment*, *115*, 2786–2797. doi:10.1016/j.rse.2011.01.026

Purves, D.W., Lichstein, J.W., & Pacala, S.W. (2007). Crown plasticity and competition for canopy space: A new spatially implicit model parameterized for 250 North American tree species. *PLOS One*, *2*(9), 1–11. doi:10.1371/journal.pone.0000870

Rautiainen, M., Stenberg, P., & Nilson, T. (2005). Estimating canopy cover in Scots pine stands. *Silva Fennica*, *39*(1), 137–142. doi:10.14214/sf.402

Sheskin, D.J. (2000). *Parametric and nonparametric statistical procedures* (2nd ed., pp. 779–783). Boca Raton: Chapman & Hall/CRC.

Smith, A.M.S., Anderson, J., & Fladeland, M. (2008). Forest canopy structural properties. In *Field measurements for forest carbon monitoring* (pp. 179–196). New York, NY: Springer. doi:10.1007/978-1-4020-8506-2

Smith, A.M.S., Falkowski, M.J., Hudak, A.T., Evans, J.S., Robinson, A.P., & Steele, C.M. (2009). A cross-comparison of field, spectral, and lidar estimates of forest canopy cover. *Canadian Journal of Remote Sensing*, *35*, 447–459. doi:10.5589/m09-038

Solberg, S., Brunner, A., Hanssen, K.H., Lange, H., Næsset, E., Rautiainen, M., & Stenberg, P. (2009). Mapping LAI in a Norway spruce forest using airborne laser scanning. *Remote Sensing of Environment*, *113*, 2317–2327. doi:10.1016/j.rse.2009.06.010

Spurr, S.H. (1948). *Aerial photographs in forestry* (pp. 340). New York, NY: Ronald Press.

Straatsma, M.W., & Middelkoop, H. (2006). Airborne laser scanning as a tool for lowland floodplain vegetation monitoring. *Hydrobiologia*, *565*, 87–103. doi:10.1007/s10750-005-1907-5

Vain, A., Yu, X., Kaasalainen, S., & Hyyppä, J. (2010). Correcting airborne laser scanning intensity data for automatic gain control effect. *IEEE Geoscience and Remote Sensing Letters*, *7*, 511–514. doi:10.1109/LGRS.2010.2040578

Vastaranta, M., Holopainen, M., Yu, X., Hyyppä, J., Hyyppä, H., & Viitala, R. (2011). Predicting stand-thinning maturity from airborne laser scanning data. *Scandinavian Journal of Forest Research*, *26*, 187–196. doi:10.1080/02827581.2010.547870

Wasser, L., Day, R., Chasmer, L., & Taylor, A. (2013). Influence of vegetation structure on lidar-derived canopy height and fractional cover in forested riparian buffers during leaf-off and leaf-on conditions. *PLOS One*, *8*, 1–13. doi:10.1371/journal.pone.0054776

VIII

Arumäe, T., Lang, M., Laarmann, D. 2020. Thinning- and tree-growth-caused changes in canopy cover and stand height and their estimation using low-density bitemporal airborne lidar measurements – a case study in hemi-boreal forests. European Journal of Remote Sensing, 53(1), 113−123.

European Journal of Remote Sensing

ISSN: (Print) 2279-7254 (Online) Journal homepage: https://www.tandfonline.com/loi/tejr20

Thinning- and tree-growth-caused changes in canopy cover and stand height and their estimation using low-density bitemporal airborne lidar measurements – a case study in hemi-boreal forests

Tauri Arumäe, Mait Lang & Diana Laarmann

To cite this article: Tauri Arumäe, Mait Lang & Diana Laarmann (2020) Thinning- and tree-growth-caused changes in canopy cover and stand height and their estimation using low-density bitemporal airborne lidar measurements – a case study in hemi-boreal forests, European Journal of Remote Sensing, 53:1, 113-123, DOI: 10.1080/22797254.2020.1734969

To link to this article: https://doi.org/10.1080/22797254.2020.1734969

EUROPEAN JOURNAL OF REMOTE SENSING
2020, VOL. 53, NO. 1, 113–123
https://doi.org/10.1080/22797254.2020.1734969

Thinning- and tree-growth-caused changes in canopy cover and stand height and their estimation using low-density bitemporal airborne lidar measurements – a case study in hemi-boreal forests

Tauri Arumäe[a,b], Mait Lang[a,c] and Diana Laarmann[a]

[a]Chair of Forest Management Planning and Wood Processing Technologies, Estonian University of Life Sciences, Tartu, Estonia; [b]Forest Survey Management Division, Estonian State Forest Management Centre, Lääne-Viru County, Estonia; [c]Tartu Observatory, Faculty of Science and Technology, University of Tartu, Tartu County, Estonia

ABSTRACT

Repeated airborne laser scanning (ALS) measurements during leaf-on and leaf-off phenophases were studied. A 15 km × 15 km test site located in northern Estonia was used that included a reference set of stands, and 870 stands with thinning carried out before, between, and after two ALS flights. The decrease in ALS-based canopy cover estimate (CC_{ALS}) caused by thinning was similar for the leaf-off and leaf-on phenophases, and for different height thresholds. The point cloud height percentile (H_{Px}) values increased in almost all thinned stands, and the increase was present for the leaf-off and leaf-on phenophases. ALS point cloud metrics (skewness, kurtosis, mode, and canopy relief ratio) showed no response to thinning (p-value >0.05). Stand-dominating species had no significant influence on H_{Px} increment or CC_{ALS} change using the leaf-on data (p-value >0.05). The minimum height filter for pulse return selection had a substantial influence on H_{Px} increment in stands thinned between the two ALS measurements. Ground points are usually excluded from H_{Px} calculation, but for stand-level analyses, their inclusion can provide additional information.

ARTICLE HISTORY
Received 21 February 2019
Revised 17 February 2020
Accepted 23 February 2020

KEYWORDS
Change detection; commercial thinning; forest management; forest height increment; canopy cover; repeated airborne laser scanning

Introduction

A common practice of forest management involves commercial thinning, for the purpose of increasing forest growth and promoting forest health (Kocoloski, Griffin, & Matthews, 2011). Smaller changes, such as thinning that removes 20% or less of the basal area, have a relatively small impact on the spectral signature (Olsson, 1994) in multispectral satellite images. With small-scale disturbances, the recovery time of the forest canopy is also shorter – the tree crowns grow denser and wider on account of the free space. Olsson (1994) showed that within four to five years the thinning effect on forest reflectance decreases, showing a forest signature similar to that before the treatment. Depending on the method of the thinning – upper-layer thinning, understory removal, high-intensity, or low-intensity – the treatment could also have a negligible effect on canopy cover (CC), altering the variability but leaving the stand mean spectral signature unchanged.

Airborne laser scanning (ALS) has immensely increased in usage over the past few decades in forest inventories. Originally designed for terrestrial mapping and construction of digital terrain models (DTM), ALS was soon discovered to have potential in monitoring and predicting forest inventory variables (Large & Heritage, 2009). Most laser scanners work in the near-infrared (NIR) spectral range, being able to penetrate the green foliage and vegetation to provide data throughout the vertical forest cross-section (Bottalico et al., 2017; Næsset, 1997a). The ability to gather such vertical data enables the prediction of the structure variables of forests (Ellis, Griscom, Walker, Gonçalves, & Cormier, 2016; Korpela, 2008; Næsset & Gobakken, 2005; Wing et al., 2012). Such data can also be used for forest planning and management (Valbuena, Eerikäinen, Packalen, & Maltamo, 2016), including monitoring forest height growth (Lang, Arumäe, Laarmann, & Kiviste, 2017; Yu, Hyyppä, Kukko, Maltamo, & Kaartinen, 2006), canopy cover estimation (Korhonen, Korpela, Heiskanen, & Maltamo, 2011), assessing biomass increment (Ene et al., 2017; Guerra-Hernández et al., 2016; Kotivuori, Korhonen, & Packalen, 2016; Næsset, Bollandsås, Gobakken, Solberg, & McRoberts, 2015; Temesgen, Strunk, Andresen, & Flewelling, 2015), mapping clear-cuts or other disturbances (Andersen, Reutebuch, McGaughey, d'Oliveira, & Keller, 2014; Nijland et al., 2015; Vastaranta et al., 2013), and mapping tree mortality or windthrow (Nyström, Holmgren, Fransson, & Olsson, 2014).

CONTACT Tauri Arumäe tauri.arumae@rmk.ee Forest Management Planning and Wood Processing Technologies, Estonian University of Life Sciences, Kreutzwaldi 5, Tartu 51014, Estonia

As with multitemporal satellite images, similar change detection methods can be applied to ALS data. Zhao et al. (2018) demonstrated a strong correlation between the field-measured and lidar-based forest height growth and biomass increment predictions, and with the availability of high-density ALS data (>7 points per square metre, p m^{-2}), change detection at the single-tree level could be realistic, provided with bi-temporal high-density ALS datasets. Hevia et al. (2016) carried out thinning experiments with different intensities in four pure and even-aged maritime pine (*Pinus pinaster* Aiton) stands and found that canopy cover estimates were good indicators for thinning detection. Such reliable methods for mapping of disturbances and forest growth are necessary for national forest stock reporting, but can also enable pre-targeting of forest inventory fieldwork. The amount of timber obtained from commercial thinning in Estonia is 12.2% of the total felling volume and 20% of the total felling area (Valgepea, Sims, Raudsaar, & Timmusk, 2017). The Estonian Land Board carries out routine laser scanning measurements over one-quarter of Estonia in every second year (Maa-amet, 2006). Bitemporal measurements in similar phenological conditions occur in every fourth year. Such sparse (<1 p m^{-2}) point clouds are influenced by changes in forest canopy and could, therefore, be used for state-level disturbance monitoring.

Lang and Arumäe (2018) used low-density ALS measurements to show that in Estonian hemiboreal forests, there is a moderate relationship between thinning intensity and canopy cover change. In this study, we used low-density nationwide bitemporal ALS measurements from routine measurements to study methods for detecting thinning using data from leaf-off (from bud swelling until leaf unfolding) and leaf-on (final leaf-unfolding period) phenophases (Lukasová, Lang, & Škvarenina, 2014). For the analysis, the forest management inventory database and the Estonian state forest thinning cutting register were used. The study focussed mainly on questions (1) how do the ALS point cloud metrics change over time in thinned stands, (2) what is the effect of phenology on detecting thinning cuttings and forest height growth using sparse ALS point clouds from bitemporal measurements, (3) are thinning events detectable if both ALS measurements are done after thinning?

Methods and materials

Test site

The Aegviidu 15 × 15 km site in the northern part of Estonia (59º 19′ 20” N, 25º 35′ 36” E) was first measured in 2008 (Anniste & Viilup, 2010). The test site is mainly dominated by coniferous hemi-boreal forests, with Scots pine (*Pinus sylvestris* L.) and Norway spruce (*Picea abies* L.) the most common tree species. A smaller proportion of the forests are dominated by deciduous species like birch (*Betula pendula* Roth and *Betula pubescens* Ehrh.) and European aspen (*Populus tremula* L.). The most common site types by the classification schema of Lõhmus (2004) are *Myrtillus, Polytrichum-Myrtillus*, and *Rhodococcum*. The forests are typical of the hemi-boreal region (Jõgiste et al., 2017), with Norway spruce in the lower and mid-layer. Most of the forests in the area are managed by the Estonian State Forest Management Centre (RMK).

Airborne LiDAR data for the Aegviidu test site

ALS measurements were carried out by the Estonian Land Board at the Aegviidu test site using a Leica ALS50-II scanner. The repeated measurements were carried out four years after the first measurements. The ALS measurements (Table 1) for the leaf-off phenophase were taken during the national topographic mapping program for DTM construction in early spring 2009 (ALS_{2009}) and the middle of spring 2013 (ALS_{2013}). The leaf-on summertime ALS measurements were taken during routine forest inventory mapping flights (Maa-amet, 2006) in 2008 and 2012 (ALS_{2008}, ALS_{2012}). Pulse repetition frequency varied between the measurements (Table 1) and the scan angle was limited to less than 28°. The influence of flight altitude and scan angle on the ALS metrics was not studied; because we used the database of routine scanning, data and repeated measurements taken at different altitudes for comparison were not available.

FUSION freeware tools (McGaughey, 2014) were used for the ALS data processing. A point cloud for each forest stand in the forest inventory database was extracted using the PolyClipData module.

Canopy cover is the proportion of vertical projections of crowns covering the ground surface, with the crowns considered solid shapes with no gaps (Jennings, Brown, & Sheil, 1999). The ALS-based

Table 1. ALS leaf-on and leaf-off measurement specifications and descriptive data.

Dataset	Flight year	Point density (p m^{-2})	Flight altitude (m)	Laser footprint Ø (m)	First to all echos ratio	Pulse freq. (kHz)	Scanning freq. (Hz)	Flight dates
Leaf-on								
ALS_{2008}	2008	0.45	2400	0.53	0.70	103.0	46.8	11 Jul, 27 Jul, 01 Sep
ALS_{2012}	2012	0.25	3800	0.86	0.74	61.0	20.9	20 Jun – 04 Jul
Leaf-off								
ALS_{2009}	2009	0.45	2400	0.54	0.66	93.0	32.0	15 May, 26 May
ALS_{2013}	2013	0.23	2400	0.54	0.68	46.7	32.0	3–4 May

proxy for canopy cover $CC_{ALS} = N_{p,canopy}/N_p$ was calculated for each stand using a threshold method (Korhonen, Ali-Sisto, & Tokola, 2015; Smith et al., 2009), where N_p was the count of returns in point cloud and $N_{p,canopy}$ was the count of returns from the canopy. The threshold was first set to breast height (1.3 m) from the ground, and all echoes above the threshold were used when calculating CC_{ALS}. This was done to reduce the saturation effect in dense forests, as was shown by Arumäe and Lang (2018). The second computation of CC_{ALS} was done using an increased threshold of 8 m above the DTM. Point cloud height distribution statistics and metrics were calculated using a minimum height filter similar to Næsset (1997b), excluding returns below 1.3 m. For an additional comparison, no minimum height filter was used, and all echoes were included for percentile calculations. For the change detection experiment, the studied point cloud height metrics were at the 25th, 50th, 80th, and 95th percentiles ($H_{P25;}$ $H_{P50;}$ H_{P80}; H_{P95}) based on previous experiments (Arumäe & Lang, 2016; Lang & Arumäe, 2018; Lang, Arumäe, & Anniste, 2012; Lang, Arumäe, Lükk, & Sims, 2014). In addition to the point cloud height percentiles, we studied the skewness, kurtosis, and mode value of the ALS point cloud height distribution and canopy relief ratio (CRR) (McGaughey, 2014):

$$\mathrm{CRR} = \left(\overline{H_{\mathrm{ALS}}} - H_{ALS,min}\right)/\left(H_{ALS,max} - H_{ALS,min}\right), \tag{1}$$

which was calculated using the mean ($\overline{H_{\mathrm{ALS}}}$), minimum ($H_{\mathrm{ALS,min}}$), and maximum ($H_{\mathrm{ALS,max}}$) heights of echoes for each forest stand.

Forest inventory and management data

Forest stand data for the Aegviidu test site were obtained from the Estonian Forest Register. The database contains forest stand map and tables with records of forest age, standing volume per unit area, basal area, relative density, site type, tree species composition, and other common forest inventory variables. The selection rules of forest stands to increase the sample size were similar to those of Lang and Arumäe (2018). The most important criteria were the size limit of at least 1 ha and more than 750 ALS returns for each stand polygon. The forest management data and commercial thinning data were obtained from the RMK database. The dates recorded in the RMK database for each thinning operation do not correspond to the actual felling work but are the dates of the field inspections, which may have been carried out several months after the actual thinning. To exclude the falsely dated thinning operations, the extracted ALS point clouds and available orthophotos were visually checked to determine the actual starting and ending times in relation to the ALS measurements.

The final dataset contained information of 870 thinned forest stands with a mean size of 2.49 ha. Most of the stands were dominated by Scots pine (398), birch (195), or Norway spruce (191). The rest of the stands in the sample were dominated by deciduous species such as European aspen, grey alder, or black alder (Table 2). The thinning is usually carried out from below and also from the dominant layer with the aim to increase the growth space for the remaining trees with the best stem properties. An additional 2,113 reference stands with no thinning were used for comparison (Table 2) with a mean size of 2.51 ha.

Statistical analysis

For the mean value comparison of CC_{ALS} or H_{P80} for different data acquisitions, a paired *t*-test was used after accepting the variance homogeneity with the *F*-test.

We applied two linear models, M_1 (2) and M_2 (3):

$$Y = b_0 + b_1 \cdot x + e, \tag{2}$$

$$Y = b_0 + b_1 \cdot x + SP + e, \tag{3}$$

where Y was CC_{ALS} and H_{P80} using on dataset ALS_{2008} or ALS_{2009}, x was CC_{ALS} or H_{P80} correspondingly on dataset ALS_{2012} or ALS_{2013}, SP was the dummy-variable component (Fox & Weisberg, 2011), b_0 and b_1 were the model parameters, and e was the error term. The dummy-variable component SP was implemented for regression model as $c_1 \cdot x_1 + c_2 \cdot x_2 + \ldots + c_k \cdot x_k$, where the dummy-variables $x_1, x_2 \ldots, x_k$ were defined as follows: x_1 equals 1 for Scots pine-dominated stand and 0 for other dominating species, x_2 equals 1 for Norway spruce dominated stand and 0 for other dominating species, x_k equals 1 for the kth dominated stand and 0 for other dominating species and $c_1, c_2 \ldots, c_k$ are parameters.

To estimate the significance of the additional variable SP in M_2, analysis of variances (ANOVA) was used. The F statistic for model comparison was as follows (Faraway, 2005):

$$F = \frac{\left(RSS_{M1} - RSS_{M2}\right)/\left(p_2 - p_1\right)}{RSS_{M2}/\left(n - p_2\right)}, \tag{4}$$

where RSS_{M1} and RSS_{M2} are the residual sums of squares for the models M_1 and M_2, respectively, p_1 and p_2 are the number of parameters for M_1 and M_2, and n is the number of observations.

The influences of thinning year (T_{Year}), site fertility index (H_{100}), and stand age at the time of thinning (A_{Thinning}) on the change in H_{P80} (ΔH_{P80}) were studied using T_{Year} as a factor, using the generalized additive models (function gam, Mixed GAM Computation Vehicle package):

$$\Delta H_{P80} = a_0 + a_1 \cdot T_{Year} + a_2 \cdot A_{Thinning} + a_3 \cdot H_{100} + e, \tag{5}$$

where a_x are the model parameters and e is the error term.

The factor level 0 was assigned to stands with T_{Year} before 2008, and for the rest of the stands, factor value was calculated as T_{Year} – 2007. This yielded factor levels 1–7 (Table 4).

Statistical analyses were carried out using R software (R Core Team, 2014).

Results

Canopy cover estimates in reference stands

The mean CC_{ALS} estimate for the reference stands from ALS_{2008} and ALS_{2012} revealed no significant change in value over the four years – the mean difference was only 0.4% (interquartile range 5.6%), and the t-test showed no statistically significant difference (p-value >0.05). The mean CC_{ALS} calculated for the reference stands using leaf-off data ALS_{2009} was 2% larger (p-value <0.05) than for ALS_{2013}, and the CC_{ALS} mean difference was dependent on stand-dominating species (Eq. 4, p-value <0.05). The interquartile range of CC_{ALS} was also larger for the leaf-off dataset (10.9%). The dominating species was not significant for leaf-on data when tested using the ANOVA model comparison (Eq. 4, p-value >0.05). There was a relatively large CC_{ALS} variation for both leaf-off and leaf-on phenophases in the reference stands, mostly due to the random character of the point cloud formation (Arumäe & Lang, 2018), and partly due to differences in leaf-off phenological stages in the case of springtime measurements (ALS_{2009} and ALS_{2013}). A substantial increase in CC_{ALS} by 2012 appeared in younger stands where the height of trees crossed the 1.3 m threshold used for CC_{ALS} calculation, and these stands were excluded from the reference data, similar to the clear-cut areas.

Canopy cover change in thinned stands

The CC_{ALS} for the stands thinned 1 year before the first ALS flight (Figure 1(a,e)), did not change significantly (t-test, p-value >0.05) during the bitemporal ALS measurements. In the stands that were thinned after the later ALS measurement (Figure 1(d,h)) a slight systematic decrease in CC_{ALS} was present. The decrease in CC_{ALS} was statistically insignificant for leaf-off data (p-value >0.05). This decrease in CC_{ALS} is most likely due to natural self-thinning and tree mortality, difference in leaf area index, or differences in scanning setups. In contrast, for leaf-off data, the results were also influenced by the earlier scanning date for ALS_{2013} compared to ALS_{2009}, which resulted in the stands being at different phenological stages.

The mean CC_{ALS} decrease in stands thinned between the two ALS flights was in the same range for both leaf-on (20.7%, interquartile range 15.4–25.1%; Figure 1(b,c)) and leaf-off data (21.5%, interquartile range 16.3–26.9%; Figure 1(f,g); Table 2). The few stands where the CC_{ALS} change was small (Figure 1(f)) were thinned with lower intensity, i.e. less than 20% of the standing wood volume was removed. The CC_{ALS} at the 8 m threshold was statistically significantly smaller compared to the CC_{ALS} at the 1.3 m threshold (for ALS_{2008} 54.3% and 65.1%, ALS_{2009} 50.3% and 62.4%, ALS_{2012} 61.1% and 52.6%, and ALS_{2013} 44.1% and 54.3%, respectively; p-value <0.01), but had no significant advantage in detecting thinning for either leaf-on or leaf-off data. A similar conclusion was made by Lang and Arumäe (2018) for a subsample of the stands using leaf-on data.

Changes in point cloud height distribution

The leaf-on ALS point cloud height percentiles H_{P25}, H_{P50}, H_{P80}, and H_{P95} showed a statistically significant (p-value <0.05) increase between the two bitemporal ALS measurements in thinned stands. The height difference was somewhat larger and more scattered for H_{P25} (Figure 1(i)) compared to higher H_{Px}. The difference between the leaf-off and leaf-on mean height increment was statistically significant (p-value <0.01).

Table 2. The Aegviidu test site characteristics based on forest inventory data. Age – A, stand basal area – G, stand mean height – H, site index – H_{100}. Interquartile range is given in brackets.

Dominating species	A (yrs)	G (m^2 ha^{-1})	H (m)	H_{100} (m)
Thinned stands (n = 870)				
Scots pine	69 (55–80)	22.0 (20–25)	16.7 (14–20)	22.1 (21–25)
Norway spruce	44 (36–52)	18.4 (15–22)	12.9 (10–16)	23.6 (21–25)
Birch	45 (35–55)	18.4 (15–22)	15.4 (12–19)	24.1 (21–25)
Other species	43 (36–49)	23.4 (19–26)	16.6 (14–19)	26.1 (22–28)
Reference stands (**n** = 2,113)				
Scots pine	85 (55–105)	19.4 (17–23)	15.1 (12–19)	18.3 (17–21)
Norway spruce	56 (29–90)	14.1 (11–22)	12.9 (7–22)	22.4 (21–25)
Birch	51 (23–73)	14.4 (7–21)	14.3 (5–20)	21.8 (17–25)
Other species	48 (38–61)	20.7 (17–24)	15.8 (15–20)	24.2 (21–25)

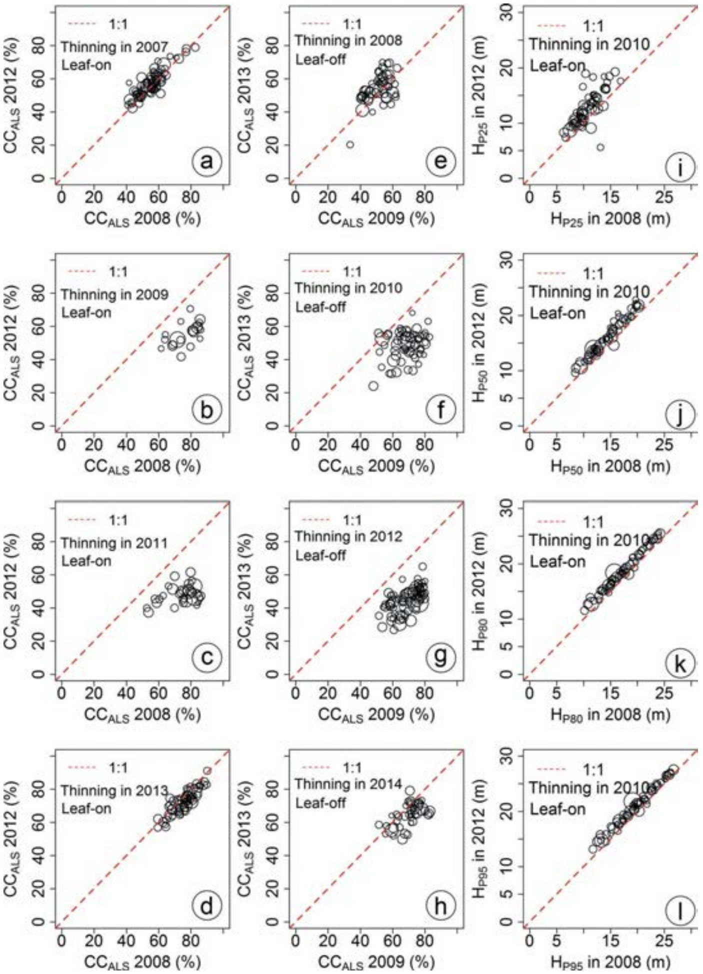

Figure 1. Examples of ALS-based canopy cover proxy (CC_{ALS}) and point cloud height distribution percentiles H_{P25}, H_{P50}, H_{P80}, and H_{P95} over four years with thinning carried out before, in between, and after the ALS measurements. Symbols are scaled to indicate stand size.

Nijland et al. (2015) compared the mean height and 95th percentile difference for thinned stands and found that distance between the height percentiles increased with thinning intensity. However, in our tests, the H_{P50} and H_{P95} difference before and after thinning did not change significantly (p-value = 0.2). The mean increase of H_{P80} for the leaf-off flight pair was 0.73 m, and for leaf-on data, the increase was 1.19 m (Table 3). The smaller increment in the H_{P80} calculated from the leaf-off flight pair is most likely because the first measurements (ALS_{2009}) were carried out in late May, whereas the measurements of ALS_{2013} were taken at the beginning of May (Table 1). Using the leaf-off dataset, the H_{P80} increment was also dependent on species composition; in thinned stands, the H_{P80} mean increment was significantly greater in evergreen coniferous forests compared to deciduous broadleaf species-dominated forests. This is most likely the result of differences in the phenological stages of the deciduous species. According to Ahas,

Table 3. The mean ALS-based canopy cover estimate (CC_{ALS}) and point cloud height distribution 80th percentile H_{P80} from leaf-off and leaf-on seasonal ALS measurements for stands with different thinning years. Standard error (S_e) is given in brackets.

Leaf-on

Thinning year	$\overline{CC_{ALS}}$ 2008 (%)	$\overline{CC_{ALS}}$ 2012 (%)	$\overline{H_{P80}}$ 2008 (m)	$\overline{H_{P80}}$ 2012 (m)
2007	56.0 (0.9)	57.8 (0.9)	18.7 (0.3)	19.8 (0.3)
2008	57.9 (1.3)	56.7 (1.2)	17.8 (0.4)	18.9 (0.4)
2009	76.6 (1.9)	54.5 (1.4)	16.6 (0.5)	17.6 (0.5)
2010	74.2 (1.0)	55.3 (0.8)	17.2 (0.5)	18.6 (0.5)
2011	74.4 (1.7)	48.9 (1.6)	16.5 (0.5)	18.2 (0.5)
2012	72.8 (0.9)	47.4 (0.8)	14.6 (0.3)	16.3 (0.4)
2013	74.5 (0.9)	71.3 (0.9)	15.7 (0.4)	17.5 (0.4)

Leaf-off

Thinning year	$\overline{CC_{ALS}}$ 2009 (%)	$\overline{CC_{ALS}}$ 2013 (%)	$\overline{H_{P80}}$ 2009 (m)	$\overline{H_{P80}}$ 2013 (m)
2008	52.3 (1.0)	55.2 (1.4)	17.8 (0.4)	18.3 (0.4)
2009	59.1 (2.5)	53.7 (1.4)	16.3 (0.5)	17.0 (0.5)
2010	68.2 (1.2)	47.9 (1.2)	17.1 (0.5)	18.2 (0.5)
2011	68.9 (1.6)	47.1 (1.2)	16.4 (0.5)	17.6 (0.5)
2012	68.8 (0.9)	45.5 (1.0)	14.6 (0.3)	16.0 (0.3)
2013	68.9 (1.1)	47.9 (1.4)	15.7 (0.4)	17.1 (0.4)
2014	70.1 (1.2)	64.5 (1.1)	16.3 (0.4)	17.1 (0.3)

Jaagus, and Aasa (2000), foliation of birch and other deciduous species in Estonia usually begins in early May and the final-leaf-unfolding phenophase occurs at the end of May, which falls within the bracket of flight times for ALS_{2009} and ALS_{2013}.

There was a systematic increase in H_{Px} of the reference stands similar to that of the thinned forest stands (Figure 2). The mean increase in H_{P80} (0.96 m; S_e = 0.02 m) of the reference stands, based on ALS_{2008} and ALS_{2012}, was significant (p-value <0.01) and slightly less than in the thinned stands (1.19 m; S_e = 0.06 m). This was due to the higher soil fertility (H_{100}) in the thinned stands compared to the reference stands (Table 2). A linear regression model (Figure 2) was fitted for leaf-on flight H_{Px} values of ALS_{2008} and ALS_{2012} for the reference stands. The linear model slope varied from 0.92 to 0.96 and was statistically significant (p-value <0.01; Figure 2). This indicates a greater height increment in younger stands (<30 years) and a smaller height increment in older stands (>60 years), which was also confirmed by a one-sided t-test (p-value <0.05). Stand-dominating species did not impact the H_{Px} change, according to a comparison of linear models (4) (p-value >0.05; Figure 2).

Other point cloud metrics

The other point cloud metrics (skewness, mode, and CRR) were mostly correlated to each other when compared using leaf-on data (R^2 = 0.35–0.64) and also to CC_{ALS} (R^2 = 0.17–0.44), except kurtosis. Surprisingly, the height distribution metrics did not change over the course of four years with structure changes caused by thinning. The four metrics did not show significant differences in their behaviour between the thinned and reference stands (p-value >0.05) and were not influenced by different thinning years except for CRR, which is caused by the calculation being based on the H_{Pmax} and H_{Pmin}.

The influence of thinning year

The model (5) (Table 4) for studying the dependence of ΔH_{P80} on T_{Year}, H_{100}, and A_{Thinning} showed no dependence on T_{Year} for stands thinned before the first ALS data measurement in 2008 for leaf-on data, or for stands thinned before 2009 using leaf-off data. Instead, ΔH_{P80} showed a significant correlation to the stand age at the year of thinning A_{Thinning} and site fertility index H_{100} (Table 4; p-value <0.05). When applied to all the thinned stands, the model (5.2) also showed a dependence of ΔH_{P80} on T_{Year} (Table 4; p-value <0.01). The determination coefficient R^2 increased significantly from 0.34 to 0.44 when a spline fitting (model 5.3) of T_{Year} was used instead of a linear relationship (Table 4). From Figure 3 we also see that the spline fitting was justified considering the shape of the relationship for both leaf-off and leaf-on data. The ΔH_{P80} showed a systematic increase for stands thinned near the second ALS data acquisition in 2012 and 2013 (Figure 3(a,c)). The fitted linear model using thinning year as a factor showed a significant difference in ΔH_{P80} between thinning years before 2007 and after 2007 (Table 4), and in the case of leaf-off data, between thinning years before 2008 and after 2008. Adding the

Table 4. The parameters of model (5) describing the change in the 80th percentile depending on the selection of stands and using leaf-on data. Factor level 0 corresponds to stands thinned before 2008, and the rest are calculated as thinning year – 2007.

Model	$\hat{a}_0$	$\hat{a}_1$	$\hat{a}_2$	$\hat{a}_3$	R^2	Model info
M5.1	*13.21*	*−0.006*	−0.013	0.0190	0.26	Model for stands thinned before the year 2007
M5.2	−70.65	0.036	−0.013	0.0255	0.34	Model without any filters to thinning year
M5.3	1.040	8.675 (s)	−0.012	0.0308	0.44	Model using spline fitting (s) on the thinning year
M5.4		0: 0.933 1: −0.149 2: −0.307 3: 0.275 4: 0.627 5: 0.611 6: 0.580 7: 0.438			0.30	Model for studying differences between thinning years. Each factor represents a different thinning year starting from 2008 (1–7). The factor 0 represents stands thinned before 2008.

*The values in italics are statistically insignificant (p-value >0.05).

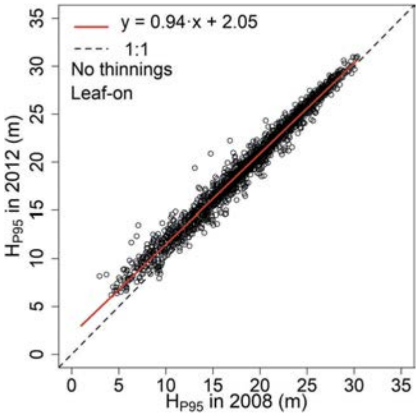

Figure 2. ALS point cloud height distribution percentile H_{P95} from 2008 and 2012 and the fitted linear model in reference stands.

H_{100} and A_{Thinning} to the model increased R^2 from 0.30 to 0.44 using leaf-on data; however, there was no significant increase in the case of leaf-off data.

We also analysed point clouds including the points from below the usual 1.3 m minimum height threshold and found different dependences of ΔH_{P80} on thinning year for the stands thinned between the two ALS measurements. In these point clouds, ΔH_{P80} decreased for the stands compared to those that were thinned before the first or after the latter ALS measurement (Figure 3(b)). A similar analysis for ΔH_{P80} using leaf-off data from ALS_{2009} and ALS_{2013} also indicated a possible decrease, but this was obscured by the influence of phenology.

Discussion

Forest canopy properties have a direct impact on the forest spectral signature measured using passive optical sensors, as well as the distribution of recorded photons from laser pulses. Changes in canopy

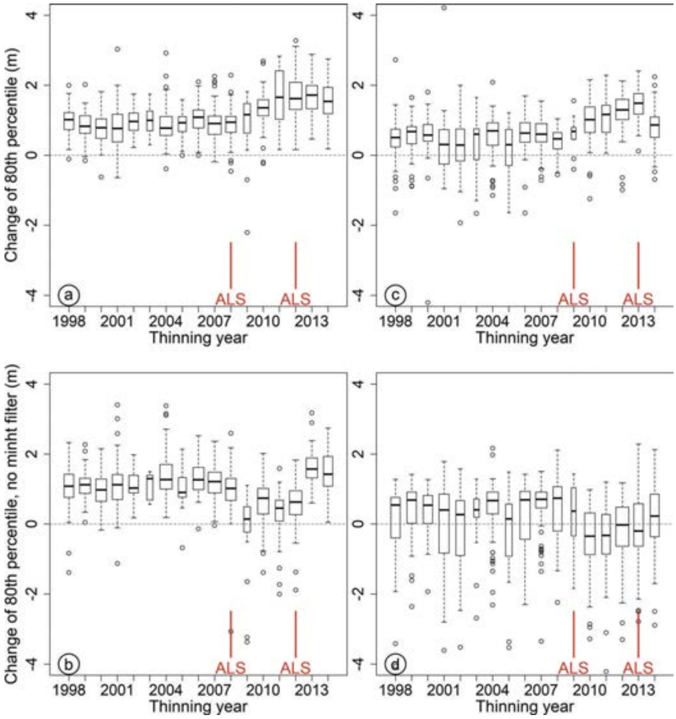

Figure 3. Boxplots showing the median, 25th, and 75th percentiles and individual outliers of the change in 80th percentile of point cloud height distribution using leaf-on data as a function of thinning year: (a) ground points excluded, (b) all points included. Leaf-off data: (c) ground points excluded, (d) all points included.

properties have an effect on the recorded discrete positions of laser pulse returns that create an ALS point cloud and that could be further linked to forest growth, disturbances, or phenology. However, there are also random effects related to the particular measurement configuration and possible systematic differences due to scanner settings and viewing angle (Keränen, Maltamo, & Packalen, 2016) between the compared datasets, but as Næsset (2009) and Wasser, Day, Chasmer, and Taylor (2013) concluded, the changes are more pronounced in the lower canopy layers. In addition to the flight configurations, the automatic gain control (AGC) influences the number of emitted photons and therefore the distribution of echoes (Vain, Yu, Kaasalainen, & Hyyppä, 2010), and can influence results when comparing the point cloud metrics from repeated ALS measurements.

CC_{ALS} as a proxy for canopy cover estimate depends on the number of returns per pulse, which can be a function of canopy structure and scanner settings. For our study, the first-to-all-echoes ratio did not significantly change for different datasets of leaf-on and leaf-off and was similar for different flying altitudes and different footprint sizes in leaf-on data, which corresponds to the findings by Næsset (2009). The first-to-all-echoes ratio in our dataset was slightly greater for the lower pulse repetition frequency compared to Næsset (2009), but that could be related to different scanners. CC_{ALS} estimates from ALS point clouds were significantly influenced by commercial thinning, as found in other studies (Ellis et al., 2016; Hevia et al., 2016). In our study, the CC_{ALS} decreased due to thinning by approximately 20% in leaf-on and leaf-off conditions. The species composition had no influence on CC_{ALS} change using leaf-on data but was relevant for leaf-off conditions. This is most likely due to the difference in the phenological stages in our leaf-off data acquisition times from 2009 and 2013. The somewhat large interquartile range of CC_{ALS} difference in the reference stands is most likely the cause of the CC_{ALS} estimation error, as was shown by Arumäe and Lang (2018), and for leaf-off data, the phenological differences also add up to the estimation errors. Similar to Arumäe and Lang (2018), raising the threshold up to 8 m systematically decreased the CC_{ALS} values using both leaf-on and leaf-off data, but provided no advantage in thinning detection.

The changes in ALS point cloud height distribution skewness, kurtosis, canopy relief ratio, and mode were not sensitive to the thinning cuttings. The point cloud height distribution percentiles did not decrease as would have been expected, opposite to findings by Nijland et al. (2015), who concluded that the range between H_{P95} and mean height estimate decreases with an increase in thinning grade in boreal forests. In our results, there was no significant difference in the distance between H_{P50} and H_{P95} before and after thinning. We observed a systematic increase in H_{Px} over the four-year period of ALS measurements, which reflected the forest height increment and partly also an effect of the stand mean height increase when smaller trees are removed (Lang, Arumäe, Laarmann & Kiviste, 2017). In our dataset, the recovery time for the forest understorey ranged from one to four years with respect to the last ALS measurements, and the height percentiles were calculated excluding the near-ground points. If the forest understorey is sparse, then the median and upper H_{Px} are influenced only by the upper layer of trees, as the returns either occur from the upper part of the canopy or are excluded by the minimum height filter. In this situation, the distance between H_{P50} and H_{P95} would not change much after thinning. Nijland et al. (2015) used measurements where the time gap from thinning to ALS data was 10 years, which meant there was also enough time for the understory vegetation to recover and therefore become "visible" to the ALS.

The H_{Px} increment was greater in younger stands compared to older forests, and this difference was similarly present in both the leaf-off and leaf-on datasets, although the H_{Px} values in the leaf-off dataset were systematically lower. This finding agrees well with existing knowledge of forest growth in Estonia (Kängsepp, Kangur, & Kiviste, 2015; Metslaid et al., 2011). We also found a smaller height increment estimate for the reference stands compared to the stands that were thinned, which can be explained by higher soil fertility in the sample of thinned stands. The mean height increment over the four-year period was statistically significant and could be further used for site index estimates, which have been shown by Kandare, Ørka, Dalponte, Næsset, and Gobakken (2017) to be predictable based on just tree height. However, site index estimates using bitemporal ALS data (Noordermeer, Bollandsås, Gobakken, & Næsset, 2018) will also be influenced by thinning cuttings. We found a characteristic pattern in the H_{P80} increment, depending on the time of thinning relative to the repeated ALS measurements. The H_{P80} increments of stands thinned before the first ALS flight were dependent not on thinning year but on the site fertility index H_{100} and stand age at thinning, which corresponds to the common knowledge of forest management practice – younger stands, or stands growing in fertile site types, have greater height increment. Initially, the height increment for the dominant and codominant tree layers is known to decrease for a couple of years after thinning, before then starting to increase (Sharma, Smith, Burkhart, & Amateis, 2006). However, our data showed a greater increment for H_{P80} in the stands with thinning year closer to the latter ALS measurement. The contradiction can be explained by the recovery of the forest canopy after thinning, and interaction with the laser pulses in a measurement configuration characterized by relatively large footprints and sparse point cloud. The tree crowns in dense forests before thinning are short, narrow, and sparse due to competition. With the increased amount of nutrients, growth space, and light for single trees, more branches at the live crown base survive, branches grow longer, and crown diameter increases as a result. At the same time, crowns become opaquer because the foliage mass of each tree is increased, and this increased photosynthetic capacity is expressed by the increased growth of breast height diameter and height of trees. With narrower, shorter, and sparser tree crowns, the probability is greater for a laser pulse to penetrate the canopy. Therefore, pulse returns are triggered either from the upper part of tree crowns or from the ground.

As time passes since thinning, tree crowns grow wider and denser and the probability of returns at the live crown base level increases. Assuming that the reflectance of branches in the NIR spectral region does not change much after thinning, the probability of a pulse return is proportional to the area of crown projection at the selected canopy height. The increase in crown projection area as branches grow is proportional to the crown radius, which is greater at the lower part of tree crowns in hemi-boreal forests. This also decreases H_{P80} of sparse point clouds. The combination of the smaller footprint in the earlier measurement and larger footprint in the later measurement may have an influence in a random direction for each stand, due to the AGC being turned on during the ALS measurements.

In addition to the tree canopy recovery, the selection of points for calculation of the point cloud height distribution percentiles has a substantial effect on the change of the percentile values in stands thinned between the two ALS measurements. If ground returns are included, then the increment of H_{P80} in stands thinned between the two ALS measurements is less compared to that of stands thinned before the first or after the second measurement. The difference in point cloud height metrics when calculated first without ground points and then with ground points included may give additional information towards the assessment of changes in forest canopy structure, and for site index estimation.

High altitude flights are more cost-effective as a larger territory is covered from each flight trajectory, but it comes with the loss of point cloud density per unit area. However, such cost-effective bitemporal low-density ALS data have still the potential for applications in National Forest Inventories for the monitoring of increment and felling volumes. There are also possibilities for large forest owners and forest management companies to use such data to monitor forest regeneration and for detecting natural disturbances, which alter canopy structure similarly to commercial thinning.

Conclusion

The study showed that the bitemporal ALS measurements carried out after thinning do not indicate the disturbance, and there are no significant changes detectable in the chronosequence of thinned stands dependent on the time that has passed since the thinning event. However, the thinnings carried out between the two ALS data acquisitions were detectable, and differences between point clouds of ALS measurements were dependent on the time passed since the first ALS measurements.

The ALS point cloud height distribution metrics skewness, kurtosis, mode, and canopy relief ratio were insensitive to thinning; instead, CC_{ALS} was the most informative ALS metric for detecting thinning-like disturbances.

While CC_{ALS} decreased after thinnings, the point cloud height percentiles remained at the same value or increased. Increase in point cloud height percentiles was similar for both thinned and reference stands similarly, using either leaf-off or leaf-on data. The fitted linear models for ΔH_{P80} were also in good agreement with the known patterns of forest stand growth. Also, the height increment estimate and changes in CC_{ALS} were not influenced by the stand-dominating species; it was only relevant when using leaf-off ALS data, which is related to differences in phenophases during ALS measurements. The inclusion of ground returns in the calculation of ΔH_{Px} decreases the change in stands thinned between the two ALS measurements, and can be used as an additional information source.

Acknowledgments

The authors would like to thank the Estonian Land Board for the airborne lidar data. Thinning data for the Aegviidu test site was retrieved from the Estonian State Forest Management Centre. This work was supported partially by the Estonian Defence Forces under Grant SLTTO19373, Estonian Environmental Investment Centre project [KIK14515] and by the Ministry of Education and Research under Grant IUT21-4. We thank Dr John Stanturf for commenting on and editing the English language. We thank Andres Kiviste for fruitful discussions. We thank all the anonymous reviewers for comments that helped us to improve the quality of the manuscript.

Disclosure statement

No potential conflict of interest was reported by the authors.

Funding

This work was supported by the Estonian Environmental Investment Centre [KIK14515]; Estonian Defence Forces [SLTTO19373];Ministry of Education and Research grant [IUT21-4].

Geolocation

Aegviidu test site is located in Estonia, 59° 19′ 20” N, 25° 35′ 36” E.

ORCID

Mait Lang http://orcid.org/0000-0002-0951-7933
Diana Laarmann http://orcid.org/0000-0002-1299-3893

References

Ahas, R., Jaagus, J., & Aasa, A. (2000). The phenological calendar of Estonia and its correlation with average air temperature. *International Journal of Biometeorology*, *44*, 159–166.

Andersen, H.-E., Reutebuch, S.E., McGaughey, R.J., d'Oliveira, M.V.N., & Keller, M. (2014). Monitoring selective logging in western Amazonia with repeat lidar flights. *Remote Sensing of Environment*, *151*, 157–165. doi:10.1016/j.rse.2013.08.049

Anniste, T., & Viilup, Ü. (2010). Metsa takseer tunnuste määramisest laserskanneerimise abil [Estimation of forest characteristics with laser scanning]. *Articles and Studies, Luua Forestry College*, *10*, 38–53.

Arumäe, T., & Lang, M. (2016). A validation of coarse scale global vegetation height map for biomass estimation in hemiboreal forests in Estonia. *Baltic Forestry*, *22*, 275–282.

Arumäe, T., & Lang, M. (2018). Estimation of canopy cover in dense mixed species forests using airborne lidar data. *European Journal of Remote Sensing*, *51*, 132–141. doi:10.1080/22797254.2017.1411169

Bottalico, F., Chirici, G., Giannini, R., Mele, S., Mura, M., Puxeddu, M., … Travaglini, D. (2017). Modeling Mediterranean forest structure using airborne laser scanning data. *International Journal of Applied Earth Observations and Geoinformation*, *57*, 145–153. doi:10.1016/j.jag.2016.12.013

Ellis, P., Griscom, B., Walker, W., Gonçalves, F., & Cormier, T. (2016). Mapping selective logging impacts in Borneo with GPS and airborne lidar. *Forest Ecology and Management*, *365*, 184–196. doi:10.1016/j.foreco.2016.01.020

Ene, L.T., Næsset, E., Gobakken, T., Bollandsås, O.M., Mauya, E.W., & Zahabu, E. (2017). Large-scale estimation of change in aboveground biomass in miombo woodlands using airborne laser scanning and national forest inventory data. *Remote Sensing of Environment*, *188*, 106–117. doi:10.1016/j.rse.2016.10.046

Faraway, J.J. (2005). *Linear models with R* (pp. 25–26). Florida: Chapman & Hall/CRC.

Fox, J., & Weisberg, S. (2011). *An R companion to applied regression* (pp. 163). Thousand Oaks, CA: SAGE Publications.

Guerra-Hernández, J., Görgens, E.B., García-Gutiérrez, J., Rodriguez, L.C.E., Tomé, M., & González-Ferreiro, E. (2016). Comparison of ALS based models for estimating aboveground biomass in three types of Mediterranean forest. *European Journal of Remote Sensing*, *49*, 185–204. doi:10.5721/EuJRS20164911

Hevia, A., Álvarez-González, J., Ruiz-Fernández, E., Prendes, C., Ruiz-González, A., Majada, J., & González-Ferreiro, E. (2016). Modelling canopy fuel and forest stand variables and characterizing the influence of thinning in the stand structure using airborne LiDAR. *Revista de Teledetección*, *45*, 41–55. doi:10.4995/raet.2016.3979

Jennings, S.B., Brown, N.D., & Sheil, D. (1999). Assessing forest canopies and understorey illumination: Canopy closure, canopy cover and other measures. *Forestry*, *72*, 59–73. doi:10.1093/forestry/72.1.59

Jõgiste, K., Korjus, H., Stanturf, J.A., Frelich, L.E., Baders, D., Donis, J., … Vodde, F. (2017). Hemiboreal forest: Natural disturbances and the importance of ecosystem legacies to management. *Ecosphere*, *8*(2), e01706. doi:10.1002/ecs2.1706

Kandare, K., Ørka, H.O., Dalponte, M., Næsset, E., & Gobakken, T. (2017). Individual tree crown approach for predicting site index in boreal forests using airborne laser scanning and hyperspectral data. *International Journal of Applied Earth Observation and Geoinformation*, *60*, 72–82. doi:10.1016/j.jag.2017.04.008

Kängsepp, V., Kangur, A., & Kiviste, A. (2015). Tree height distribution dynamics in young naturally regenerated study plots. *Forestry Studies*, *63*, 100–110. doi:10.1515/fsmu-2015-0011

Keränen, J., Maltamo, M., & Packalen, P. (2016). Effect of flying altitude, scanning angle and scanning mode on the accuracy of ALS based forest inventory. *International Journal of Applied Earth Observation and Geoinformation*, *52*, 349–360. doi:10.1016/j.jag.2016.07.005

Kocoloski, M., Griffin, W.M., & Matthews, H.S. (2011). Estimating national costs, benefits, and potential for cellulosic ethanol production from forest thinnings. *Biomass and Bioenergy*, *35*, 2133–2142. doi:10.1016/j.biombioe.2011.02.010

Korhonen, L., Ali-Sisto, D., & Tokola, T. (2015). Tropical forest canopy cover estimation using satellite imagery and airborne lidar reference data. *Silva Fennica*, *49*, 18. doi:10.14214/sf.1405

Korhonen, L., Korpela, I., Heiskanen, J., & Maltamo, M. (2011). Airborne discrete-return LIDAR data in the estimation of vertical canopy cover, angular canopy closure and leaf area index. *Remote Sensing of Environment*, *115*, 1065–1080. doi:10.1016/j.rse.2010.12.011

Korpela, I. (2008). Mapping of understory lichens with airborne discrete-return LiDAR data. *Remote Sensing of Environment*, *112*, 3891–3897. doi:10.1016/j.rse.2008.06.007

Kotivuori, E., Korhonen, L., & Packalen, P. (2016). Nationwide airborne laser scanning based models for volume, biomass and dominant height in Finland. *Silva Fennica*, *50*, 28. doi:10.14214/sf.1567

Lang, M., & Arumäe, T. (2018). Assessment of forest thinning intensity using sparse point clouds from repeated airborne lidar measurements. *Forestry Studies*, *68*, 40–50. doi:10.2478/fsmu-2018-0004

Lang, M., Arumäe, T., & Anniste, J. (2012). Estimation of main forest inventory variables from spectral and airborne lidar data in Aegviidu test site, Estonia. *Forestry Studies*, *56*, 27–41. doi:10.2478/v10132-012-0003-7

Lang, M., Arumäe, T., Laarmann, D., & Kiviste, A. (2017). Estimation of change in forest height growth. *Forestry Studies*, *67*, 5–16. doi:10.1515/fsmu-2017-0009

Lang, M., Arumäe, T., Lükk, T., & Sims, A. (2014). Estimation of standing wood volume and species composition in managed nemoral multi-layer mixed forests by using nearest neighbour classifier, multispectral satellite images and airborne lidar data. *Forestry Studies*, *61*, 47–68. doi:10.2478/fsmu-2014-0010

Large, A.R.G., & Heritage, G.L. (2009). Laser scanning – Evolution of the discipline. In G.L. Heritage & A.R.G. Large (Eds.), *Laser scanning for the environmental sciences* (pp. 1–20). Chichester, UK: John Wiley & Sons Ltd.

Lõhmus, E. (2004). *Eesti metsakasvukohatüübid* [Forest site types in Estonia]. Tartu, Estonia: Loodusfoto.

Lukasová, V., Lang, M., & Škvarenina, J. (2014). Seasonal changes in NDVI in relation to phenological phases, LAI and PAI of beech forests. *Baltic Forestry*, *20*, 248–262.

Maa-amet. (2006). Ortofotod aastate ja objektide kaupa [Database of ortophotos and objects by Estonian land board]. Retrieved from http://geoportaal.maaamet.ee/est/Andmed-ja-kaardid/Ortofotod/Ortofotod-aastate-ja-objektide-kaupa-p27.html.

McGaughey, R.J. (2014). *FUSION/LDV: Software for LIDAR data analysis and visualization. March 2010 – FUSION, version 3.42*. United States Department of Agriculture Forest Service Pacific Northwest Research Station, University of Washington, Seattle.

Metslaid, S., Sims, A., Kangur, A., Hordo, M., Jõgiste, K., Kiviste, A., & Pertti, H. (2011). Growth patterns from different forest generations of Scots pine in Estonia. *Journal of Forest Research*, *16*, 237–243. doi:10.1007/s10310-011-0275-4

Næsset, E. (1997a). Estimating timber volume of forest stands using airborne laser scanner data. *Remote Sensing of Environment*, *61*, 246–253. doi:10.1016/S0034-4257(97)00041-2

Næsset, E. (1997b). Determination of mean tree height of forest stands using airborne laser scanner data. *ISPRS Journal of Photogrammetry & Remote Sensing*, *52*, 49–56. doi:10.1016/S0924-2716(97)83000-6

Næsset, E. (2009). Effects of different sensors, flying altitudes, and pulse repetition frequencies on forest canopy metrics and biophysical stand properties derived from small-footprint airborne laser data. *Remote Sensing of Environment*, *113*, 148–159. doi:10.1016/j.rse.2008.09.001

Næsset, E., Bollandsås, O.M., Gobakken, T., Solberg, S., & McRoberts, R.E. (2015). The effects of field plot size on model-assisted estimation of aboveground biomass change using multitemporal interferometric SAR and airborne laser scanning data. *Remote Sensing of Environment*, *168*, 252–264. doi:10.1016/j.rse.2015.07.002

Næsset, E., & Gobakken, T. (2005). Estimating forest growth using canopy metrics derived from airborne laser scanner data. *Remote Sensing of Environment*, *96*, 453–465. doi:10.1016/j.rse.2005.04.001

Nijland, W., Coops, N.C., Macdonald, S.E., Nielsen, S.E., Bater, C.W., & Stadt, J.J. (2015). Comparing patterns in forest stand structure following variable harvests using airborne laser scanning data. *Forest Ecology and Management*, *354*, 272–280. doi:10.1016/j.foreco.2015.06.005

Noordermeer, L., Bollandsås, O.M., Gobakken, T., & Næsset, E. (2018). Direct and indirect site index determination for Norway spruce and Scots pine using bitemporal airborne laser scanner data. *Forest Ecology and Management*, *428*, 104–114. doi:10.1016/j.foreco.2018.06.041

Nyström, M., Holmgren, J., Fransson, J.E.S., & Olsson, H. (2014). Detection of windthrow trees using airborne laser scanning. *International Journal of Applied Earth Observation and Geoinformation*, *30*, 21–29. doi:10.1016/j.jag.2014.01.012

Olsson, H. (1994). Changes in satellite-measured reflectances caused by thinning cuttings in boreal forest. *Remote Sensing of Environment*, *50*, 221–230. doi:10.1016/0034-4257(94)90072-8

R Core Team. (2014). *R: A language and environment for statistical computing. R foundation for statistical computing*. Vienna. Retrieved from http://www.R-project.org

Sharma, M., Smith, M., Burkhart, H.E., & Amateis, R.L. (2006). Modelling the impact of thinning on height development of dominant and codominant loblolly pine trees. *Annual Forest Science*, *63*, 349–354. doi:10.1051/forest:2006015

Smith, A.M.S., Falkowski, M.J., Hudak, A.T., Evans, J.S., Robinson, A.P., & Steele, C.M. (2009). A cross-comparison of field, spectral, and lidar estimates of forest canopy cover. *Canadian Journal of Remote Sensing*, *35*, 447–459. doi:10.5589/m09-038

Temesgen, H., Strunk, J., Andresen, H.-E., & Flewelling, J. (2015). Evaluating different models to predict biomass increment from multi-temporal lidar sampling and remeasured field inventory data in south-central Alaska. *Mathematical and Computation Forestry & Natural Resource Sciences*, *7*, 66–80.

Vain, A., Yu, W., Kaasalainen, S., & Hyyppä, J. (2010). Correcting airborne laser scanning intensity data for automatic gain control effect. *IEEE Geoscience and Remote Sensing Letters*, *7*, 511–514. doi:10.1109/LGRS.2010.2040578

Valbuena, R., Eerikäinen, K., Packalen, P., & Maltamo, M. (2016). Gini coefficient predictions from airborne lidar remote sensing display the effect of management intensity on forest structure. *Ecological Indicators*, *60*, 574–585. doi:10.1016/j.ecolind.2015.08.001

Valgepea, M., Sims, A., Raudsaar, M., & Timmusk, T. (2017). Raied [Fellings]. In M. Raudsaar, K.-L. Siimon, & M. Valgepea (Eds.), *Aastaraamat mets 2017* [Yearbook Forest 2017] (pp. 111–143). Tallinn, Estonia: Keskkonnaagentuur.

Vastaranta, M., Kantola, T., Lyytikäinen-Saarenmaa, P., Holopainen, M., Kankare, V., Wulder, M.A., … Hyyppä, H. (2013). Area-based mapping of defoliation of Scots pine stands using airborne scanning LiDAR. *Remote Sensing*, *5*, 1220–1234. doi:10.3390/rs5031220

Wasser, L., Day, R., Chasmer, L., & Taylor, A. (2013). Influence of vegetation structure on lidar-derived canopy height and fractional cover in forested riparian buffers during leaf-off and leaf-on conditions. *PLoS ONE*, *8*, e54776. doi:10.1371/journal.pone.0054776

Wing, B.M., Ritchie, M.W., Boston, K., Cohen, W.B., Gitelman, A., & Olsen, M.J. (2012). Prediction of understory vegetation cover with airborne lidar in an interior ponderosa pine forest. *Remote Sensing of Environment*, *124*, 730–741. doi:10.1016/j.rse.2012.06.024

Yu, X., Hyyppä, J., Kukko, A., Maltamo, M., & Kaartinen, H. (2006). Change detection techniques for canopy height growth measurements using airborne laser scanner data. *Photogrammetric Engineering and Remote Sensing*, *72*, 1339–1348. doi:10.14358/PERS.72.12.1339

Zhao, K., Suarez, J.C., Garcia, M., Hu, T., Wang, C., & Londo, A. (2018). Utility of multitemporal lidar for forest and carbon monitoring: Tree growth, biomass dynamics, and carbon flux. *Remote Sensing of Environment*, *204*, 883–897. doi:10.1016/j.rse.2017.09.007

CURRICULUM VITAE

First name: Tauri
Surname: Arumäe
Citizenship: Estonian
Date of Birth: 04.11.1987
Addresses: Institute of Forestry and Rural Engineering,
Estonian University of Life Sciences, Kreutzwaldi 5,
51014 Tartu, Estonia
State Forest Management Centre, Sagadi Village,
Haljala Municipality, 45403 Lääne-Viru County
E-mail: tauri.arumae@rmk.ee

Education:

2012–2019	PhD studies in forestry, Institute of Forestry and Rural Engineering, Estonian University of Life Sciences
2009–2011	Master's studies in forest industry, Institute of Forestry and Rural Engineering, Estonian University of Life Sciences
2006–2009	Bachelor's studies in forestry, Institute of Forestry and Rural Engineering, Estonian University of Life Sciences
1994–2006	Võru Kreutzwald Gymnasium

Professional employment:

2011–…	State Forest Management Centre, remote sensing specialist

Research interests:

Remote sensing of forests

Foreign languages:

English, German, French

Training and special courses:

2016	Forest Canopy Height Mapping with Radar Interferometry, ForestSAT2016, Santiago, Chile
2015	Reconstruction of Stand Structure, Tallinn, Estonia

2014	Trans-Atlantic Training (SAR), Kraków, Poland
2014	Hands-on LiDAR processing course, ForestSAT2014, Riva del Garda, Italy

Projects:

2015–2019	Institutional grant IUT21-4: The carbon dynamics in Estonian forests affected by sustainable management.
2011–2016	Ministry of Education and Research Targeted Funding project SF0180009Bs11: Quantitative remote sensing of vegetation covers.
2010–2013	Estonian Science Foundation Research Grant project ETF8290: Integration of remote sensing, forest growth and reflectance models with existing databases into continuous inventory systems of hemi-boreal forests.

ELULOOKIRJELDUS

Eesnimi: Tauri
Perekonnanimi: Arumäe
Kodakondsus: Eesti
Sünniaeg: 04.11.1987
Aadressid: Metsandus- ja maaehitusinstituut, Eesti Maaülikool, Kreutzwaldi 5, 51014 Tartu, Eesti
Riigimetsa Majandamise Keskus, Sagadi küla, Haljala vald, 45403 Lääne-Viru maakond
E-post: tauri.arumae@rmk.ee

Haridus:

2012–2019	Eesti Maaülikool, metsandus- ja maaehitusinstituut, metsandus, doktoriõpe
2009–2011	Eesti Maaülikool, metsandus- ja maaehitusinstituut, metsatööstus, magistriõpe
2006–2009	Eesti Maaülikool, metsandus- ja maaehitusinstituut, metsandus, bakalaureuseõpe
1994–2006	Võru Kreutzwaldi Gümnaasium

Teenistuskäik:

2011–…	Riigimetsa Majandamise Keskus, kaugseirespetsialist

Teadustöö suunad: Metsade kaugseire

Võõrkeelte oskus: Inglise, saksa, prantsuse

Täiendkoolitus:

2016	Metsa kõrguse mõõtmine radari interferomeetriaga, ForestSAT2016, Santiago, Tšiili
2015	Puistu struktuuri rekonstrueerimine, Tallinn, Eesti
2014	LiDARi andmetöötluse kursus, ForestSAT2014, Riva del Garda, Itaalia
2014	Trans-Atlantic training (SAR), Kraków, Poola

Projektid:

2015–2019	Institutsionaalne uurimistoetus IUT21-4: Eesti metsade süsiniku dünaamika ja jätkusuutlik majandamine.
2011–2016	Sihtfinantseerimine projekt SF0180009Bs11: Taimkatte kvantitatiivne kaugseire.
2010–2013	Eesti Teadusfondi uurimistoetus projekt ETF8290: Kaugseire, metsanduslike andmebaaside ning metsakasvu ja heleduse mudeli lõimimine pideva metsakorralduse süsteemi poolboreaalsete metsade jaoks

LIST OF PUBLICATIONS

Publications indexed in the Thomson Reuters Web of Science database

Olesk, A., Praks, J., Antropov, O., Zalite, K., **Arumäe, T.**, Voormansik, K. 2016. Interferometric SAR Coherence Models for Characterization of Hemiboreal Forests Using TanDEM-X Data. Remote Sensing, 8(9), 700.

Arumäe, T., Lang, M. 2016. A Validation of Coarse Scale Global Vegetation Height Map for Biomass Estimation in Hemiboreal Forests in Estonia. Baltic Forestry, 22(2), 275–282.

Arumäe, T., Lang, M. 2018. Estimation of canopy cover in dense mixed-species forests using airborne lidar data. European Journal of Remote Sensing, 51(1), 132–141.

Hovi, A., Lindberg, E., Lang, M., **Arumäe, T.**, Peuhkurinen, J., Sirparanta, S., Pyankov, S., Rautiainen, M. 2019. Seasonal dynamics of albedo across European boreal forests: Analysis of MODIS albedo and structural metrics from airborne LiDAR. Remote Sensing of Environment, 224, 365–381.

Arumäe, T., Lang, M., Laarmann, D. 2020. Thinning- and tree-growth-caused changes in canopy cover and stand height and their estimation using low-density bitemporal airborne lidar measurements – a case study in hemi-boreal forests. European Journal of Remote Sensing, 53(1), 113–123.

Publications in other peer-reviewed research journals

Kodar, A., Lang, M., **Arumäe, T.**, Eenmäe, A., Pisek, J., Nilson, T. 2011. Leaf area index mapping with airborne lidar, satellite images and ground measurements in Järvselja VALERI test site. Forestry Studies, 55, 11–32.

Lang, M., **Arumäe, T.**, Anniste, J. 2012. Estimation of main forest inventory variables from spectral and airborne lidar data in Aegviidu test site, Estonia. Forestry Studies, 56, 27–41.

Arumäe, T., Lang, M. 2013. A simple model to estimate forest canopy base height from airborne lidar data. Forestry Studies, 58, 46–56.

Lang, M., Kodar, A., **Arumäe, T.** 2013. Restoration of above canopy reference hemispherical image from below canopy measurements for plant area index estimation in forests. Forestry Studies, 59, 13–27.

Lang, M., **Arumäe, T.**, Lükk, T., Sims, A. 2014. Estimation of standing wood volume and species composition in managed nemoral multi-layer mixed forests by using nearest neighbour classifier, multispectral satellite images and airborne lidar data. Forestry Studies, 61, 47–68.

Arumäe, T., Lang, M. 2016. ALS-based wood volume models of forest stands and comparison with forest inventory data. Forestry Studies, 64, 5–16.

Lang, M., **Arumäe, T.**, Laarmann, D., Kiviste, A. 2017. Estimation of change in forest height growth. Forestry Studies, 67, 5–16.

Lang, M., **Arumäe, T.** 2018. Assessment of forest thinning intensity using sparse point clouds from repeated airborne lidar measurements. Forestry Studies, 68, 41–51.

Articles in proceedings in a book or in a collection

Lang, M., **Arumäe, T.** 2014. Kaugseire praktilistes metsanduslikes rakendustes Eestis. Aan, A., Narusk, K. (Toim.). Kaugseire Eestis 2014: 128−137. Tallinn: Keskkonnaagentuur.

Lang, M., **Arumäe, T.**, Nikopensius, M. 2016. Puistute biomassi ja süsiniku hulga hindamine kaugseire abil. Peterson, U., Lillemaa, T. (Toim.). Kaugseire Eestis 2016: 58−66. Tõravere: Tartu Observatoorium.

Lang, M., Kaha, M., **Arumäe, T.** 2018. Kaugseire praktilised metsanduslikud rakendused – puistute liigilise koosseisu kaardistamine ja harvendusraiete tuvastamine. Peterson, U., Lillemaa, T. (Toim.). Kaugseire Eestis 2018: 69–76. Tartu Ülikooli Tartu observatoorium.

Published meeting abstracts

Lang, M., Anniste, J., Lükk, T., **Arumäe, T.** 2012. Forestry database update in Aegviidu test site, Estonia, using multi source kNN. ForestSat2012, Oregon State University, Corvallis, Oregon, USA. 11–14. September, 2012.

Popular scientific publications

Lang, M., Kardakov, A., Lükk, T., **Arumäe, T.**, Korjus, H. 2011. Metsanduslik andmehõive ajas, ruumis ja pildis. Eesti Mets, 4, 6−12.

Kangur, A., Märdla, S., **Arumäe, T.**, Jürgenson, H., Kask, P. 2015. Üksikpuu kõrguse mõõtmine. Eesti Mets, 2, 34−39.

VIIS VIIMAST KAITSMIST

BIRGIT AASMÄE
ANTIMICROBIAL RESISTANCE OF ESCHERICHIA COLI AND ENTEROCOCCI ISOLATED FROM SWINE, CATTLE AND DOGS AND MASTITIS PATHOGENS ISOLATED IN ESTONIA IN 2006–2015.
EESTIS AASTATEL 2006–2015 SIGADELT, VEISTELT JA KOERTELT ISOLEERITUD ESCHERICHIA COLI JA ENTEROCOCCUS'E PEREKONNA MIKROOBIDE NING LEHMADELT ISOLEERITUD MASTIIDIPATOGEENIDE ANTIBIOOTIKUMIRESISTENTSUS.
Dotsent **Piret Kalmus** ja professor **Toomas Orro**
13. detsember 2019

KAIA KASK
THE EFFECTS OF HEAT STRESS SEVERITY ON PHOTOSYNTHESIS AND VOLATILE ORGANIC COMPOUND EMISSIONS IN BLACK MUSTARD AND TOBACCO.
KUUMASTRESSI MÕJU MUSTA KAPSASROHU (*BRASSICA NIGRA* L.) JA VÄÄRISTUBAKA (*NICOTIANA TABACUM* L.) FOTOSÜNTEESILE JA LENDUVÜHENDITE EMISSIOONIDELE.
Professor **Ülo Niinemets**, vanemteadur **Astrid Kännaste**
5. märts 2020

MÄRT REINVEE
APPLICABILITY OF LOW-COST ELECTROMYOGRAPHS IN ERGONOMIC ASSESSMENT
MADALA MAKSUMUSEGA ELEKTROMÜOGRAAFIDE RAKENDATAVUS ERGONOOMIKALISES HINDAMISES
Emer. dots. **Jaak Jaaniste**, prof. **Mati Pääsuke**
13. märts 2020

ANRI AINO ELISA TIMONEN
EPIDEMIOLOGY OF MYCOPLASMA BOVIS INTRAMAMMARY INFECTION IN DAIRY HERDS
MYCOPLASMA BOVIS'E PÕHJUSTATUD UDARANAKKUSE EPIDEMIOLOOGIA PIIMAVEISEKARJADES
Dotsent **Piret Kalmus**, dotsent **Kerli Mõtus**
11. juuni 2020

ANNE INGVER
IMPACT OF FARMING SYSTEM, PRE-CROP AND WEATHER CONDITIONS TO YIELD AND QUALITY OF SPRING WHEAT
VILJELUSSÜSTEEMI, EELVILJA JA ILMASTIKU MÕJU SUVINISU SAAGILE JA KVALITEEDILE
Dotsent **Evelin Loit**, vanemteadur **Ilmar Tamm**
16. juuni 2020

ISSN 2382-7076
ISBN 978-9949-698-26-4 (trükis)
ISBN 978-9949-698-27-1 (pdf)